Dynamic mobility management at cordon level : evaluation of different pricing-based strategies

Louis Balzer

Thesis National Number: 2023ENTP0006

A THESIS OF ENTPE
Member of the Université de Lyon

Doctoral school N°162
(Mechanics–Energy–Civil engineering–Acoustics)

To obtain the graduation of
PhD in Civil Engineering

Defended on September 15th, 2023, by:
Louis Balzer

Dynamic mobility management at cordon level: evaluation of different pricing-based strategies

In front of the following examination committee:

SOLNON Christine, Professor, INSA Lyon	Committee chair
BOGENBERGER Klaus, Professor, TU Munich	Reviewer
GEROLIMINIS Nikolas, Professor, EPFL	Reviewer
CATS Oded, Professor, TU Delft	Examiner
VERHOEF Erik, Professor, VU Amsterdam	Examiner
LECLERCQ Ludovic, Research director, Univ Eiffel/ENTPE	Supervisor

Numéro national de thèse (NNT) : 2023ENTP0006

THÈSE DE DOCTORAT DE L'ENTPE
Membre de l'Université de Lyon

École Doctorale N°162
(Mécanique-Energie-Génie Civil-Acoustique)

Spécialité / discipline de doctorat :
Génie Civil

Soutenue publiquement le 15/09/2023, par :
Louis Balzer

Gestion dynamique de la mobilité au niveau d'un cordon : évaluation de différentes stratégies à base de tarification

Devant le jury composé de :

SOLNON Christine, Professeure, INSA Lyon	Présidente
BOGENBERGER Klaus, Professeur, TU Munich	Rapporteur
GEROLIMINIS Nikolas, Professeur, EPFL	Rapporteur
CATS Oded, Professeur, TU Delft	Examinateur
VERHOEF Erik, Professeur, VU Amsterdam	Examinateur
LECLERCQ Ludovic, Directeur de recherche, Univ Eiffel/ENTPE	Directeur de thèse

"*Walking is still the best form of short-distance transportation. It's the most convenient, the cheapest, and the most healthful. Countless years of technological advance have not changed that.*"

Chetter Hummin, in *Prelude to Foundation* from Isaac Asimov.

Abstract

Automotive congestion in urban regions is a worldwide challenge. Changing travel behaviors can achieve a more sustainable use of the transportation network. Travelers should be encouraged to use sustainable modes such as public transportation (PT) instead of modes associated with large negative externalities such as private cars. A Tradable Credit Scheme (TCS) is a policy aiming at reducing the negative externalities of transportation. The regulator distributes credits for free to travelers. Accessing the transportation network requires credits, and the required amount depends on the sustainability of the travel choice. Travel alternatives inducing large negative externalities require more credits than sustainable ones. The credits can be traded directly between travelers or through a central bank. The trading activity determines the credit price.

In this thesis, we propose TCS as a tool to nudge private car drivers to switch to PT and carpooling. The TCS is compared to other demand management policies already deployed in some cities: congestion pricing and license plate rationing (LPR). TCS has the advantages of being budget-neutral, as opposed to pricing, and more flexible than LPR. Another use of TCS is proposed: the regulation of ride-hailing (RH) services, which tend to compete with PT. The different regions in the city are regulated as credits are needed to access the regions, and more credits are needed in regions with excellent PT services. The TCS aims to promote combined trips, where travelers use RH in sparse areas and PT in dense areas.

A simulation framework based on the trip-based Macroscopic Fundamental Diagram (MFD) is deployed. It allows us to compute the traffic states and accounts for the congestion dynamics and the heterogeneity of the trips. It also includes multi-modal congestion effects for a large-scale network, typically the size of a city. It is faster to solve than simulation based on micro-simulation, which makes the framework fit for computing the traffic state under the equilibrium and performing optimization of the TCS. An ad-hoc method is developed to find the equilibrium by linearizing the MFD model and solving quadratic problems.

The proposed TCS are evaluated on a realistic case study based on the city of Lyon (FR). The typical use case permits the evaluation of the effect of different TCS on travel time, mode choices, and carbon emissions. It also allows quantifying the heterogeneous impacts of TCS on the different travelers according to their values of time, origins, and destinations.

Keywords: Congestion dynamics, Demand management, Macroscopic fundamental diagram, On-demand mobility, Tradable credits.

Résumé

La congestion automobile dans les zones urbanisées est un problème mondial. Le changement des habitudes de déplacements permet une utilisation plus durable des réseaux de transport. Les usagers doivent être encouragés à utiliser des modes de transport durables, tel que les transports en commun (TC) à la place de modes générant de notables externalités négatives, tels que la voiture particulière.

Un système de crédits échangeables (TCS) est une politique de mobilité visant à réduire les externalités négatives associées au transport. Le régulateur utilise des crédits qu'il distribue gratuitement aux usagers. L'accès au réseau de transport requiert des crédits, et la quantité dépend du niveau de durabilité du choix de trajet. Les trajets générant beaucoup d'externalités requièrent plus de crédits que ceux qui sont durables. Les crédits peuvent être échangés directement entre les usagers ou par le biais d'une banque centrale. Les échanges déterminent le prix du crédit.

Dans cette thèse, nous proposons d'utiliser le TCS comme un outil pour encourager les chauffeurs de voitures particulières à se reporter sur les TC ou le covoiturage. Le TCS est comparé à d'autres politiques de management de la demande : le péage urbain et la circulation alternée. Le TCS a les avantages d'opérer à budget neutre, à l'inverse du péage urbain et d'être plus flexible que la circulation alternée.

Une autre utilisation du TCS est proposée pour réguler les services de voiture de tourisme avec chauffeur (VTC), qui peuvent concurrencer les TC. Les différentes régions de la ville sont régulées puisqu'il est nécessaire d'utiliser des crédits pour y accéder, et plus la couverture TC est excellente, plus la quantité de crédits nécessaires est élevée. Le TCS cherche à promouvoir des trajets où VTC et TC se complètent, c'est-à-dire où les usagers utilisent les VTC dans les zones peu denses et les TC dans les zones denses.

Un cadre de simulation basé sur la version du diagramme fondamentale macroscopique (MFD) orientée trajet est déployé. Il permet de calculer les états de trafic en prenant en compte la dynamique de la congestion et l'hétérogénéité des trajets. Ce cadre comprend aussi les effets multimodaux de la congestion pour un réseau à grande échelle, typiquement la taille d'une ville. Il est plus rapide à résoudre qu'une simulation basée sur une représentation microscopique de la congestion, ce qui rend cette méthode idéale pour calculer les états d'équilibre et optimiser le TCS. Une méthode sur mesure est développée pour trouver l'équilibre en linéarisant le modèle MFD et résolvant des problèmes quadratiques.

Les TCS proposés sont évalués sur un cas d'étude réaliste basé sur Lyon. Ce cas d'usage typique permet d'évaluer les effets de différents TCS sur les temps de trajet, les choix modaux, et les émissions de carbone. Il permet aussi de quantifier l'impact hétérogène du TCS sur les différents usagers selon leurs valeurs du temps, origines, et destinations.

Mots Clés : Crédits échangeables, Diagramme fondamental macroscopique, Management de la demande, Mobilité à la demande, Modélisation dynamique.

Acknowledgements

I thank my supervisor, Prof. Leclercq, for providing me with opportunities for research, collaboration, and dissemination of my work. I could not expect to have such a friendly and respectful supervisor. The excellent working environment at LICIT-ECO7 positively affected my research. The two generations of PhD students with whom I shared the office kept the morale high: Elise, Cécile, Loïc, and then Maryia, Jiajie, Ali, Fei, and Zhixiong. I want to thank also the other PhD students Mélanie, Alexandre, and Mathis, who started their PhD with me; Manon for supporting me as a deputy coordinator; the lab post-docs Andres, Pierre, Kinjal, and Matthieu, for sharing their wisdom; Anne-Christine for the weekly cake and creating cohesion in the lab.

The work done during my thesis included cooperation with European partners. I thus thank the TU Munich team led by Prof. Bogenberger and Dr. Loder for the two joint seminars. I also thank colleagues from the TU Delft Jesper and Prof. Cats for welcoming me to Delft.

I warmly thank my family for supporting me in my choices and being there for both the joyful and the sad events. Thank you, Annabelle, for being at my side all these years.

Contents

Abstract **v**

Résumé **vii**

Acknowledgements **ix**

1 Introduction **1**

1.1 Context and background 1
1.2 Research objectives and questions 2
1.3 Thesis contributions 2
1.3.1 Scientific contributions 2
1.3.2 Societal relevance 3
1.3.3 Publication list 3
1.3.4 Thesis outline 4

2 Literature review and scope of the thesis **7**

2.1 Demand management policies 7
2.1.1 Concepts 8
2.1.2 Objectives 10
2.1.3 User behavior 10
2.1.4 Charging scheme 11
2.1.5 Experiments 11
2.1.6 Models and solutions methods 12
2.1.7 Position compared to other demand management schemes . . . 17
2.2 Traffic representations 19
2.2.1 Discussion of traffic representation from the literature on TCS . 20
2.2.2 Macroscopic Fundamental Diagram 20
2.3 Case study: Lyon 24

3 Modal equilibrium for the trip-based macroscopic fundamental diagram framework under static tradable credit schemes **27**

3.1 Methodological framework 28

3.1.1 Mode choice . . . 29
3.1.2 Network equilibrium . . . 30
3.2 Computing the modal equilibrium . . . 34
3.3 Derivation of the travel times with respect to the modal shares . . . 36
3.4 Optimization of the credit charge . . . 38
3.4.1 Minimizing total travel time . . . 39
3.4.2 Minimizing the total network emissions . . . 40
3.4.3 Mixed objective function considering both emissions and travel times . . . 42
3.5 Numerical example . . . 43
3.5.1 Preliminary analysis . . . 43
3.5.2 Results . . . 44
3.6 Conclusions . . . 51

4 Comparison of the tradable credit scheme against other demand management policies 53
4.1 Methodological framework . . . 53
4.1.1 Mode choice . . . 54
4.1.2 Initial DMS . . . 54
4.1.3 Equilibrium computation . . . 55
4.2 Demand management strategies . . . 56
4.2.1 LPR . . . 56
4.2.2 Pricing . . . 57
4.2.3 TCS . . . 57
4.2.4 TPS . . . 57
4.2.5 Spatial variations of DMS . . . 57
4.3 Computing the modal equilibrium . . . 59
4.3.1 No DMS . . . 59
4.3.2 LPR . . . 59
4.3.3 Pricing . . . 59
4.3.4 TCS . . . 60
4.3.5 TPS . . . 61
4.4 Benchmarking the different demand management policies . . . 63
4.4.1 Comparing the DMS with uniform charging settings . . . 66
4.4.2 Different spatial charges . . . 68
4.4.3 Different cycle lengths . . . 71
4.5 Conclusions . . . 77

5 Dynamic tradable credit scheme for multimodal urban networks 79
5.1 TCS models in urban areas . . . 79
5.2 Problem formulation . . . 80
5.2.1 Multimodal generalized bathtub . . . 81
5.2.2 Dynamic Tradable Credit Scheme . . . 84
5.2.3 Mode and departure time choice . . . 84
5.2.4 Equilibrium formulation . . . 85
5.3 Methodological Framework . . . 86
5.3.1 Credit price . . . 87
5.3.2 Assignment . . . 87
5.3.3 Optimization of the charging profile . . . 88
5.4 Case Study . . . 90
5.4.1 Simulation settings . . . 91
5.4.2 TCS impact analysis . . . 93
5.4.3 Comparison with the trip-based MFD . . . 99
5.5 Conclusions . . . 100

6 Rebalancing on-demand service operations with tradable credit scheme 103
6.1 Motivation . . . 103
6.2 Methodology . . . 104
6.3 Regulating fleet size in each region with TCS . . . 106
6.3.1 Calculating the equilibrium . . . 107
6.3.2 Simulating the day-to-day markets evolution and the transition to equilibrium . . . 109
6.4 Case study . . . 112
6.5 Numerical results . . . 114
6.6 Conclusions . . . 121

7 Conclusion 123
7.1 Contribution to the research questions . . . 123
7.2 Research perspectives . . . 125

A App. MFD under static TCS 127
A.1 Notations . . . 127
A.2 Numerical evaluation for the condition of uniqueness . . . 129
A.3 Sensitivity of the PT travel times . . . 129
A.4 Sensitivity of the threshold for the search space . . . 130

B App. Comparison of DMS **131**

B.1 Sensitivity of the PT penalty distribution 131

C App. Dynamic TCS **133**

C.1 Notations 133

C.2 Algorithm for credit charge optimization 135

C.3 Sensitivity of the carpooling penalty 135

C.4 Total travel time and carbon emissions 136

D App. On-demand TCS **137**

D.1 Notations 137

Bibliography **139**

List of Figures

1.1 Structure of the thesis. 5

2.1 Traffic demand management with TCS and TPS. 9
2.2 Evolution of the distance traveled by the virtual traveler. 22
2.3 Evolution of the accumulation on the network. 23
2.4 (a) The urban area under consideration (Mariotte et al., 2020, ©OpenStreetMap); (b) The IRIS areas merged in 10 regions and the access points merged in five boundaries (circles). From (Balzer & Leclercq, 2022f). 25
2.5 (a) Departure times, (b) trip lengths, and (c) PT travel times distributions. 26

3.1 Each OD pair has car and PT alternatives. 29
3.2 Decomposition of the travel time following events. In this illustration, group i enters at the event 1 and exits at the event 4. 31
3.3 The iterative process to find the car shares and credit price at equilibrium. (a) One step and (b) full convergence process. 34
3.4 Flowchart of the search for the equilibrium. 36
3.5 (a) Time- and (b) distance-based representations of the inter-event periods. 37
3.6 Speed (a), accumulation (b) and production (c) at the modal equilibrium for a credit charge of 200 credits and no TCS. 44
3.7 (a) Error on the travel times, and (b) error on the modal decisions. . . 44
3.8 (a) Error between modal shares and decisions vs. iteration, (b) vs. computation time, (c) evolution of the credit price, and (d) modal shares at equilibrium. 45
3.9 (a) Trip lengths and (b) PT travel times for ST and (c) departure times for DT. 46
3.10 Modal shares at the equilibrium for the three scenarios with SC2. . . . 47
3.11 (a) Number of car users, (b) toll price in EUR, and (c) total travel time for different credit charges. 47
3.12 (a) CO_2 emission per distance and (b) CO_2 total emissions for different credit charges. 48
3.13 Total travel time vs. CO_2 emissions for different credit charges. The green and red points are found by minimizing total travel time and the mixed objective function. 48

3.14 (a) Total travel time and (b) mixed objective function optimizations. . 49
3.15 (a) Trade balances, (b) time gains, and (c) net gains for the credit charges found by minimizing the total travel time and the mixed objective. 50

4.1 Distribution of days with PT penalty. 64
4.2 Comparison of the uniform DMS for a cycle of one day: (a) total travel time vs. penalty cost, (b) social cost vs. carbon emission, (c) car share and equivalent toll price. 67
4.3 Comparison of the distributions of the (a) social and (b) trade gains between uniform TCS with a validity cycle of one day and pricing. . . 68
4.4 Comparison of the uniform DMS for a cycle of ten days: (a) total travel time vs. penalty cost, (b) social cost vs. carbon emission, (c) car share and equivalent toll price. 69
4.5 Social cost vs. carbon emissions for (a) pricing and (b) TCS for a validity cycle of one day. 70
4.6 Total travel time vs. carbon emissions with pricing without PT penalty. 70
4.7 Distribution of the permits prices, averaged over the two working weeks, for a validity cycle of one day. 71
4.8 (a) Social cost vs. carbon emission and (b) car share and toll equivalent for D-specific DMS for a validity cycle of one day. 71
4.9 (a) Social cost vs. carbon emission and (b) car share and toll equivalent for OD-specific DMS for a validity cycle of one day. 72
4.10 (a) Social cost vs. carbon emission and (b) car share and toll equivalent for D-specific DMS for a validity cycle of ten days. 72
4.11 (a) Social cost vs. carbon emission and (b) car share and toll equivalent for OD-specific DMS for a validity cycle of ten days. 73
4.12 TCS-U with the different cycles: (a) car share and (b) equivalent toll. The credit ratio is 33%. 73
4.13 TCS-U with the different cycles: (a) total travel time, (b) satisfaction rate, (c) social cost, (d) total traveled distance, (e) mean car speed, and (f) carbon emissions. The credit ratio is 33%. 75
4.14 (a) Social and (b) trade gains distribution with TCS-U over the different cycles. The credit ratio is 33%. 76
4.15 TCS-D with the different cycles: (a) car share and (b) equivalent toll. The macro credit ratio is 33%. 76
4.16 TCS-OD with the different cycles: (a) car share and (b) equivalent toll. The macro credit charge is 33%. 76

5.1 Framework of the multimodal bathtub under TCS. 81
5.2 Discretization of the accumulation computation. 84
5.3 Algorithm flowchart. 86
5.4 Update of the credit charging profile from blue to red. 90

5.5 The distribution of the desired arrival times. 91

5.6 Travel time distribution (without TCS). The charging period T_{charges} (30 min) is represented by the green line. 92

5.7 Quality of the SUE: (a) user distribution vs. demand weighted by the logit, and (b) distribution of the relative error between the logit and user distribution over demand. 93

5.8 Total travel cost vs. carbon emissions for different static and dynamic TCS. The numbers are the charge over allocation ratios for the static cases. For comparison, the no TCS case leads to a total travel cost of 2.63×10^6EUR and a carbon emission of 275 t. 94

5.9 Comparison of the static and dynamic TCS for different parameters: (a) credit charge and (b) toll equivalent with respect to the departure time slots. 94

5.10 Evolution of the mode shares and the departure times for (a) solo car, (b) PT, (c) carpool, and (d) total shares. 95

5.11 Effect of the different dynamic TCS of the mean traffic speed: (a) mean car and PT speeds with dynamic TCS ('mid') and without TCS, and (b) mean car speed for the TCS 'cong' and 'emis'. 96

5.12 Variations in departure time normalized by the trip length. A positive value means the traveler starts their trip later with TCS (scenario 'mid') than without. 96

5.13 Distribution of the travel cost gains: (a) normalized by the VoT and (b) absolute travel cost. 97

5.14 Distribution of the benefits of the TCS: (a) trade gains (money earned or spent through the market) and (b) user cost gains. 97

5.15 (a) Mode shift and (b) user cost gains with respect to the desired arrival times. The blue line is the average, and the red lines are the average plus/minus the standard deviation. 98

5.16 (a) Mode shift and (b) user cost gains per distance with respect to trip lengths. The blue line is the average, and the red lines are the average plus/minus the standard deviation. 99

5.17 Comparison of the mean car speeds with and without TCS for the bathtub and trip-based MFD resolutions. 99

5.18 Variations of the objectives measures between the bathtub and trip-based MFD: (a) total travel cost and (b) carbon emission. 100

6.1 A trip between an origin o in region 3 and a destination d in region 1 has three alternatives: RH, PT, or RH till the border i and then PT. . 105

6.2 The two timescales of TCS: drivers' activity and assignment, and credit charge changes by the regulator. 107

6.3 Inter-dependencies between drivers, travelers, and credit market. . . . 107

6.4 Simulation of the day-to-day RH operations. 110

6.5 Driver assignment depending on the evaluation of the marginal gains. . 111

6.6 Departure time distribution of the background traffic and the MaaS customers. 113

6.7 Evolution of (a) the average actual (Act.) RH revenue and its estimation (Est.) and (b) number of active RH drivers. The black dashed lines are the equilibrium values for the corresponding TCS computed with the heuristic method. 115

6.8 Evolution of (a) the credit price and (b) credit balance. The black dashed lines are the equilibrium values for the corresponding TCS. . . 116

6.9 Evolution of (a) the equivalent license prices and (b) the number of RH drivers active in the city center. The black dashed lines are the equilibrium values for the corresponding TCS. 117

6.10 Mode choice evolution: (a) absolute and (b) relative. The reference is the no TCS case. The black vertical dotted lines mark the TCS changes. 118

6.11 (a) Number of active drivers, (b) credit price, and (c) number of license 1 holders when providing a warm start for each TCS change. 119

6.12 (a) Total travel time, (b) travel cost, and (c) driven distance (including pick-up distance). Without warm starts of the credit price. 120

6.13 Total travel time and PT revenue. 120

A.1 Computation of the dot product of the car travel time differences and weighted modal share differences. 129

A.2 (a) Total travel time vs. carbon emissions and (b) toll equivalent for different variations of the PT travel times. The numbers in (a) are the credit charges. 129

A.3 Cost function values vs. computation time for different maximum allowed variations with (a) no TCS; (b) a credit charge of 200 credits; and (c) a credit charge of 300 credits. 130

B.1 TCS-U with different PT penalty distribution: (a) PT distribution; (b) toll equivalent vs. car share; (c) total travel time vs. satisfaction rate; and (d) social cost vs. carbon emissions. 131

C.1 Carpooling shares for the different carpooling penalties. 136

C.2 Total travel time vs. carbon emissions for different static and dynamic TCS. The reference case (no TCS) is also presented. 136

List of Tables

2.1 Comparison of TPS-related works. 14
2.2 Comparison of TCS-related works. 14

3.1 Parameters for CO_2 emission curve for passenger cars. These numerical values are for speeds in km/h and emissions in g/km. 41
3.2 The default parameters used for the simulation. 43
3.3 The credit prices and differences in modal shares at equilibrium for the three scenarios with the demand SC2. 46
3.4 Total travel time and carbon emissions with the two objective functions. 50

4.1 Comparison of the different DMS 63
4.2 Parameters used for the simulation 64

5.1 Comparison of related contributions on TCS 80
5.2 The parameters used for the simulation. 92

6.1 PT mean speeds (m/s) and headtimes (between brackets, min) for the different region OD pairs. 112
6.2 Demand distribution for the different region OD pairs. 113
6.3 Credit charges and introduction day. 114
6.4 Mode shares (%) without TCS and with the last TCS ([40,20,0]) for the different pairs of regions. Red means the mode share decreases with the TCS and blue means it increases. 119

A.1 Summary of parameters notations. 127
A.2 Summary of variables notations. 128
A.3 Other notations. 128

C.1 Summary of parameters and variables notations. 133
C.2 Sensitivity of the carpooling penalty. 136

D.1 Summary of parameters and variables notations. 137

List of Abbreviations

BPR	Bureau of Public Roads
CC	Credit Cap
DMS	Demand Management Scheme
DUE	Deterministic User Equilibrium
MaaS	Mobility-as-a-Service
MCC	Market-Clearing Condition
MFD	Macroscopic Fundamental Diagram
MSA	Method of Successive Average
OD	Origin-Destination
SUE	Stochastic User Equilibrium
TCS	Tradable Credit Scheme
TPS	Tradable Permit Scheme
VoT	Value of Time

Chapter 1

Introduction

1.1 Context and background

Urban mobility is an essential component of the modern economy. The automotive congestion issue was identified more than a century ago by Pigou, 1920. According to Pigou, some markets, such as the road network, are poorly balanced: the individual costs do not account for the negative externalities. A car driver faces some fuel consumption, maintenance, and consumables costs, but the driver does not face the cost of pollution, congestion, noise, and other adverse outcomes. Instead, other individuals (inhabitants and road users) undergo these costs. According to Schroten et al., 2019, the external cost of passenger cars was 565 billion EUR in 2016 in the European Union. This figure accounts for accidents, congestion, and environmental costs. For reference, the EU Gross Domestic Product (GDP) was 14 800 billion EUR (Eurostat, 2017). It means the external costs of passenger cars represent almost 4% of the EU GDP. Furthermore, climate change requires modern society to cut greenhouse gas emissions drastically. Transportation is responsible for a significant share of these emissions, with, between other, the use of private cars. Urban networks are suitable for reducing private car rides as sustainable alternatives exist, such as riding bikes or using PT. A Demand Management Scheme (DMS) encourages car drivers to become PT passengers or bike riders. It can be achieved in two ways: by increasing the car driving cost to compensate for the negative externalities or restricting the use of cars. The first solution is taxing the negative externality to achieve the social optimum. W. S. Vickrey, 1963 proposes a congestion charging scheme that differentiates between on- and off-peak periods. He proposed to fit vehicles with an electronic device to charge the car owner automatically.

In this thesis, we focus on the second option. The idea of rationing access to the road network was proposed a few decades ago by Verhoef et al., 1997. A regulator sets the number of cars allowed to use the road network to ensure an acceptable level of externalities, such as congestion and pollution. In the case of a Tradable Credit Scheme (TCS), credits are distributed for free to each potential traveler. Each travel alternative requires a specific amount of credits. Those credits can be traded between travelers.

TCS effects must be understood before planning a possible implementation in real conditions. The number of credits required for the different travel alternatives is crucial. The more constraining the TCS is, the more travel behavior changes are expected, and the more the traffic state will vary. Quantifying the sensitivity of the objectives, such as total travel time and carbon emissions, with respect to the TCS parameters is a challenging task as it involves the dynamics of the congestion on the

studied network, the travelers' behaviors, and the credits trade. The outcomes of a TCS need to be estimated in a simulation framework to compute the results under different settings and provide a policy a priori fulfilling the regulator's objectives. Deploying a TCS already optimized reduces the need to perform large modifications after deployment to realign the TCS with the city's goals.

This thesis has been pursued in cooperation with the project *DIT4TraM*[1], funded by the European Union's Horizon 2020 research and innovation program under Grant Agreement no. 953783.

1.2 Research objectives and questions

This thesis is built around the following research questions:

- TCS has mainly been investigated by representing the transportation network with static functions or a bottleneck representation. How does the formulation change when introducing a **dynamic representation of the network**? How relevant is the introduction of **trip heterogeneity and congestion dynamics** for evaluating TCS? (Chapter 3)
- Most studies are based on a toy network or academic examples. What impacts can we expect in the case of a **real scenario**? (Chapter 3)
- Some design choices are required to define a TCS. Furthermore, TCS is only one of several possible DMS. What is the effect of being able to **stock** the credits earned one day to use on another day? What is the effect of trip-specific charges? How does TCS perform **against other DMS**? How is a **time-dependent** charging scheme better than a static one? (Chapter 4 and 5)
- How does the TCS affect travelers with **different revenue levels**? (Chapter 5)
- TCS is applied to the travelers, i.e., to the demand side. How could we use TCS to regulate transportation offers? What are the insights of using a TCS to regulate **on-demand services**? (Chapter 6)

1.3 Thesis contributions

1.3.1 Scientific contributions

This research work done during this PhD thesis is articulated around the previous research questions. By addressing them, the thesis provides the following contributions:

- A simulation framework for evaluating TCS with a **trip-based MFD framework** is formulated. The TCS aims at nudging commuters from private cars to transit. The developed method finds the equilibrium. (Chapter 3)
- A realistic scenario is designed for the city of **Lyon** (FR). The TCS is evaluated, compared, and discussed based on this use case. (Chapter 3, 4, and 5)

[1] https://dit4tram.eu/

- TCS is compared against **congestion pricing and license plate rationing**. (Chapter 4). A **time-dependent** TCS is also introduced and compared to the static variant. (Chapter 5)
- The developed framework allows for **equity consideration**. Especially the effect of travelers' revenue on TCS behavior is assessed. (Chapter 5)
- A TCS for **ride-hailing services** is designed, integrated into a simulation environment, evaluated, and discussed. (Chapter 6)

1.3.2 Societal relevance

We use the 17 goals of the United Nations for sustainable development[2] to present the societal relevance of this thesis:

- The decrease of car shares to the profit of PT ridership decreases the exhaust gas emissions. It fits goal 3: *Good health and well-being*, as car use reduction contributes to better air quality, and goal 14: *Climate action* thanks to decreased carbon emissions. As the TCS nudges travelers to more sustainable modes, it also fits goal 11: *Sustainable cities and communities*.
- The reduction of the congestion level reduces the total travel time. It thus reduces commute and transport costs. It fits goal 8: *Decent work and economic growth*.
- The TCS for RH services promotes using RH vehicles as a complementary to PT and not a competition to PT. It thus fits goal 12: *Responsible consumption and production*.

1.3.3 Publication list

Peer-reviewed journal articles

- Balzer, L., & Leclercq, L. (2022f). Modal equilibrium of a tradable credit scheme with a trip-based MFD and logit-based decision-making. *Transportation Research Part C: Emerging Technologies*, *139*, 103642. https://doi.org/10.1016/J.TRC.2022.103642
- Balzer, L., & Leclercq, L. (2022g). Modal dynamic equilibrium under different demand management schemes. *Transportation*, 1–38. https://doi.org/10.1007/s11116-022-10338-0
- Balzer, L., Ameli, M., Leclercq, L., & Lebacque, J. P. (2023). Dynamic tradable credit scheme for multimodal urban networks. *Transportation Research Part C: Emerging Technologies*, *149*, 104061. https://doi.org/10.1016/J.TRC.2023.104061

Peer-reviewed conference proceedings

- Balzer, L., & Leclercq, L. (2022e). Mode shift with tradable credit scheme: a simulation study in Lyon. *Transportation Research Procedia*, *62*, 229–235. https://doi.org/10.1016/J.TRPRO.2022.02.029

[2] https://sdgs.un.org/goals

Conference presentations

- Balzer, L., & Leclercq, L. (2022d). Trip-based MFD model with tradable credit scheme: investigating modal equilibrium. *Transportation Research Board Annual Meeting*
- Balzer, L., & Leclercq, L. (2022a). Mode share equilibrium with tradable credit scheme and license plate rationing. *Symposium of the European Association for Research in Transportation (hEART)*
- Balzer, L., & Leclercq, L. (2022b). Mode share equilibrium with tradable credit scheme over different time cycles. *Triennial Symposium on Transportation Analysis (TRISTAN)*
- Balzer, L., & Leclercq, L. (2022c). Tradable credit scheme: an alternative to license plate rationing and congestion pricing to foster modal shift. *Transportation Research Arena*
- Balzer, L., Provoost, J., Leclercq, L., & Cats, O. (2022). Tradable mobility credits and permits: state of the art and future research directions. *Transportation Research Arena*
- Balzer, L., Ameli, M., Leclercq, L., & Lebacque, J.-P. (2022). Tradable Credit Scheme for Multimodal Urban Networks. *Symposium on Management of Future Motorway and Urban Traffic Systems (MFTS)*
- Balzer, L., Ameli, M., Leclercq, L., & Lebacque, J.-P. (2023). Modeling Tradable Credit Scheme for Multimodal Urban Networks with Departure Time: a Bathtub Approach. *Transportation Research Board Annual Meeting*

Working papers

- Balzer, L., Provoost, J., Leclercq, L., & Cats, O. (2021). *Tradable mobility credits and permits: state of the art and concepts-Deliverable D4.1-Project DIT4TraM* (tech. rep.). https://dit4tram.eu/downloads/

1.3.4 Thesis outline

The thesis is divided into seven chapters. The thesis structure is summarized in Fig. 1.1.

Chapter 2 sets the scope of this thesis. It reviews the different TCS proposed in the literature, describes the traffic representation adopted for this thesis, and introduces the case study of Lyon to illustrate the proposed TCS in a real scenario.

In chapter 3, a uniform TCS nudges commuters to ride transit instead of driving their personal car. The travel times are computed with the trip-based MFD. An ad-hoc gradient-based framework computes the mode choices and the credit price for the SUE. The TCS parameter: the number of credits needed to drive a car is optimized to reduce total travel time and carbon emissions.

Chapter 4 extends the previous chapter to evaluate and compare different DMS. The SUE is computed over several days to account for credit validity of several days, meaning the credit of a day can be used on another day. The proposed TCS and TPS

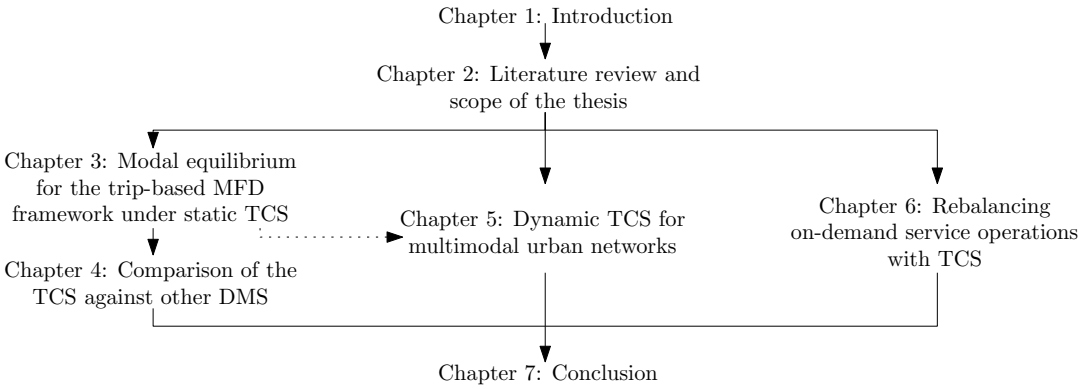

Figure 1.1: Structure of the thesis.

are trip-specific to account for the service level of each trip's transit alternative. The extended framework permits a comprehensive comparison of TCS against congestion pricing, LPR, and TPS. The evaluations are based on environmental, economic, and social aspects of the DMS.

Chapter 5 goes deeper into the evaluation of the TCS for a dynamic congestion framework. The travelers choose their departure times on top of the mode choices. Carpooling is proposed on top of the car and PT. The PT speeds depend on the congestion level. The credit charge is departure-time-dependent. These extensions of the study require a modification of the framework to accommodate the additional degrees of freedom.

The competition between RH and PT services is addressed in chapter 6. The proposed TCS changes the traffic management perspective: the transportation offer is regulated instead of the demand. This final chapter proposes a TCS to nudge RH drivers to operate in the suburbs instead of the city center, where the transit offer is satisfying. It promotes a cooperative operation of PT and RH, where travelers board an RH vehicle in the suburbs and then switch to transit in the city center.

Chapter 7 concludes the thesis. The main results are summed up. Future research directions are also presented.

Chapter 2

Literature review and scope of the thesis

This thesis deals with the control of traffic by economic measures. This chapter sets the scope of the thesis with respect to the existing literature. The first section defines the different DMS proposed in the scientific literature. The second section details the traffic representation we adopted and the reasons behind this choice. The last section of this chapter presents the case study of Lyon we use to illustrate the methodology developed in chapters 3, 4, and 5.

2.1 Demand management policies

This section is an updated version of deliverable 4.1 for the EU project Horizon2020 DIT4TraM (Balzer et al., 2021).

Urban mobility faces challenges in terms of congestion, pollution, and sustainability. Transportation networks are not optimally loaded, as the transportation modes, routes, and departure times of travelers are chosen according to their individual needs and desires, which currently lacks coordination. This leads to a user equilibrium, which typically deviates from the system optimum, i.e., the optimal use of the transportation network with regard to collectives goals. Consequently, users undergo from sub-optimal travel conditions, e.g., longer travel times, and the society suffers from the negative traffic externalities, e.g., pollution. To improve social welfare and reach the social optimum, suitable institutions can require or help to redistribute (or reduce) travel demand in space or time. This process is called 'demand management'. The objective of this thesis is to develop, simulate and compare demand management strategies that are based on the novel concepts of tradable credit and tradable permit schemes (TCS and TPS). By rationing and increasing or decreasing the cost of some travel behaviors, demand management schemes foster the re-distribution of the travel demand other the different alternatives. The latter is designed to achieve a reduction of the negative externalities (e.g., delays, small passenger occupancy, pollution, or costs) of multi-modal transportation networks. In this chapter, we provide an overview of the state-of-the-art literature on tradable credit and permit schemes. We compile, characterize and synthesize scientific contributions related to TCS and TPS. Both aspects of proposed policies of the travel supply and demand are investigated. Other demand management policies are succinctly presented to put TCS and TPS into perspective. The literature review explicitly identifies some gaps, both in terms of policies and traffic and demand representations.

2.1.1 Concepts

When using economic measures to induce changes in the usage of road networks, two alternatives exist. The first is price-based management, in which payments are required to access infrastructure. The authority determines the price (i.e., toll) of specific segments. The extent of infrastructure usage is not restricted, but as the travel costs of some alternatives increase, travelers shift to other options in time, space, or mode. The second option concerns quantity-based measures. With this form of demand management, the usage levels on the network(s) are fixed using mobility rights (Verhoef et al., 1997). The users are given an initial allocation of those rights and may trade them amongst themselves. The price of those rights results from the trading between the users rather than being set by the authority, as is the case for congestion pricing. By letting the users trade the mobility rights, this form of demand management is mainly decentralized. There is no money exchange from the users to the authority, as the travelers are exclusively buying and selling mobility rights from and to other travelers. The regulation of those mobility rights can help the system reach states with a smaller price of anarchy. At the time of writing, quantity-based schemes have not been implemented yet for traffic management purposes. However, they are currently used to reduce the carbon emissions of some industries. The EU Emissions Trading System (ETS) (Bayer & Aklin, 2020) is a framework in which large polluting companies spend a credit for each ton of carbon dioxide released into the atmosphere. Generally, the quantity-based measures that have been proposed in the literature can be categorized as permit or credit-based schemes. However, the concepts of tradable credits and permits are not used consistently in the existing literature. In the following sections, we propose definitions for credit and permit schemes that correspond as much as possible to the available state-of-the-art contributions regarding quantity-based demand management.

Tradable credits

In the TCS, credits are a commodity needed to access the transportation network. The credits are indifferentiable (e.g., like currency units): we cannot distinguish one credit from another as they have the same value and are used similarly. However, the number of credits needed to access the transportation network may depend on the chosen route, departure time, and transportation mode. An initial number of credits is distributed, equally or not, among eligible travelers. These credits can be sold and bought amongst the travelers through a trading mechanism without the interference of a central authority. The distribution scheme can account for the travelers' heterogeneity and ability to buy credits or flexibility (like low-income travelers or workers not able to telework). Yang and Wang, 2011 formalized an early mathematical framework for TCS. Now, in most available works, the interval of credit assignment is a day, while only a few contributions investigate the possibility of credits being transferred to the next day. In Ye and Yang, 2013, the credits are allocated for a span of several days, and the price is updated each day based on the number of credits still available. Y. Tian and Chiu, 2015 define consumption periods for the TCS, at the end of which the users need to balance their credit account by using the credit market. If they fail, they need to fill the gap by buying credits at a high price from the authority. In Guo et al., 2019, the charges and the allocation are updated between each period. The contributions of Miralinaghi and Peeta, 2016, 2018, 2019, 2020 consider the transfer of credits to a different period. The different frameworks presented in the works of

Miralinaghi & Peeta account for interest rate (inflation), switch to greener personal cars via advantageous credit charges, and future price perception.

Tradable permits

The TPS is similar to a credit scheme in the sense that it allows access to the transportation network. However, in contrast to credits, permits are specific to a link and a timeslot. After an initial allocation, the users can trade the individual permits. As the permits do not provide the same access to the network, there is one price and one market for each individual permit. In this review, we also consider some schemes where no trading of permits takes place between users. Instead, the permits are auctioned by the authority. In comparison to TCS, there are fewer contributions regarding TPS in the literature. TPS has been formalized by Akamatsu, 2007 for a single Origin-Destination (OD) pair and by Akamatsu and Wada, 2017 for several OD pairs in a network of links. For using a given link at a particular time, the user needs to buy a corresponding permit. To avoid queuing at bottlenecks, the number of issued permits per time unit equals the link capacity. W. Liu et al., 2014 regulate a bottleneck with expirable parking permits to encourage users to arrive earlier and reduce queuing. P. Wang et al., 2018 propose a TPS for a network of links represented by flow-dependent travel time (BPR) functions, while accounting for a transit alternative. The permits are OD-based, while their quantity is selected to minimize the overall system cost. We summarize the global framework of TCS and TPS in Fig. 2.1.

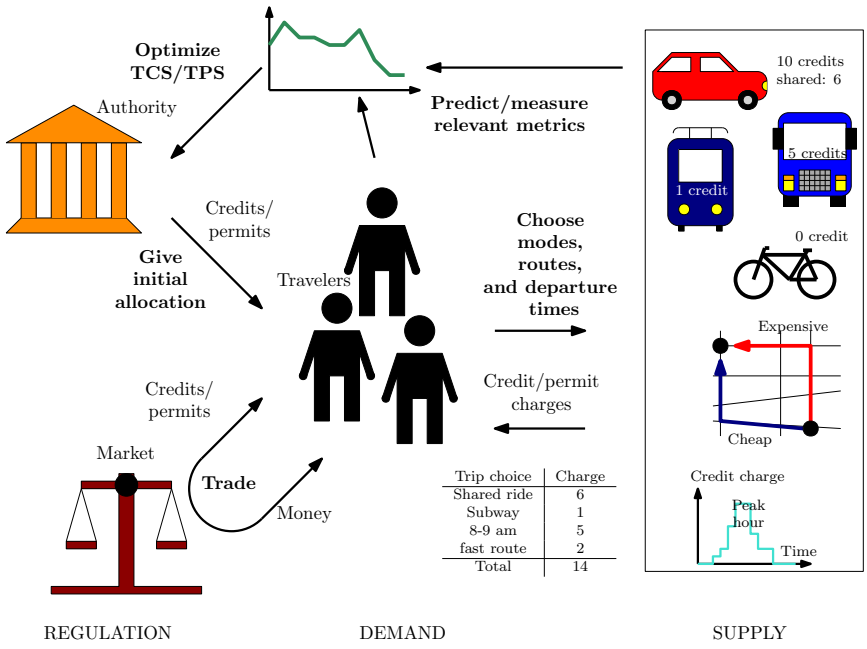

Figure 2.1: Traffic demand management with TCS and TPS.

The regulating authority gives the initial allocations of credits and permits. Travelers trade credits and permits between themselves. Depending on their travel choices, they spend credits or permits, some alternatives being more expensive than others. Some relevant metrics are used to quantify the effect of TCS or TPS and optimize them.

2.1.2 Objectives

When introducing TCS, the main objective is to reduce externalities generated by transport, particularly those induced by congestion. The total travel time, i.e., the sum of travel times of all travelers acts as a metric for the social cost of congestion. When considering the departure time problem and the fact that users need to be at their destination at a given time, the "total schedule delay" is used. This is typical for the morning commute case: on top of the travel time, the users experience a disutility if they arrive earlier, and a usually higher one if they arrive later (Arnott et al., 1990). The environmental externalities of congestion are addressed by accounting for the emission of greenhouse gases and toxic emissions or by quantifying the change in the total fuel consumption. The social and political aspect is considered by defining and measuring the equity of the TCS. Already without any demand management policies, the travelers have different travel costs. On top of that, the TCS or TPS might profit some travelers at the expense of others. One needs to choose between equity in the sense of results, i.e., the absolute travel costs are similar for all travelers, or in the sense of opportunities, i.e., the improvement of travel costs is the same for everybody. The challenge is to account for the different OD pairs and revenue levels.

2.1.3 User behavior

Different behavioral responses are used to drive the user equilibrium closer to the social equilibrium and attain the political goals regarding congestion, pollution, and equity. This leverage can be achieved among various travel modes, such as private cars, public transportation, and shared mobility forms. The common denominator between these modes is that congestion, pollution, and equity issues can persist, and that capacity is limited, whereby the same principle of leveraging behavioral response (by means of TCS and TPS) can be applied. Travelers will be stimulated to change their departure times by introducing a time-varying credit charge or permits with a specific time window as it becomes more expensive to drive or use public transportation during peak hours. The road network is spatially heterogeneous: some links are overused, while others are underused. The same phenomenon occurs for public transportation, as vehicles on certain lines can become overcrowded, and the capacity of the service network can be exceeded. By charging the links or the areas differently, the users change their routes, and the demand can be better distributed over the network. Public transportation and shared mobility are often underutilized because travel time is longer and may involve walking and waiting as compared to a private car with a single occupant. Furthermore, passenger comfort is generally lower. By charging the user of privately owned cars, some users may shift to public transportation or share travel costs by ride-pooling/ridesharing. Differentiated charging schemes are introduced to foster the usage of different types of private cars, such as zero- or low-emission, or autonomous vehicles. As the travel costs of some trips change with the introduction of a demand management scheme, the demand might vary with the travel costs. Thus, some contributions consider the travel demand as elastic. If the travel cost decreases, additional travelers will switch to a given mode, and if it increases, some users will cancel their trips or use alternative travel modes.

2.1.4 Charging scheme

The charging scheme is usually variable, i.e., non-constant and dependent on several parameters. It provides freedom to the authority to stimulate road users to change their choices in a direction suitable to the respective goals. Previous work has considered different parameters, on which the credit charges are based, including:

Link: the charge is the sum of the charges of the links used during the trip (Yang & Wang, 2011).

Time: the credit charge is dynamic in the temporal domain (Nie & Yin, 2013).

Distance: the charge is proportional to the traveled distance (Shirmohammadi et al., 2013).

Area: the charge is fixed for all users in a given area (Shirmohammadi et al., 2013).

Class: the credit charge or allocation depends on the class of the user, usually its value of time (VoT) as a proxy for its wealth. In F. Xiao et al., 2013, the poorer users get more credits to compensate for their travel time increase.

Vehicle: the charge depends on the type of vehicle. In Miralinaghi et al., 2019, low emission vehicles require a lesser charge to foster them against conventional (ICE) vehicles.

Negative charge: the charge can be negative, to work as an incentive. In F. Xiao et al., 2019, negative credits charges on some links replace the initial allocation. All of the above-mentioned studies have been limited to car traffic.

2.1.5 Experiments

No full-scale TCS has been implemented yet. However, several aspects have been independently studied using field experiments, serious games, or surveys. Ettema et al., 2010; Knockaert et al., 2012 present the results of a peak avoidance experiment in The Netherlands: car drivers receive money when they do not drive during the peak hour. During the experiment, car usage decreased. However, most car drivers resumed commuting by car when the incentives stopped. The incentives need to be continued to maintain the peak hours avoidance. It poses an issue about the sustainability of such a scheme, since one would constantly need funds to finance the incentives. The MOBIS experiment in Switzerland introduced a Pigovian pricing scheme (Axhausen et al., 2021). Each participant pays a tax corresponding to the external cost of its travel. It represents the costs of one's travel decision undergone by the rest of the society (congestion, pollution, and health). The Pigovian tax increased the private costs by about 16% and reduced the external cost by 5%. Different serious games have been proposed. The participants react to a fictive TCS via a computer-based interface. In the experimental game of Aziz et al., 2015, the participants choose routes subject to personal mobility carbon allowances. They trade those allowances on a multi-unit double-auction market. The participants are learning from the system and improving their usage of the carbon allowances. In Dogterom et al., 2018, a distance-based TCS is set up. Here, the participants have an initial quota of kilometers per car allowed. They can reschedule their activities or change mode to decrease the usage of their credit. Additionally, they can sell the remaining credits or buy additional ones at a fixed

price. The results of the experiments show that about two-thirds of the participants change their car use. In Y. Tian et al., 2019, another experimental game is proposed, where participants have credits and money budgets. They choose their routes and trade with a multi-unit double-auction market. From the experiments, it emerges that participants are spending more credits in the beginning, after which they start saving some credits for later use. The authors also noticed a learning behavior as the number of satisfied bids and asks increased over time. Brands et al., 2020 conducted an experiment with participants regarding parking permits. The scenario that the authors selected is the following: participants need to park their car downtown. To do so, they have to secure parking permits that they can buy and sell daily. Permit prices fluctuate on a daily basis as well. If they fail, they will face a monetary penalty. The outcomes showed that most of the decisions were rational, while participants with higher levels of education tend to earn more money from the trade than others. This implies concerns about the equity of such a scheme. Other contributions are based on surveys to assess the public reaction to a TCS and the population's preferences between TCS and the more common congestion pricing. In Krabbenborg et al., 2020; Krabbenborg et al., 2021, the acceptability of TCS is investigated. A survey is used to understand the reasons behind the acceptability, and a case study with a fictive city is introduced to compare pricing and TCS. In the survey, public support varies from 30% to 50%, depending on how the credits are initially distributed . The highest level of support occurs when the credits are uniformly distributed among car users. The majority of the participants of the case study rejected the TCS: only 20% accepted the TCS, while 56% agreed with the congestion pricing. One essential argument is that congestion pricing has already been successfully implemented in the real world. Hence, it is argued that there is no need for the complexity of another scheme such as TCS. The results of this study highlight the importance of the user experience and the communication of the advantages of TCS and TPS, especially compared to congestion pricing.

2.1.6 Models and solutions methods

TCS and TPS contributions from the literature mainly focus on finding the system equilibrium, i.e., the traffic assignment under the TCS or TPS, and comparing it with the status quo case. The majority of past works, such as Yang and Wang, 2011, are then developing methods to find the TCS and TPS parameters that minimize the sum of the costs for all users. Different assumptions are made for the analytical formulations and numerical simulations. The conditions under which the credits and permits are traded as well as the representations of the traffic supply and demand are categorized. In the following sub-sections, underlining the common features and differences of the contributions on TCS and TPS.

Market settings

Most of the literature does not make explicit that the trade mechanism and the credit price are determined by a market-clearing condition (MCC): the price is non-zero if and only if all the credits are consumed, like in Yang and Wang, 2011. It is assumed that the users trade between themselves, but the exact mechanism is not specified. In Ye and Yang, 2013, the authority updates the credit price over the days, depending on the difference between credits consumption and allocation. In W. Liu et al., 2015; Su and Park, 2015, the permits for using the highway are auctioned. The travelers bidding

the highest amount of money are buying the permits. The contribution of Y. Tian and Chiu, 2015 focuses on the trade of credits using a double-auction market and how the marginal value of the credits depends on the travelers. In a double-auction market, each player (here, the potential traveler) enters the market to buy or sell credits with a chosen quantity and price, after which the market mechanism maximizes the number of credits traded. Several contributions account for transaction costs. They represent either a tax or a valuation of the effort (time and energy) spent to trade credits in order to prevent speculation and market abuse. Nie, 2012 introduced transaction costs proportional to the traded quantity. In Bao et al., 2014, the transaction costs are linearly proportional to both price and traded quantity. The transaction costs in Zhang, Lu, Hu, and Liu, 2021 are a constant, multiplied by the traded quantity to a power that is equal to or greater than one. It represents the fact that, by increasing the traded quantity, the difficulty to find trading partners increases.

Demand representation

The equilibrium is usually defined by the Deterministic User Equilibrium (DUE): no user can unilaterally improve its travel cost by changing mode, departure time, or route. In Yang and Wang, 2011, TCS is implemented, while assuming DUE. Some contributions account for Cournot-Nash players (CN) to represent transportation companies: a CN player (here a potential traveler) cooperates with other players from the same entity (usually a company) to minimize the entity's costs and not its individual costs, for instance in He et al., 2013. The Stochastic User Equilibrium (SUE) accounts for perception errors. It is reached when the decisions of the users match their current affectation. The decision model is often the logit. The probability of choosing an alternative depends on the travel cost of this alternative compared to the costs of the other options. In Ye and Yang, 2013, TCS is implemented while assuming SUE. Under a TCS or TPS, the users are selling or buying credits or permits to reduce their travel time. The parameter named Value of Time (VoT) is defined to quantify the amount of money a user is ready to pay to reduce its travel time. Some contributions account for different VoT to represent different types of users and especially travelers with different revenues, to differentiate the impact of the TCS on low-income and high-income travelers. In X. Wang et al., 2012, the TCS accounts for VoT heterogeneity, as the credit charge depends on the class of the traveler. Human behavior is often suboptimal. The following biases are known:

Loss aversion: travelers selling credits are earning money, and those buying credits are losing money. Under loss aversion, the users value the money they lose more than the money they earn (Bao et al., 2014).

Cognitive illusion: the travelers do not consider the cost of spending credits as long as the number of spent credits does not exceed the allocation (Han & Cheng, 2016).

Perception error: As both, the supply and demand affect the credit price, its value is uncertain. Therefore, travelers are prone to random errors when predicting the credit price (Zhang, Lu, & Hu, 2021b).

Framing and labelling: users are more eager to spend the credits from the allocation (which are provided for free) than additional ones they need to buy on the market (Bao et al., 2016). The difference to cognitive illusion is that,

even if they do not need to buy additional credits, they still consider the cost of spending the credits they got for free.

Comparison of TPS contributions

The different contributions about TPS for traffic management are summarized in Table 2.1. For each contribution, we check which behavioral response is considered along with the supply representation. The letter 'E' means the model accounts for elastic demand without explicitly considering different transportation modes.

Table 2.1: Comparison of TPS-related works.

Reference	Congestion model	Mode	Route	Departure time
Akamatsu, 2007	Vickrey	E	✓	✓
Akamatsu and Wada, 2017	Vickrey		✓	✓
Lessan et al., 2020	Vickrey			✓
W. Liu et al., 2015	Vickrey			✓
W. Liu et al., 2014	Vickrey	✓		✓
Sakai et al., 2015	Vickrey		✓	✓
Shirmohammadi and Yin, 2016	Vickrey			✓
Su and Park, 2015	MATSim		✓	✓
Wada and Akamatsu, 2013	Vickrey		✓	✓
J. P. Wang et al., 2018	BPR	✓	✓	
P. Wang et al., 2018	Vickrey			✓
L. L. Xiao, Liu, and Huang, 2021	Vickrey	✓		✓
Sakai et al., 2017	Vickrey			✓

Most TPS frameworks use a fixed-capacity bottleneck to represent the congestion. The leverage of the TPS is then changing the departure time distribution. The number of emitted permits per bottleneck is equal to the capacity for time periods, which prevents the formation of queues. One paper deals with the BPR functions. In this paper, the authors optimize the number of emitted permits to minimize the total travel time. The representation and investigation of the route and mode choices are under-represented.

Comparison of TCS contributions

Relevant contributions on TCS are compared in Table 2.2. It compares the behavioral responses taken into account and considers emissions of pollutants, transaction costs, and human biases.

Table 2.2: Comparison of TCS-related works.

Reference	Mode	Route	Departure time	Emission	Transaction cost	Human biases
Bao et al., 2016	E	✓				Framing and labeling
Bao et al., 2014		✓			✓	Loss aversion

Bao et al., 2017	E	✓				
Bao et al., 2019			✓			
Chen et al., 2016		✓				
de Palma et al., 2018	✓	✓				
Gao and Hu, 2015	✓					
Gao, Liu, et al., 2019		✓				
Gao, Liu, et al., 2019		✓				
Gao and Sun, 2014		✓		✓		
Gao et al., 2018	✓					
Gao et al., 2016	✓					
Guo et al., 2019	E	✓				
Han and Cheng, 2016		✓				Cognitive illusion
Han and Cheng, 2017		✓				
He et al., 2013		✓			✓	
Jia et al., 2016			✓			
Jiang et al., 2017		✓				
Li and Gao, 2014		✓				
Lian et al., 2019		✓			✓	
Miralinaghi and Peeta, 2018	E	✓		✓		
Miralinaghi and Peeta, 2016	E	✓		✓		
Miralinaghi and Peeta, 2019	✓	✓		✓		
Miralinaghi and Peeta, 2020		✓		✓		Loss aversion
Miralinaghi et al., 2019			✓			Loss aversion
Nie, 2015			✓			
Nie, 2012	E	✓			✓	
Nie, 2017b	✓					

Nie and Yin, 2013	✓	✓	✓			
Seilabi et al., 2020	✓	✓				
Shirmohammadi et al., 2013	E	✓				
L. J. Tian et al., 2013	✓		✓			
G. Wang et al., 2019		✓				
G. Wang et al., 2014b		✓				
G. Wang et al., 2014a		✓				
G. Wang, Li, et al., 2020	E	✓				
G. Wang, Xu, et al., 2020	E	✓		✓		
X. Wang and Yang, 2012	E					
X. Wang et al., 2014	E	✓				
X. Wang et al., 2012	E	✓				
H. Wang and Zhang, 2016		✓				
Z. Wu et al., 2020	✓	✓			✓	Loss aversion
D. Wu et al., 2012	✓	✓				
L. L. Xiao et al., 2015	✓		✓			
F. Xiao et al., 2019		✓				
F. Xiao et al., 2013	✓					
Xu and Grant-Muller, 2016	✓					
Yang and Wang, 2011	E	✓				
Ye and Yang, 2013		✓				
Zang et al., 2020	✓	✓				
Zang et al., 2018	✓	✓				
Zhang, Lu, and Hu, 2021a	E	✓			✓	
Zhang et al., 2020	✓	✓				

Zhang, Lu, and Hu, 2021b	E	✓			Perception error
Zhang, Lu, Hu, and Liu, 2021		✓		✓	
Zhou et al., 2020	✓				
W. Zhu et al., 2017		✓	✓		

Most of the proposed TCS methods in the scientific literature leverage the route choice and represent the congestion with a network of BPR functions. The mode choice is often only indirectly considered via elastic demand, and the departure time problem is under-represented. Only a few papers account for the vehicles' emissions, as most of them only focus on minimizing the total travel time or its monetary equivalent. Human biases in transactions are sometimes considered, but the majority of publications assumes that trade induces no costs and that users are perfectly rational. In Nie, 2012; Shirmohammadi et al., 2013, the authority sells additional credits at a fixed and relatively high price on top of the distribution the initial allocation for free. In case the demand for car travel is huge, the credit price rises until it reaches the authority price. At this point, the travelers directly buy credits from the authority. In this framework, a traveler can always travel with any mode anytime on any route, even if it can be expensive and the credit price is bounded. This framework can be interpreted as a hybrid between TCS and congestion pricing: the credit cap can be violated when there is a relatively large need to drive personal cars or prevent the credit prices from becoming too high. In a more decentralized framework, the credits are not given by the authority, but earned by car drivers traveling off-peak (Nie, 2015) or by using alternative routes (F. Xiao et al., 2019; W. Zhu et al., 2017). The authority does not determine the number of credits, but only chooses which behaviors lead to a loss or gain of credits.

2.1.7 Position compared to other demand management schemes

TCS and TPS are not the only policies relative to demand management. To provide some context and references, we now compare some relevant contributions in terms of demand management for traffic regulation: urban tolls, license plate rationing (LPR), and peak-avoidance incentives.

Road pricing

Congestion pricing was proposed for several cities and implemented in some (Bhatt et al., 2008; Croci & Douvan, 2016; Eliasson, 2014; Gu et al., 2018). In the following, we list some examples of implementations:

- Singapore is the earliest city in 1975 with the Area License Scheme: a paper to show on the windshield. In 1998, it was replaced by the Electronic Road Pricing replaced. The toll is time- and space-specific: the charging rate changes every 30 minutes, and an embedded device records when tolling gates are crossed.
- In London, a Congestion Charge was introduced in 2003 with a fixed price per day. CCTV reads the plate numbers, which are automatically processed.

- In Stockholm, an urban toll was implemented in 2007 after a previous experiment in 2006. The cordon-based toll is active during peak hours and changes every 30 minutes. Plate numbers are read and processed automatically as well.

Other major cities had projects for the implementation of urban tolls, which were discarded, for instance, in New York City and Hong Kong (Gu et al., 2018). The advantages of congestion pricing are that the approach is relatively simple to apply and its implementation in different cities proves the pertinence of this policy. The urban tolls generate additional revenue for the city council to fund the infrastructure and administration necessary for applying and enforcing the policy. Its drawbacks are that it is perceived as another tax for car drivers on top on fuel tax and license registration, and it penalizes low-income inhabitants more than high-income ones. TCS and TPS address both aspects, since the money flow stays between the citizens, and part of the credit/permit consumption is already covered by the initial allocation.

License plate rationing

Different cities implement license plate rationing (LPR) occasionally to curb traffic emissions during pollution peaks. With LPR, cars are allowed to drive on a given day according to their plate number. In the typical implementation of the LPR, cars with odd plate numbers can drive every second day and cars with even plates every other day only. Some vehicles are exempt from the policy, usually low-emissions ones. In Nie, 2017a, 2017b, the author argues that LPR is ineffective because it fosters purchasing a second car to circumvent the policy. He presents TCS as a good alternative. Goddard, 1997 takes the case of Mexico City as an example to underline the perverse effect of the LPR (named Non-Driving Day in the paper). As it encourages inhabitants to buy a second car in the long term, more cars than before and higher exhaust gas levels were observed in the streets. Though the method is fast and simple to implement, it is the least flexible policy and does not account for the real utility of driving a car. In a TCS or TPS, a traveler who needs to drive a car on a specific day is likely to secure enough credits/permits by bidding a high enough price. With a policy based on LPR, this traveler would be forced to find an alternative or face a fine.

Peak avoidance incentives

Incentives have been proposed in the literature as an effective method for demand management. Multiple incentive-based frameworks have been proposed to foster changes in travel behavior, aiming to shift demands away from car traffic peak hours (Ettema et al., 2010; Fahrioglu & Alvarado, 2000; Hu et al., 2015; Knockaert et al., 2012; C. Zhu et al., 2015) or encourage the use of more sustainable travel modes (de Kruijf et al., 2018). The authors argue that incentives may be a more popular policy instrument than traditional taxation methods. However, in comparison to taxation methods and permit/credit schemes, the costs to financially compensate drivers are expensive for authorities. Also, the approach arguably does not ensure an equitable pay-for-use policy, as people who already traveled outside the rush hour are not fairly compensated, even though they already showed the desired behavior before the system was implemented. In TPS and TCS, there is no money flow from the authority to the travelers, which results in lower costs for authorities and a fairer distribution of charges among all travelers.

Perspectives

In this literature review, two demand management schemes were compared: Tradable Permit Scheme (TPS) and Tradable Credit Scheme (TCS). The main difference is the flexibility of the mobility schemes. The literature mainly focuses on TCS. Most contributions do not make explicit the market mechanism as they only focus on the assignment at equilibrium. The first gap identified in the literature is the representation of traffic. Congestion models are usually based on Vickrey bottleneck or BPR function. They are relatively simple (with fixed capacity and static travel times). They allow to derive properties feeding analytical discussions. It is questionable, however, if such a representation is sufficient to prepare for real-life implementations. The second gap concerns mode changes during a trip. In most publications, private car travel has been at the center of attention of the proposed schemes. Some works consider public transport or carpooling as a potential mode shift, but research is lacking with regard to comprehensive, mode-agnostic schemes. A TCS or TPS would arguably be more interesting, if different transport modes could be combined, such that demand can be shifted to other modes, where capacity is not saturated. Some contributions account for different modes, but only a few allow the users to change modes during the trip. Thus, inter-modality is usually lacking: a traveler might drive its car to a park-and-ride facility, take a train and finish its trip with a shared bike.

The literature lacks simulation of TCS and TPS for a real city, even though it is necessary to get a more precise estimation of the effects of the TCS. Most of the contributions use relatively standardized or straightforward networks as use-cases (e.g. Sioux Falls or Nguyen-Dupuis).

Our review supports the plan of extending the numerical and analytical discussions at the equilibrium for different TCS and TPS, using large-scale dynamic congestion simulation environment. It is the main focus of the thesis.

2.2 Traffic representations

This section is built upon parts from Balzer and Leclercq, 2022f and Balzer, Ameli, Leclercq, and Lebacque, 2023.

The review of the work on TCS led us to identify some gaps in the literature regarding the representation of the transportation network when evaluating TCS and other DMS. Assessing the effect of a TCS in a city gives requirements regarding the congestion representation:

- It needs to be **large-scale** to encompass the whole city and not only a few streets.
- As the policy affects the demand, the demand distribution changes. Departure times and trip lengths are expected to vary. The traffic representation needs to account for the **traffic dynamics** and the **trips heterogeneity**.
- It is always preferable to have a simulation framework that is **fast to compute**.

2.2.1 Discussion of traffic representation from the literature on TCS

Most of the literature about TCS represents the congestion using the BPR function (Bureau of Public Roads, 1964). Each link is represented by a static function where the travel time depends on the traffic flow. It is fast to compute and represents a large area. Its explicit analytical formulation makes it suitable for deriving properties such as the existence or uniqueness of the equilibrium under TCS. It, however, fails to account for traffic dynamics, as the travel time function does not account for the departure time distribution.

Another widespread model for congestion management is Vickrey bottleneck (Arnott et al., 1990; W. S. Vickrey, 1969). The road is assumed to be of fixed capacity, and demand exceeding the capacity is stacked into a vertical queue. It is fast to compute, accounting for variation in the departure time distribution. It also allows for extensive analytical discussions regarding the equilibrium under congestion pricing or TCS. In 1991, Vickrey relaxed the fixed capacity assumption (W. Vickrey, 2020) (work published posthumously) with a new model, named the *classical bathtub model*. The main idea is to define the network as an undifferentiated movement area with a mean speed function. The mean speed is defined as a function of network density and network characteristics (Arnott, 2013; Fosgerau & Small, 2013). Therefore, the network speed decreases as demand increases. These extensions, however, still fail to represent the trip heterogeneity.

A small part of the works uses traffic simulators: DynusT in Y. Tian and Chiu, 2015 and MATSim (Axhausen, 2016) in Su and Park, 2015. It allows for a realistic and complex representation of congestion and assignment. However, analytical discussions are limited. As there is no mathematical description of the congestion, properties such as optimal parameters, existence, uniqueness, or stability of the equilibrium under TCS or TPS cannot be analytically proven. They tend to require significant computational power to compute a scenario. This can be an issue when searching the state of the transportation system at equilibrium or optimizing the TCS.

2.2.2 Macroscopic Fundamental Diagram

We choose to represent the traffic mechanics with the MFD in this thesis. It is designed to represent the traffic conditions of a large network (typically a city) at a macroscopic scale. As the current congestion level depends on the instantaneous number of vehicles on the network, departure time distribution is accounted for. The travel demand can be represented as agents with different trip lengths. It allows for the study of the heterogeneity of the trips. Even if the analytical formulation of the MFD is not explicit as the BPR function or Vickrey model, it still allows for some discussion on the existence and unicity of the equilibrium in chapter 3. The computational effort is low enough to perform iterative simulations.

This section provides a summarized description of the MFD framework to cover the knowledge required to read this PhD thesis. We refer to Mariotte, 2018 for more details. Relationships between mean speed and density for urban networks were formulated in Godfrey, 1969 and Mahmassani et al., 1984. Daganzo, 2007 introduces the MFD concept to formalize congestion dynamics while keeping the network still tractable at a large urban scale. The studied network is split between regions, and the speed in each region is assumed to be spatially homogeneous. Only the one-region case is presented in the following. For multi-reservoirs scenario, see Mariotte and

Leclercq, 2019. The network outflow or speed depends on the accumulation. The instantaneous speed on the network V is a function of the accumulation n, i.e., the number of vehicles driving in the network. The dynamics of the accumulation follows

$$\dot{n} = \dot{n}_{in} - P(n)/L, \tag{2.1}$$

$\dot{n}_{in}$ the rate of trip generation, L the typical trip length, and $P(n)$ the production. The production (vehicle times distance over time) is linked to the speed by

$$P(n) = nV(n). \tag{2.2}$$

Leclercq et al., 2017; Mariotte et al., 2017 introduced the trip-based MFD to consider any trip length distribution. The mean speed is a function of vehicle accumulation, which is the key state variable of the classical bathtub and MFD models. Lamotte and Geroliminis, 2018 described a numerical resolution method to compute the departure times distribution at equilibrium. Jin, 2020 introduced an extension for the classical bathtub model, named *generalized bathtub*. The author presented a numerical framework for computing travel times. The key state variable is the distribution of the remaining trip lengths of the travelers, which was also introduced in Lamotte and Geroliminis, 2018. However, departure time optimization was not addressed. Recently, Ameli et al., 2022 applied the Mean Field Game theory to compute the deterministic user equilibrium, and Lebacque et al., 2022 computed the Stochastic User Equilibrium (SUE) for the generalized bathtub model.

The travel time T_i of a traveler with a departure time t_d, mode m, and trip length l_m is computed by integrating the MFD speed over the time the traveler evolves in the network:

$$l_m = \int_{t_d}^{t_d+T_i} V_m\left(\{n_m(s), m \in \mathcal{M}\}\right) \mathrm{d}s. \tag{2.3}$$

$\mathcal{M}$ is the set of possible travel modes (typically cars or public transportation), and n_m is the accumulation of mode m.

The travel times can be calculated using the virtual traveler introduced in Lamotte and Geroliminis, 2018. We follow the trajectory of a fictional traveler who enters the network at the origin of time and stays there indefinitely. We define $t \mapsto z_m(t)$ the traveled distance of the virtual traveler for mode m as a function of the time, and $s \mapsto n_m(s)$ the accumulation as a function of the traveled distance. The travel time of a traveler is computed by:

$$T_i = \int_{z_m(t_d)}^{z_m(t_d)+l_m} \frac{1}{V_m\left(\{n_m(s), m \in \mathcal{M}\}\right)} \mathrm{d}s. \tag{2.4}$$

In this thesis, we assume that the speeds on the network are always greater than a minimal speed $V_0 > 0$ to avoid numerical issues. It means we assume the network never reaches a complete gridlock.

The trajectory of the virtual traveler and the calculation of the arrival times $\hat{t}_a = t_d + T_i$ is presented in Figure 2.2.

The concept of trip-based MFD has been extended to account for different transportation modes, especially buses. Considering different transportation modes requires integrating different vehicle types into the road network. Multimodal macroscopic congestion models consider different travel times for the different vehicles and

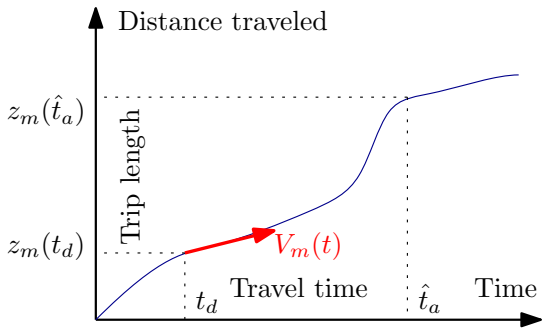

Figure 2.2: Evolution of the distance traveled by the virtual traveler.

their interactions, especially between personal cars and buses. We can distinguish different approaches to represent multimodality in the literature: (i) the speeds for buses and cars are the same, and the bus dwelling time is explicitly considered (Dakic et al., 2021); (ii) the bus speed is affine in the car speed (Loder et al., 2017; Loder et al., 2019); (iii) modes other than the private car undergo an additional delay depending on the congestion level (Loder et al., 2021); (iv) each mode has its speed function, which is affine in the accumulation of every mode in the system (Paipuri & Leclercq, 2020). In this thesis, we use the second approach in chapter 5 to capture the impact of car congestion on PT without adding too much complexity and calibration requirements.

In this thesis, we proceed with two different resolutions of Eq. 2.4 to compute the travel times. The first consists in computing the exact solution by considering a group of travelers as an agent and using an event-based resolution. We will refer to this method as the *trip-based MFD*. The second consists in representing the travel demand as a continuous distribution and approximating the travel time by discretizing the time. The computational burden is, however, smaller than the exact resolution. We will refer to this method as the *generalized bathtub*.

Event-based representation (Trip-based MFD)

Different OD pairs and/or departure times are associated with different groups. If different routes are considered for the same OD pair, each route is represented by a different group. All the users of the same group enter the network simultaneously (same departure time), follow the same route (same trip length), and have the same travel time for each mode. The car ratio in the group i on day d is noted $x_{d,i}$, and the vector of the car ratio of all the groups is $\mathbf{x_d} \in [0,1]^N$. The number of travelers in group i is γ_i. It means when the group i is traveling, its contribution to the car accumulation is $\gamma_i x_{d,i}$.

In the MFD framework, the speed of mode m for group i V_i^m is assumed to be the same for all groups sharing the same mode at the same time. This speed corresponds to the multi-modal MFD curves, which typically depend on the accumulation of both cars n_{car} and PT vehicles (usually buses) n_{PT}: $V_i^m = V_i^m(n_{\text{car}}(t), n_{\text{PT}}(t))$.

Fig. 2.3 illustrates the evolution of the accumulation over time for trip-based MFD set-up. When a group of travelers i, with γ_i travelers and a car share $x_{d,i}$ starts its trips at the time t_i, the departure curves increase by $\gamma_i x_{d,i}$. The accumulation, seen as the difference between the departure and arrival curves, then increases. After a

travel time T_i, the group i leaves the network, and the accumulation decreases by the amount $\gamma_i x_{d,i}$.

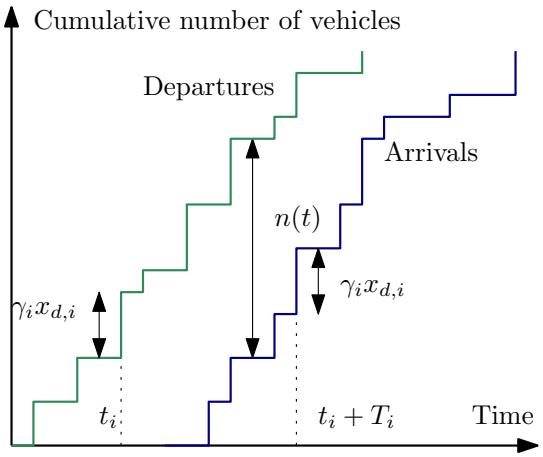

Figure 2.3: Evolution of the accumulation on the network.

The resolution of the travel times consists in calculating the next event: the departure or arrival of a group of travelers. The accumulations and mean speeds are then updated.

Time discrete representation (Generalized bathtub)

The generalized bathtub model provides a set of equations per transport mode. For each mode m, we define a virtual traveler $t \mapsto z_m(t)$ which keeps track of the cumulative traveled distance since the origin of times, as introduced by Lamotte and Geroliminis, 2018 (a.k.a. characteristic travel distance in Jin, 2020). We also define $H_m(t)$ as the accumulation, i.e., the number of vehicles of type m in the network at time t. The number of active trips with a remaining distance higher than x at t is denoted $k_m(x,t)$. This state variable is specific to the generalized bathtub. The accumulation is then computed by $H_m(t) = k_m(x=0,t)$. The accumulation is a state variable common to both MFD and bathtub representations. The speed of mode m v_m depends on the accumulations of all modes (Loder et al., 2017; Loder et al., 2021; Loder et al., 2019; Paipuri et al., 2021; Paipuri & Leclercq, 2020). The coupling between the modes in the bathtub model occurs through the speed functions.

The accumulation at time t consists of the trips that started before t and are long enough to be ongoing by t. Therefore, we introduce the density, with respect to departure time t_d, of the number of vehicles with trip length longer than l: $F_m(l,t_d)$. The traffic dynamics are based on the formulation of Ameli et al., 2022 and extended here to account for different modes. The bathtub dynamics of mode $m \in \mathcal{M}$ is given by Eq. 2.5.

$$\begin{cases} z_m(t) & = \int_0^t v_m(\{H_{m'}(s)\}_{m' \in \mathcal{M}}) \mathrm{d}s \\ H_m(t) & = \int_0^t F_m(z_m(t) - z_m(t_d), t_d) \mathrm{d}t_d \\ F_m(l,t_d) & = \int_{l' > l, l' \in \mathcal{L}} \int_{t_a \in \mathcal{T}_a} \sum_{c \in \mathcal{C}} f(c, l', t_a, t_d, m) \mathrm{d}l' \mathrm{d}t_a \end{cases} \tag{2.5}$$

The first equation states that the mean speed depends on the accumulations and

computes the trajectory of the virtual traveler $z_m(t)$. The second computes the accumulation $H_m(t)$: the sum of the trips that started earlier and are long enough to remain active. It depends on the trajectory of the virtual traveler $z_m(t)$. The third equation is the computation of the density $F_m(l, t_d)$ based on the traffic assignment f. $t_a \in \mathcal{T}_a$ is the desired arrival time and $c \in \mathcal{C}$ is the socioeconomic class (see chapter 5).

The arrival time $\hat{t}_a$ is computed by using the inverse of the virtual traveler $x \mapsto z_m^{-1}(x)$. The inverse is correctly defined as long as the mode speeds are always non-zero. We assume the mean speeds are always strictly positive, meaning we exclude the possibility of a complete gridlock. A user starting at t_d with a trip of length l and using mode m will arrive at

$$\hat{t}_a = t_d + z_m^{-1}(z_m(t_d) + l). \tag{2.6}$$

2.3 Case study: Lyon

This thesis deals with managing the traffic demand and the nudge to different travel alternatives in an urban context. Application of TCS or other DMS is proposed n the chapters 3, 4, and 5 in the MFD context for the general case. To quantify the expected impact of DMS in terms of congestion mitigation, pollution reduction, and individual effect of heterogeneous drivers on a real metropolis, we set up a case study based on Lyon.

We use the network of Lyon Metropolis to calculate the travel times. The individual travelers are gathered into groups departing from an identical region at the same time and traveling to another common region. The MFD for the whole region has been experimentally determined in Mariotte et al., 2020. The demand is based on IRIS areas, which are French administrative areas with between 1 800 and 5 000 inhabitants (INSEE, 2021). We regroup the OD pairs into a city partition of 10 regions to aggregate the demand and define relevant groups departing simultaneously. Furthermore, the perimeter is split into five regions to characterize trips starting or ending outside of Lyon Metropolis. Thus 224 OD pairs are considered because one OD pair has no demand for the considered period. The trip lengths and PT travel times are estimated using the average of those values at the IRIS level weighted by the demand. The considered road network, along with the regions and the boundaries forming the 15 origins and destinations, is represented in Fig. 2.4.

A scenario is developed to test the proposed methodology. We consider the demand between 7:00 and 10:00 and split it into 15 minute subperiods (Ameli, Alisoltani, et al., 2021). Each period has its own PT travel time obtained from the navigator HERE and demand level per OD pair. The PT travel times for the trip from and to Lyon Metropolis are obtained using the HERE API (HERE Developer, 2020). For every subperiod and OD pair, the PT travel time is retrieved by sending a request to the navigator. The data from the navigator HERE considers the historical traffic conditions for each PT trip at a given hour of the day. Regarding the PT travel times for trips originating or ending outside of Lyon Metropolis, an average PT speed of 3 m/s (10.8 km/h) is used for chapters 3 and 4. This value is chosen to match the mean PT speed obtained from the navigator while being slightly lower to account for the inconvenience of switching mode at the city border (Park+Ride).

For chapter 5, as we consider the multimodal effect of the congestion, we account

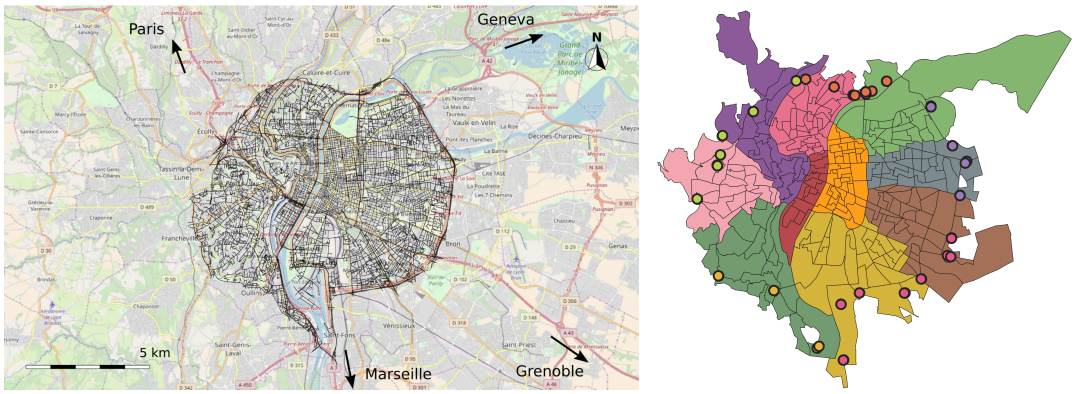

(a) (b)

Figure 2.4: (a) The urban area under consideration (Mariotte et al., 2020, ©OpenStreetMap); (b) The IRIS areas merged in 10 regions and the access points merged in five boundaries (circles). From (Balzer & Leclercq, 2022f).

for the effect of congestion on the PT level of service. We calibrated the affine dependence formulation from Loder et al., 2017 with the travel times and distances retrieved from the city navigator HERE Developer, 2020. The travel demand acts as the weighting factor. The PT speed is assumed affine in the car speed. As the PT trips may consist of different modes (subway, tramway, and bus), we obtain a macroscopic calibration of the PT speed, regardless of the PT vehicles. It is computed by (numerical values for speed in m/s):

$$V_{\mathrm{PT}} = 0.12 V_{\mathrm{car}} \left(H_{\mathrm{car}} + \frac{1}{2} H_{\mathrm{pool}} \right) + 3.17. \tag{2.7}$$

Note that the constant factor is higher and the proportionality factor lower than in Loder et al., 2017. In the former study, the authors represented the speed of buses only, whereas we consider tramways and subways as well. These modes are not or very little impacted by congestion. A mean car speed of 50 km/h leads to a mean PT speed of 17.4 km/h. For comparison, a similar car speed with Loder's models leads to a PT speed of 15.4 km/h for the center of Zurich and 20.6 km/h for the neighborhood of Wiedikon.

The departure times are generated uniformly for each subperiod. This scenario has 384 200 trips (or travelers). We use heterogeneous groups to ensure we have a proper granularity both in trips and departure times. They are aggregated with a maximum of 250 or 1 000 travelers per group and a minimum of two groups per OD pair and per hour. The distributions of the departure times, trip lengths, and PT travel times are shown in Fig. 2.5. It can be seen that there are no overlapping of the PT travel times and the trip lengths, meaning that the attractiveness of the PT strongly depends on the OD pair.

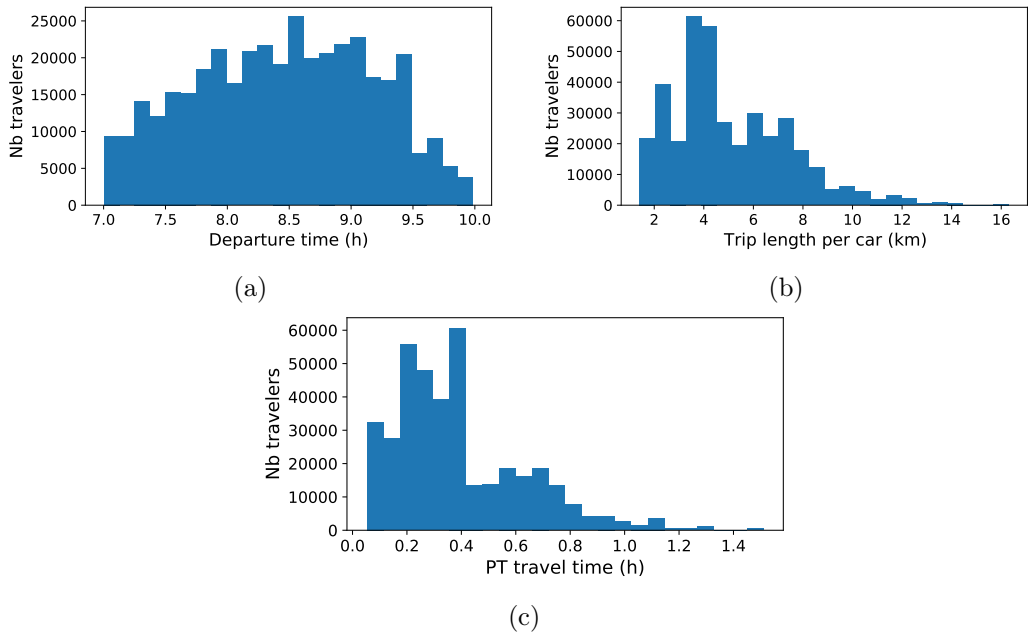

Figure 2.5: (a) Departure times, (b) trip lengths, and (c) PT travel times distributions.

Chapter 3

Modal equilibrium for the trip-based macroscopic fundamental diagram framework under static tradable credit schemes

This chapter is an updated version of the paper Balzer and Leclercq, 2022f.

In this chapter, we investigate the equilibrium distribution of the users between private cars and transit, considering TCS and traffic dynamics with a trip-based MFD. We aim to investigate how TCS can foster PT when the demand is elastic and user choices are based on the perceived costs of all alternatives. Most of the literature about TCS was about driving the users to choose optimal routes or departure times. Some works introduced elastic demand but without explicitly considering transit. Re-routing the drivers or spreading the demand over time mitigate the congestion and reduce exhaust gas emissions. However, switching modes can address other externalities, such as the scarcity of parking places or the ecological footprint of automotive fleets over their life cycles. It is an auspicious research direction and fits with a trip-based MFD framework as it considers the dynamics of congestion.

The proposed TCS is simple: the credit charge is constant and independent of the travel distance. It is applied on a day-to-day basis: each evening, the users choose if they will take the car or ride transit on the next morning, depending on the expected travel times of each alternative and the credit price. They get an allocation of credits for free from the regulator and can trade them with each other using an ad hoc application. The credit price depends on the offer and demand. A more advanced (dynamic) credit charge scheme may improve overall system performance. Nevertheless, we believe that users would more easily get used to the trading system if a daily credit charge is applied to all car trips. In such a case, they do not need to account for their departure time in their decision process. Considering our numerical test case, we will show in this chapter that such a daily charging scheme significantly improves travel conditions compared to the reference scenario without TCS.

The users are assumed to have given trip lengths and departure times, and their only degree of freedom is their modal choice: car or transit. The analytical properties of the MFD are used in order to compute the gradient of the travel times with regard to the modal choices. This information is then used to derive the demand equilibrium.

An application of this method optimizes the credit charge to reduce the total travel time and the total network emissions. No assumptions are made about the credit price regulation mechanism. The credit price is thus treated as a variable along the modal shares to reach the modal equilibrium, which needs to satisfy the MCC, as in many contributions.

The main contribution of this chapter is a modeling and calculation framework based on the trip-based MFD to derive the stochastic user equilibrium with mode choices. It can be broken into four methodological steps: the first is formulating a TCS for an MFD where the degrees of freedom are the modal choices. The second is quantifying the relationship between the travel times and the modal shares in a trip-based MFD framework. The third one is a method to compute the modal equilibrium of the TCS with MFD by using the linearization of the travel times to quantify the delay induced by one user on the other users. The fourth one is a simple method using the previous results to optimize the credit charge to improve social welfare. For convenience, the notations used in this chapter and in the following are summed up in A.1.

This chapter is organized as follows. In Sect. 3.1, we present the framework. Sect. 3.2 formulates the modal equilibrium and its computation. The quantification of the marginal delay induced by a user, i.e., the derivation of the travel times is presented in Sect. 3.3. The credit charge optimization is discussed in Sect. 3.4. A numerical example is provided in Sect. 3.5 for a realistic test case corresponding to the morning commute in Lyon Metropolis. Sect. 3.6 concludes this chapter.

3.1 Methodological framework

The network is represented by a trip-based MFD framework considering the whole city as a single region (Mariotte et al., 2017, Lamotte and Geroliminis, 2018, Jin, 2020). The demand consists of N groups describing different clusters of travelers, each cluster having the same OD pair and departure time.

Here, we further simplify this relationship by assuming that the PT offer and operations do not change and are defined by the actual functioning of the PT network. PT travel times change in time based on historical observations corresponding to a typical day. That means we consider the changes in PT travel times related to the existing adaptation of timetables during the peak hour and usual traffic conditions. We retrieve PT travel times directly from existing timetables and usual PT travel times in the Lyon Metropolis network during peak hours with respect to a given OD pair:

$$V_i^{\mathrm{PT}} = \frac{l_i^{\mathrm{PT}}}{T_i^{\mathrm{PT}}}, \tag{3.1}$$

where l_i^{PT} and T_i^{PT} are retrieved from the city planner and depend on the departure time and OD pair of the group i. $V_i^{\mathrm{car}}(t)$ depends on $n^{\mathrm{car}}(t)$ and $n^{\mathrm{PT}}(t)$. Because we assume that the PT operation is the same every day, that means $n^{\mathrm{PT}}(t)$ does not change over days. So, we can directly fit $V_i^{\mathrm{car}}(t)$ as a function of $n^{\mathrm{car}}(t)$ based on historical data, and this will consider the usual interactions between cars and PT over the network. So, the car speed MFD reduces to a function of the accumulation of cars only. Thus the relationship for cars becomes:

$$l_i^{\text{car}} = \int_{t_i}^{t_i+T_i^{\text{car}}} V_i^{\text{car}}(n^{\text{car}}(t))\mathrm{d}t. \tag{3.2}$$

Note that for this chapter and the following (4), we omit the super- and subscript 'car' to lighten the notation. Furthermore, we remove the subscript i in the speed as it is common for all the groups because they travel in the same reservoir in this thesis.

3.1.1 Mode choice

The users have two alternatives to complete their trips: private car or PT (See Fig. 3.1).

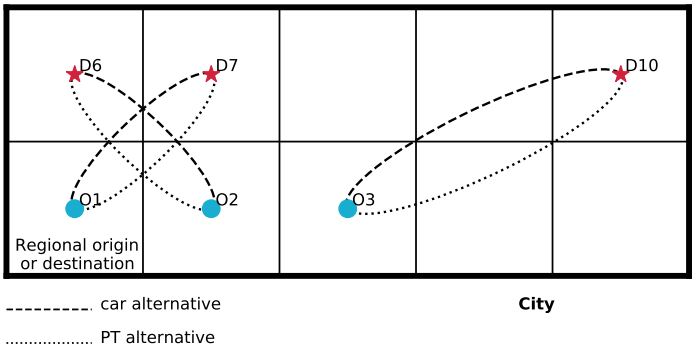

Figure 3.1: Each OD pair has car and PT alternatives.

The travel costs of group i for each mode are the monetary evaluation of the travel time plus the credit charge for the car:

$$\begin{cases} C_i^{\text{car}} &= \alpha T_i(\mathbf{x}) + (\tau - \kappa)p^{\text{TCS}}; \\ C_i^{\text{PT}} &= \alpha T_i^{\text{PT}} - \kappa p^{\text{TCS}}, \end{cases} \tag{3.3}$$

where α is the Value of Time (VoT), τ the credit charge, i.e., the number of credits one needs to take its car, κ the allocation, i.e., the number of credits given by the regulator to each traveler for free, and p^{TCS} the credit price, the money spent to buy one credit from another user or the money received after selling one credit to another user. Aside from the travel time difference, a PT user earns money by selling its credits since it does not need them. A car user spends money to purchase additional credits to pay the credit charge, since $\kappa < \tau$. Otherwise, the TCS is useless. The travelers are assumed homogeneous in the sense that they all have the same VoT. Considering heterogeneity is possible in this framework (with a VoT α_i specific to each group i) but not considered in this study. A user taking the car has to spend τ credits. The group i then spends in total $\gamma_i x_i \tau$ credits.

We drop the day-specific notation d for the modal shares $\mathbf{x}$ as we consider a single day in this chapter.

Note that even if we do not formerly consider trip cancellation because of high travel costs due to the TCS, the current framework makes no difference between a traveler canceling its trip and a transit rider. The PT travel times do not depend on the number of passengers, and no credits are needed to ride PT. Thus, trip cancellation

is equivalent to switching to PT with respect to the traffic conditions and the credit trade.

The number of cars allowed on the network per day is $\sum_i^N \gamma_i \frac{\kappa}{\tau}$. It is the parameter chosen by the control authority. The authority does not choose the credit price p^{TCS} as it results from the credits trade and is not known a priori. This aspect is an essential difference with congestion pricing, where the local authority fixes the price to pay to drive a car. In Sect. 3.4, we assume the allocation κ is fixed and we optimize the credit charge τ. Optimizing the allocation under a fixed credit charge is equivalent, as only the ratio matters.

The decision process follows a logit model. It assumes independent users' perceiving costs with an added error term following a Gumbel distribution. It is a well-established mode choice model that has a single parameter θ. We adhere to the independence assumption for error between alternatives as costs for PT and cars do not depend on each other directly. The probability of group i to drive a car given the modal shares $\mathbf{x}$ and its associated traffic conditions and the credit price is:

$$\psi_i(\mathbf{x}, p^{\text{TCS}}) = \frac{e^{-\theta C_i^{\text{car}}}}{e^{-\theta C_i^{\text{car}}} + e^{-\theta C_i^{\text{PT}}}}. \tag{3.4}$$

Since each group represents several travelers, ψ_i is the ratio of users in group i willing to drive their car. A similar approach can be found in Ye and Yang, 2013, where the logit is used not as a probability but as a ratio of flows taking a particular path.

The travel time T_i is computed by splitting the integral from Eq. (2.4) every time a new event occurs, see Fig. 3.2. An event is either the entry or the exit of a group in the network. Between two consecutive events, the accumulation does not change. Thus the speed is constant. We can then easily solve the integral as the terms under the small integrals are constant. Let us note $e_{i,s}$ the event corresponding to the entry of group i and $e_{i,e}$ the event relative to its exit. Then

$$\begin{aligned} T_i &= \sum_{e=e_{i,s}+1}^{e_{i,e}} \int_{z(t_{e-1})}^{z(t_e)} \frac{1}{V(n_{e-1})} \mathrm{d}s \\ &= \sum_{e=e_{i,s}+1}^{e_{i,e}} \frac{z(t_e) - z(t_{e-1})}{V(n_{e-1})} \\ &= \sum_{e=e_{i,s}+1}^{e_{i,e}} T_e, \end{aligned} \tag{3.5}$$

with T_e the time elapsed between the event $e-1$ and e, and $n_{e-1} = n(z(t_{e-1}))$.

3.1.2 Network equilibrium

Network equilibrium is reached when the actual mode shares are equal to the modal decisions given the same modal shares. The equilibrium is only implicitly defined as we need to know the modal shares to determine travel times, while mode shares calculations require travel times estimations. It is a classical fixed-point problem representing users who are satisfied with their assignments. It can be expressed as:

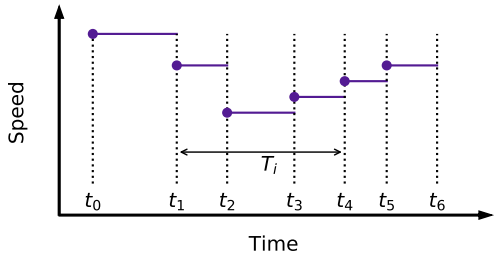

Figure 3.2: Decomposition of the travel time following events. In this illustration, group i enters at the event 1 and exits at the event 4.

$$\mathbf{x} = \psi(\mathbf{x}, p^{\mathrm{TCS}}); \tag{3.6a}$$

$$\tau \sum_{i=1}^{N} \gamma_i x_i \leq \kappa \sum_{i=1}^{N} \gamma_i; \tag{3.6b}$$

$$x_i \geq 0 \ \forall i; \tag{3.6c}$$

$$x_i \leq 1 \ \forall i; \tag{3.6d}$$

$$p^{\mathrm{TCS}} \geq 0; \tag{3.6e}$$

$$p^{\mathrm{TCS}} \left(\sum_{i=1}^{N} \gamma_i (\kappa - \tau x_i) \right) = 0. \tag{3.6f}$$

Eq. (3.6a) define the Stochastic User Equilibrium (SUE) under logit decision-making. Eq. (3.6b) is specific to the TCS: the number of consumed credits cannot exceed the overall allocation. Since the groups can trade credits between themselves, this constraint is at the system level and not the group level. Eq. (3.6c), (3.6d) and (3.6e) delimit the admissible domain for the variables. There is no assumption on the credit price mechanism. It is a positive variable that has to be determined along with the modal shares. Eq. (3.6f) is the MCC as in Yang and Wang, 2011: the price is zero or all the credits are consumed. TCS is a quantity-based demand management strategy. It means the number of trips by car is limited (Eq. (3.6b)), but the price is not fixed. On the opposite, congestion pricing is a price-based strategy. The price is fixed, but the quantity is not limited. To change the proposed framework to congestion pricing, it is enough to remove Eq. (3.6b), (3.6e), and (3.6f). The credit price p^{TCS} would then be treated as a parameter.

Theorem 1. *The proposed TCS admits at least one equilibrium state.*

Proof. The proof of existence is inspired by Ye and Yang, 2013 and resorts to the fixed-point theorem. First, let us define the following function Ψ, which represents a possible model for the system dynamics of the system:

$$\Psi : (\mathbf{x}, p^{\mathrm{TCS}}) \mapsto \left(\psi(\mathbf{x}, p^{\mathrm{TCS}}), \left[p^{\mathrm{TCS}} - \left(\sum_{i=1}^{N} \gamma_i (\kappa - \tau \psi_i \left(\mathbf{x}, p^{\mathrm{TCS}} \right)) \right) \right]_+ \right). \tag{3.7}$$

The modal shares are updated following the logit-based decisions, and the price decreases if some credits are not used while always been positive. Let us show that Ψ is continuous. The positive part function $[\cdot]_+$ is continuous. The accumulation between

two consecutive events is the sum of the modal shares of the groups present on the network at that time, so the accumulation is continuous with regard to the modal shares. The speed V is assumed continuous in the accumulation. The travel times T_i are continuous in the speed V (Eq. (2.4)). The modal choices ψ_i are continuous in the travel times T_i (Eq. (3.3) and (3.4)), so the function Ψ is continuous.

Let us find a compact convex Ω such as the image of Ω by ψ stays in Ω, i.e., $\Psi : \Omega \mapsto \Omega$. As the modal decision goes to zero when the price goes to infinity: $\forall\ i \in [1, N]$ and $\forall\ \mathbf{x}$,

$$0 \leq \psi_i(\mathbf{x}, p^{\text{TCS}}) \leq 1 - \frac{e^{-\theta\alpha T_i^{\text{PT}}}}{e^{-\theta\tau p^{\text{TCS}}} + e^{-\theta\alpha T_i^{\text{PT}}}} \xrightarrow{p^{\text{TCS}} \to \infty} 0, \tag{3.8}$$

we can find a price $p^{\text{TCS},*} \geq 0$ satisfying $\sum_{i=1}^{N} \gamma_i(\kappa - \tau\psi_i(\mathbf{x}, p^{\text{TCS}})) \geq 0\ \forall\ \mathbf{x},\ p^{\text{TCS}} \geq p^{\text{TCS},*}$. Let us set $p^{\text{TCS},+} = \max_{p^{\text{TCS}} \leq p^{\text{TCS},*}} \left(\left[p^{\text{TCS}} - \left(\sum_{i=1}^{N} \gamma_i(\kappa - \tau\psi_i(\mathbf{x}, p^{\text{TCS}})) \right) \right]_+ \right)$. Then setting $\Omega = [0,1]^N \times [0, p^{\text{TCS},+}]$ works. By applying the fixed-point theorem to Ψ on Ω, we get a point $(\mathbf{x}, p^{\text{TCS}})$ satisfying $\mathbf{x} = \psi(\mathbf{x}, p^{\text{TCS}})$ and $p^{\text{TCS}} = \left[p^{\text{TCS}} - \left(\sum_{i=1}^{N} \gamma_i(\kappa - \tau x_i) \right) \right]_+$. This couple $(\mathbf{x}, p^{\text{TCS}})$ satisfies Eq. (3.6a-3.6f), which proves the existence of an equilibrium. □

Proving the uniqueness of the solution is challenging because: (i) travel times have no explicit formulation (see Eq. (2.4)) and (ii) the travel time of one group depends on the modal decisions of many other groups sharing the network at the same time. This coupling is the main difference with the previous contributions based on BPR-like functions, where the travel time on a link depends only on the number of vehicles on this link. Here, we prove the uniqueness of the equilibrium under the condition that the Cartesian product of the difference in car travel times and the difference of the weighted modal shares is strictly positive. Mathematically, it means that:

$$(\mathbf{T_1} - \mathbf{T_2})^T \cdot \gamma \cdot (\mathbf{x_1} - \mathbf{x_2}) > 0\ \forall\ \mathbf{x_1} \neq \mathbf{x_2}, \tag{3.9}$$

with γ being the matrix $N \times N$ with $\{\gamma_i, i \in [1, N]\}$ on the diagonal and zeros outside. Each individual term of the Cartesian product represents the variation in car travel time multiplied by the weighted corresponding change in mode shares. When all groups traveling at the same time experience the same trend in mode shares, all terms are positive as an increase of car share for those groups increases the total number of vehicles in the region. So car travel times increase for everyone (and when all car shares decrease, so do the car travel times). Note that the logit mode choice and the MFD model tend to favor such a collective trend, but it may happen in some specific circumstances that some individual terms be negative. For example, it is the case when a group has a very long trip length and may experience reverse trending along its trip compared to other groups that stay a shorter period of time in the region. The mean herd should generally compensate for this, but it depends on how the simulation goes. For a given test case, we can assess if this assumption is valid by randomly sampling multiple couples $(\mathbf{x_1}, \mathbf{x_2})$ and numerically verify through simulation that Eq. (3.9) always holds. It is not an absolute proof of uniqueness (which we believe is hardly possible because of the implicit nature and dependencies of $\mathbf{T}$), but, at least this provides a process to check uniqueness for any test case one like to study. Note that A.2 provides such a check for the numerical test case.

Theorem 2. *If Eq. (3.9) holds, the equilibrium state is unique.*

Proof. Let us take two equilibrium points $[\mathbf{x_1}, p_1]$ and $[\mathbf{x_2}, p_2]$. Once again, the proof is inspired by Ye and Yang, 2013. MCC and the credit cap tell us that:

$$\begin{aligned}
&(p_1 - p_2)\tau \sum_{i=1}^{N} \gamma_i \left(x_{1,i} - x_{2,i}\right) \\
&= p_1 \sum_{i=1}^{N} \tau\gamma_i x_{1,i} - p_2 \sum_{i=1}^{N} \tau\gamma_i x_{1,i} - p_1 \sum_{i=1}^{N} \tau\gamma_i x_{2,i} + p_2 \sum_{i=1}^{N} \tau\gamma_i x_{2,i} \\
&= p_1 \left(\sum_{i=1}^{N} \gamma_i\kappa - \sum_{i=1}^{N} \tau\gamma_i x_{2,i} \right) + p_2 \left(\sum_{i=1}^{N} \gamma_i\kappa - \sum_{i=1}^{N} \tau\gamma_i x_{1,i} \right) \\
&\geq 0.
\end{aligned} \tag{3.10}$$

By dividing the numerator and the denominator of the logit in Eq. (3.4) by $e^{-\theta\kappa p^{\mathrm{TCS}}}$, for $i \in [1, N]$:

$$\psi_i(\mathbf{x}, p^{\mathrm{TCS}}) = \frac{e^{-\theta(\alpha T_i(\mathbf{x}) + \tau p^{\mathrm{TCS}})}}{e^{-\theta(\alpha T_i(\mathbf{x}) + \tau p^{\mathrm{TCS}})} + e^{-\theta\alpha T_i^{\mathrm{PT}}}}, \tag{3.11}$$

we remark that ψ_i is decreasing with $\alpha T_i(\mathbf{x}) + \tau p^{\mathrm{TCS}}$. Thus,

$$\begin{aligned}
&\sum_{i=1}^{N} \gamma_i \left((\alpha T_i(x_1) + \tau p_1) - (T_i(x_2) + \tau p_2) \right) \left(\psi_i(\mathbf{x_1}, p_1) - \psi_i(\mathbf{x_2}, p_2) \right) \\
&= \alpha(\mathbf{T}(\mathbf{x_1}) - \mathbf{T}(\mathbf{x_2}))^T \cdot \gamma \cdot (\psi_\mathbf{1} - \psi_\mathbf{2}) + \sum_{i=1}^{N} (p_1 - p_2)\tau\gamma_i(\psi_{1,i} - \psi_{2,i}) \\
&= \alpha(\mathbf{T}(\mathbf{x_1}) - \mathbf{T}(\mathbf{x_2}))^T \cdot \gamma \cdot (\mathbf{x_1} - \mathbf{x_2}) + \tau(p_1 - p_2) \sum_{i=1}^{N} \gamma_i(x_{1,i} - x_{2,i}) \\
&\leq 0.
\end{aligned} \tag{3.12}$$

Eq. (3.9) makes the first term strictly positive for $\mathbf{x_1} \neq \mathbf{x_2}$. Using Eq. (3.10), the second term is positive. It implies that $\mathbf{x_1} = \mathbf{x_2}$. As they are equilibrium points, $\psi_\mathbf{1} = \psi_\mathbf{2}$, and thus $p_1 = p_2$ since the function $p^{\mathrm{TCS}} \mapsto \psi(\mathbf{x_1}, p^{\mathrm{TCS}})$ is strictly decreasing. The equilibrium point is thus unique. □

To conclude this section, let sum up the main assumptions of the modeling framework.

- The trip lengths and departure times of the users are given for each OD pair.
- The travel times using PT only depend on departure time and OD pair.
- The travel times using the car depends on the time evolution of car accumulation, which results from all modal shares at the group level.
- The users' decisions follow a logit-based rule. They have the same VoT.
- The control authority uniformly distributes for free among all users a total quantity of credits equal to $\sum_{i=1}^{N} \gamma_i\kappa$. They then trade them between themselves.
- The credit price is zero or all credits are effectively used (MCC).

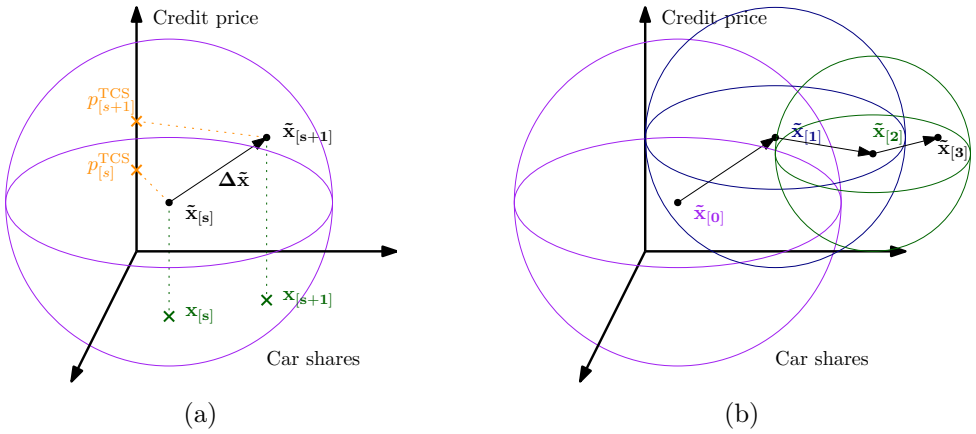

Figure 3.3: The iterative process to find the car shares and credit price at equilibrium. (a) One step and (b) full convergence process.

3.2 Computing the modal equilibrium

Contrarily to works based on Vickrey bottleneck and BPR functions, there is no implicit formulation of the SUE for a trip-based MFD formulation. We cannot directly transpose the existing methodology to calculate the equilibrium and have to develop a new one. This section presents the proposed workflow to find the modal equilibrium for a given credit charge, i.e., the number of credits needed to drive a car. It follows an iterative process based on the linearization of the equilibrium problem and the local resolution of a quadratic optimization problem (QP).

We define $\tilde{\mathbf{x}} = [\mathbf{x}, p]$. The iterative convergence process is illustrated in Fig. 3.3. During step s, the travel times are linearized around the point $\tilde{\mathbf{x}}_{[\mathbf{s}]}$. It permits to formulate a QP and to solve it in the neighborhood of the reference point. The solution $\tilde{\mathbf{x}}_{[\mathbf{s+1}]}$ is then used as the new reference point. The process is repeated until the SUE is reached.

Let us start from an arbitrary mode choice vector $\mathbf{x_0}$ and a credit price p_0. The travel time for group i is $T_{0,i}$ and its corresponding decision is $\psi_{0,i}$. The decision vector is noted $\psi_{\mathbf{0}}$. The car travel delay induced by the group j on the group i is noted $\nabla T_{i,j}$.

The vector of logit choices is linearized according to the change in the modal shares and credit price $\boldsymbol{\Delta}\tilde{\mathbf{x}} = [\boldsymbol{\Delta}\mathbf{x}; \Delta p^{\mathrm{TCS}}]$:

$$\psi = \psi_{\mathbf{0}} + \tilde{\nabla}\psi \cdot \boldsymbol{\Delta}\tilde{\mathbf{x}} + \mathbf{o}(\boldsymbol{\Delta}\tilde{\mathbf{x}}), \tag{3.13}$$

where the operator $\tilde{\nabla}\cdot$ represents the gradient with respect to $\tilde{\mathbf{x}} = [\mathbf{x}; p^{\mathrm{TCS}}]$. The gradient of the decision is defined by:

$$\begin{cases} \psi_{0,i} & = \frac{e^{-\theta(\alpha T_{0,i} + (\tau-\kappa)p_0)}}{e^{-\theta(\alpha T_{0,i} + (\tau-\kappa)p_0)} + e^{-\theta(\alpha T_i^{\mathrm{PT}} - \kappa p_0)}}; \\ \tilde{\nabla}\psi_{i,j} & = \psi_{0,i}(\psi_{0,i} - 1)\theta\alpha\nabla T_{i,j}; \\ \tilde{\nabla}\psi_{i,N+1} & = \psi_{0,i}(\psi_{0,i} - 1)\theta\tau, \end{cases} \tag{3.14}$$

for $i \in [1, N]$ and $j \in [1, N]$. $\psi_{0,i}$ is the decision given the starting point, $\tilde{\nabla}\psi_{i,j}$ is the reaction of the group i to an increase of the car share of a group j, and $\tilde{\nabla}\psi_{i,N+1}$ is the reaction of the group i to an increase of the credit price. We note that the sign of

the gradient of the decision is opposed to the gradient of time. It confirms the general intuition that if the car travel time increases, the car will be less chosen. Similarly, if the credit price increases, the car will be less chosen as well.

The optimization process aims to find an equilibrium point, i.e., a point $\tilde{\mathbf{x}}$ satisfying $\psi = \mathbf{I_x} \cdot \tilde{\mathbf{x}}$, with $\mathbf{I_x}$ the matrix of size $N \times (N+1)$ with 1 on the diagonal and 0 outside, such that $\mathbf{x} = \mathbf{I_x} \cdot \tilde{\mathbf{x}}$.

At the same time, the MCC should hold, i.e., the credit price is zero or all the credits are consumed. We integrate the MCC in the cost function to not treat it as a quadratic hard constraint. It is numerically advantageous since all the constraints are then affine.

The objective function J to minimize is defined as

$$J = \frac{1}{2} \left\| (\tilde{\nabla}\psi - \mathbf{I_x}) \cdot \mathbf{\Delta}\tilde{\mathbf{x}} + \psi_\mathbf{0} - \mathbf{x_0} \right\|_2^2 + \eta p^{\text{TCS}} \frac{1}{\sum_{i=1}^N \gamma_i} \left(\sum_{i=1}^N \gamma_i (\kappa - \tau x_i) \right), \quad (3.15)$$

with η being the weight associated to the MCC.

The optimization problem is formulated as a quadratic problem:

$$\frac{1}{2} \mathbf{\Delta}\tilde{\mathbf{x}}^\mathbf{T} \cdot \mathbf{p}^{\text{TCS}} \cdot \mathbf{\Delta}\tilde{\mathbf{x}} + \mathbf{q} \cdot \mathbf{\Delta}\tilde{\mathbf{x}}, \quad (3.16)$$

by defining the symmetric matrix $\mathbf{p}^{\text{TCS}}$ and the vector $\mathbf{q}$ with

$$\begin{cases} \mathbf{p}^{\text{TCS}} & = (\tilde{\nabla}\psi - \mathbf{I_x})^\mathbf{T} \cdot (\tilde{\nabla}\psi - \mathbf{I_x}) + \eta \mathbf{I_p}; \\ \mathbf{q} & = (\tilde{\nabla}\psi - \mathbf{I_x})^\mathbf{T} \cdot (\psi_\mathbf{0} - \mathbf{x_0}) + \eta \mathbf{i_p}, \end{cases} \quad (3.17)$$

where $\mathbf{I_p}$ is a symmetric matrix of size $(N+1)^2$ and $\mathbf{i_p}$ a vector of size $N+1$ defined by

$$\begin{cases} I_{p^{\text{TCS}},i,N+1} = I_{p^{\text{TCS}},N+1,i} & = -\frac{\gamma_i}{\sum_{j=1}^N \gamma_j} \tau \text{ for } i \in [1,N] \text{ and 0 elsewhere;} \\ i_{p^{\text{TCS}},i} & = -\frac{\gamma_i}{\sum_{j=1}^N \gamma_j} \tau p_0 \text{ for } i \in [1,N]; \\ i_{p^{\text{TCS}},N+1} & = \frac{1}{\sum_{i=1}^N \gamma_i} \left(\sum_{i=1}^N \gamma_i (\kappa - \tau x_{0,i}) \right). \end{cases} \quad (3.18)$$

The first terms of $\mathbf{p}^{\text{TCS}}$ and $\mathbf{q}$ stand for the modal equilibrium and the second ones stand for the MCC. The constraints on the search space and on the credit consumption are then:

$$\begin{cases} \Delta\tilde{x}_i & \leq \min(1 - x_{0,i}, \epsilon_x) \text{ for } i \in [1,N] \\ \Delta\tilde{x}_i & \geq \max(-x_{0,i}, -\epsilon_x) \text{ for } i \in [1,N] \\ \Delta\tilde{x}_{N+1} & \leq \epsilon_p \\ \Delta\tilde{x}_{N+1} & \geq \max(-x_{0,N+1}, -\epsilon_p) \\ \tau \sum_{i=1}^N \Delta\tilde{x}_i & \leq \kappa N - \tau \sum_{i=1}^N x_{0,i}. \end{cases} \quad (3.19)$$

As we linearize several terms around a starting point, we do not want to explore the entire solution space but only the local neighborhood to find a better local solution. This is why we introduce two thresholds ϵ_x and ϵ_p that represent the maximum variations allowed respectively for the modal shares and the credit price. The new optimal

solution $\tilde{\mathbf{x}}$ is used as the new starting point for the next iteration, and a new QP is formulated and solved. It lasts until a given number of iterations occurred or the cost function J has reached a satisfying precision. Fig. 3.4 summarizes the workflow.

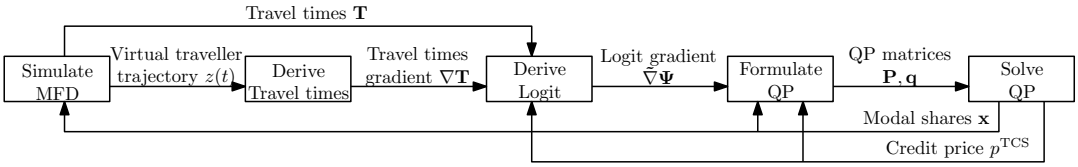

Figure 3.4: Flowchart of the search for the equilibrium.

In the numerical application, the QP (Eq. (3.16) and (3.19)) is solved using the Python package CVXOPT (Andersen et al., 2021).

We also implement the classical MSA algorithm as a benchmark (Sheffi, 1985). For each iteration k, the modal shares are updated according to:

$$\mathbf{x}_{[k+1]} = \mathbf{x}_{[k]} + \frac{1}{k}\left(\psi(\mathbf{x}_{[k]}, p^{\text{TCS}}) - \mathbf{x}_{[k]}\right). \tag{3.20}$$

It is swift to compute and very generic. It can be used for several assignment problems: route, time, or mode choice. However, it does not deal with the credit price as it only updates the modal shares. It does not enforce the TCS conditions and, in particular, the MCC and the total credit cap as it cannot hurdle specific constraints. It means that by using the MSA to find the equilibrium, there is no guarantee that the number of car users does not exceed the limit imposed by the credit cap. One could argue that some modifications can be implemented not to violate the TCS conditions. For the sake of simplicity, this path will not be investigated as it would add another level of iterations, and the MSA in this work only acts as a benchmark.

3.3 Derivation of the travel times with respect to the modal shares

Equilibrium calculation requires the computation of the variables $\nabla T_{i,j}$. The operator $\nabla\cdot$ is the gradient with respect to the modal shares $\mathbf{x}$. The car travel time of group i can be approximated by

$$T_i = T_{0,i} + \nabla\mathbf{T_i} \cdot \mathbf{\Delta x} + o(\mathbf{\Delta x}). \tag{3.21}$$

The $\{\nabla\mathbf{T_i}, \forall\ i\}$, previously defined as the delay undergone by one group because of the others, can also be seen as the derivatives of the travel times with respect to the modal shares.

We aim to quantify how the groups' modal choices influence the travel times of another group *a priori*, i.e., without running several simulations for testing every possible scenario or search direction. A similar idea was used by Simoni et al., 2015 for marginal cost-based pricing: the authors estimated the delay caused by one user for each time step to update the pricing scheme. The delay induced by one user on the others was quantified to change the urban toll for each period. The estimation was done *a posteriori* as MATSim was used to simulate the network, and thus analytical derivations were limited.

By calculating the gradient of inter-event times ∇T_e, we can find the gradient of travel time of group i ∇T_i by summing the changes in each inter-event period during group i's trip:

$$\nabla \mathbf{T_i} = \sum_{e=e_s+1}^{e_e} \nabla \mathbf{T_e}. \tag{3.22}$$

Let us name l_e the distance traveled by the virtual traveler during T_e, i.e. between the events times t_{e-1} and t_e and let us note $V_e = V(n_{e-1})$ the speed during this period. The event-scale variables T_e, t_e, l_e and V_e satisfy the following equations:

$$l_e = T_e V_e, \tag{3.23}$$

and

$$T_e = t_e - t_{e-1}. \tag{3.24}$$

These relationships can be seen in Fig. 3.5.

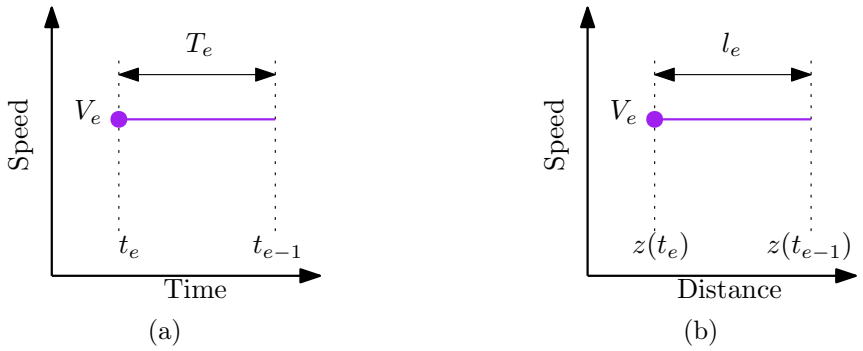

Figure 3.5: (a) Time- and (b) distance-based representations of the inter-event periods.

As the speed appears in the expression of T_e, it should be noted that its gradient $\nabla \mathbf{V_e}$ with respect to the modal shares $\mathbf{x}$ is expressed by:

$$\begin{cases} \nabla V_{e,i} = & \gamma_i \frac{\mathrm{d}V}{\mathrm{d}n}(n_{e-1}) \text{ if group } i \text{ is in the network between } e-1 \text{ and } e; \\ & 0 \text{ otherwise.} \end{cases} \tag{3.25}$$

We need to switch cases depending on the nature of the event $e-1$ and e. Note that as the departure times are assumed to be given, $\nabla \mathbf{t_e} = 0$ if e is an entry. Furthermore, the trip length of a given group i is constant too, so its gradient is zero $\nabla \mathbf{l_i} = 0$.

- Case I: t_{e-1} and t_e are both entries of groups in the network.
  Since entry times are constant, by Eq. (3.24),

$$\nabla \mathbf{T_e} = 0. \tag{3.26}$$

- Case II: t_{e-1} is an exit and t_e is an entry.
  Since $t_{e-1} = \sum_{g=1}^{e-1} \nabla \mathbf{T_g}$,

$$\nabla \mathbf{T_e} = -\nabla \mathbf{t_{e-1}} = -\sum_{g=1}^{e-1} \nabla \mathbf{T_g}. \tag{3.27}$$

- Case III: t_e is the exit of a group i, i.e. $e_{i,e} = e$ (t_{e-1} being an entry or an exit).

  We decompose the trip length into the distance traveled between events, starting from the entry of i:

  $$l_i = \sum_{g=e_{i,s}+1}^{e} l_g. \tag{3.28}$$

  By using Eq. (3.23) and knowing that l_i is constant, applying the gradient gives:

  $$\sum_{g=e_{i,s}+1}^{e} \nabla \mathbf{T_g} V_g + T_g \nabla \mathbf{V_g} = 0. \tag{3.29}$$

  By calculating the gradient of inter-event period one after another in a time ascending manner, we can compute $\nabla \mathbf{T_e}$:

  $$\nabla \mathbf{T_e} = -\frac{1}{V_e}\left(T_e \nabla \mathbf{V_e} + \sum_{g=e_{i,s}+1}^{e-1} \nabla \mathbf{T_g} V_g + T_g \nabla \mathbf{V_g}\right). \tag{3.30}$$

  It is worth noticing the two parts of the gradient: a local contribution linked to the speed variation and the cumulative shift of the events. This shift is due to earlier or later completion of trips for groups ending their trips while group i is in the network.

The gradient of the travel time is then computed following the algorithm 1. The first loop addresses the events, and the inner ones focus on the groups. As there are $2N$ events (one entry and one exit per group), the number of operations to compute the gradient of the travel times $\nabla \mathbf{T}$ in one point $\mathbf{x_0}$ is $O(N^2)$, i.e., at most proportional to N^2.

for Each event e in a time ascending manner **do**
  for Each user i present on the network at this time, i.e., $e_{i,s} < e \leq e_{i,e}$ **do**
    Compute the gradient of the speed $\nabla V_{e,i}$ according to Eq. (3.25);
  end
  Compute the marginal times $\nabla \mathbf{T_e}$ with Eq. (3.26), (3.27) or (3.30) depending on the types of the events $e-1$ and e;
  for Each user i present on the network at this time, i.e., $e_{i,s} < e \leq e_{i,e}$ **do**
    Add the contribution of this period $\nabla \mathbf{T_e}$ to the gradient of the travel time $\nabla \mathbf{T_i}$ as in Eq. (3.22);
  end
end

Algorithm 1: Computation of the gradient of the travel times relative to the modal choices.

3.4 Optimization of the credit charge

Previously the credit charge was supposed given. However, the purpose of introducing a TCS is to improve the welfare of the society undergoing the externalities of network usage. In this study, we choose to minimize the total travel time only or combine total travel time and total network carbon emissions by optimizing the credit charge level. Note that minimizing total carbon emissions alone has a trivial optimal point: the credit charge level should be infinite, so everyone takes PT. This option has obvious

drawbacks in terms of travel times (and acceptability), and this is why we better investigate a mixed objective function.

3.4.1 Minimizing total travel time

The first objective function is the total travel time TTT. It is the sum of the travel times per group and per mode, weighted by the corresponding modal ratio at equilibrium:

$$TTT = \sum_{i=1}^{N} \gamma_i \left(x_i T_i + (1 - x_i) T_i^{\mathrm{PT}} \right). \tag{3.31}$$

Let derive TTT with respect to τ to determine its sign:

$$\frac{\mathrm{d}TTT}{\mathrm{d}\tau} = \sum_{i=1}^{N} \gamma_i \frac{\mathrm{d}x_i}{\mathrm{d}\tau} (T_i - T_i^{\mathrm{PT}}) + \gamma_i x_i \nabla \mathbf{T_i} \cdot \frac{\mathrm{d}\mathbf{x}}{\mathrm{d}\tau}. \tag{3.32}$$

Since we assume the network is always at equilibrium, the derivatives of $\mathbf{x}$ and ψ are equal. We remind that the modal choices ψ depend on the credit charge, credit price, and modal shares:

$$\frac{\mathrm{d}x_i}{\mathrm{d}\tau} = \frac{\mathrm{d}\psi_i}{\mathrm{d}\tau} = \frac{\partial \psi_i}{\partial \tau} + \frac{\partial \psi_i}{\partial p^{\mathrm{TCS}}} \frac{\mathrm{d}p^{\mathrm{TCS}}}{\mathrm{d}\tau} + \nabla \psi_{\mathbf{i}} \cdot \frac{\partial \psi}{\partial \tau}. \tag{3.33}$$

Since the price mechanism is not explicit, $\frac{\mathrm{d}p^{\mathrm{TCS}}}{\mathrm{d}\tau}$ would require numerical approximations. For that, the solution space has to be sampled and the modal equilibrium calculated. We would then have the price for different credit charges and interpolate the derivative. This process is, however, costly and not fit for directly determining the optimal direction of the credit charge. In order to circumvent the costly and prone-to-uncertainty estimation of the gradient of the price, a coarser but more robust and intuitive method is introduced. The general principle is to estimate the variations of the total travel time over an actual equilibrium for a given credit charge.

The changes in total travel time are the combined effect of improving the traffic conditions and the modal report. When the credit charge increases, the number of cars on the network decreases. The users still driving their cars benefit from better traffic conditions, and users shifting from car to PT usually experience an increase in travel time. The total travel time variation is estimated by:

$$\Delta TTT = N_c \Delta TT_c + \Delta N_c (TT_{\mathrm{c}}^w - TT_{\mathrm{PT}}^w), \tag{3.34}$$

with $TT_{\mathrm{c}} = \frac{\sum_{i=1}^{N} \gamma_i x_i T_i}{\sum_{i=1}^{N} \gamma_i x_i}$ the mean travel time per car and $N_c = \sum_{i=1}^{N} \gamma_i \frac{\kappa}{\tau}$ the number of car users supposing the credit cap constraint is active, i.e., all the credits are consumed. $TT_{\mathrm{c}}^w = \frac{\sum_{i=1}^{N} \gamma_i w_i T_i}{\sum_{i=1}^{N} \gamma_i w_i}$ and $TT_{\mathrm{PT}}^w = \frac{\sum_{i=1}^{N} \gamma_i w_i T_i^{\mathrm{PT}}}{\sum_{i=1}^{N} \gamma_i w_i}$ are the mean travel time per car and per PT of users that are actually shifting from car to PT. The weights are the absolute values of the gradient of the logit $w_i = -\frac{\mathrm{d}\psi_i}{\mathrm{d}C_{i,\mathrm{car}}}$. These weights give more importance to users prone to modal shift. By increasing the credit charge by a tiny quantity $\Delta\tau$, the N_c car users will benefit from a reduction of their travel times by

ΔTT_c and ΔN_c car users will be forced to switch to PT, increasing their travel time by $TT^w_{\text{PT}} - TT^w_{\text{c}}$.

By defining the typical accumulation on the network $\bar{n} = N_c \frac{TT_c}{T_{\text{dept}}}$, with T_{dept} the time windows in which the departure times take place; the mean traveled distance by car, weighted by the modal shares $L_m = \frac{\sum_{i=1}^{N} \gamma_i x_i l_i}{\sum_{i=1}^{N} \gamma_i x_i}$; the mean speed over the whole simulation $\bar{V} = \frac{L_m}{TT_c}$ and the local slope of the speed δ_v, such that $\Delta\bar{V} = -\delta_v \Delta\bar{n}$, we can derive the travel time variation of car users $\Delta TT_c = L_m \delta_v \frac{1}{\bar{V}^2} \Delta\bar{n}$. The increase of the total travel time due to the modal shift is $(TT^w_{\text{PT}} - TT^w_{\text{c}}) \sum_{i=1}^{N} \gamma_i \frac{\kappa}{\tau^2} \Delta\tau$ and the decrease due to the improvement of the travel condition is $L_m \delta_v \frac{1}{\bar{V}^2} \bar{n} \sum_{i=1}^{N} \gamma_i \frac{\kappa}{\tau^2} \Delta\tau$. Thus, the global variation of the total travel time becomes

$$\begin{aligned} \Delta TTT &= -L_m \delta_v \frac{1}{\bar{V}^2} \bar{n} \sum_{i=1}^{N} \gamma_i \frac{\kappa}{\tau^2} \Delta\tau + (TT^w_{\text{PT}} - TT^w_{\text{c}}) \sum_{i=1}^{N} \gamma_i \frac{\kappa}{\tau^2} \Delta\tau \\ &= \left(-L_m \delta_v \frac{1}{\bar{V}^2} \bar{n} - TT^w_{\text{c}} + TT^w_{\text{PT}} \right) \sum_{i=1}^{N} \gamma_i \frac{\kappa}{\tau^2} \Delta\tau \end{aligned} \tag{3.35}$$

Thus the gradient of the total travel time can be approximated by:

$$\frac{\mathrm{d}TTT}{\mathrm{d}\tau} \approx \left(-L_m \delta_v \frac{1}{\bar{V}^2} \bar{n} - TT^w_{\text{c}} + TT^w_{\text{PT}} \right) \sum_{i=1}^{N} \gamma_i \frac{\kappa}{\tau^2} \tag{3.36}$$

3.4.2 Minimizing the total network emissions

The total network emissions of carbon dioxide is quantified using a macroscopic emission model COPERT IV for passenger cars (Ntziachristos et al., 2009). It quantifies the impact of network usage on global warming. It is also a proxy for fuel consumption. The PT part in emissions is supposed constant because we assume that the PT operations are unchanged (same number of vehicles and timetables). A straightforward extension would be to correlate the emissions to the change in PT operation to accommodate the demand. However, the contribution compared to personal cars is much lower, so this would change neither our conclusion nor the methodology. Only personal cars emissions are considered in this work.

In Ingole et al., 2020, the authors coupled the COPERT IV emissions laws to an accumulation-based MFD framework. It is very much what we need to do here, and we process the same way. For a given time period, emissions are the product of the total travel distance by all vehicles multiplied by the emission factor. The emission factor depends only on the mean speed. The total travel distance according to Edie's definition between two consecutive events is $n_e T_e V_e$. The total carbon dioxide emissions E is estimated by summing the contributions from all the inter-event periods:

$$E = \sum_{e=1}^{2N} n_e T_e V_e E_{\text{dist}}(V_e), \tag{3.37}$$

where $V \mapsto E_{\text{dist}}(V)$ is the emission model giving the emission per distance as a function of the mean speed.

The emission function representative for a French typical vehicle fleet is represented by the fourth-order polynomial from Lejri et al., 2018, see Table 3.1 for the coefficient values:

$$E_{\text{dist}}(V) = c_1V^4 + c_2V^3 + (c_3 + 2c_1c_0^2)V^2 + (c_4 + c_2c_0^2)V + (c_5 + \frac{c_3}{3}c_0^2 + \frac{c_1}{5}c_0^4). \tag{3.38}$$

Table 3.1: Parameters for CO_2 emission curve for passenger cars. These numerical values are for speeds in km/h and emissions in g/km.

Coefficient	Value
c_0	12.5
c_1	1.304×10^{-5}
c_2	-0.003269
c_3	0.3103
c_4	-13.52
c_5	371.4

As for the total travel time, a coarse but robust estimation of the variation of the emissions is calculated to avoid requiring numerical approximations of the price gradient with respect to the credit charge. As before, the changes in the network emissions come from the modal report (total traveled distance changes) and the improvement of the traffic conditions (mean speed changes). As the credit charge increases, the total emissions decrease on one side because fewer users are taking their car and the total travel distance decreases. On the other side, the emission per distance decreases because the mean speed globally increases. It means:

$$\begin{aligned}\Delta E &= \Delta L_{\text{tot}} E_{\text{dist}}(\bar{V}) + L_{\text{tot}} \frac{dE_{\text{dist}}}{dV}(\bar{V})\Delta V \\ &= \Delta N_c L_m^w E_{\text{dist}}(\bar{V}) - L_{\text{tot}} \frac{dE_{\text{dist}}}{dV}(\bar{V})\delta_v \Delta\bar{n},\end{aligned} \tag{3.39}$$

with $L_{\text{tot}} = \sum_{i=1}^{N} \gamma_i x_i l_i$ the total traveled distance of all the cars. It is equal to $\sum_{e=1}^{2N} n_e T_e V_e$. $L_m^w = \frac{\sum_{i=1}^{N} \gamma_i w_i l_i}{\sum_{i=1}^{N} \gamma_i w_i}$ is the mean travel distance by car of users shifting to PT. It is weighted by the absolute values of the gradient of the logit. When the credit charge increases by a tiny $\Delta\tau$, ΔN_c are forced to shift to PT and thus the total traveled distance per car decreases by $\Delta N_c L_m^w$. On parallel, as the typical accumulation decreases by $\Delta\bar{n}$, the traffic conditions are improved, and the carbon emission per distance decreases by $-\frac{dE_{\text{dist}}}{dV}(\bar{V})\delta_v\Delta\bar{n}$. The decrease of the carbon emissions due to modal report is $L_m^w E_{\text{dist}}(\bar{V}) \sum_{i=1}^{N} \gamma_i \frac{\kappa}{\tau^2}\Delta\tau$ and the decrease due to the better traffic condition is $-L_{\text{tot}} \frac{dE_{\text{dist}}}{dV}(\bar{V})\delta_v\bar{n}\frac{1}{\tau}\Delta\tau$. The global variation of the carbon emissions becomes:

$$\begin{aligned}\Delta E &= -L_m^w E_{\text{dist}}(\bar{V}) \sum_{i=1}^{N} \gamma_i \frac{\kappa}{\tau^2}\Delta\tau + L_{\text{tot}} \frac{dE_{\text{dist}}}{dV}(\bar{V})\delta_v\bar{n}\frac{1}{\tau}\Delta\tau \\ &= \left(-L_m^w E_{\text{dist}}(\bar{V}) \sum_{i=1}^{N} \gamma_i \frac{\kappa}{\tau} + L_{\text{tot}} \frac{dE_{\text{dist}}}{dV}(\bar{V})\delta_v\bar{n}\right)\frac{1}{\tau}\Delta\tau.\end{aligned} \tag{3.40}$$

The gradient of the total network emissions is then approximated using

$$\frac{\mathrm{d}E}{\mathrm{d}\tau} \approx \left(-L_m^w E_{\mathrm{dist}}(\bar{V}) \sum_{i=1}^{N} \gamma_i \frac{\kappa}{\tau} + L_{\mathrm{tot}} \frac{dE_{\mathrm{dist}}}{dV}(\bar{V}) \delta_v \bar{n} \right) \frac{1}{\tau}. \tag{3.41}$$

As the mean speed decreases with the network accumulation ($\delta_v \geq 0$) and the emission per distance decreases with speeds on the typical range for urban network $\left(\frac{dE_{\mathrm{dist}}}{dV}(\bar{V}) \leq 0\right)$, the gradient of the total network emissions is always negative.

Note that this estimation and gradient method can be applied to other pollutants such as NO_x or PM as the emission functions are similar. Emission curves with coefficient values can be found in Lejri et al., 2018.

3.4.3 Mixed objective function considering both emissions and travel times

The objective function is the monetary evaluation of the total travel time and network emissions. It is chosen as $\alpha TTT + \Gamma P_{\mathrm{carbon}} E$. P_{carbon} is the price of the carbon per weight and Γ is the coefficient associated to the CO_2 emissions. It is used to compensate for the difference in the order of magnitude between the total CO_2 emissions and the total travel time.

Once again, since the trip-based MFD relies on an implicit formulation of the travel times, the optimal credit charge will not be explicitly given. However, we can compute an approximation of the derivative of the objective function. We propose to solve this minimization problem by dichotomy: the search domain is halved at every step by looking at the sign of the derivative $\alpha \frac{\mathrm{d}TTT}{\mathrm{d}\tau} + \Gamma P_{\mathrm{carbon}} \frac{\mathrm{d}E}{\mathrm{d}\tau}$. A lower and higher bounds are chosen at the initialization, and the first credit charge is the average. The recursive process goes through the following steps:

- The equilibrium is computed;
- The approximation of the gradient of the objective function with respect to the credit charge is computed;
- If negative, the new credit charge is the average of the previous credit charge and higher bound. The lower bound takes the value of the previous credit charge. If positive, the new credit charge is the average of the previous credit charge and the lower bound. The higher bound takes the value of the previous credit charge;
- When the higher and lower bounds are equal, the process stops as a local minimum has been found.

As the credit charge value is taken as an integer, the process always ends in a finite number of steps. The same process is used when minimizing TTT only. Repeating the process with different starting points mitigates the risk of finding only a local minimum.

3.5 Numerical example

In order to illustrate the proposed method, we design a large-scale scenario using representative data from a regular morning peak hour in Lyon Metropolis.

The departure times are generated uniformly for each subperiod. This scenario has 384 200 trips (or travelers). We use heterogeneous groups to ensure we have a proper granularity both in trips and departure times. They are aggregated with a maximum of 250 travelers per group and a minimum of two groups per OD pair and per hour. Thus, 2 163 groups are generated.

The default parameters used for the simulation can be found in Table 3.2. The VoT is chosen based on the work of Fosgerau et al., 2007. The carbon price is based on the European Union Emissions Trading Scheme (see International Carbon Action Partnership, 2021). The maximum allowed variations ϵ_x and ϵ_p are taken as the inverse of the current iteration index (See A.4 for a comparison with constant values). Practically, this reduces the exploration space size at each iteration to narrow the search when we come close to the modal equilibrium. The iteration process stops once the cost function J is below the desired precision J_{Goal}, i.e., when the modal equilibrium is reached.

Table 3.2: The default parameters used for the simulation.

Parameter	Notation	Value
VoT	α	10.8 EUR/h
Endowment	κ	100 credits
Credit charge	τ	200 credits
Price weight	η	1
Cost function goal	J_{Goal}	10^{-3}
Initial price	$p^{\text{TCS}}(0)$	0.01 EUR/credit
Initial modal shares	$\mathbf{x_0}(0)$	$\mathbf{0}$
Logit parameter	θ	1 1/EUR
Emission weight	γ	50
Carbon price	P_{carbon}	20 EUR/tonne

3.5.1 Preliminary analysis

First, we present the simulation results without and with TCS. It shows the congestion dynamics and helps to apprehend the scenario better. The speed, accumulation, and production at the modal equilibrium along the simulation time are to be found in Fig. 3.6. The production is the product of the mean speed and the accumulation. It is the distance traveled by all the vehicles in the network per unit of time.

The traffic does not enter the hyper-congested regime, as the production does not decrease because of high accumulation. Under hyper-congestion, the PT alternative would be highly attractive, and thus, the car shares would decrease. Nevertheless, it undergoes clear loading, congested, and unloading stages. It permits to demonstrate the method capabilities for a realistic peak hour scenario.

Second, before investigating in details the equilibrium process, we assess the errors made by the linearization of the travel times. 50 pairs of modal shares $(\mathbf{x_0}, \mathbf{x_1})$ are randomly and separately generated following a uniform distribution. Simulations are carried out to define the exact values of $\mathbf{T}(\mathbf{x_1})$ and $\mathbf{T}(\mathbf{x_0})$. Then, the travel times

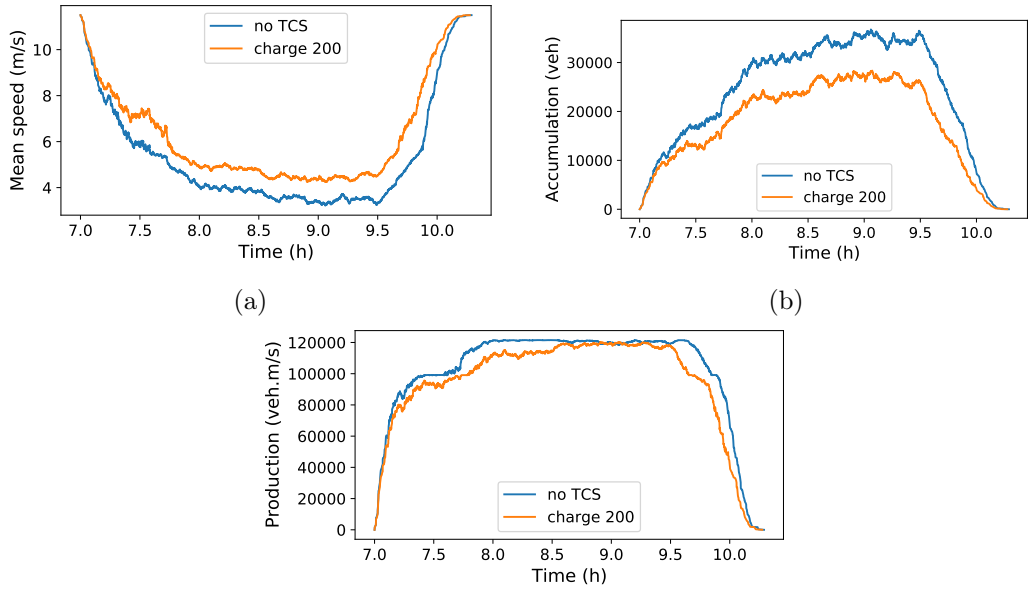

Figure 3.6: Speed (a), accumulation (b) and production (c) at the modal equilibrium for a credit charge of 200 credits and no TCS.

and modal decisions are linearized around $\mathbf{x_0}$. Their values are approximated at $\mathbf{x_1}$ with the linearization. The norm of the error is normalized using the norm of the differences: $\|\mathbf{T}(\mathbf{x_1}) - \mathbf{T}(\mathbf{x_0})\|_2$ and $\|\psi(\mathbf{x_1}) - \psi(\mathbf{x_0})\|_2$. The results are presented in Fig. 3.7. The error of the linearization of the travel time and logit is lower than 45%,

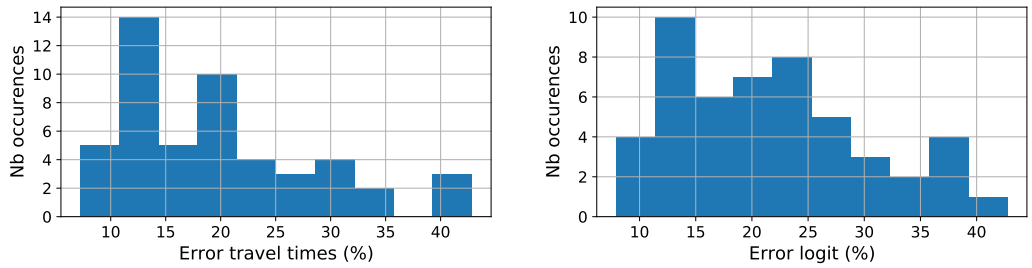

Figure 3.7: (a) Error on the travel times, and (b) error on the modal decisions.

with most of the occurrences below 25%. It is satisfying as $\mathbf{x_1}$ is not always in the neighborhood of $\mathbf{x_0}$.

3.5.2 Results

Comparing methods for computing equilibrium

We directly feed the MSA with the optimal price derived by the new method based on travel times linearization. We do this because this method can only derive the modal shares and not the equilibrium price. Thus using another price value may lead to a different equilibrium and prevent us from a fair benchmarking. Note that, as MSA

fails to calculate equilibrium prices, it greatly reduces the potential of this method in practice.

Each method is run with 20 iterations. The modal errors $\frac{1}{2}\|\mathbf{x} - \psi\|_2^2$, modal shares, and computation times are compared in Fig. 3.8 with an initial price of 0.00551 EUR/credit. The MSA is fast to compute but fails to reach high precision.

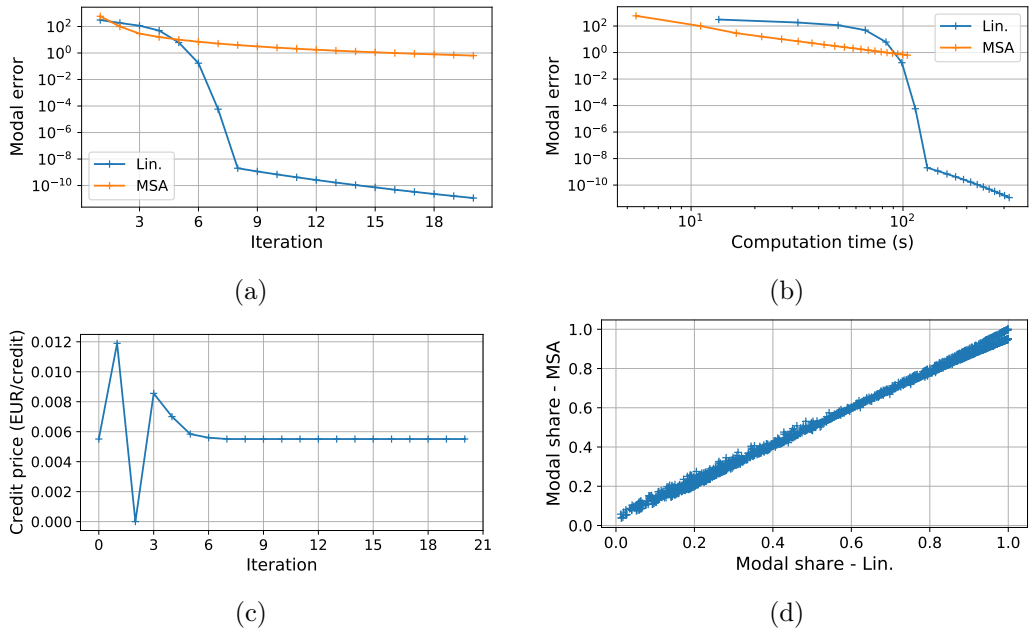

Figure 3.8: (a) Error between modal shares and decisions vs. iteration, (b) vs. computation time, (c) evolution of the credit price, and (d) modal shares at equilibrium.

The proposed methodology increases the computation burden by about one order of magnitude to increase the precision by about ten orders of magnitude. Both methods found almost the same modal shares and credit price at equilibrium. The error between the modal share is only 4%.

To further highlight the limits of the MSA, we run another equilibrium computation with another initial price of 0.001 EUR/credit. The equilibrium number of car users is then 217 695 with the MSA, which violates the credit cap as the limit is $\sum_1^N \gamma_i \kappa/\tau = 192\ 100$.

Importance of departure times and trip lengths

Most of the TCS frameworks proposed in the literature are based on Vickrey bottleneck and BPR functions. They cannot account for the congestion dynamics and trip heterogeneity at the same time. We generate some alternative scenarios to highlight the importance of considering the heterogeneity in departure times and trip lengths. We show that the behavior of the TCS is greatly affected by a change in the departure time distribution or by the homogenization of the trips.

As Vickrey bottleneck assumes that every traveler has the same trip, we create a scenario named ST, where all travelers have the same trip length and PT travel time. These parameters are computed by averaging the trip lengths and PT travel times weighted by the demand. As the BPR function does not consider the departure times,

we create a scenario named DT where the departure times are generated with a different distribution. In the reference scenario, the departure times follow the reference distribution given in Fig. 2.5. In scenario DT, they follow the normal distribution of mean 5400 s and standard deviation 1800 s. See Fig. 3.9 for the differences between the reference scenario, ST, and DT.

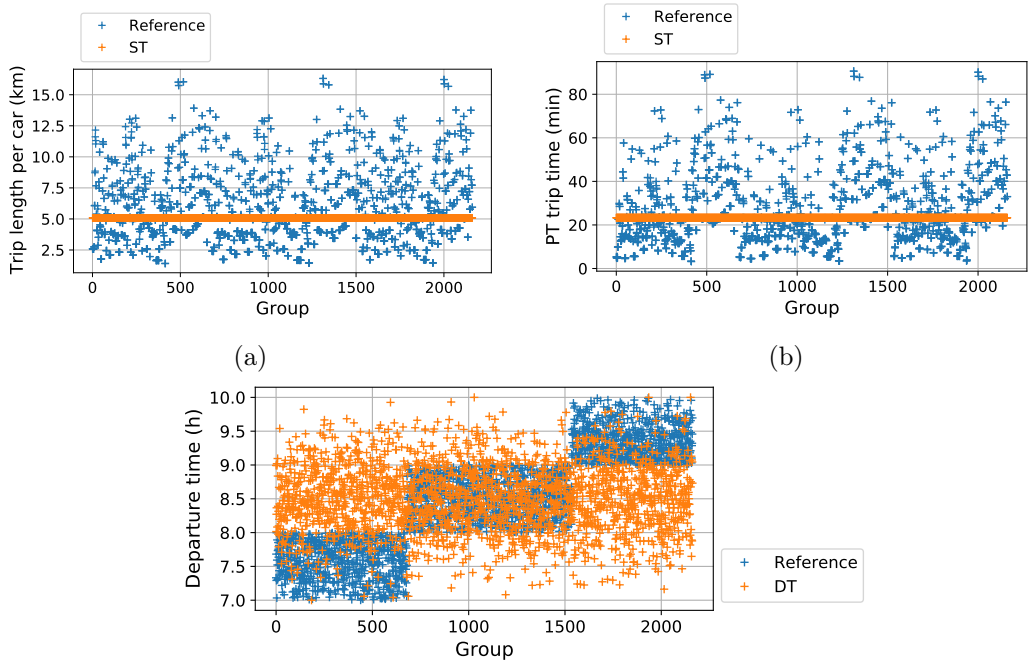

Figure 3.9: (a) Trip lengths and (b) PT travel times for ST and (c) departure times for DT.

The corresponding credit prices and modal shares at equilibrium are compared in Table 3.3 and Fig. 3.10. With a more concentrated distribution of the departure

Table 3.3: The credit prices and differences in modal shares at equilibrium for the three scenarios with the demand SC2.

Scenario	Price (EUR/credit)	Difference price	Difference modal shares
Reference	0.00551	-	-
ST	0.00820	+48.8%	46.3%
DT	0	-100%	43.0%

times in DT, the traffic is significantly more congested. A credit charge of 200 credits is not a constraint anymore, as even without TCS, the PT is more attractive than the car. Thus the credits in DT do not have any monetary value. The difference of the modal shares is more than 40%. Neglecting the congestion dynamics and assuming homogeneity of the trips leads to significant errors in estimating the modal shares at equilibrium. This simulation proves the necessity to consider both the heterogeneity in trip lengths and departure times.

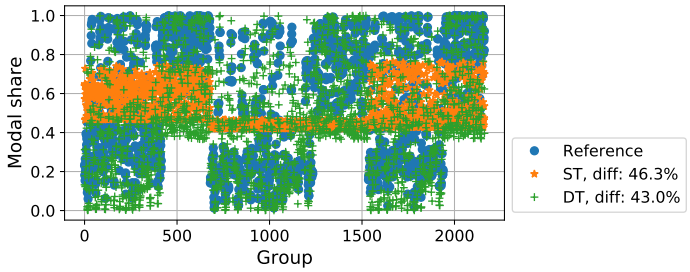

Figure 3.10: Modal shares at the equilibrium for the three scenarios with SC2.

Sensitivity analysis

Different credit charges are investigated to assess the impact of different TCS on the transportation system. The equilibriums are computed for credit charges between 100 and 460 credits with a step size of 20 credits. The number of car users and the toll equivalent $p^{\text{TCS}}(\tau - \kappa)$, i.e., the money a group has to spend to purchase the credits (on top of its allocation, which is for free) needed to take its car, are presented in Fig. 3.11 for the different credit charges. The TCS is only active from a credit charge

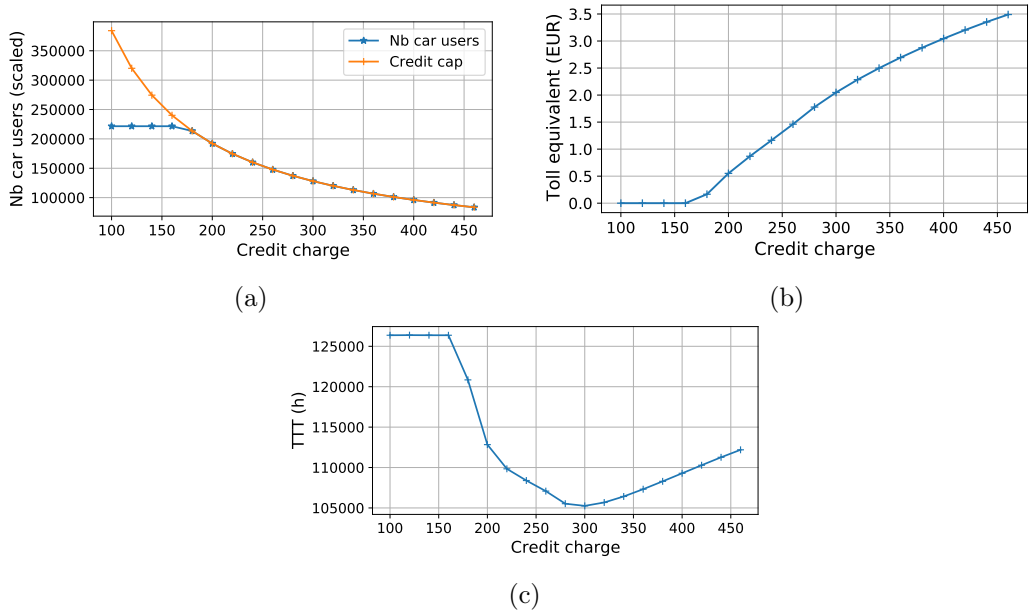

Figure 3.11: (a) Number of car users, (b) toll price in EUR, and (c) total travel time for different credit charges.

of about 180 credits. Before, it does not constraints anyone on switching from car to PT. It can be seen that the price is zero when the credit cap is not constraining. It is in line with the MCC. As expected, the toll equivalent increases with the credit charge. It is expected: by augmenting the credit charge, the number of cars allowed on the network is reduced, and the ability to drive a car, here seen as a commodity, becomes scarce and thus more expensive. For a credit charge of 460 credits, which means less than one-quarter of the users can drive their private cars, the toll equivalent is around 3.5 EUR. Such a price is reasonable. For comparison, a transit ticket costs about 2 EUR in Lyon Metropolis as of 2021. The evolution of the total travel time combines the increase of travel times for users switching from car to PT and the decrease caused by better traffic conditions for those still traveling by car. The behavior of the total

travel time as a function of the credit charge is not intuitive as it results from those two different phenomena which drive the sum in opposite directions. There seems to be a minimum for the total travel time at around 300 credits.

The impact of the TCS on network carbon emissions is also investigated in Fig. 3.12. The emission per distance decreases with the credit charge, as the lower accumulation

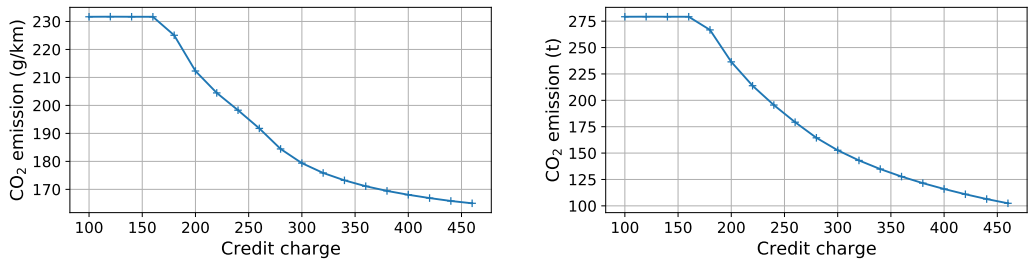

(a) (b)

Figure 3.12: (a) CO_2 emission per distance and (b) CO_2 total emissions for different credit charges.

permits better traffic conditions and a more efficient operating of the internal combustion engines. The total network emissions decrease even more as the improvement of the performance of the combustion engines is coupled with a diminution of the number of cars on the network, i.e., the total traveled distance. A credit charge of 340 credits cuts the total network carbon emissions by two.

In Fig. 3.13 , we investigate the trade-off between total travel time and carbon emissions. The Pareto front for minimizing simultaneously total travel time and car-

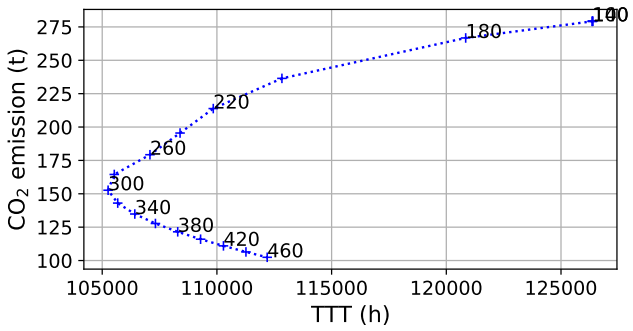

Figure 3.13: Total travel time vs. CO_2 emissions for different credit charges. The green and red points are found by minimizing total travel time and the mixed objective function.

bon emissions, i.e., the set of non-dominated solutions, starts at a credit charge of about 300 credits.

As the results are related to the PT level of service, we provide a sensitivity analysis with the PT travel times in A.3.

Optimize the credit charge

The credit charge optimization process by dichotomy is launched with an initial higher bound of 500 credits and an initial lower bound of 100 credits. The convergence of

the process can be found in Fig. 3.14 for minimizing the total travel time only and the mixed objective function. In this particular case study, only one initialization is enough because both objective functions are convex. However, it may not be the case for other case studies and demand scenarios. In such cases, considering multiple uniformly distributed starting points over the full range of possible values can still guarantee optimality.

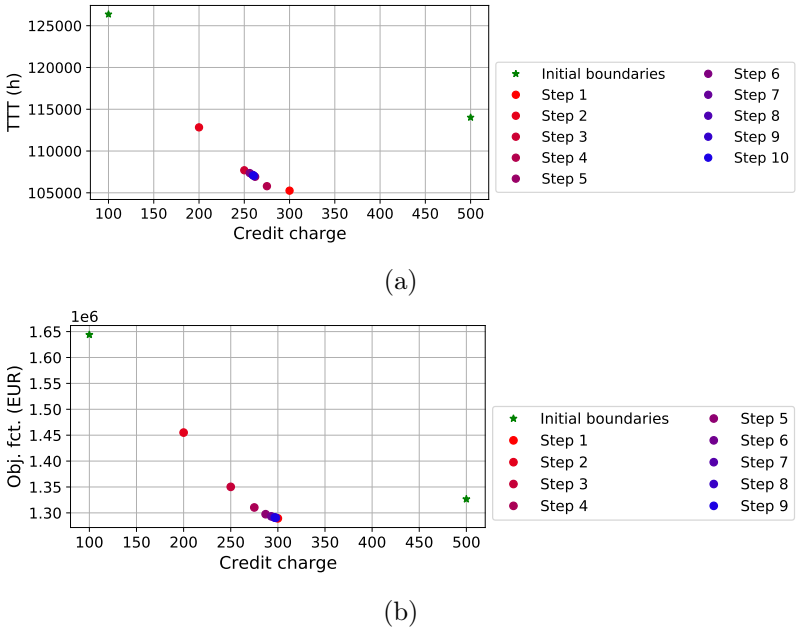

Figure 3.14: (a) Total travel time and (b) mixed objective function optimizations.

By trying to minimize the total travel time, the optimization process finds a credit charge of 260 credits, corresponding to a total travel time of 107 082 h. The optimal credit charge is actually 295 credits for a total travel time of 105 237 h. The error is only 2%. It decreases the total travel time by 15% by increasing the PT share by 20 points from 42% to 62%. The optimization process with the mixed objective ends with a charge of 297 credits for a social cost of 1 290 878 EUR. The actual optimal credit charge is 330 credits for a social cost of 1 283 803 EUR. The proposed method found a value for the social cost 0.2% away from the optimum in only nine iterations. To put it into perspective, using a greedy method and testing every credit charge between 100 and 500 credits would require 400 iterations, which means increasing the computation time by one to two orders of magnitude. Although the difference between the found and the optimal credit charge is relatively large, the difference with the objective function is minimal because the function is flat around the optimum. As expected, the credit charge found by minimizing the mixed objective is higher than the one minimizing the total travel time. It decreases carbon emissions by 45% and the total travel time by 17% by decreasing the car share by 24 points.

The total travel time and carbon emissions are compared in Table 3.4 for the credit charges found by minimizing the total travel time (260 credits) and the mixed objective function (297 credits). When minimizing the total travel time, the total travel time and the carbon emissions are higher than when minimizing the mixed objective. We would expect the total travel time to be lower. By looking at those operating points in Fig. 3.13, the credit charge of 260 credits found by minimizing the total travel time is not part of the Pareto front. However, relative to the total travel

Table 3.4: Total travel time and carbon emissions with the two objective functions.

Objective	Total travel time (h)	Carbon emissions (t)
No TCS	126 369	279.2
Total travel time	107 082	179.3
Mixed objective	105 239	154.3

time without TCS, the error stays small.

We now look at the consequences for the different groups in Fig. 3.15 in terms of money earned with the credit trade:

$$p^{\text{TCS}}(\kappa - x_i\tau), \tag{3.42}$$

time gain:

$$x_{i|\text{no TCS}}T_{i|\text{no TCS}} + (1 - x_{i|\text{no TCS}})T_i^{\text{PT}} - \left(x_iT_i + (1-x_i)T_i^{\text{PT}}\right) \tag{3.43}$$

and net gain composed of the money balance from the trade of credits plus the change in travel times:

$$p^{\text{TCS}}(\kappa - x_i\tau) + \alpha\left(x_{i|\text{no TCS}}T_{i|\text{no TCS}} + (1 - x_{i|\text{no TCS}})T_i^{\text{PT}} - \left(x_iT_i + (1-x_i)T_i^{\text{PT}}\right)\right). \tag{3.44}$$

Positive values for these three indicators are gains, which means the implementation of the TCS brings benefits (additional revenue, reduced travel time). On the opposite, negative values are losses, which means the group suffers from the TCS (additional expenditure, increased travel time). The groups spend up to 2 EUR and earn up to

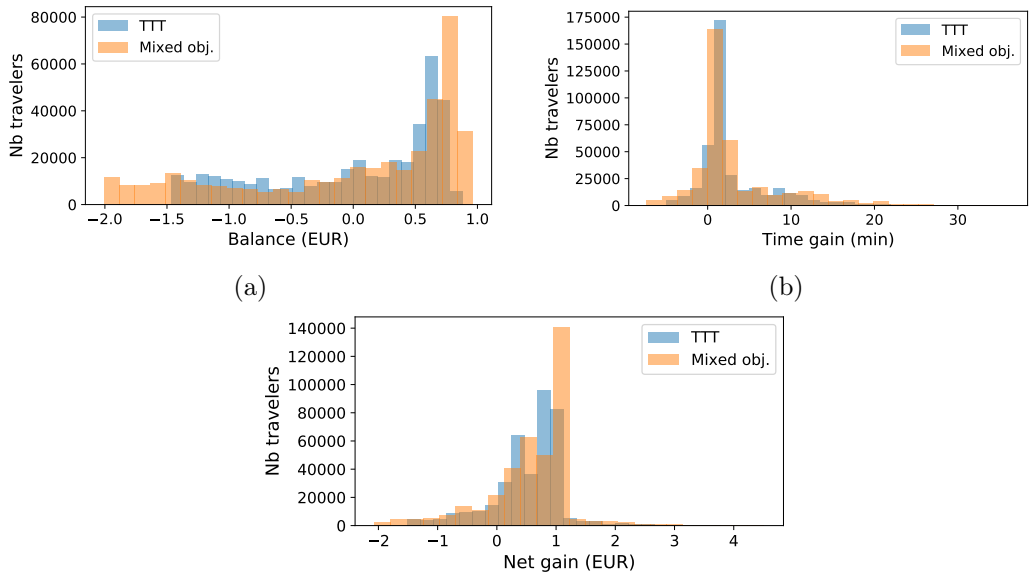

(a) (b)

(c)

Figure 3.15: (a) Trade balances, (b) time gains, and (c) net gains for the credit charges found by minimizing the total travel time and the mixed objective.

1 EUR with the credit trade. Most of the groups save travel times, and the TCS increases some travel times by at most only five minutes. When it comes to the net gain of the system, most groups are net winners with a gain up to 1 EUR. Few

travelers are losing up to 2 EUR.

3.6 Conclusions

A TCS is implemented within a trip-based MFD framework. The users are assumed to have fixed departure times and routes. They can choose between driving their private car and paying a credit charge or riding the PT using a logit model. No assumptions are made about the credit price mechanism. Such a framework account for the time evolution of traffic dynamics, including congestion effects and heterogeneous trip characteristics, unlike most existing modeling frameworks about TCS in the literature that resort to Vickrey bottleneck approaches and BPR functions.

We linearized travel times with respect to modal shares in the trip-based framework. We then derived an iterative solution method to determine the network equilibrium under the TCS constraints. Iterations consist of a local search around the last best solution following the linearized descent gradient. This method reaches model equilibrium with fewer iterations and greater precision than the classical MSA. Furthermore, it directly determines the equilibrium price value, which is not possible with the MSA. After deriving the modal equilibrium for a given credit charge, we looked for the optimal credit charge value related to the best compromise between total travel time and carbon emissions using a dichotomy-based approach. A scenario based on the network and the demand of Lyon Metropolis are presented to illustrate the TCS and the methods to compute the travel times gradient, modal equilibrium, and optimal credit charge. Depending on the chosen objective function, the optimized credit charge decreases the total travel time by about 17% and the carbon emissions by about 45%. Minimizing a mixed objective of total travel time and network emissions results in a higher credit charge than minimizing the total travel time alone. We believe that the proposed methodology is a good compromise between traffic dynamics resolution and easiness to implement and calibrate the framework for real large-scale cases. It permits not only to assess and optimize the results of the TCS at the network level (total travel time, emissions) but also to determine the consequences of the trading and choices at the individual level. This is essential to investigate the acceptability of such a scheme and look for refined tuning of the initial credit allocation. By considering the distribution of the gains, we highlight that the TCS benefits most of the users. However, there is still a minority for which the travel costs are increasing with the TCS. In this work, the credits are uniformly allocated. Especially, the allocation does not consider the heterogeneity of the OD pairs. Future work should consider leveraging the credit allocation to make the TCS profitable for as many users as possible.

Finally, the linearization method we have developed in this chapter to approximate the trip-based model outputs locally can have many other applications. It can be used to determine how the system responds to changes in control actions, e.g., traffic lights management, traffic management strategies, e.g., congestion pricing, or in users' behaviors, e.g., mode choices or departure times. One possible valuable extension of the proposed framework is to consider multi-reservoir settings to refine the spatial description of traffic conditions.

Chapter 4

Comparison of the tradable credit scheme against other demand management policies

This chapter is an updated version of the paper Balzer and Leclercq, 2022g.

This chapter compares different demand management policies: Tradable Credit Scheme (TCS), Tradable Permit Scheme (TPS), congestion pricing, and License Plate Rationing (LPR). The framework presented in the previous chapter is thus extended to account for different Demand Management Schemes (DMS). Furthermore, the credits and permits are issued with a fixed validity period of several days. Users get their credits or permits at the beginning of the period and are free to use or trade them as they want during this period. The equilibrium is thus computed over several days to evaluate the effect of being able to stock the credits and use them another day. The need to use the car depends on the day. Indeed, some specific activities might necessitate a personal car, like buying groceries or picking up children at school. To represent the costs of some activity cancellation or modification when a traveler cannot drive its car, we introduce a penalty if it rides PT on given days. This chapter also accounts for travelers not having access to a personal car, i.e., captive PT riders.

This chapter is organized as follows. In Sect. 4.1, we present the extended methodological framework. The proposed TCS and TPS are introduced in Sect. 4.2 along with LPR and pricing. The computation of the modal equilibrium is detailed in Sect. 4.3. The different DMS are benchmarked on the Lyon test case in Sect. 4.4. Sect. 4.5 concludes this chapter.

4.1 Methodological framework

The travelers from the same Origin-Destination (OD) pair are aggregated into N groups with respect to their departure times. Each group i has a fixed trip length l_i and departure time t_i. Among each group, some users take their cars while others take PT. We assume a part of each group does not have access to a personal car, and those travelers are captive PT riders. We note r_i the ratio of travelers having access to a car. There are γ_i travelers per group. $x_{d,i}$ is the fraction of car owners from the group i driving their car on day d. Thus, the fraction of the group i driving a car on the day d is $r_i x_{d,i}$. The contribution of group i to the number of car drivers is $\gamma_i r_i x_{d,i}$. $\mathbf{x_d}$ is the vector of the car shares of all groups for day d. It means, on day d, $\sum_{i=1}^{N} r_i \gamma_i x_{d,i}$

travelers drive their cars while the rest, $\sum_{i=1}^{N} \gamma_i \left((1 - r_i) + r_i(1 - x_{d,i})\right)$, ride PT. The ratio r_i is set to one in chapter 3, meaning we assumed everybody could drive a car. Group sizes are flexible and should be tuned to achieve the right balance between computation time (the larger group size, the better) and the dynamic description of the demand level (the number of travelers with the same departure time for the same OD pairs has to fall below a given threshold).

4.1.1 Mode choice

A trip-based MFD framework represents the urban transportation network. See chapter 3 for details. Captive PT riders obviously always ride transit. The remaining travelers choose between driving a car or riding PT according to the associated costs. The travel costs for a group i for a day d are given by:

$$\begin{cases} C_{i,\text{car}}(d) & = \alpha T_i(\mathbf{x_d}) + P_{k_i}; \\ C_{i,\text{PT}}(d) & = \alpha T_{i,\text{PT}} + \mu_i(d), \end{cases} \tag{4.1}$$

where α is the value-of-time (VoT) and P_{k_i} is the monetary cost associated to the demand management mechanism. k_i is the class of the trip of the group i. $\mu_i(d)$ is the penalty for using PT on one specific day d. It represents the perceived annoyance of having no other choice than using PT on a specific day when the traveler has a clear need for its personal car because it has to pick up someone or buy groceries. We name those travelers mandatory car users. The initial framework considers a single day. Furthermore, there was no PT penalty, i.e., $\mu_i(d)$ is equal to zero for all travelers, and the DMS cost P_{k_i} is the same for all travelers. The trip-dependent charges are detailed in the next section. They are part of this new contribution.

The decision process is based on the logit model (Daganzo & Sheffi, 1977). The ratio of group i which *wants* to take the car is:

$$\psi_{d,i}(\mathbf{x_d}, P_{k_i}) = \frac{e^{-\theta C_{i,\text{car}}}}{e^{-\theta C_{i,\text{car}}} + e^{-\theta C_{i,\text{PT}}}}, \tag{4.2}$$

with θ the coefficient of the logit.

4.1.2 Initial DMS

The baseline scenario is without DMS. Costs associated with DMS are set to zero:

$$P_{k_i} = 0. \tag{4.3}$$

All users who want to take their cars can drive without restriction or additional costs. The modal shares only depend on the differences of car and PT travel times and PT penalties.

Chapter 3 only focuses on TCS. Credits are distributed and traded among all the users. Each user gets κ credits from the regulator. A user needs to spend τ credits to drive its car. The credit price p^{TCS} is not known a priori and results from the offer and demand during credit trading. In practice, it is an output of the equilibrium process in addition to the modal share of each group.

The TCS specific cost is:

$$P_{k_i} = \tau p^{\text{TCS}}. \tag{4.4}$$

Note that in chapter 3, car drivers spend $(\tau - \kappa)p$ and PT riders earn κp. It is equivalent to the current formulation of the logit-based decision by multiplying both sides of the fraction in Eq. (4.2) with $e^{-\theta\kappa p}$.

4.1.3 Equilibrium computation

Since the framework considers a single day, we drop the notation d. The equilibrium is reached when the modal decisions of all groups ψ are equal to the corresponding modal shares $\mathbf{x}$. Furthermore, the consumed credits cannot exceed the allocated credits. The equilibrium under TCS is given by

$$\begin{cases} \psi & = \mathbf{x}; \\ p^{\text{TCS}} \left(\sum_{i=1}^{N} \gamma_i (\kappa - \tau x_i) \right) & = 0; \\ \sum_{i=1}^{N} \gamma_i (\tau x_i - \kappa) & \leq 0. \end{cases} \tag{4.5}$$

The two last lines of Eq. (4.5) are specific to TCS: the credit cap and the market-clearing condition (MCC). The MCC constrains the credit price: the credit price is zero, or the credits issued for this cycle are completely consumed. It is a classical assumption for a TCS at equilibrium. Note that captive PT users only influence the credit market as they sell their allocation to car drivers. They do not impact the traffic conditions.

It is formulated as an optimization problem:

$$J = \frac{1}{2} \sum_{i=1}^{N} (x_i - \psi_i)^2 + \eta \frac{1}{\sum_{i=1}^{N} \gamma_i} p^{\text{TCS}} \sum_{i=1}^{N} \gamma_i (\kappa - \tau x_i), \tag{4.6}$$

with η the coefficient related to the MCC. It is computationally advantageous to add the MCC in the objective function to avoid non-linear constraints. The global constraints are

$$\begin{cases} 0 \leq x_i \leq 1 \ \forall \ i \in [1, N]; \\ p^{\text{TCS}} \geq 0; \\ \sum_{i=1}^{N} \gamma_i \left(\tau x_i - \kappa \right) \leq 0. \end{cases} \tag{4.7}$$

The optimization problem is linearized and formulated as a Quadratic Problem (QP) to be solved iteratively until convergence is reached:

$$\frac{1}{2} \mathbf{\Delta \tilde{x}^T} \cdot \mathbf{P} \cdot \mathbf{\Delta \tilde{x}} + \mathbf{q} \cdot \mathbf{\Delta \tilde{x}}. \tag{4.8}$$

The variable $\tilde{\mathbf{x}}$ are the modal shares and the credit price: $\tilde{\mathbf{x}} = [\mathbf{x}; p^{\text{TCS}}]$, and $\mathbf{\Delta \tilde{x}}$ its variation. Its size is $N + 1$. $\mathbf{P}$ is a symmetric matrix, and $\mathbf{q}$ is a vector. The computation of this matrix and vector is based on the linearization of the travel times with respect to the modal shares:

$$T_i = T_{0,i} + \nabla_{\mathbf{x}} \mathbf{T_i} \cdot \mathbf{\Delta x} + o(\mathbf{\Delta x}) \ \forall \ i \ \in [1, N]. \tag{4.9}$$

One major contribution of chapter 3 is quantifying the delay induced by one user to the users (a.k.a. marginal external delay) in a trip-based MFD framework for a single day equilibrium.

4.2 Demand management strategies

The initial framework needs to be extended in many directions to assess the demand management strategies we have identified. It includes introducing new variables and constraints to handle a time horizon, i.e., the possibility that users can define their strategy over multiple days. We will introduce heterogeneity in user preferences over time to reproduce specific modal constraints that users may have. Also, constraints that reproduce the user behaviors should be tuned to represent not only TCS but also LPR and pricing. Finally, we want to investigate how the DMS can account for spatial adjustments, like OD or destination-specific settings. Again, adequate constraints should be defined before calculating the equilibrium.

First, we allow $\mu_i(d)$ to be non-zero on some days d to represent user- and day-specific need for a car on some days over the time horizon. Based on the trip of the group i, the charging mechanism, i.e., the toll (pricing), the number of credits needed (TCS), or the kind of permit (TPS), depends on k_i, the class of the trip of the group i. We assume the cost or restriction of car usage may be distributed over space, for example, depending on the OD pair. The DMS force some travelers to shift from car to PT. The segmentation of the DMS determines the magnitude of this shift: a TPS allows for closer control by setting OD-specific caps, and OD-specific credit charging schemes account for the heterogeneity of the PT network coverage. Some trips are more straightforward to complete with PT than others: it is usually more challenging to shift from car to PT for a trip in the suburbs than downtown. We note N_K the number of different charges, i.e., the number of different trips classes. For example, in an OD-specific charging scheme, N_K is the number of OD pairs.

The network regulator can implement different measures that foster modal shifts to manage the demand and decrease total travel time and/or carbon emission. We present here how to integrate each scheme in our modeling framework.

4.2.1 LPR

License Plate Rationing is one of the most basic and easy-to-implement DMS. It has been put in practice multiple times in different cities during pollution peaks. The LPR policy, as it has been implemented in several European cities, states that a car can be used on odd days if the plate number is odd and on even days if the plate number is even. Some users are exempt from this regulation, like low-emission vehicle owners. We assume each user owns at most one car. Thus, some users cannot drive their cars every two days. For the others, there is no additional cost:

$$\begin{cases} P_{k_i} & = \infty \text{ for those not allowed to drive;} \\ P_{k_i} & = 0 \text{ for those allowed to drive.} \end{cases} \tag{4.10}$$

It is similar to the no DMS case, except the car shares of the groups not allowed to drive are set to zero. The ratio of groups not concerned by the LPR is a parameter the authority can use to regulate the number of cars driving in the network. A ratio of 0% is a rigid LPR where the whole population undergoes the LPR, while a ratio of 100% is equivalent to the no DMS case. This ratio permits calibrating the LPR to reach given objectives in terms of congestion and pollution.

4.2.2 Pricing

Users need to pay a toll fixed by the regulator to use their car. So travellers from the group i face a toll of

$$P_{k_i} = p_{k_i}. \tag{4.11}$$

Note that given the user decision model and the mode choice, implementing an incentive scheme, i.e., rewarding travelers taking the PT with, let us say 2 EUR instead of charging those who drive their cars, is equivalent to the pricing scheme with a toll of 2 EUR. The modal shares at equilibrium are the same. The only difference is the monetary flow: the regulator would give $\gamma_i p_{k_i} ((1 - x_i)r_i + 1 - r_i)$ to the group i with the incentive scheme, whereas the group i gives $r_i \gamma_i p_{k_i} x_i$ to the regulator with pricing.

4.2.3 TCS

The credit price is the same for the whole validity period at equilibrium. If the price were higher for a day, credit sellers would sell on this day, and the buyers would buy on another day. For example, if the credits are valid for a week and cost 1 EUR on Monday and 2 EUR on Tuesday, a user would buy credits on Monday and sell them on Tuesday. The demand would thus increase on Monday and the offer on Tuesday till the prices are the same every day, and the market reaches its equilibrium. The TCS specific cost is:

$$P_{k_i} = \tau_{k_i} p^{\mathrm{TCS}}. \tag{4.12}$$

Note that in opposition to Eq. (4.4), the TCS specific cost is not the same for all travelers' groups.

4.2.4 TPS

The difference with TCS is that the permits are only valid for specific time periods or regions. The permits depend on the destination or the OD pair in this work. Each user of group i gets a fraction $\kappa_{k_i}^{\mathrm{TPS}}$ of a permit (or one permit every $1/\kappa_{k_i}^{\mathrm{TPS}}$ days). A user needs to spend one permit specific to the class k_i of its trip to drive its car. The prices of each type of permit $p_{k_i}^{\mathrm{TPS}}$ are not directly defined by the regulator and not known a priori. They result from permit trading. The main difference with the TCS is that there is one market per permit, so each permit can have a different price. Same as for the TCS, each permit price is constant over the validity cycle. The TPS specific cost is the price of the adequate permit:

$$P_i = p_{k_i}^{\mathrm{TPS}}. \tag{4.13}$$

4.2.5 Spatial variations of DMS

Every traveler faces the same credit charge in the uniform (U-) TCS, regardless of the corresponding OD-pair. However, every user has a different trip, and the corresponding PT alternative is relatively worse or better than taking the car compared to other users' trips. Thus a U-TCS could be sub-optimal by not considering such heterogeneity and creating spatial inequalities. We propose destination (D-) and OD-pair (OD-) variations for each DMS to account for this spatial heterogeneity. We make the price, credit charge or permit allocation ratio proportional to the quality of the PT alternative over the car option, w_k. w_k is computed as the trip length per car over the PT

travel time, weighted by the demand. We use the subscript k as the index for both the D or OD, as the process to compute both spatial DMS are similar. w_k is homogeneous to a speed. Since instantaneous car speed is the same for every traveler and depends on the mode choices, the car trip length is used instead of the car travel time. Let us explain the spatial DMS design for the case of a D-specific charging scheme. k refers to D. For the OD-specific case, the computation of the credit charges, permit allocations, and tolls are similar; one only needs to replace D by OD.

$$w_k = \frac{\sum_{i=1}^{N} \delta_i^k \gamma_i \frac{l_i}{T_i^{\mathrm{PT}}}}{\sum_{i=1}^{N} \delta_i^k \gamma_i}, \tag{4.14}$$

with $\delta_i^k = 1$ if and only if the D of the trip of i is k. It is zero otherwise. We define a macro credit charge τ for the TCS. We assume the allocation κ is the same for all travelers. The credit cap is set by the ratio of the charge and the allocation, so it is enough to vary one while keeping the other constant to tune the TCS. For D-TCS, the credit charge is proportional to the quality of the PT alternative: it is expensive to drive a car when the PT alternative is good and more affordable when the transit travel time is relatively high. It is computed using

$$\tau_k = \tau w_k \frac{\sum_{i=1}^{N} \gamma_i}{\sum_{i=1}^{N} \gamma_i w_{k_i}}. \tag{4.15}$$

k_i is the D of the group i. We define a macro permit ratio κ^{TPS}. It is the ratio of permits distributed averaged over all the travelers. The permit allocation per class of trip k is inversely proportional to the quality of the PT. It is more difficult for travelers with good transit alternatives to take their cars. It is defined by:

$$\kappa_k^{\mathrm{TPS}} = \frac{\kappa^{\mathrm{TPS}}}{w_k} \frac{\sum_{i=1}^{N} \gamma_i}{\sum_{i=1}^{N} \gamma_i \frac{1}{w_{k_i}}}. \tag{4.16}$$

Eq. (4.15) and (4.16) ensure the DMS is proportional to the quality of the PT alternative and the averaged number of allowed personal cars is $\frac{\kappa}{\tau}$ or κ^{TPS} times the number of travelers, i.e.,

$$\begin{cases} \frac{\sum_i^N \gamma_i \kappa}{\sum_i^N \gamma_i \tau_{k_i}} & = \frac{\sum_i^N \gamma_i \kappa}{\sum_i^N \gamma_i \tau} = \frac{\kappa}{\tau}; \\ \frac{\sum_i^N \gamma_i \kappa_{k_i}^{\mathrm{PT}}}{\sum_i^N \gamma_i} & = \frac{\sum_i^N \gamma_i \kappa_k^{\mathrm{TPS}}}{\sum_i^N \gamma_i} = \kappa^{\mathrm{TPS}}. \end{cases} \tag{4.17}$$

The macro toll price is p. For the D-specific tolls, the corresponding pricing for the class of trip k is p_k. It is computed similarly to the TCS, proportional to the quality of the PT alternative:

$$p_k = p w_k \frac{\sum_{i=1}^{N} \gamma_i}{\sum_{i=1}^{N} \gamma_i w_{k_i}}. \tag{4.18}$$

It ensures that the averaged faced toll price is p:

$$\frac{\sum_i^N \gamma_i p_{k_i}}{\sum_i^N \gamma_i} = \frac{\sum_i^N \gamma_i p}{\sum_i^N \gamma_i} = p. \tag{4.19}$$

4.3 Computing the modal equilibrium

This section presents how the solution method for calculating the SUE under TCS presented in chapter 3 should be extended to account for the new variables and constraints introduced in Sect. 4.2. The modifications to account for the new constraints related to LPR and pricing are relatively straightforward. The main contribution here is the modifications related to the time horizon, i.e., the validity cycle. In the initial problem, the SUE was calculated over the same time horizon as the demand management strategy, i.e., over one day. Now, we have a hierarchical problem where prices and quantities are equilibrated over the entire validity cycle while the modal shares are still equilibrated for each day.

The different DMS modify the costs and constraints linked to using private cars. The modal equilibrium is then different following the considered policy. We assume the regulator sets the parameters relative to the different DMS: travelers exempt from LPR, toll price, credit charge, and permit allocation. The presented framework aims at computing the equilibrium and comparing the DMS. This chapter does not optimize the DMS, even though we compare different implementations.

4.3.1 No DMS

As no constraints link the different days, the equilibrium is computed separately for each day. The solutions are different for each day because of the distribution of the PT penalties changes.

The equilibrium is reached when the modal decisions of all groups ψ_d are equal to the corresponding modal shares $\mathbf{x_d}$:

$$\psi_{\mathbf{d}} = \mathbf{x_d} \; \forall \; d. \tag{4.20}$$

With those modifications, the equilibrium computation is the same as with the initial framework, by dropping the terms and constraints linked to the price, the credit cap, and the MCC; or simply by setting $\tau = 0$ in the Eq. (4.5) to (4.8).

4.3.2 LPR

Groups not allowed to drive are removed from the vectors as their modal shares are set to zero, and they do not contribute to the congestion as they ride PT. The equilibrium solution method is the same as for no DMS in Eq. (4.20), excluding the groups not allowed to drive. The travelers allowed to drive are the ones exempted from the LPR and the ones for which the license plate number matches the ones allowed for this day (odd numbers on odd days and even numbers on even days).

4.3.3 Pricing

The pricing equilibrium method is similar to the no DMS case in Eq. (4.20). The difference is in the logit decision ψ, as users account for the toll on top of the travel time. As it is not a quantity-based DMS, no constraints connect the different days. Thus the modal shares are computed by applying the iterative method independently for each day.

4.3.4 TCS

As we now consider that the credits can be valid for a given period, the modal shares and credit price have to be computed over the complete validity cycle c. In particular, the credit cap applies to the whole validity cycle and not every single day independently. The consumed credits over the cycle cannot exceed the allocated credits during the same period. Furthermore, the credit charge is not the same for all the travelers' groups. We need to reformulate the equilibrium problem to consider several days, the ratio of travelers having access to a car, and the credit charge heterogeneity. The equilibrium differs from Eq. (4.5):

$$\begin{cases} \psi_{\mathbf{d}} & = \mathbf{x_d} \ \forall \ d \in [1, c]; \\ p^{\text{TCS}} \left(\sum_{i=1}^{N} \sum_{d=1}^{c} \gamma_i (\kappa - \tau_{k_i} r_i x_{d,i}) \right) & = 0; \\ \sum_{i=1}^{N} \sum_{d=1}^{c} \gamma_i (\tau_{k_i} r_i x_{d,i} - \kappa) & \leq 0. \end{cases} \tag{4.21}$$

The two last lines of Eq. (4.21) are specific to TCS: the credit cap and the MCC. The MCC concerns credit consumption over the whole validity cycle.

The optimization problem covers the days forming the validity cycle, and not a single day as in Eq. (4.6):

$$J = \frac{1}{2} \sum_{d=1}^{c} \sum_{i=1}^{N} (x_{d,i} - \psi_{d,i})^2 + \eta \frac{1}{\sum_{i=1}^{N} \gamma_i} p^{\text{TCS}} \sum_{d=1}^{c} \sum_{i=1}^{N} \gamma_i (\kappa - \tau_{k_i} r_i x_{d,i}). \tag{4.22}$$

The cost function is the sum of the assignment errors over the days plus the MCC, which spans over the validity cycle too. The global constraints are also modified:

$$\begin{cases} 0 \leq x_{d,i} \leq 1 \ \forall \ i \in [1, N], \ d \in [1, c]; \\ p^{\text{TCS}} \geq 0; \\ \sum_{d=1}^{c} \sum_{i=1}^{N} \gamma_i \left(\tau_{k_i} r_i x_{d,i} - \kappa \right) \leq 0. \end{cases} \tag{4.23}$$

The optimization problem is linearized and formulated as a QP to be solved iteratively until convergence is reached:

$$\frac{1}{2} \mathbf{\Delta \tilde{x}^T} \cdot \mathbf{P} \cdot \mathbf{\Delta \tilde{x}} + \mathbf{q} \cdot \mathbf{\Delta \tilde{x}}. \tag{4.24}$$

The quadratic formulation is similar, however, the matrices and vectors are larger to account for the whole validity cycle. The variable $\mathbf{\tilde{x}}$ are the modal shares for each day of the cycle and the credit price: $\mathbf{\tilde{x}} = [\mathbf{x_1}; \ldots; \mathbf{x_c}; p^{\text{TCS}}]$, and $\mathbf{\Delta \tilde{x}}$ its variation. Its size is $Nc + 1$. The symmetric matrix $\mathbf{P}$ and the vector $\mathbf{q}$ are defined by

$$\begin{cases} \mathbf{P} & = (\tilde{\nabla} \mathbf{\Psi} - \mathbf{I_x})^{\mathbf{T}} \cdot (\tilde{\nabla} \mathbf{\Psi} - \mathbf{I_x}) + \eta \mathbf{I_p}; \\ \mathbf{q} & = (\tilde{\nabla} \mathbf{\Psi} - \mathbf{I_x})^{\mathbf{T}} \cdot (\mathbf{\Psi} - \mathbf{I_x} \cdot \mathbf{\tilde{x}_0}) + \eta \mathbf{i_p}. \end{cases} \tag{4.25}$$

The first terms of $\mathbf{P}$ and $\mathbf{q}$ stand for the modal equilibrium and the second ones stand for the MCC. $\mathbf{I_x}$ the pseudo-identity matrix of size $(Nc + 1) \times Nc$, so that $\mathbf{I_x} \cdot \mathbf{\tilde{x}} = [\mathbf{x_1}; \ldots; \mathbf{x_c}]$. $\mathbf{\Psi}$ is the concatenation of the modal decisions of every day of

the cycle: $\mathbf{\Psi} = [\psi_\mathbf{1}; \ldots; \psi_\mathbf{c}]$. $\tilde{\nabla}\mathbf{\Psi}$ is defined by:

$$\tilde{\nabla}\mathbf{\Psi} = \begin{pmatrix} \nabla_{\mathbf{x_1}}\psi_\mathbf{1} & \mathbf{0} & \mathbf{0} & \mathbf{0} & \nabla_{p^{\text{TCS}}}\psi_\mathbf{1} \\ \mathbf{0} & \nabla_{\mathbf{x_2}}\psi_\mathbf{2} & \mathbf{0} & \mathbf{0} & \nabla_{p^{\text{TCS}}}\psi_\mathbf{2} \\ \mathbf{0} & \mathbf{0} & \ddots & \mathbf{0} & \vdots \\ \mathbf{0} & \mathbf{0} & \mathbf{0} & \nabla_{\mathbf{x_c}}\psi_\mathbf{c} & \nabla_{p^{\text{TCS}}}\psi_\mathbf{c} \end{pmatrix}. \tag{4.26}$$

This equation reflects the fact that the logit decision on a day is impacted by the car shares on all days, because it drives the credit consumption, which affects the credit price and thus the car travel costs. $\nabla_{\mathbf{x_d}}\psi_\mathbf{d}$ and $\nabla_{p^{\text{TCS}}}\psi_\mathbf{d}$ are respectively the gradients of the modal decision on day d with respect to the modal shares on day d and to the credit price. $\mathbf{I_p}$ is a symmetric matrix of size $(Nc+1)^2$ and $\mathbf{i_p}$ a vector of size $Nc+1$ defined by:

$$\begin{cases} I_{p,N(d-1)+i,Nc+1} & = I_{p,Nc+1,N(d-1)+i} \\ & = -\frac{\gamma_i}{\sum_{j=1}^N \gamma_j}\tau_{k_i} r_i \text{ for } (i,d) \in [1,N]\times[1,c] \\ & \text{ and 0 elsewhere;} \\ i_{p,N(d-1)+i} & = -\frac{\gamma_i}{\sum_{j=1}^N \gamma_j}\tau_{k_i} r_i p_0^{\text{TCS}} \text{ for } (i,d) \in [1,N]\times[1,c]; \\ i_{p,Nc+1} & = \frac{1}{\sum_{i=1}^N \gamma_i}\left(\sum_{d=1}^c \sum_{i=1}^N \gamma_i(\kappa - \tau_{k_i} r_i x_{0,d,i})\right). \end{cases} \tag{4.27}$$

The constraints of the iterative linearized problem are

$$\begin{cases} \Delta x_{d,i} & \leq \min(1 - x_{0,d,i}, \epsilon_x) \ \forall\ i \in [1,N],\ d \in [1,c]; \\ \Delta x_{d,i} & \geq \max(-x_{0,d,i}, -\epsilon_x) \ \forall\ i \in [1,N],\ d \in [1,c]; \\ \Delta p^{\text{TCS}} & \leq \epsilon_p; \\ \Delta p^{\text{TCS}} & \geq \max(-p_0^{\text{TCS}}, -\epsilon_p); \\ \sum_{d=1}^c \sum_{i=1}^N \gamma_i \tau_{k_i} r_i \Delta x_{d,i} & \leq \sum_{d=1}^c \sum_{i=1}^N \gamma_i \left(\kappa - \tau_{k_i} r_i x_{0,d,i}\right), \end{cases} \tag{4.28}$$

with ϵ_p a parameter restricting the search space for the credit price around the current best solution. When a better solution is found, the search space is moved around the new best one and linearizations are performed again.

4.3.5 TPS

As the permits are also issued for a cycle of c days, the equilibrium in the TPS case is defined over the validity cycle by:

$$\begin{cases} \psi_\mathbf{d} & = \mathbf{x_d} \ \forall\ d \in [1,c]; \\ p_k^{\text{TPS}}\left(\sum_{i=1}^N \delta_i^k \sum_{d=1}^c \gamma_i(\kappa_k^{\text{TPS}} - r_i x_{d,i})\right) & = 0 \ \forall\ k \in [1,N_K]; \\ \sum_{i=1}^N \delta_i^k \sum_{d=1}^c \gamma_i(r_i x_{d,i} - \kappa_k^{\text{TPS}}) & \leq 0 \ \forall\ k \in [1,N_K], \end{cases} \tag{4.29}$$

with $\delta_i^k = 1$ if and only if group i's trip is part of the k's class of trip, and 0 otherwise. The main differences with the TCS are several permit caps and MCC (one per type of permit). The decision vector is larger than the TCS one as there is one price per D or OD. The equilibrium is formulated as an optimization problem:

$$J = \frac{1}{2}\sum_{d=1}^c \sum_{i=1}^N (x_{d,i} - \psi_{d,i})^2 + \eta^{\text{TPS}} \frac{1}{\sum_{i=1}^N \gamma_i} \sum_{d=1}^c \sum_{i=1}^N \gamma_i p_{k_i}^{\text{TPS}} \left(\kappa_{k_i}^{\text{TPS}} - r_i x_{d,i}\right), \tag{4.30}$$

with η^{TPS} the coefficient related to the MCC. Note that the coefficient δ_i^k does not appear since all the N_K MCC are summed together, and each group appears exactly once in the MCC concerning its corresponding type of permit. Here again, the MCC are included in the cost function to keep all constraints linear. The global constraints are

$$\begin{cases} 0 \leq x_{d,i} \leq 1 \ \forall \ i \in [1, N], \ d \in [1, c]; \\ p_k^{\text{TPS}} \geq 0 \text{ for } k \in [1, N_K]; \\ \sum_{d=1}^{c} \sum_{i=1}^{N} \gamma_i \delta_i^k \left(\kappa_k^{\text{TPS}} - r_i x_{d,i} \right) \leq 0 \text{ for } k \in [1, N_K]. \end{cases} \tag{4.31}$$

The optimization problem is linearized and formulated as a QP to be solved iteratively around the current best solution:

$$\frac{1}{2} \mathbf{\Delta \bar{x}^T} \cdot \mathbf{P} \cdot \mathbf{\Delta \bar{x}} + \mathbf{q} \cdot \mathbf{\Delta \bar{x}}. \tag{4.32}$$

The variable $\mathbf{\bar{x}}$ are the modal shares for each day of the cycle and the permits prices: $\mathbf{\bar{x}} = [\mathbf{x_1}; \ldots; \mathbf{x_c}; p_1^{\text{TPS}}; \ldots; p_{N_K}^{\text{TPS}}]$, and $\mathbf{\Delta \bar{x}}$ is its variation. Its size is $Nc + N_K$. The symmetric matrix $\mathbf{P}$ and the vector $\mathbf{q}$ are defined by:

$$\begin{cases} \mathbf{P} & = (\bar{\nabla} \mathbf{\Psi} - \mathbf{I_x})^{\mathbf{T}} \cdot (\bar{\nabla} \mathbf{\Psi} - \mathbf{I_x}) + \eta^{\text{TPS}} \mathbf{I_p}; \\ \mathbf{q} & = (\bar{\nabla} \mathbf{\Psi} - \mathbf{I_x})^{\mathbf{T}} \cdot (\psi_{\mathbf{0}} - \mathbf{I_x} \cdot \mathbf{\bar{x}_0}) + \eta^{\text{TPS}} \mathbf{i_p}. \end{cases} \tag{4.33}$$

The first terms of $\mathbf{P}$ and $\mathbf{q}$ stand for the modal equilibrium and the second ones stand for the MCC. $\mathbf{I_x}$ is the pseudo-identity matrix of size $(Nc + N_K) \times Nc$, so that $\mathbf{I_x} \cdot \mathbf{\bar{x}} = [\mathbf{x_1}; \ldots; \mathbf{x_c}]$. $\bar{\nabla} \mathbf{\Psi}$ is defined by:

$$\bar{\nabla} \mathbf{\Psi} = \begin{pmatrix} \nabla_{\mathbf{x_1}} \psi_{\mathbf{1}} & \mathbf{0} & \mathbf{0} & \mathbf{0} & \nabla_{p_1^{\text{TPS}}} \psi_{\mathbf{1}} & \ldots & \nabla_{p_{N_K}^{\text{TPS}}} \psi_{\mathbf{1}} \\ \mathbf{0} & \nabla_{\mathbf{x_2}} \psi_{\mathbf{2}} & \mathbf{0} & \mathbf{0} & \nabla_{p_1^{\text{TPS}}} \psi_{\mathbf{2}} & \ldots & \nabla_{p_{N_K}^{\text{TPS}}} \psi_{\mathbf{2}} \\ \mathbf{0} & \mathbf{0} & \ddots & \mathbf{0} & \vdots & \ldots & \vdots \\ \mathbf{0} & \mathbf{0} & \mathbf{0} & \nabla_{\mathbf{x_c}} \psi_{\mathbf{c}} & \nabla_{p_1^{\text{TPS}}} \psi_{\mathbf{c}} & \ldots & \nabla_{p_{N_K}^{\text{TPS}}} \psi_{\mathbf{c}} \end{pmatrix}. \tag{4.34}$$

$\nabla_{\mathbf{x_d}} \psi_{\mathbf{d}}$ and $\nabla_{p_k^{\text{TPS}}} \psi_{\mathbf{d}}$ are respectively the gradients of the modal decision on day d with respect to the modal shares on day d and to the permit price of type k. $\mathbf{I_p}$ is a symmetric matrix of size $(Nc + N_K)^2$ and $\mathbf{i_p}$ a vector of size $Nc + N_K$ defined by:

$$\begin{cases} I_{p,N(d-1)+i,Nc+k_i} & = I_{p,Nc+k_i,N(d-1)+i} \\ & = -\frac{\gamma_i}{\sum_{j=1}^{N} \gamma_j} r_i \text{ for } (i,d) \in [1, N] \times [1, c] \\ & \text{ and 0 elsewhere;} \\ i_{p,N(d-1)+i} & = -\frac{\gamma_i}{\sum_{j=1}^{N} \gamma_j} r_i p_{k_i,0}^{\text{TPS}} \text{ for } (i,d) \in [1, N] \times [1, c]; \\ i_{p,Nc+k} & = \frac{1}{\sum_{i=1}^{N} \gamma_i} \left(\sum_{d=1}^{c} \sum_{i=1}^{N} \delta_i^k \gamma_i (\kappa_{k_i}^{\text{TPS}} - r_i x_{0,d,i}) \right) \\ & \text{for } k \in [1, N_K]. \end{cases} \tag{4.35}$$

The constraints are

$$\begin{cases} \Delta x_{d,i} & \leq \min(1 - x_{0,d,i}, \epsilon_x) \text{ for } i \in [1, N]; \\ \Delta x_{d,i} & \geq \max(-x_{0,d,i}, -\epsilon_x) \text{ for } i \in [1, N]; \\ \Delta p_k^{\text{TPS}} & \leq \epsilon_p^{\text{TPS}} \text{ for } k \in [1, N_K]; \\ \Delta p_k^{\text{TPS}} & \geq \max(-p_{k,0}^{\text{TPS}}, -\epsilon_p^{\text{TPS}}) \text{ for } k \in [1, N_K]; \\ \sum_{d=1}^{c} \sum_{i=1}^{N} \gamma_i r_i \delta_i^k \Delta x_{d,i} & \leq \sum_{d=1}^{c} \sum_{i=1}^{N} \gamma_i \delta_i^k \left(\kappa_k^{\text{TPS}} - r_i x_{0,d,i}\right) \\ & \text{for } k \in [1, N_K], \end{cases} \tag{4.36}$$

with ϵ_p^{TPS} a parameter restricting the search space for the permit prices around the current best solution during the iterative process.

The class of trip k can be the destination D or the OD pair in this work. We compare the different options in Table 4.1. The initial framework of Sect. 4.1, i.e., our previous work on TCS with trip-based MFD corresponds to TCS-U for $c = 1$.

Table 4.1: Comparison of the different DMS

Strategy	Type	Allocation	Charge	Nb charges	Nb markets	Nb variables
No DMS	-	-	-	-	-	N
LPR	rationing	-	-	-	-	$\leq N$
Pri-U	price	-	p	1	-	N
Pri-D	price	-	p_k	N_D	-	N
Pri-OD	price	-	p_k	N_{OD}	-	N
TCS-U	quantity	κ	τ	1	1	$cN + 1$
TCS-D	quantity	κ	τ_k	N_D	1	$cN + 1$
TCS-OD	quantity	κ	τ_k	N_{OD}	1	$cN + 1$
TPS-D	quantity	κ_k^{TPS}	1	N_D	N_D	$cN + N_D$
TPS-OD	quantity	κ_k^{TPS}	1	N_{OD}	N_{OD}	$cN + N_{OD}$

The computational complexity of the TCS and TPS is substantially higher than the other DMS as the QP size is higher. It is necessary because of the credit/permit cap and MCC over the whole validity cycle. Note that the uniform variant of the TPS is the same as the uniform variant of the TCS since there is a unique market. Thus the TPS-U is not considered because it would be redundant.

4.4 Benchmarking the different demand management policies

The users are aggregated into groups by ensuring at least two groups per hour for the same OD and that groups never gather more than 1 000 users. It is a trade-off between numerical complexity and an accurate representation of the demand dynamics at the OD level. Thus 1 374 groups are formed, representing the total demand of 384 200 travelers. To account for different days, we consider a horizon of two working weeks, i.e., $h = 10$ days. We suppose that 10% of the travelers do not have access to a car and that this ratio is homogeneous across the different groups. Table 4.2 sums up the main parameters. The numerical value for the VoT is based on the work of Fosgerau

Table 4.2: Parameters used for the simulation

Parameter	Notation	Value
VoT	α	10.8 EUR/h
MCC weight TCS	η	1
MCC weight TPS	η^{TPS}	1
Logit parameter	θ	1 1/EUR
Horizon length	h	10 days
Validity cycle	c	{1, 2, 5, 10} days
PT penalty	$\mu_i(d), i \in [1, N], d \in [1, h]$	{0, 10} EUR
Ratio of car access	$r_i, i \in [1, N]$	0.9

et al., 2007. The PT penalty is set to 10 EUR. This value ensures that almost all ($> 99\%$) mandatory car users, i.e., travelers willing to take their car the days they face the penalty, are satisfied in the no DMS case. Captive PT riders do not face the PT penalty, as they do not choose their modes. The distributions the PT penalties over the days can be found in Fig. 4.1. The sensibility to the PT penalty distribution is discussed in Appendix B.1.

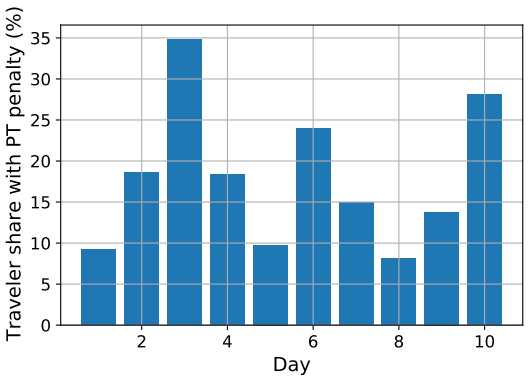

Figure 4.1: Distribution of days with PT penalty.

To compare the different DMS, we quantify various aspects: travel disutility, users' satisfaction, pollution, equivalent toll, and individual gains.

Travel disutility To assess the disutility of the travels, in the sense of travel time and PT penalty, we calculate the average total travel time TTT and penalty cost PC over the overall time horizon (ten days). The social cost SC is defined as the sum of them, with TTT being weighted by the VoT α.

$$\begin{cases} TTT &= \frac{1}{h}\sum_{d=1}^{h}\sum_{i=1}^{N}\gamma_i\left(r_i x_{d,i} T_i(\mathbf{x_d}) + (r_i(1-x_{d,i}) + 1 - r_i)T_i^{\mathrm{PT}}\right) \\ PC &= \frac{1}{h}\sum_{d=1}^{h}\sum_{i=1}^{N}\gamma_i r_i(1-x_{d,i})\mu_i(d) \\ SC &= \alpha TTT + PC \end{cases} \tag{4.37}$$

Note that travelers without access to a car do not face PT penalties. Their travel time and thus social costs remain unchanged by the DMS.

Satisfaction Furthermore, to better assess DMS acceptability at an individual level, we compute the satisfaction rate, defined as the ratio of mandatory car users

driving their cars. It is a proxy measuring how critical needs for cars can still be fulfilled under the DMS.

Pollution We also consider the cars' carbon emissions averaged over the time horizon using a COPERT IV model, i.e., assuming the emission per distance and vehicle depends on the instantaneous mean speed.

Equivalent toll To compare the financial consequences for the users of the different DMS, we assess the equivalent toll of the DMS: pricing, TCS, and TPS. The equivalent toll is the out-of-pocket money needed to drive a car. It is the average money spent by car drivers.

- The equivalent toll price is the toll price in a uniform pricing case. However, for D- and OD-specific tolling, the equivalent toll price may differ from the macro toll (weighted by the travel demand) as it is weighted by the realized car demand. The equivalent toll price for D- and OD-pricing schemes is computed as:
$$\frac{\sum_{i=1}^{N} \gamma_i x_i p_{k_i}}{\sum_{i=1}^{N} \gamma_i x_i}, \tag{4.38}$$
with k_i being the destination (for D-variant) or the OD-pair (for OD-variant) of the group i.
- It is defined by $p^{\mathrm{TCS}}(\tau - \kappa)$ for the uniform TCS. For the D- and OD-variants, it is computed with:
$$\frac{\sum_{i=1}^{N} \gamma_i x_i p^{\mathrm{TCS}}(\tau_{k_i} - \kappa)}{\sum_{i=1}^{N} \gamma_i x_i}. \tag{4.39}$$
- For TPS, it is computed in a similar manner:
$$\frac{\sum_{i=1}^{N} \gamma_i x_i p_{k_i}^{\mathrm{TPS}}(1 - \kappa_{k_i})}{\sum_{i=1}^{N} \gamma_i x_i}. \tag{4.40}$$

Individual gains The social cost gains are the difference between the perceived costs with the actual DMS and without DMS. It is defined independently of the DMS for a group i by:
$$\begin{aligned} r_i \Bigg(& x_i^{\text{no DMS}} \alpha T_i^{\text{no DMS}} + (1 - x_i^{\text{no DMS}})(\alpha T_i^{\mathrm{PT}} + \mu_i) \\ & - \big(x_i \alpha T_i + (1 - x_i)(\alpha T_i^{\mathrm{PT}} + \mu_i) \big) \Bigg). \end{aligned} \tag{4.41}$$
The trade gain is the money a traveler earns with the DMS. When negative, it means the travelers of the corresponding group are losing money, i.e., they spend more money than they earn with the DMS.

- It is negative for pricing as the travelers' money flows to the regulator. It is defined by:
$$-p_{k_i} r_i x_i. \tag{4.42}$$
- For the TCS, the trade gains are defined by:
$$p^{\mathrm{TCS}}(\kappa - r_i \tau_{k_i}^{\mathrm{TCS}} x_i). \tag{4.43}$$

- For the TPS, the trade gains are defined by:

$$p_{k_i}^{\mathrm{TPS}}(\kappa_{k_i}^{\mathrm{TPS}} - r_i x_i). \tag{4.44}$$

In the following, different labels are used to name the different configurations of the DMS in the figures.

- For pricing, it is the macro toll level p in euro.
- For LPR, it is the ratio of the population exempted from (or non-complying to) LPR.
- For TCS, it is the ratio of the allocation over the macro credit charge κ/τ (short credit ratio). For the uniform case, this ratio also represents the maximum ratio of car drivers over all the travelers. The maximum car share is unknown for the D- and OD cases, as the groups face different credit charges.
- For TPS, it is the macro permit allocation κ^{TPS}. It also represents the maximum car share.

Furthermore, to avoid any confusion, the labeling of the DMS follows the conventions [DMS]-[charging], [DMS]-[charging][validity cycle], or [DMS]-[charging][validity cycle][DMS parameter] depending on the context. So TCS-D10-50% refers to the TCS with a D-specific charging scheme with a validity cycle of ten days and a ratio allocation over charge of 50%, i.e., at the maximum, every second traveler can drive a car.

For all the presented results, the convergence quality is measured by the quadratic cost over the validity cycle length J/c. It is smaller than 1.4×10^{-2}.

4.4.1 Comparing the DMS with uniform charging settings

First, we compare the different DMS: pricing, LPR, and TCS with uniform charging settings. The different DMS are associated with different parameters and settings (credit charge for TCS, toll price for pricing, exemption ratio for LPR), and there is no direct equivalence between them. Comparing two individual scenarios corresponding to two different DMS may appear challenging. However, a fair comparison can be achieved by assessing the different DMS globally using a wide range of parameters covering the most plausible values. We can then compare the network performances at equilibrium by analyzing the relative positioning of the associated curves. Thus, we compare the DMS as a whole, and we do not pair single configurations. The effects on travel time, satisfaction rate, carbon emission, social cost, equivalent toll, and car share of the DMS with uniform settings are compared in Fig. 4.2 for a validity cycle of one day. As expected, implementing a DMS decreases the satisfaction rate because restrictions or increased costs for car travel push users towards PT options. The satisfaction rate decreases rapidly with LPR and falls as low as 50%. Such a policy is myopic and affects users respectless of their actual needs. When fully enforced, half of the mandatory car users cannot use it (exemption rate of 0%). The satisfaction rate only begins to drop for a relatively high toll with pricing. It is only when the toll price reaches the penalty value that mandatory car users start considering PT options. A uniform TCS with an allocation/charge ratio of 33% (maximum one car driver every three travelers) reduces the satisfaction rate by less than 5 points. With

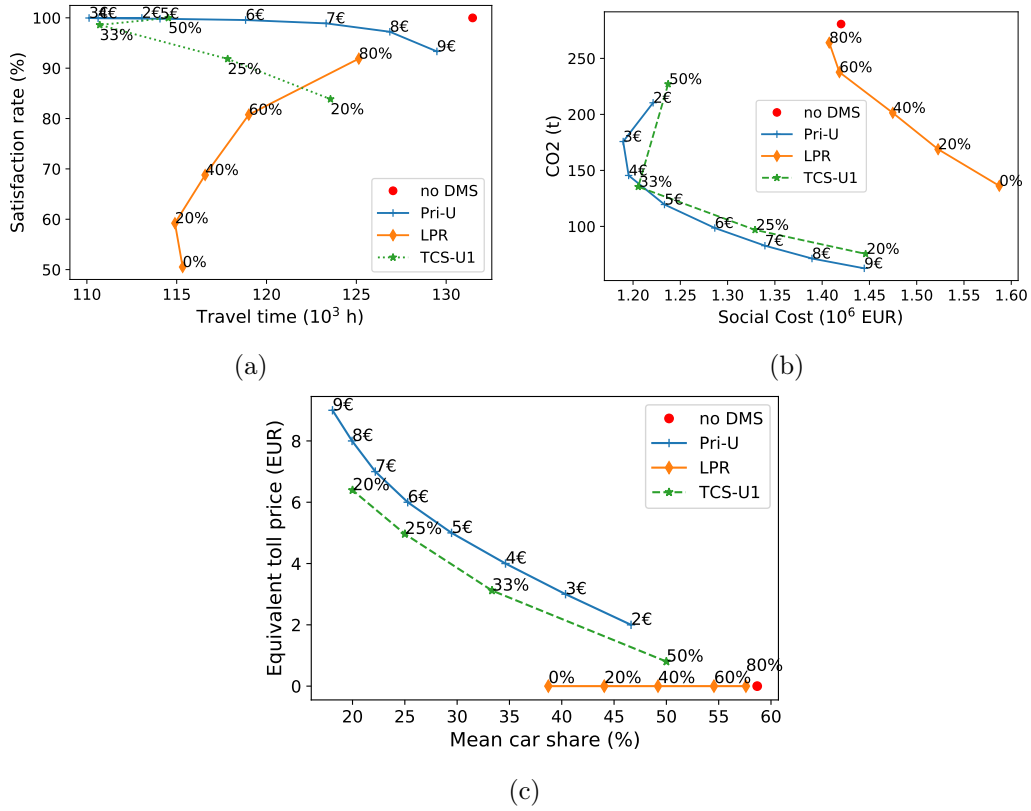

Figure 4.2: Comparison of the uniform DMS for a cycle of one day: (a) total travel time vs. penalty cost, (b) social cost vs. carbon emission, (c) car share and equivalent toll price.

the same settings, the network carbon emissions drop by around 50% and the social cost by about 15%. The same effects can be observed with an urban toll of 4 EUR, but the equivalent toll for a TCS of 33% is only about 3.1 EUR, see Fig. 4.2c. The equivalent toll with TCS is about 1 EUR cheaper than pricing to achieve the same car share reduction. Indeed, as a part of the needed credits are given by the regulator, car drivers only need to buy the remaining credits. The Pareto fronts formed by the pricing are slightly better than the TCS-U. They are better than the LPR, which reduces carbon emissions at the expense of the satisfaction rate and social costs. They enable better compromises between carbon emissions and social costs. The LPR is limited when reducing the modal share and cannot lead to a car share of less than 39%. The mean car share without any restrictions is 59%.

We also look at the distributions of the social gains: the congestion pricing and the TCS give analog distributions. The toll level of 4 EUR and credit ratio of 33% were chosen for the comparison as they give similar social costs and carbon emissions. It permits the comparison of the individual impacts of all DMS, considering the same general output in terms of network performances. We compare those gains in Fig. 4.3. The distribution of social costs, i.e., accounting for the change in travel time and PT penalty, are similar. Some travelers lose the equivalent of 20 EUR, while a few earn up to 70 EUR over the time horizon. However, the bulk of the population earns a social gain between 0 and 10 EUR. So the vast majority of the travelers are better off with TCS or pricing in terms of travel conditions. As the TCS is revenue-neutral, some travelers earn money by selling the credits they do not need. In particular, a specific user can pay some days but get money on other days, reducing its overall

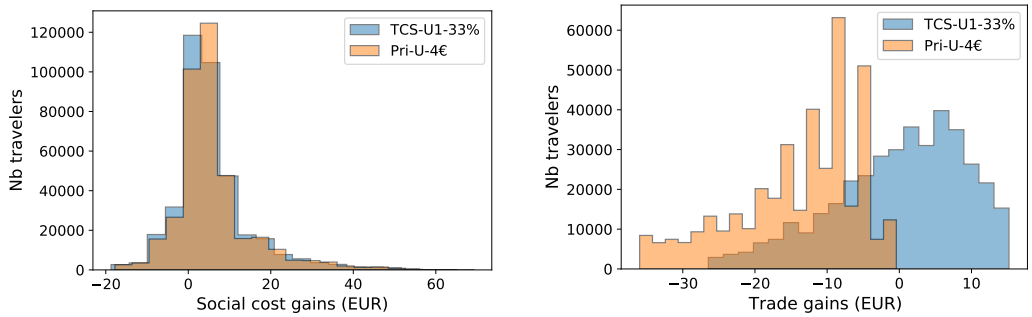

(a) (b)

Figure 4.3: Comparison of the distributions of the (a) social and (b) trade gains between uniform TCS with a validity cycle of one day and pricing.

balance over the time horizon. With pricing, some travelers spend on average up to 4 EUR per day because of the toll, while they spend a maximum of 3.1 EUR per day for buying credits with TCS. Without redistribution, all users spend money under a pricing scheme. This result illustrates one advantage of TCS over pricing: some travelers are rewarded for their choices.

We compare travel time, satisfaction rate, carbon emission, and social cost for the DMS with uniform setting and a cycle length of ten days in Fig. 4.4. The main improvement by increasing the validity cycle from one to several days is that the drop in satisfaction rate with TCS is smaller. Less than 3% of necessary car trips are canceled in the very restricting case of one car trip per working week per traveler (credit ratio of 20%). By giving more flexibility for the credit consumption, it is easier and cheaper for the mandatory car drivers to fulfill their needs. With a validity cycle of ten days, the Pareto fronts of TCS-U and pricing for satisfaction rate vs. total travel time and carbon emissions vs. social costs overlap. It is not surprising, as the credit price is the same every day when the validity cycle equals the horizon under consideration. The modal shares with TCS-U10 are then equivalent to congestion pricing with a toll of $p = p^{\text{TCS}}\tau$ (the allocation does not matter when it comes to the modal shares, see the remark following Eq. (4.4)). It thus leads to the same modal shares and same traffic conditions. Note that the equivalent toll price is still 1 to 2 EUR cheaper with TCS (Fig. 4.4c), thanks to the initial allocation of κ credits.

4.4.2 Different spatial charges

We now assess the effect of charging differently the travelers according to their destinations or OD-pairs in Fig. 4.5 for TCS and pricing. Increasing the spatial resolution from uniform to destination and then OD negatively affects the Pareto fronts of carbon emissions vs. social costs. It means when choosing the macro toll price of credit ratio to reach a desired carbon reduction, the associated social costs with the U-variant are lower than with the OD-variant. In other words, reducing carbon emissions requires a greater sacrifice with the OD-variant than with the U-variant. For pricing, reaching a carbon level of 100 t requires a toll between 6 and 7 EUR for the uniform variant. The corresponding social cost is 1.3×10^6 EUR. The OD pricing variant with a macro toll of 8 EUR leads to the same pollution reduction. However, the corresponding social cost is 1.4×10^6 EUR, 8% higher. We would expect the opposite since the OD- and D-schemes try to account for the relative burden of switching from car to PT. To

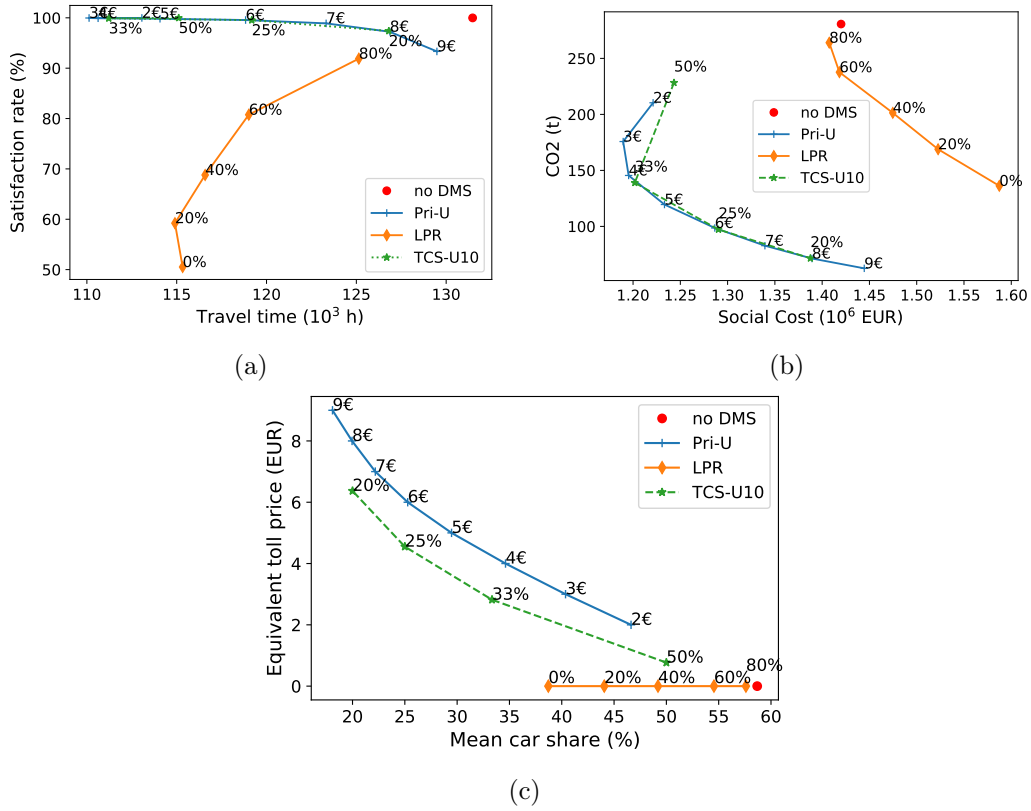

Figure 4.4: Comparison of the uniform DMS for a cycle of ten days: (a) total travel time vs. penalty cost, (b) social cost vs. carbon emission, (c) car share and equivalent toll price.

understand this difference, we compute the modal equilibrium for pricing without PT penalty (i.e., with $\mu_i(d) = 0\ \forall i, d$) in Fig. 4.6. We represent the total travel time instead of the social cost because without PT penalty, the penalty cost is zero, and thus the social cost is the total travel time weighted by the VoT. It seems that without PT penalty, the D- and OD-specific pricing charging schemes lead to better compromises in terms of congestion and pollution for low total travel time. Especially, the OD variant leads to total travel times below 105×10^3 h. However, those specific schemes do not account for the day-specific need to use the car, which appears to play a crucial role when calculating the equilibrium situations, more important than the quality of the PT coverage. Note that the PT penalty represents the same cost as a travel time of about one hour with the chosen parameters.

We compute the distribution of the permit prices for TPS-D and TPS-OD with a macro permit ratio of respectively 30% and 40% (they lead to similar carbon emissions and social costs) in Fig. 4.7. With the D-variant, the permit prices are only between 4.4 and 6.3 EUR, while they go from 0.1 to 11.8 EUR with the OD setting. It is explained by the smaller number of markets in the D case where larger quantities of permits are traded than the OD-variant. A larger trade quantity stabilizes the market, as the effect of the marginal utility of a permit for a traveler (especially when it absolutely needs to drive a car) is less representative.

The performances of D-specific DMS are compared in Fig. 4.8, and the OD-specific in Fig. 4.9 for a validity cycle of one day. For the D-case, pricing is slightly better than TCS and TPS because its Pareto front dominates the trade-off proposed by

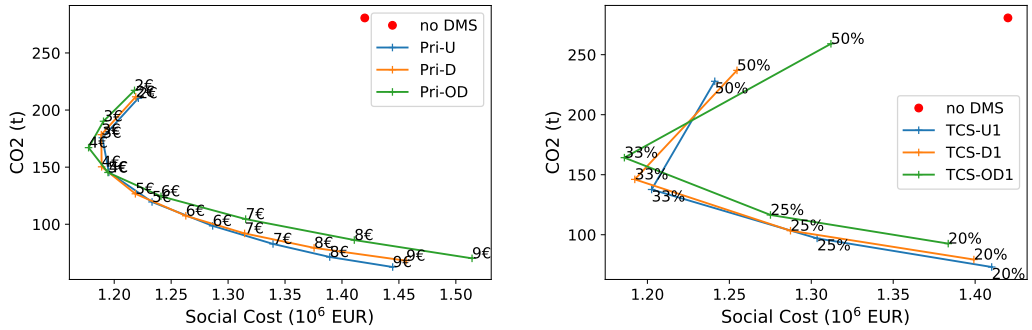

(a) (b)

Figure 4.5: Social cost vs. carbon emissions for (a) pricing and (b) TCS for a validity cycle of one day.

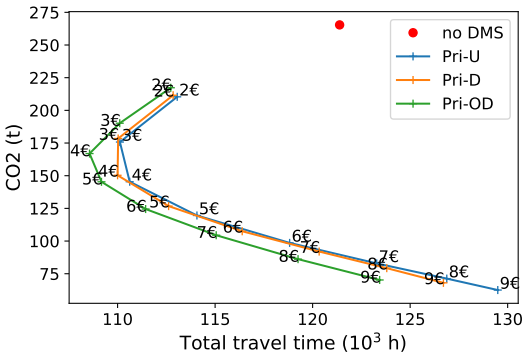

Figure 4.6: Total travel time vs. carbon emissions with pricing without PT penalty.

TCS-D and TPS-D. For a carbon level of 100 t, the corresponding social cost is about 1.3×10^6 EUR with pricing and more than 1.35×10^6 EUR with TCS and TPS. For a given car share, the equivalent toll faced by the users is lower with TCS, by 1 to 2 EUR for pricing and some dozens of cents for TPS. Note that the equivalent toll price (y-axis) differs from the macro toll price (labels), as the first is weighted by the travel demand (car and PT), and the realized car demand weights the second. We draw the same conclusions for the OD-specific case as for the D-specific case: better compromises with pricing, especially it can lead to a social cost of less than 1.2×10^6 EUR, while it is not the case with TCS or TPS. The TPS leads to similar or worse compromises in the OD case than pricing and TCS. Especially, the TPS-OD is adequate to reduce the carbon emission but not the social cost. This scheme is expected to be the least flexible since there are 224 different types of permits, and travelers trade exclusively along with travelers with the same route.

When the validity cycle is ten days, the results are slightly different, see Fig. 4.10 for D- and Fig. 4.11 for OD-specific DMS. As noticed and explained before, pricing and TCS are equivalent when the validity cycle is ten days, the number of days under consideration, because the credit price is constant over the days. For the D-specific variants, pricing, TCS, and TPS are equivalent for social costs and carbon emissions. The flexible consumption of credits and permits compensates their drawbacks in comparison to pricing. For the same mean car share over the horizon of ten days, the equivalent toll with TCS and TPS is lower than pricing by 1 to 2 EUR. For the OD-specific cases, TPS leads to better compromises for high carbon emissions reduction. For the same pollution levels, let us say by dropping to 100 t of carbon emissions,

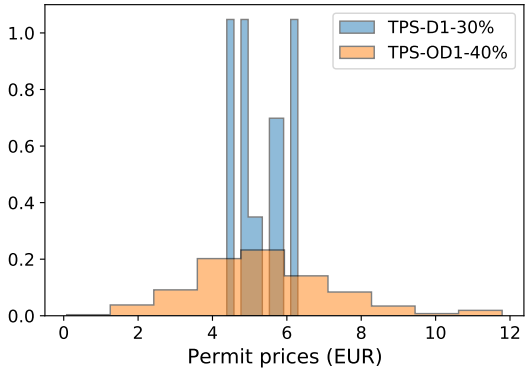

Figure 4.7: Distribution of the permits prices, averaged over the two working weeks, for a validity cycle of one day.

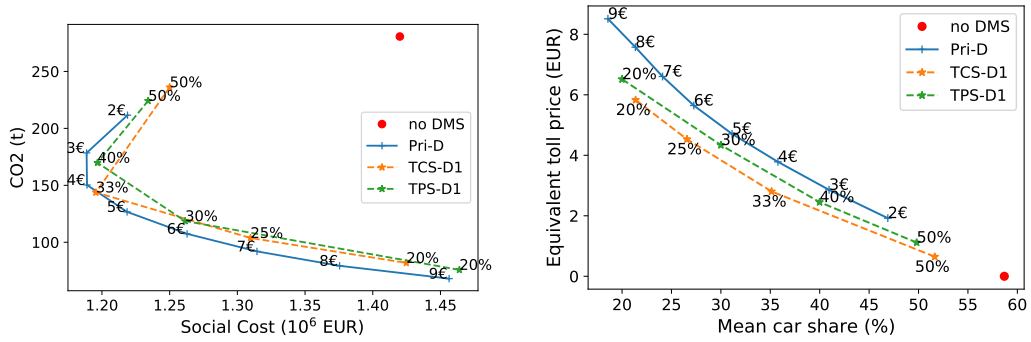

(a) (b)

Figure 4.8: (a) Social cost vs. carbon emission and (b) car share and toll equivalent for D-specific DMS for a validity cycle of one day.

the social cost is 1.4×10^6 EUR for pricing (7 EUR) and TCS (between 20% and 25 %), and only 1.3×10^6 EUR for TPS (30%). Furthermore, to reach this carbon reduction objective, the equivalent toll is 3.4 EUR with TPS, 4-5 EUR with TCS, and 6 EUR with pricing. TPS-OD leads to better compromises and is cheaper for travelers than TCS-OD and OD-specific pricing for a validity cycle of ten days. Here again, increasing the cycle improves the quantity-based DMS.

4.4.3 Different cycle lengths

We compare the TCS for different validity cycles: one, two, five, and ten days. We investigate the impacts on mode share, traffic conditions, and credit price.

TCS-Uniform

The effects of a longer validity cycle for a uniform TCS for a credit ratio of 33% on car share and equivalent toll price are showed in Fig. 4.12 . According to Fig. 4.12, increasing the validity cycle leads to more variations in the number of cars per day. As expected, with a validity cycle of one day, the car share is 33% every day. For a cycle of two to ten days, it oscillates between 25% and 45%. It is low on days with fewer mandatory car drivers to save them for days with high demand, i.e., lots of

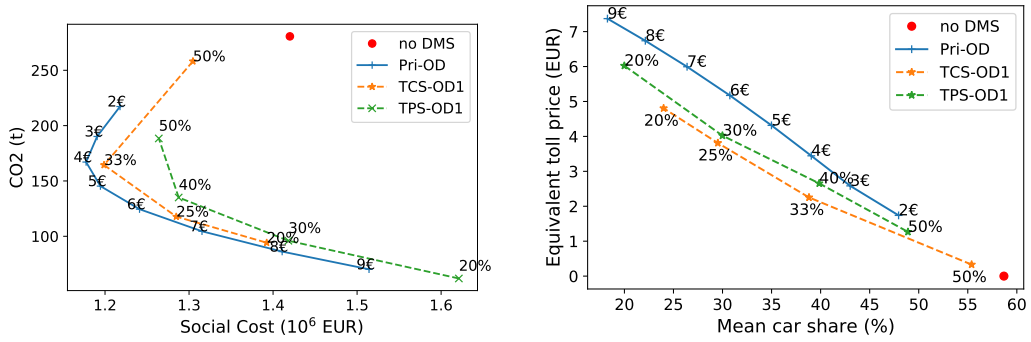

(a) (b)

Figure 4.9: (a) Social cost vs. carbon emission and (b) car share and toll equivalent for OD-specific DMS for a validity cycle of one day.

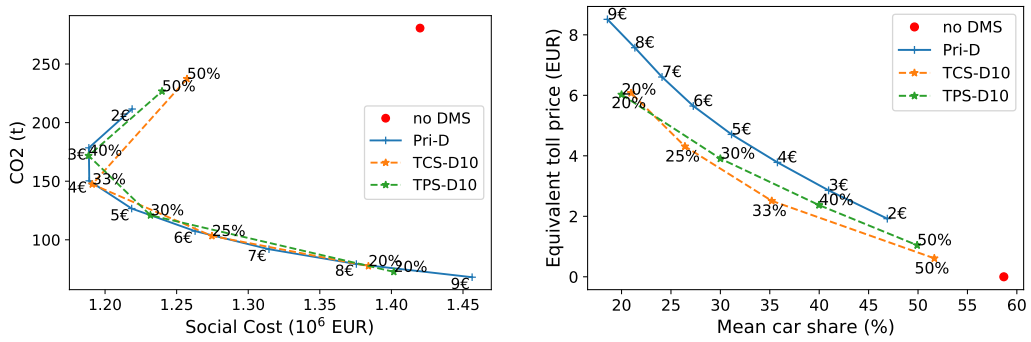

(a) (b)

Figure 4.10: (a) Social cost vs. carbon emission and (b) car share and toll equivalent for D-specific DMS for a validity cycle of ten days.

mandatory car drivers. This effect is easily observed for two days during the cycle formed by days 3 (high demand) and 4 (low demand). However, a longer validity cycle stabilizes the price. The equivalent toll increases from 2.4 EUR to 6 EUR for a cycle of one day, whereas it is practically constant and equal to 2.8 EUR for a cycle of five days. The Pareto front social cost vs. emission slightly improves as the validity cycle increases. We compute some day-to-day indicators in Fig. 4.13: total travel time, satisfaction rate, social cost, the total traveled distance by car, mean car speed, and carbon emissions. The variations of the total travel time because of the cycle length are minimal with respect to their absolute values. The satisfaction rate increases with the validity cycle lengths. On day 3, lots of travelers need to drive their cars. The satisfaction rate is less than 94% for a cycle of one day and almost 100% for five and ten days. The consequence is that the penalty cost, and thus the social costs present a peak on day 3 for a cycle of one day: 1.35×10^6 EUR against an average value of 1.2×10^6 EUR. The total travel distance, the mean speed, and thus the network carbon emissions present more variations across the days as the cycle length increases. It is because the number of cars per day is not fixed. Only the average over the validity cycle is. The carbon emission varies by about 50% with a cycle length of five or ten days: from less than 120 t on day 1 to a peak around 180 t on day 3 when lots of travelers are mandatory car drivers. It is relatively constant with a cycle of one day. However, the average stays almost the same over the days since the number of cars driving over the horizon of ten days is the same regardless

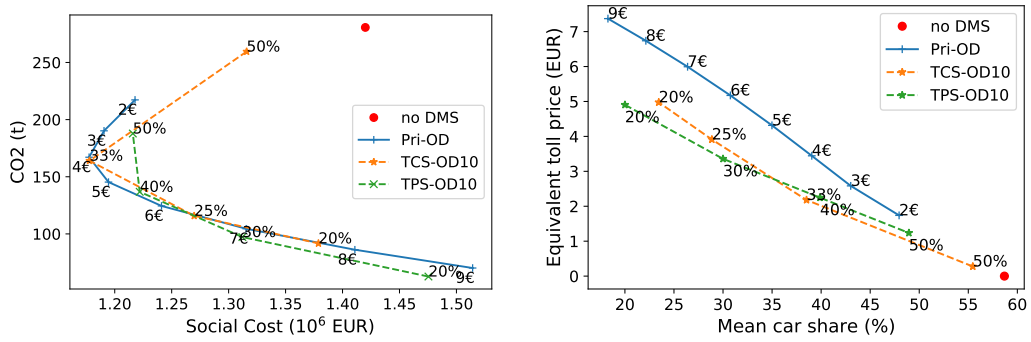

(a) (b)

Figure 4.11: (a) Social cost vs. carbon emission and (b) car share and toll equivalent for OD-specific DMS for a validity cycle of ten days.

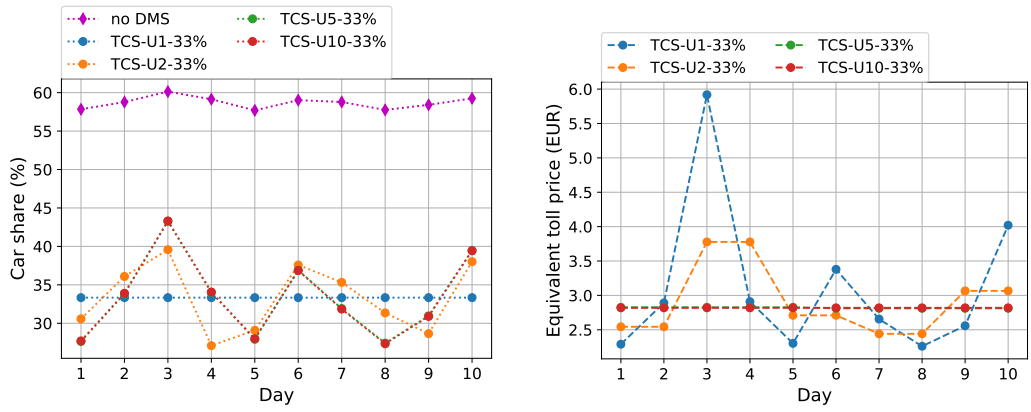

(a) (b)

Figure 4.12: TCS-U with the different cycles: (a) car share and (b) equivalent toll. The credit ratio is 33%.

of the validity cycle. Increasing the validity cycle gives more flexibility to travelers. It leads to a better satisfaction rate, almost total satisfaction at the expense of the variability of the traffic conditions. However, the average travel conditions (travel time and emissions) are similar regardless of the validity cycle.

The distribution of the social and trade gains is presented in Fig. 4.14. The validity cycle has little impact on the distribution of the social and trade gains among the travelers over the two working weeks because the main effects of the validity cycle are the variability of the indicators like prices and total travel times over the days, the average values remain similar. The validity cycle does not affect the distribution of the gains and, in that sense, does not affect the equity of the DMS.

TCS-Destinations

The effects on car share and equivalent toll price of a longer validity cycle for a D-specific TCS are showed in Fig. 4.15 for a macro credit ratio of 33%. The car share with a validity cycle of one day is around 35%. It is not constant and equal to the macro credit ratio of 33% because as all the users are not facing the same credit charges, the consumption of all the credits does not lead to the number of cars on the

network. Especially, the observed car share is higher than the macro credit ratio, as travelers with bad PT alternatives, and thus more prone to drive the car, face lower credit charges. With a higher validity cycle, the car share varies between 30% and 45%. Increasing the validity cycle leads to more variations in the number of cars per day, with up to 15-point changes for cycles of five and ten days, but stabilizes the price. The equivalent toll oscillates between 2 and more than 5 EUR for a validity cycle of one day and stays around 2.5 EUR for five and ten days. The Pareto front social cost/emission slightly improves as the validity cycle increases. Note that for a cycle of ten days, even if the credit price is constant over the days, the equivalent toll is not. As for the similar observation regarding the car shares, since the credit charge is D-specific, the toll equivalent depends on the destination. As different travelers, with different destinations, are driving their cars on different days, the equivalent toll varies because it depends on the car shares (see Eq. (4.39)). Here again, the conclusions are the same: a large validity cycle stabilizes the price at the expense of the variability of the traffic conditions.

TCS-OD pairs

The effects on car share and equivalent toll price of a longer validity cycle for an OD-specific TCS are shown in Fig. 4.16 for a macro credit ratio of 33%. This credit ratio is chosen as it leads to a similar emission/social cost compromise are the U and D variant for ratios of 33%, see Fig. 4.5.

The car share varies between 36% and 41% for a cycle of one day. As explained earlier, the car share is not constant and equal to the macro credit ratio for the D-case because all travelers are not facing the same credit charge. Increasing the validity cycle allows more variability for the car share: between 33% and 47%. The equivalent toll oscillates between 1.4 and 4 EUR for a validity cycle of one day and varies only between 2 and 2.5 EUR for five and ten days. The Pareto fronts social cost/emissions and slightly improves as the validity cycle increases. Here again, the conclusions are the same: a large validity cycle stabilizes the price at the expense of the variability of the traffic conditions.

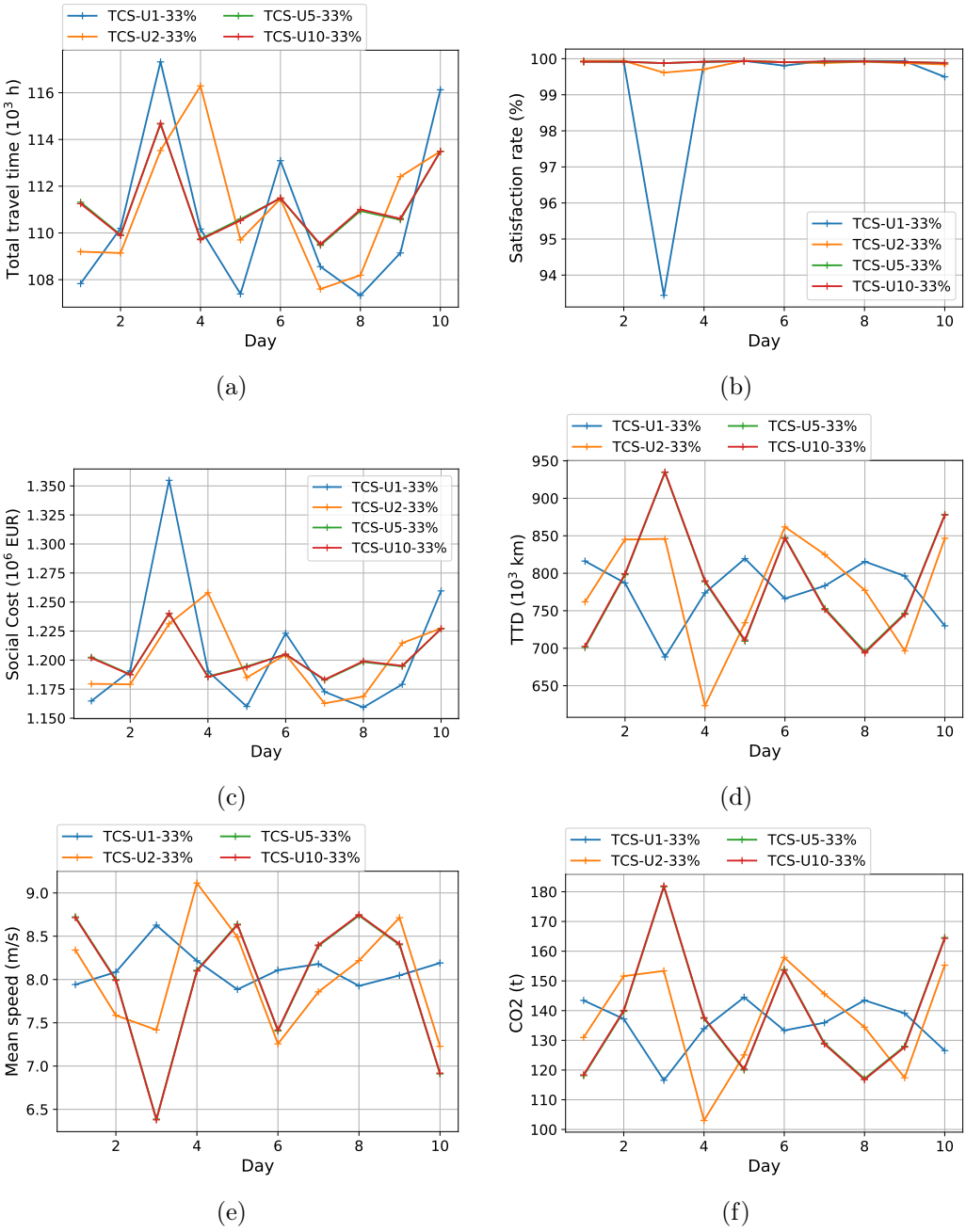

Figure 4.13: TCS-U with the different cycles: (a) total travel time, (b) satisfaction rate, (c) social cost, (d) total traveled distance, (e) mean car speed, and (f) carbon emissions. The credit ratio is 33%.

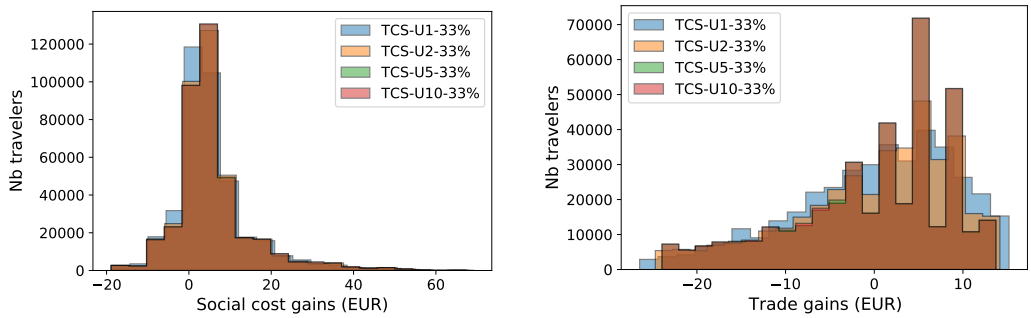

(a) (b)

Figure 4.14: (a) Social and (b) trade gains distribution with TCS-U over the different cycles. The credit ratio is 33%.

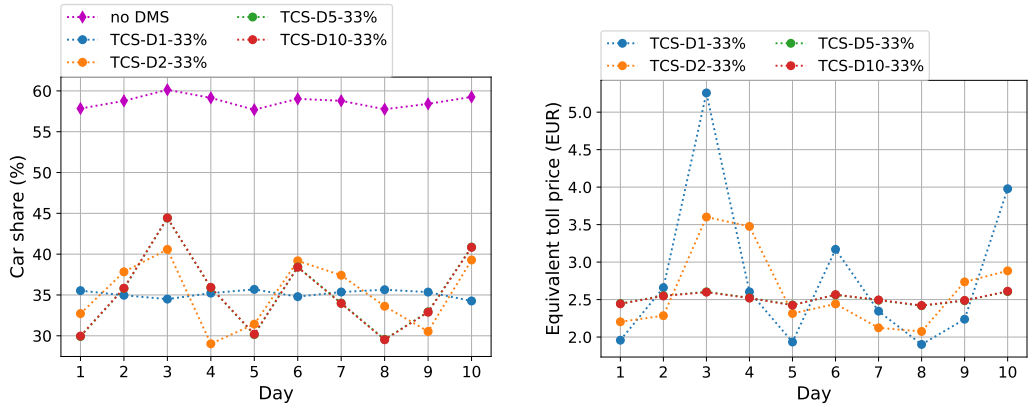

(a) (b)

Figure 4.15: TCS-D with the different cycles: (a) car share and (b) equivalent toll. The macro credit ratio is 33%.

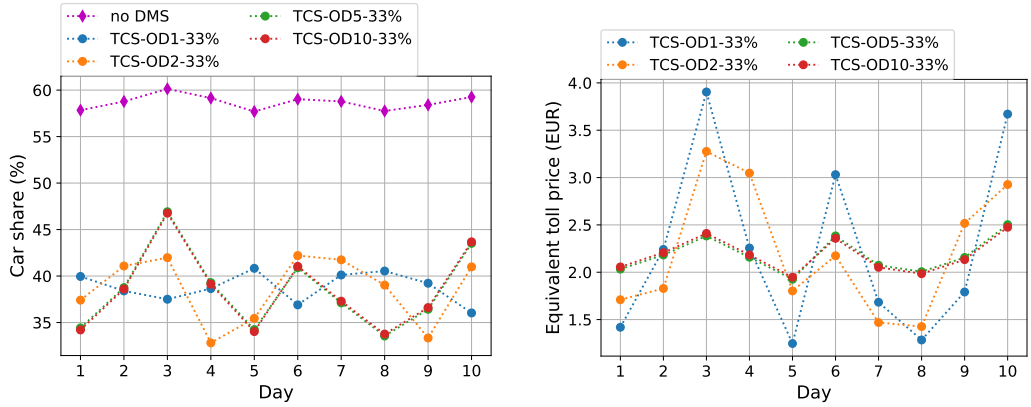

(a) (b)

Figure 4.16: TCS-OD with the different cycles: (a) car share and (b) equivalent toll. The macro credit charge is 33%.

4.5 Conclusions

This study provides a deeper look into TCS and TPS performances compared to pricing and LPR when considering congestion dynamics and a time horizon during which the credits/permits can be used. The credits/permits are issued with a validity period of several days. Every day is specific because, even if the demand stays the same, traveling by car brings a different utility for each traveler and day by introducing a penalty term. The framework accounts for captive PT travelers. The developed methodology is applied on a typical morning commute in Lyon. The complexity of the case study (more than 380 000 travelers) permits a realistic benchmarking of the different DMS in a dynamic environment.

The results draw several conclusions with regard to the impacts on the transportation system:

- Pricing and TCS allow for better social cost and carbon emissions compromises than the established LPR or even TPS.
- For similar reductions of social cost and carbon emissions, the equivalent toll faced with TCS is significantly smaller than the pricing toll. Furthermore, TCS is neutral. There is no money flow from the users to the regulator. It is indeed a decentralized policy with a collective bound. A traveler can occasionally drive its car without spending a single euro with a large enough validity cycle, only by stocking its credits. However, a similar money balance at equilibrium can be achieved through toll revenue distribution, but travelers would need to advance the money.
- Charging schemes accounting for the quality of the PT alternative do not reduce even further social costs and carbon emissions for this specific case study. They do not seem robust, as the presence of a day-specific need to drive a car might be more important than the heterogeneity of the PT coverage. However, this observation should be confirmed by studying other case studies and different settings.
- A validity cycle of several days for the credits leads to similar or even better congestion and pollution reduction performances. It stabilizes the credit price and increases the satisfaction rate by providing more flexibility for travelers.

The performances of the congestion pricing are similar to the TCS. However, there are some advantages to the quantity-based DMS. Thanks to the credit cap, the regulator has less uncertainty about the maximum number of vehicles on the network. The TCS defines an overall objective in terms of car usage, while the marketplace defines the credit price. It does not need to find and set the price leading to the desired mode shift. Achieving the same results with congestion pricing requires fine-tuning the tolls to find the targeted equilibrium, which is challenging in practice. The method can easily be transferred to other test cases and scenarios.

Chapter 5

Dynamic tradable credit scheme for multimodal urban networks

This chapter is an updated version of the paper Balzer, Ameli, Leclercq, and Lebacque, 2023.

The previous chapters aimed at estimating the effect of the TCS in a dynamic traffic set-up and compare TCS with other DMS. In this chapter, we propose an extended framework to account for departure time choice on top of mode choice; the effect of car congestion on PT operations; the heterogeneity of travelers' VoT; an additional travel alternative (carpooling); time-dependent credit charging.

5.1 TCS models in urban areas

We proceed with a literature review on traffic congestion models and multimodality in TCS frameworks.

Considering different vehicles may not be enough to account for the diversity of mobility supply, especially with the rise of ride-hailing and -sharing services. A passenger car offers two different transportation alternatives if driven alone or used for carpooling. Certain recent contributions in the literature (L. L. Xiao et al., 2016, 2021; L. L. Xiao, Liu, Huang, & Liu, 2021; Yu et al., 2019) have promoted carpooling to foster more sustainable travel behavior by reducing the number of vehicles in circulation. In the general framework, two travelers with similar trips would use only one car instead of two cars. On the one hand, users can drive on the High Occupancy Vehicle (HOV) lane, with the travelers sharing the expenses: fuel, congestion pricing, or credit/permit purchase. On the other hand, carpooling induces a penalty representing the detour, waiting time or the discomfort of not driving alone. The aim of this work is to integrate time-dependent TCS, congestion dynamics and multimodality, including carpooling, into a single framework.

A substantial part of the literature on TCS is aimed at optimizing travelers' route choices by charging the links of the networks, e.g., Yang and Wang, 2011. The implementation of these contributions in an urban area is complex in practice. The present work focuses on mode and departure time choices at the network level. Most studies in the literature have used *Vickrey bottleneck* model to address TCS at the network level to reduce congestion (Jia et al., 2016; Miralinaghi et al., 2019; Nie, 2015; Nie & Yin, 2013; L. J. Tian et al., 2013; L. L. Xiao et al., 2015). Furthermore, Bao et al., 2019 considered *Chu model* (Chu, 1995), which is based on the BPR function. In

the studies mentioned, the credit charge is dynamic, meaning the number of credits required to pass the bottleneck is time-dependent (i.e., based on the choice of departure time). The purpose is to encourage travelers to switch from on-peak to off-peak hours. However, most considered only a single transportation mode with a homogeneous traveler profile. Miralinaghi et al., 2019; L. J. Tian et al., 2013; L. L. Xiao et al., 2015 accounted for different Values of Time (VoT) to represent the heterogeneity of monetary valuation of travel time for the personal car with Vickrey bottleneck.

We consider a multimodal extension of the generalized bathtub model (Jin, 2020) to address the network equilibrium with a heterogeneous demand profile and investigate the effect of a TCS on mode and departure time choices.

Moreover, we take into account environmental measures (CO2 emissions) not only to evaluate the performance of TCS but also to optimize the dynamic charging profile. In the literature, few studies consider environmental goals with TCS at the link level (Gao & Sun, 2014). To highlight our contributions, we compare the most relevant studies on TCS at the network level, including the departure time choice problem in Table 5.1, along with previous works on MFD under TCS. This study addresses the gap between realistic congestion representation and dynamic TCS. It should be recalled that dynamic TCS means that the credit charge may change depending on the time. The time- and mode-dependent TCS is aimed at fostering shifts of mode and departure times to mitigate congestion and reduce the carbon footprint of the transportation network. We consider three travel modes: personal car, PT, and carpooling.

Table 5.1: Comparison of related contributions on TCS

Article	Congestion model			Travel choice				Different VoT	Dynamic charging scheme	Pollution
	Vickrey	Trip-based MFD	Multimodal generalized bathtub	Departure time	Car	PT	Carpool			
Nie and Yin, 2013	✓			✓	✓					
L. J. Tian et al., 2013	✓			✓	✓	✓		✓	✓	
Nie, 2015	✓			✓	✓				✓	
L. L. Xiao et al., 2015	✓			✓	✓			✓	✓	
Jia et al., 2016	✓			✓	✓				✓	
Miralinaghi et al., 2019	✓			✓	✓			✓	✓	
Bao et al., 2019	✓			✓	✓				✓	
R. Liu et al., 2022		✓		✓	✓			✓	✓	
Chapters 3 and 4		✓			✓	✓				✓
This work			✓	✓	✓	✓	✓	✓	✓	✓

The remainder of this chapter is organized as follows. In Sect. 5.2, we present the multimodal generalized bathtub framework with the TCS: congestion dynamics, TCS, users' decision, and equilibrium formulation. Sect. 5.3 formulates the computation of the SUE and the optimization of the credit charge profile. The case study and the associated results are presented in Sect. 5.4 for a realistic morning commute scenario in Lyon (France) with 384 200 trips in total. Sect. 5.5 concludes this chapter.

5.2 Problem formulation

This section describes the proposed methodological framework to address the TCS problem, including the SUE calculation based on the multimodal generalized bathtub under TCS. Fig. 5.1 depicts an overview of the different components and interactions in our framework. In Fig. 5.1, the travelers get a fixed amount of credits daily from the regulator. They choose their transportation mode *and departure time* according to the credit charging profiles and scheduling preferences. The regulator determines the

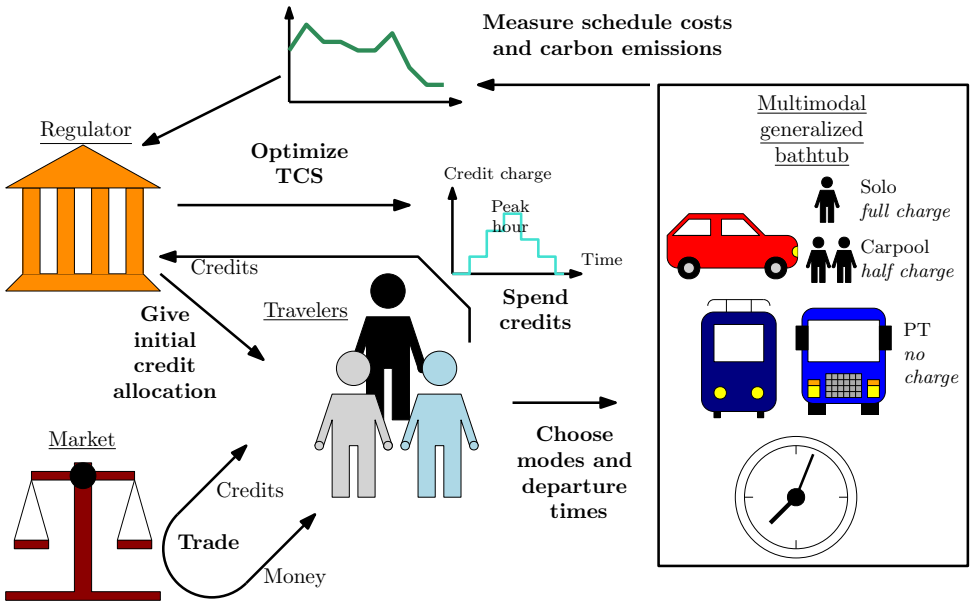

Figure 5.1: Framework of the multimodal bathtub under TCS.

credit charging profile to achieve its economic and environmental goals. The following subsection presents the congestion model based on the generalized bathtub. Then the TCS is presented with a dynamic charging profile. Finally, we present the user choice model and the SUE formulation.

For convenience, the notations are summed up in C.1.

5.2.1 Multimodal generalized bathtub

Here we introduce the concepts, assumptions, and notations related to the congestion model.

In this framework (see Fig. 5.1), travelers have different characteristics: trip length $l \in \mathcal{L}$, desired arrival time, $t_a \in \mathcal{T}_a$, and scheduling preferences α_c, $\tilde{\beta}_c$, and $\tilde{\gamma}_c$ associated to their socioeconomic class $c \in \mathcal{C}$. The capital and curly letter represents the domain of validity of the respective parameter or variable. They choose their departure times $t_d \in \mathcal{T}_d$ and travel modes $m \in \mathcal{M}$ according to the corresponding travel costs. $\mathcal{M}$ is the discrete set of all available transportation modes.

The demand scenario defines their VoT, trip length, and desired arrival time for all users. It is described by the distribution $d = d(c, l, t_a)$. D denotes the total number of travelers. Traffic assignment will allocate each user to a departure time and a mode. We represent the user distribution by the distribution f that encompasses all their characteristics (VoT, trip length, desired arrival time, departure time, mode) $f = f(c, l, t_a, t_d, m)$. In this chapter, we consider three transportation modes: car solo (one traveler per car), carpooling (two travelers per car), and public transportation (PT). ζ_m is the waiting time linked to mode m. We set it to zero for the solo car drivers and PT riders. We neglect the PT waiting time (typically half of the head time) as we focus on the morning commute scenario when the PT frequency is high and the average waiting time is only a few minutes. It represents the extra time related to carpooling (waiting and small detour time). We assume no distinction between driver's and passenger's travel time and credit charge when carpooling. It means the

driver waits at its origin, and its waiting time in its car is equivalent to the passenger walking time to the driver's origin during ζ_m. Then both start their trips.

The user cost of mode m is calculated based on the arrival time obtained by bathtub dynamics equations. This congestion model assumes all trips take place in the same overall region, where the speed is spatially uniform. The mean speed for a given time is a function of the number of vehicles (personal cars, buses, tramways) circulating in the network at this time. A vehicle enters the network at the departure time t_d and leaves it once it has driven its trip length l.

To address the realistic demand profile based on trip data, we use the discretization approach to represent the formulation of the multimodal generalized bathtub to compute the arrival times via the trajectory of the virtual traveler z_m and the accumulation H_m, which are inter-dependent.

Discretization

The discretization approach aims to compute the arrival times of the multimodal generalized bathtub (Eq. (2.5)) in uniform intervals. Note that the discretization is not applied in the previous chapters 3 and 4, since we used a more advanced trip-based MFD simulation framework, wherein the arrival times are computed following an event-based simulation: the state variables are updated each time a vehicle enters or leaves the network. The equilibrium computation was based on the linearization of the travel times with respect to the mode choices. This former approach is not suited here for the following reasons: (i) the travel time linearization while accounting for departure time becomes too complex as it adds another dimension to the problem; (ii) for each trip length, departure time, and mode, we would need one agent to account for the effect of this specific demand on the congestion. The computational cost of event-based resolution of the trip-based MFD increases quickly with the number of agents, as the state variables are updated each time an agent enters or leaves the network. The main difference between the two approaches is that the trip-based MFD framework follows each traveler and tracks its remaining travel distance. On the contrary, the generalized bathtub focuses on the distribution of the remaining trip lengths with fixed time steps. It is advantageous in terms of complexity and computation time to use the generalized bathtub framework, which is continuous. However, in a later section (5.4.3), we will simulate the optimal TCS solution with the more advanced trip-based MFD formulation to show that using the simplified approximation through the discretization of the generalized bathtub model in the optimization process makes perfect sense.

We approximate the solution $(z_m(t), H_m(t))$ as piece-wise affine functions calculated at nodal points. The numerical resolution of the bathtub requires the discretization of the trip length, departure time, and desired arrival times. The values of those discretized parameters and variables are identified by the following indexes:

$$\begin{cases} i_l = \lfloor (l - l_{\min})/\Delta_l + 0.5 \rfloor; \\ i_{t_d} = \lfloor t_d/\Delta_t + 0.5 \rfloor; \\ i_{t_a} = \lfloor (t_a - t_{a,\min})/\Delta_{t_a} + 0.5 \rfloor, \end{cases} \tag{5.1}$$

with $l_{\min}$ the minimum trip length and $t_{a,\min}$ the minimum desired departure time. $\lfloor x \rfloor$ is the integer part of x, i.e., the highest integer smaller than x. The first admissible

departure time is taken as reference, i.e., is zero. The simulation time shares the same discretization as the departure times.

One can come back to the continuous value of the variables from the indexes:

$$\begin{cases} l = l_{\min} + i_l \Delta_l; \\ t = i_t \Delta_t; \\ t_a = t_{a,\min} + i_{t_a} \Delta_{t_a}. \end{cases} \tag{5.2}$$

In the rest of the chapter, we use both the discrete and continuous formulations for the arguments of the functions interchangeably. The discrete versions of the demand and the assignment are defined by:

$$\begin{cases} d(c, i_l, i_{t_a}) & = \int_{\Theta(i_{t_a})} \int_{\Theta(i_l)} d(c, l, t_a) \mathrm{d}t_a \mathrm{d}l; \\ f(c, i_l, i_{t_a}, i_{t_d}, m) & = \int_{\Theta(i_{t_a})} \int_{\Theta(i_l)} \int_{\Theta(i_{t_d})} f(c, l, t_a, t_d, m) \mathrm{d}t_a \mathrm{d}l \mathrm{d}t_d; \end{cases} \tag{5.3}$$

with

$$\begin{cases} \Theta(i_{t_a}) & = [t_{a,\min} + (i_{t_a} - 0.5)\Delta_{t_a}, t_{a,\min} + (i_{t_a} + 0.5)\Delta_{t_a}], \\ \Theta(i_l) & = [l_{\min} + (i_l - 0.5)\Delta_l, l_{\min} + (i_l + 0.5)\Delta_l], \\ \Theta(i_{t_d}) & = [(i_{t_d} - 0.5)\Delta_t, (i_{t_d} + 0.5)\Delta_t]. \end{cases} \tag{5.4}$$

$$\begin{cases} z_m(i_t) & = z_m(i_{t-1}) + \Delta_t v_m \left(\{H_{m'}(i_{t-1}) + \sum_{c, i_{t_a}, i_l} f(c, i_l, i_{t_a}, i_t, m')\}_{m' \in \mathcal{M}} \right) \\ H_m(i_t) & = \sum_{i_{t_d} \leq i_t} F_m \left(\max(0, \lfloor \frac{(z_m(i_t) - z_m(i_{t_d}) - l_{\min})}{\Delta_l} \rfloor), i_{t_d} \right) \\ F_m(i_l, i_{t_d}) & = \sum_{i_{l'} \geq i_l} \sum_{c, i_{t_a}} a_{i_{t_d}, i_{l'}} f(c, i_{l'}, i_{t_a}, i_{t_d}, m) \end{cases} \tag{5.5}$$

Recall that F_m is a density with respect to t_d. $F_m(i_l, i_{t_d})$ is defined as the integral of $F_m(l, t_d)$ over $\Theta(i_{t_d})$. z_m and H_m are initialized with zero. The second part of the first equation allows us to account for the accumulation due to the trips starting during the current time step i_t. It counterbalances the fact that the bathtub tends to underestimate the congestion compared to the exact solution (computed via the trip-based MFD framework). Without this correction, the underestimation can be significant: with the case study, the equilibrium without TCS based on the generalized bathtub corresponds to gridlock with the exact solution (trip-based MFD). Adding the accumulation of trips starting during the current time step does not increase the computation time and memory requirements. On the contrary, increasing the time discretization to reach a satisfying precision mobilizes more resources.

The dynamics computation involves the resolution of Eq. (2.5) time step after step. The integration of the virtual traveler trajectory is straightforward: on each time step i_t, the traveled length z_m increased with the speed corresponding to the previous accumulation $H_m(i_{t-1})$ plus the trips starting in this step. The accumulation computation is represented by the yellow area in Fig. 5.2.

The accumulation at the time $t = \Delta_t i_t$ gathers all vehicles that have already started their trips and have a remaining travel distance strictly positive. Each square contributes to the accumulation at i_t with $a_{i_{t_d}, i_l} \in [0, 1]$ the ratio of the square above the line $t_d \mapsto z_m(i_t) - z_m(t_d)$ (i.e., the yellow part) multiplied by the number of trips starting at i_{t_d} with trip length i_l, $\sum_{c, i_{t_a}} f(c, i_l, i_{t_a}, i_{t_d}, m)$.

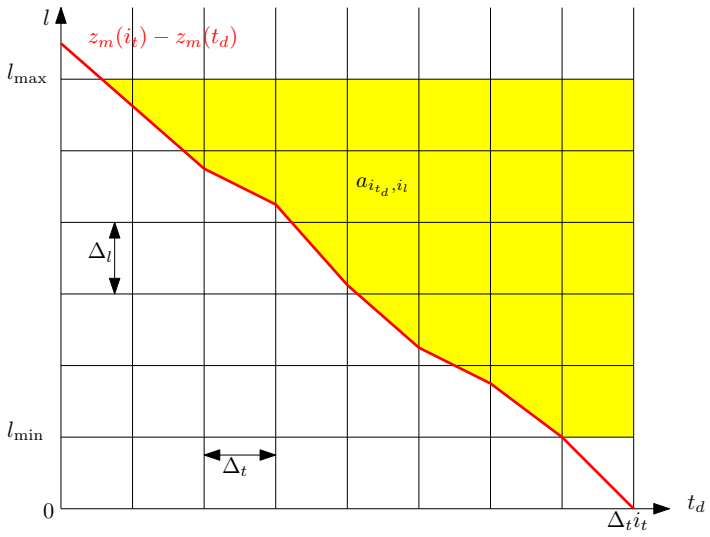

Figure 5.2: Discretization of the accumulation computation.

5.2.2 Dynamic Tradable Credit Scheme

After presenting how traffic dynamics are affected by travelers' choices, we introduce the proposed demand management policy designed for the regulator to incite travelers to change their behaviors. Some mobility alternatives require credits depending on the transportation mode m and departure time t_d. The credit charge is significant for highly congestive modes like private cars during peak hours and low for more sustainable choices like PT or carpooling outside peak hours. The regulator should set the charging profile $\tau(t_d, m)$ according to congestion and carbon emissions goals. In the following, the regulator only chooses the profile for car drivers $\tau(t_d, \text{car})$. It is free for PT riders: $\tau(t_d, \text{PT}) = 0$ and only the half for carpoolers as we assume two travelers per car: $\tau(t_d, \text{pool}) = \frac{1}{2}\tau(t_d, \text{car})$. Travelers receive a free initial allocation of κ credits from the regulator. They can trade the credits between themselves in a dedicated market. The credit price p is not fixed by the regulator. This is the main difference with congestion pricing: with TCS, the regulator defines the quantity and not the price, while for pricing, the regulator sets up the price but not the quantity. When equilibrium is reached, TCS and pricing may lead to the same results, but TCS makes it easier to meet collective optimum as the quantity is defined by design. It is determined by the law of supply and demand in the market. We do not consider the details of the trade mechanism. We adopt the widely used Market Clearing Condition (MCC), as in Yang and Wang, 2011 and the previous chapters, to represent the market mechanism: the price is zero or all issued credits are spent.

5.2.3 Mode and departure time choice

Travelers' choices depend on the travel times depending on the traffic dynamics, the different alternatives, and the additional cost caused by the TCS, depending on the credit charge and the credit price. The travel time (TT) of a traveller leaving at t_d and arriving at $\hat{t}_a$ is

$$TT = \hat{t}_a - t_d. \tag{5.6}$$

The travel cost (TC) accounts for the early or late arrival on top of the TT. The TC of a traveler of the class c with the desired arrival time t_a finishing its trip at $\hat{t}_a$ is

$$TC = \alpha_c \left((\hat{t}_a - t_d) + \tilde{\beta}_c \max(0, t_a - \hat{t}_a) + \tilde{\gamma}_c \max(0, \hat{t}_a - t_a) \right). \tag{5.7}$$

α_c, $\tilde{\beta}_c$, and $\tilde{\gamma}_c$ are respectively the VoT (money per time) and the normalized marginal cost (no unit) for early and late arrival.

The user cost (UC) is obtained by adding the TCS-related cost, i.e., the monetary value of the required credits:

$$UC = TC + p \cdot \tau(t_d, m). \tag{5.8}$$

Both TC and UC depend on trip length, departure time, mode, desired arrival time, and class. However, we do not make it explicit in the equations to keep the notations light.

We assume the users' decision processes follow the logit model to account for irrationality and uncertainty in their choices while keeping the framework tractable. The discrete logit-based decision depends on the UC of all alternatives regarding departure time and mode choice and on the logit parameter θ_c:

$$\psi(c, i_l, i_{t_a}, i_{t_d}, m) = \frac{e^{-\theta_c UC(c, i_l, i_{t_a}, i_{t_d}, m)}}{\sum_{i_{t'_d}, m'} e^{-\theta_c UC(c, i_l, i_{t_a}, i_{t'_d}, m')}}. \tag{5.9}$$

$\psi(c, i_l, i_{t_a}, i_{t_d}, m)$ is the ratio of travelers with characteristics c, i_l, i_{t_a} *wanting* to travel at t_d with mode m. It may be different from the *actual* travel choices $f(c, i_l, i_{t_a}, i_{t_d}, m)/d(c, i_l, i_{t_a})$. We assume all travelers have access to all modes. We especially consider all travelers have access to a car: the one they own, if they own one, or a shared or rental car. Such an assumption can also be found in L. J. Tian et al., 2013; L. L. Xiao, Liu, Huang, and Liu, 2021.

5.2.4 Equilibrium formulation

The SUE formulation is based on Lebacque et al., 2022. It is extended to account for the mode choice and the TCS constraints. The SUE is reached when the user distribution matches the logit distribution:

$$d(\omega)\psi(\omega) = f(\omega) \ \forall \ \omega \in \Omega, \tag{5.10}$$

with $\Omega = \mathcal{C} \times \mathcal{L} \times \mathcal{T}_a \times \mathcal{T}_d \times \mathcal{M}$ the space of all travelers' characteristics and degrees of freedom. The demand conservation requires the travel demand with specific characteristics to match the sum of the user distributions with the same characteristics:

$$\sum_{i_{t_d}, m} f(c, i_l, i_{t_a}, i_{t_d}, m) = d(c, i_l, i_{t_a}) \ \forall \ c, i_l, i_{t_a}. \tag{5.11}$$

The TCS-specific constraints are, respectively, the credit cap (CC): the consumed credits cannot exceed the allocated amount, the MCC, and the positivity of the price:

$$\begin{cases} \sum_{\omega\in\Omega} f(\omega)\tau(\omega) \leq D\kappa; \\ \left(\sum_{\omega\in\Omega} f(\omega)\tau(\omega) - D\kappa\right) p = 0; \\ p \geq 0. \end{cases} \tag{5.12}$$

5.3 Methodological Framework

Our contribution consists in computing the SUE under TCS, i.e., finding the travelers' choices (mode and departure time) and the credit price; and optimizing the credit charge τ to fulfill societal goals in terms of total travel cost and carbon emissions. Previous works on the generalized bathtub (Ameli et al., 2022; Lebacque et al., 2022) focused on calculating departure time distribution, excluding mode choice and optimization of TCS variables, i.e., a part of the blue inner loop. The equilibration of the multimodal generalized bathtub model under TCS is decomposed into two imbricated loops. The outer loop increases (respectively decreases) the price if too many (too few) credits are consumed until the MCC and CC hold: (i) price is zero and some credits are not used, or (ii) all credits are consumed. The inner loop changes the travelers' departure times and travel modes until their logit-based decisions match their actual travel choices. The two loops form two imbricated fixed-part problems to be solved. Fig. 5.3 presents the two loops: blue for the assignment and green for the credit price. The red one indicates the optimization of the charging profile. It is not part of the fixed-point problem. The role of this third loop is presented in subsection 5.3.3.

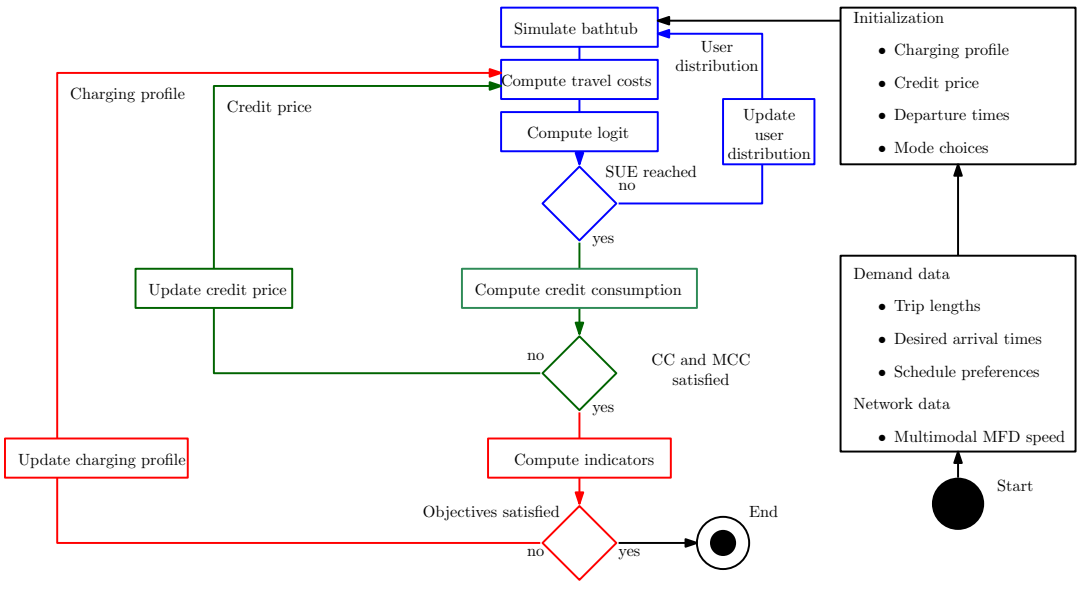

Figure 5.3: Algorithm flowchart.

5.3.1 Credit price

We define the credit consumption excess R as

$$R = \frac{1}{D} \sum_{\omega \in \Omega} f(\omega) \left(\frac{\tau(\omega)}{\kappa} - 1 \right). \tag{5.13}$$

It is the normalized number of credits used minus the initial allocation. The CC dictates it should be negative: we accept unused credits but not the consumption of non-existing ones. The CC error is defined as the positive part of R:

$$E_{\text{CC}} = \max(0, R). \tag{5.14}$$

The MCC error is defined as

$$E_{\text{MCC}} = p\kappa|R|. \tag{5.15}$$

It is high when the price is non-zero, and all credits are not consumed. We use the absolute value of R to ensure a positive metric for the MCC error.

We change the credit price if one of the error measures E_{CC} or E_{MCC} is higher than the given respective thresholds E^*_{CC} and E^*_{MCC}. The price variation of the CC and MCC loop for the iteration $i_{\text{step,pri}}$ of the price loop is

$$\Delta p = \frac{1}{\sqrt{i_{\text{step,pri}}}} \frac{1}{\kappa} R. \tag{5.16}$$

The amplitude of the change decreases as the loop iterates to force convergence but not too fast to allow for space exploration. This process is typical when solving a fixed-point problem, e.g., the Method of Successive Average (MSA) (Sheffi, 1985). We bound Δp by $\pm\epsilon_p$, a fixed threshold, to prevent large oscillations. The price is then updated by ensuring it stays positive:

$$p = \max(p + \Delta p, 0). \tag{5.17}$$

The price loop iterates until the maximum number of iterations is reached or both CC and MCC errors fall below the given thresholds.

5.3.2 Assignment

The SUE error quantifies the difference between user distribution and logit-based decision:

$$E_{\text{SUE}} = \frac{1}{D} \sum_{\omega \in \Omega} |f(\omega) - d(\omega)\psi(\omega)|. \tag{5.18}$$

The assignment loop starts with an initial solution based on free flow mean speed and then iterates until the maximum number of iterations is reached or the SUE error falls below a threshold E^*_{SUE}. A heuristic reassignment algorithm is designed to correct the worst decisions (assignment far from logit) with a procedure similar to the MSA. We first rank the assignment based on the SUE error. Then, we choose the proportion of the assignments with larger errors and reassign their departure time and mode choice. This procedure is inspired by Sbayti et al., 2007. The proportion corresponds to the step size of the algorithm. A search index is defined and initialized with $r = 1$. For each iteration of the SUE loop, the fraction $1/r$ of the assignment characteristics $\omega \in \Omega$ where the assignment error $|f(\omega)/d(\omega) - \psi(\omega)|$ is the largest, is updated. We

name this part of the travel characteristics $\mathcal{F}$. The rest of the characteristics define the ensemble $\bar{\mathcal{F}}$. Thus $\mathcal{F} \cup \bar{\mathcal{F}} = \Omega$ and $\mathcal{F} \cap \bar{\mathcal{F}} = \varnothing$. The step size formulation is the same as the step size of the MSA method; however, we use the smart step size approach (Ameli et al., 2020) to update the step size for the following iterations. If the new user distribution leads to a smaller SUE error E_{SUE}, then the search index stays the same. Otherwise, the search index r increases by one, decreasing the search radius. The convergence of this approach is discussed in Ameli, 2019. We stop once the SUE error falls below a given threshold or the best solution (lowest SUE error) is returned if the maximum number of iterations is reached.

As we modify the user distribution, we need to ensure the conservation of the travel demand (Eq. (5.11)). The total change of the user distributions from $\mathcal{F}$ is spread among the configurations not selected to be changed ($\bar{\mathcal{F}}$). We first need to ensure the sum of the unchanged user distributions $\bar{C}$ of $\bar{\mathcal{F}}$ (positive) is big enough to absorb the sum of the changes C of $\mathcal{F}$ (positive or negative) if we use the update coefficient $1/r$:

$$\begin{cases} C &= \sum_{\omega \in \mathcal{F}} \frac{1}{r}(d(\omega)\psi(\omega) - f(\omega)); \\ \bar{C} &= \sum_{\omega \in \bar{\mathcal{F}}} f(\omega). \end{cases} \tag{5.19}$$

If $\bar{C}$ is larger than C, then we can use the update factor $\mu = 1/r$ as we can ensure the demand conservation by counterbalancing the deviation from the demand d using $\bar{\mathcal{F}}$. If it is not the case, the update factor μ is scaled down:

$$\begin{cases} \mu = \frac{1}{r} & \text{if } \bar{C} \geq C; \\ \mu = \frac{\bar{C}}{C}\frac{1}{r} & \text{if } \bar{C} < C. \end{cases} \tag{5.20}$$

The user distribution update follows:

$$\begin{cases} f_{\text{new}}(\omega) &= (1-\mu) f(\omega) + \mu d(\omega)\psi(\omega), \ \forall \omega \in \mathcal{F}; \\ f_{\text{new}}(\omega) &= \left(1 - \frac{C}{\bar{C}}\right) f(\omega), \ \forall \omega \in \bar{\mathcal{F}}. \end{cases} \tag{5.21}$$

It means we use $1/r$ as an update factor, except if the change quantity C is higher than the unchanged one $\bar{C}$. In this case, we cannot ensure the demand conservation without scaling down the update factor μ.

5.3.3 Optimization of the charging profile

The charging profile is updated using an iterative heuristic method to decrease congestion and pollution. We estimate the variation of the travel costs and the carbon emissions for a change in car share for each charging period W of duration T_{charges} (typically half an hour). An alternative method for credit profile optimization could have been Bayesian optimization as in (R. Liu et al., 2022). As we could derive an analytical approximation for the gradient considering the system dynamics, we better stick to the proposed heuristic that converges quickly with reasonable accuracy. Fig. 5.4 presents the updating process. We do not account for the change of early and late penalties but only consider the travel time variation to have a robust measure. We do not consider carpooling in this approximation, as the corresponding share is relatively small. Let us define Ω_m^W the subspace of Ω restricted to mode m and departure time included in the charging period W, i.e., $\Omega_m^W = \mathcal{C} \times \mathcal{L} \times \mathcal{T}_a \times (\mathcal{T}_d \cap W) \times \{m\}$. $\Omega_m^W\{l\}$ is the subpart further restricted to trips of length l, i.e., $\Omega_m^W\{l\} = \mathcal{C} \times \{l\} \times \mathcal{T}_a \times (\mathcal{T}_d \cap W) \times \{m\}$. We define several aggregates over this period W for each mode m:

- the average speed $\bar{v}_m = \frac{\sum_{t\in W} H_m(t)v_m(t)}{\sum_{t\in W} H_m(t)}$;
- the average travel cost $\bar{TC}_m = \frac{\sum_{\omega\in\Omega_m^W} f(\omega)TC(\omega)}{\sum_{\omega\in\Omega_m^W} f(\omega)}$;
- the average travel time $\bar{TT}_m = \frac{\sum_{\omega\in\Omega_m^W} f(\omega)TT(\omega)}{\sum_{\omega\in\Omega_m^W} f(\omega)}$;
- the average trip length $\bar{l}_m = \sum_{l\in\mathcal{L}} \frac{\sum_{\omega\in\Omega_m^W\{l\}} f(\omega)l}{\sum_{\omega\in\Omega_m^W\{l\}} f(\omega)}$.

The ratio between the average accumulation $\frac{\sum_{t\in W} H_m(t)\Delta_t}{T_{\text{charges}}}$ and the number of travelers $\sum_{\omega\in\Omega_m^W} f(\omega)$ is named $\tilde{H}_m$. It is approximated using the travel times: $\tilde{H}_m = \bar{TT}_m/T_{\text{charges}}$. We now compute the effect of a traveler switching from car to PT, i.e., when $\sum_{\omega\in\Omega_{\text{car}}^W} f(\omega)$ decreases by one. It corresponds to a reduction of the mean car accumulation by $\tilde{H}_{\text{car}}$. A decrease in car ridership affects the average TC of all modes by increasing the mean speeds. This variation is approximated by

$$\delta_v \bar{TC}_m = -\frac{\mathrm{d}\bar{\alpha}\frac{\bar{l}_m}{\bar{v}_m}}{\mathrm{d}\sum_{\omega\in\Omega_{\text{car}}^W\{l\}} f(\omega)} = \bar{\alpha}\frac{\mathrm{d}v}{\mathrm{d}H_m}\tilde{H}_m\frac{\bar{l}_m}{\bar{v}_m^2}. \tag{5.22}$$

$\bar{\alpha}$ is the average VoT. The variation of total travel cost is approximated by $\sum_{\omega\in\Omega_m^W} f(\omega)\delta_v\bar{TC}_m$

The marginal total travel cost variation ΔTC_{tot} due to a decrease in car ridership, i.e., because a user switches from car to PT, is the change of travel cost for this user plus the effect on the rest of the travelers:

$$\Delta TC_{\text{tot}} = \bar{TC}_{\text{PT}} - \bar{TC}_{\text{car}} + \sum_m \sum_{\omega\in\Omega_m^W} f(\omega)\delta_v\bar{TC}_m. \tag{5.23}$$

The carbon emission per distance e depends on the mean network speed. We use the COPERT IV (Ntziachristos et al., 2009) model of Lejri et al., 2018. It allows for efficient estimation of the pollution while accounting for the effect of the congestion dynamics through the variations of the mean car speed across time. We only consider private car carbon emissions, but the model can easily be tuned to account for different fleet compositions. We do not account for the variation of PT carbon emissions due to occupancy (more weight) or operational (more vehicles) changes. Indeed, a large part of the PT fleet uses low-carbon technologies: electric propulsion for subways, tramways, and some buses; and natural gas for some other buses. The change in PT carbon emissions is thus neglected. We approximate the carbon emissions by using the mean car speed over the charging window $e(\bar{v}_{\text{car}})$. The total distance driven by car is $l_{\text{tot}} = \sum_{l\in\mathcal{L}} l\sum_{\omega\in\Omega_{\text{car}}^W\{l\}} f(\omega)$. The marginal carbon emission decreases when a traveler switches to PT consists of the emission of a car $e(\bar{v}_{\text{car}})\bar{l}$ and the effect of better traffic conditions $l_{\text{tot}}\frac{\mathrm{d}e}{\mathrm{d}\sum_{\omega\in\Omega_{\text{car}}^W} f(\omega)}$.

$$\Delta E = -e(\bar{v}_{\text{car}})\bar{l} - l_{\text{tot}}\frac{\mathrm{d}e}{\mathrm{d}\sum_{\omega\in\Omega_{\text{car}}^W} f(\omega)} = -e(\bar{v}_{\text{car}})\bar{l} - l_{\text{tot}}\frac{\mathrm{d}e}{\mathrm{d}v_{\text{car}}}(\bar{v}_{\text{car}})\frac{\mathrm{d}v_{\text{car}}}{\mathrm{d}H_{\text{car}}}\tilde{H}_{\text{car}} \tag{5.24}$$

The global objective function Obj_W to minimize over the charging period W is a combination of the total travel cost TC_{tot} and carbon emissions E. It is defined by

$$Obj_W = TC_{\text{tot}} + \chi_{\text{opt}} E, \tag{5.25}$$

with χ_{opt} the optimization parameter chosen to tune the relative importance of pollution compared to congestion. Its variations in reaction to a credit charge increase, i.e., a decrease in car ridership, is

$$\Delta Obj_W = \Delta TC_{\text{tot}} + \chi_{\text{opt}} \Delta E. \tag{5.26}$$

The variation of the objective function ΔObj_W is computed for each charging period. The credit charge of the period with the highest absolute variation is updated: it increases if negative and decreases if positive. The other charging periods are changed only if the difference between two consecutive periods is too high. In our case study, the credit charge of the concerned period is updated by one allocation κ. We allow a maximum difference of one allocation κ between consecutive periods. If needed, the other charging periods are updated to fulfill this requirement. This constraint limits the effect of travelers waiting for the change of period to start their trip and leading to a travel peak just at the period change. This process of 'braking' to avoid a high toll is presented in Lindsey et al., 2012. We provide the pseudo-code in C.2 along a small example in Fig. 5.4. Period 5 is chosen to be updated (highest

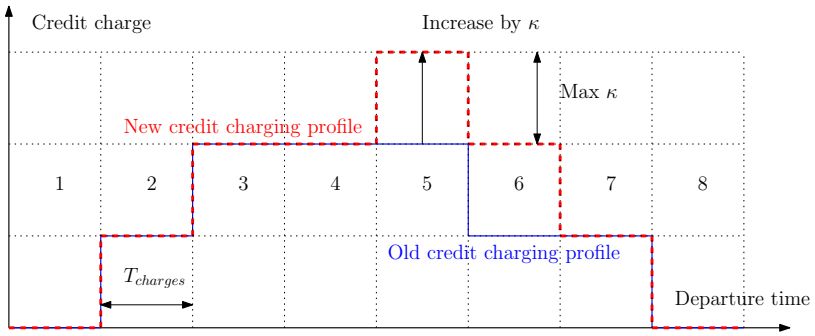

Figure 5.4: Update of the credit charging profile from blue to red.

absolute gradient) by increasing the charge by κ. The charge in period 6 is increased to have no credit charge difference of more than κ.

The SUE is then computed with the new TCS profile, the estimation of the gradient of the objective function for the new equilibrium is estimated, and the credit profile is updated again. The optimization ends if a loop is detected, meaning we reached a charging profile that has already been considered or if the maximum number of iterations is reached.

5.4 Case Study

The city of Lyon, France, serves as the framework for deriving travelers' choices and credit prices at equilibrium, along with optimizing the dynamic credit charge to minimize total travel time and carbon emissions. In the following, we introduce the case study. The effects of TCS, both at the global and individual scale, are then presented.

Finally, the trip-based MFD cross-validates the results by providing a finer resolution of the traffic dynamics.

5.4.1 Simulation settings

The travel demand considered for the case study represents the typical morning commute of 384 200 travelers in Lyon (France) between 7:00 and 10:00. There are ten regions and five boundaries, creating 224 different OD-pairs with non-zero demand. The travel demand consists of trips in Lyon and through Lyon, i.e., we also account for travelers starting or/and ending their trip outside the city. The synthetic desired arrival times are generated by adding the travel time in free flow conditions for a travel by personal car. The distribution is shown in Fig. 5.5. The distribution has a bell shape: the demand is low at 7:00 and 10:00 and high between 8:00 and 9:00.

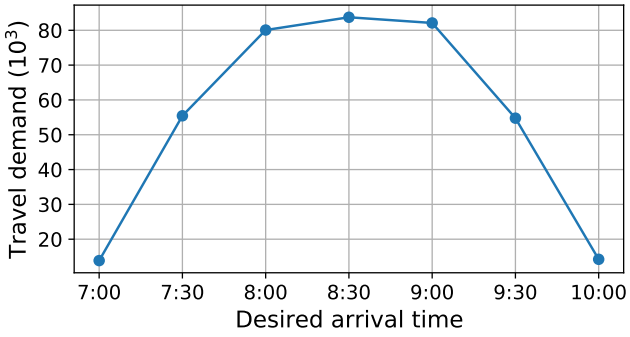

Figure 5.5: The distribution of the desired arrival times.

An MFD speed function represents the network capacity. All trips occur in the same region. The mean speed depends only on the car accumulation (solo drivers and carpoolers). We assume the number of operating buses is given and thus already accounted for in the speed function. The speed function does not depend explicitly on the accumulation of buses.

The trip length is discretized with 50 steps, and the departure time with 100 steps. We validate these choices in 5.4.3. We assume seven possible desired arrival times: every 30 min from 7:00 to 10:00. These numerical values are chosen as a trade-off between computation times, numerical rounding errors, and simulation precision. To account for the equity of the TCS concerning the travelers' wealth, we consider travelers with a low VoT of 10.8 EUR/h for low revenue and a high VoT of 21.6 EUR/h to represent high revenue. We assume they are evenly distributed across the travel demand. These VoT correspond to the order of magnitude of the VoT distribution of Lyon's inhabitants, as used in Ameli, Lebacque, et al., 2021. The normalized early factor is chosen as 1/2 and the late one as 2. This means that being late is worse than traveling a long time, which is worse than arriving early. It is a common assumption when computing the travel cost as a proxy for the perceived user cost. The normalized ratios are similar to Arnott et al., 1990. This choice of discretization leads to 210 000 different combinations of travelers' characteristics and trip choices: 50 trip lengths, 100 departure times, seven desired arrival times, two VoT, and three modes.

The trip-based MFD provides the exact travel times by solving the implicit equation $l_m = \int_{t_d}^{\hat{t}_a} V_m(s)\mathrm{d}s$. It serves as our plant in this case study. The two main differences between the trip-based model and the generalized bathtub are: (i) trip

lengths and desired arrival times which are individually assigned to each traveler in the trip-based model while being represented by distributions in the generalized bathtub; and (ii) the generalized bathtub uses discretization with arbitrarily fixed steps, whereas the trip-based MFD is solved following an event-based discretization (starts and ends of trips). The trip-based MFD (event-based resolution) solution is expensive to compute for such a large set of trips. The trip-based framework updates the state variable each time a trip begins or ends, i.e., up to thirty thousand times (twice per agent and one agent per trip length, departure time, and mode). With the generalized bathtub, we count less than 200 time steps for the generalized bathtub (the departure times plus additional time steps to wait for the completion of the last trip). One simulation lasts about 470 s with the trip-based MFD and only 0.1 s with the generalized bathtub. The trip-based framework is used only to confirm that the generalized bathtub approximation provides a close approximation of the system states for the optimal solution.

We estimate the carpooling penalty ζ_{pool} with an additional 10 min. The sensitivity of this parameter is discussed in C.3. The main parameters used for the numerical computation are gathered in Table 5.2. Note that the endowment value κ is only meaningful when compared to the charging profile τ, as only the ratio matters.

Table 5.2: The parameters used for the simulation.

Parameter	Notation	Value
VoT	α_c	$\{10.8, 21.6\}$ EUR/h
Scaled early factor	$\tilde{\beta}$	1/2
Scaled late factor	$\tilde{\gamma}$	2
Endowment	κ	1 credit
SUE goal	E^*_{SUE}	10^{-2}
CC goal	E^*_{CC}	5×10^{-3}
MCC goal	E^*_{MCC}	5×10^{-3}
Maximum price variation	ϵ_p	1 EUR
Logit parameter	θ_c	1 1/EUR
Optimization parameter	χ_{opt}	$\{0, 10^{-4}, 10^{-3}\}$
Carpooling penalty	ζ_{pool}	10 min
Charging period	T_{charges}	30 min

The charging period is chosen based on the travel time distribution without TCS, in Fig. 5.6. The credit charge changes every 30 min, and most trips (about 90%) last

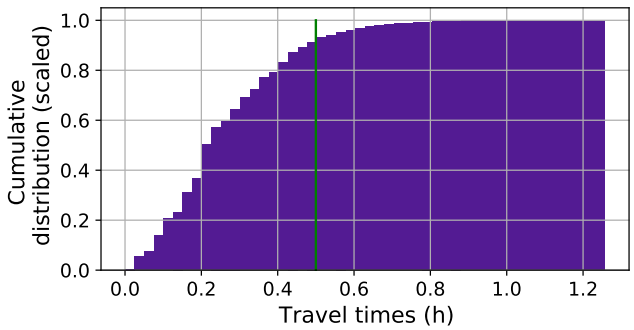

Figure 5.6: Travel time distribution (without TCS). The charging period T_{charges} (30 min) is represented by the green line.

less than this period. This means most of the trips finish at most in the period after which they started. It is essential not to have too many trips impacting many periods, as these travelers would impact the traffic conditions without paying the appropriate charge. This is in line with marginal cost pricing: the traveler pays for the externality they cause to the rest of the travelers.

We assess the convergence quality as a verification. The SUE loop is run until the SUE error falls below the given threshold E^*_{SUE}, i.e., when the user distribution is close enough to the logit decisions. The resulting assignment for an optimized TCS (referred to as 'mid' later in the text) is shown in Fig. 5.7 versus the demand weighted by the logit-based decision. Most of the points in Fig. 5.7(a) are on the diagonal,

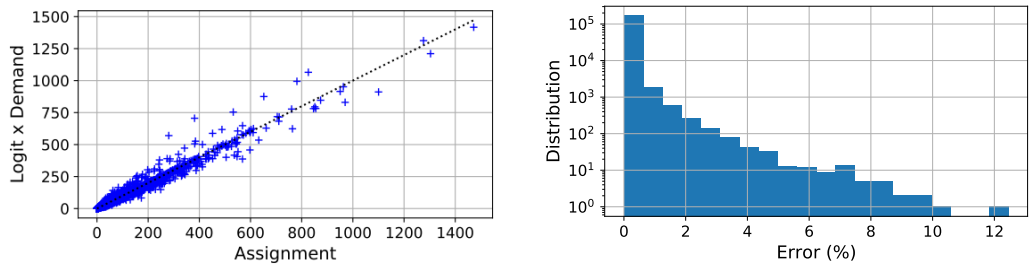

(a) (b)

Figure 5.7: Quality of the SUE: (a) user distribution vs. demand weighted by the logit, and (b) distribution of the relative error between the logit and user distribution over demand.

meaning the assignment matches the logit. Some points deviate, but as the error distribution shows (Fig. 5.7(b)), their number is low, and the error is small (max 12% for one point), thus the impact is marginal.

5.4.2 TCS impact analysis

We first assess the global effects of optimized TCS on the network: total travel cost, carbon emissions, credit charge, assignment changes. The aim of the algorithm proposed and presented in 5.3.3 is to minimize carbon emissions and the total travel cost. The total travel cost is the sum of all travelers the travel costs, i.e., the proxy for the economic losses caused by congestion. Different coefficients define the objective function to vary the importance of minimizing carbon emissions: 0, 10^{-4}, and 10^{-3}. We keep the solutions forming the Pareto front, i.e., those with no other solution being better simultaneously for the total travel cost and carbon emission reduction. As a benchmark, we also compute the equilibrium under static credit charging, with different charge over allocation ratios $\tau(\text{car})/\kappa$ between 3 and 16. The Pareto front is shown in Fig. 5.8, with the static solutions and the no TCS case for comparison. A static charge of 4 credits means that, on average, only one car can drive for every four travelers (one solo driver or two carpoolers). It already enables a reduction of the the total travel cost of about 19% and a 59% reduction of pollution. Dynamic charging profiles improve teose metrics even further: 20% for congestion and 90% for pollution. It is possible to reach similar pollution levels with static charging, as it decreases when the charge increases (fewer car drivers). However, it is achieved at the expense of the total travel cost reduction. To achieve a low carbon footprint, the TCS significantly penalizes the car, and many travelers switch to PT and carpooling. Since the mode shift is significant, the improvement of traffic does not offset the use

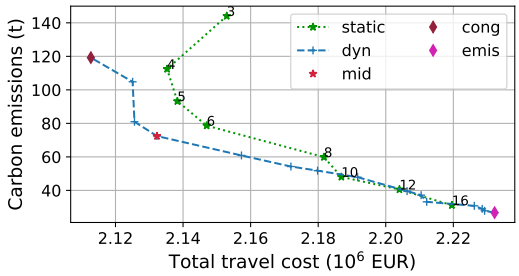

Figure 5.8: Total travel cost vs. carbon emissions for different static and dynamic TCS. The numbers are the charge over allocation ratios for the static cases. For comparison, the no TCS case leads to a total travel cost of 2.63×10^6EUR and a carbon emission of 275 t.

of slower modes, and the total travel cost increases due to increased travel times. The total travel cost reduction of 20% (dynamic charging 'cong') cannot be reached with static charging. Although static charging enables a the total travel cost reduction of 19%, the associated carbon emissions are 36% higher than the dynamic TCS 'cong'. We keep the dynamic solutions with the lowest total travel cost ('cong') and the lowest CO2 emission ('emis') for further comparison against static charging. An intermediate case of dynamic charging ('mid') is compared versus the no TCS scenario. See C.4 for comparing the TCS in terms of total travel time and carbon emissions.

The static and dynamic credit charge and equivalent toll profiles are presented in Fig. 5.9. We plot the charge for solo car drivers. It is half for carpoolers and zero for transit riders. The equivalent toll charge is defined as $(\tau(t_d, \text{car}) - \kappa)p$. It corresponds to the out-of-pocket money a traveler needs to pay to start a solo car trip at t_d. As

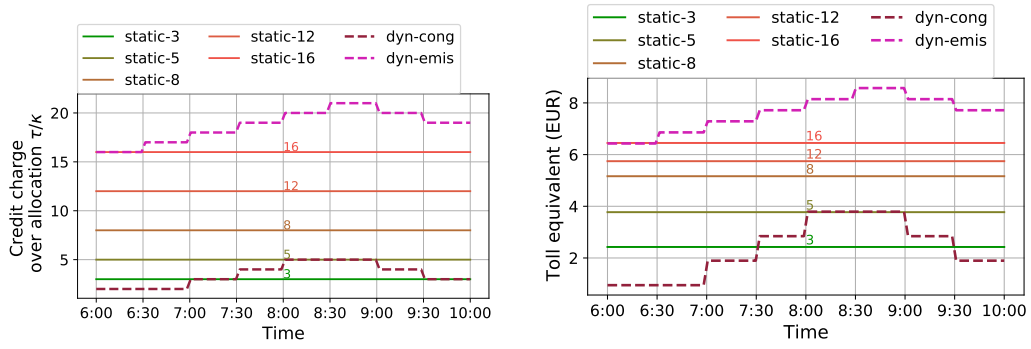

(a) (b)

Figure 5.9: Comparison of the static and dynamic TCS for different parameters: (a) credit charge and (b) toll equivalent with respect to the departure time slots.

expected, it is more expensive to drive a car during the high-demand period of the peak hour. Increasing the magnitude of carbon emissions increases the credit charge (Fig. 5.9(a)) as pollution tends to increase with car usage: the 'emis' scheme leads to an equivalent toll (Fig. 5.9(b)) of about 8 EUR, while it stays below 4 EUR in the 'cong' case.

We compare the modal shares for the different scenarios in Fig. 5.10. As expected, we see in Fig. 5.10(a) that the share of solo drivers diminishes with TCS as the associated user costs increase. On closer inspection it can be seen that the car share

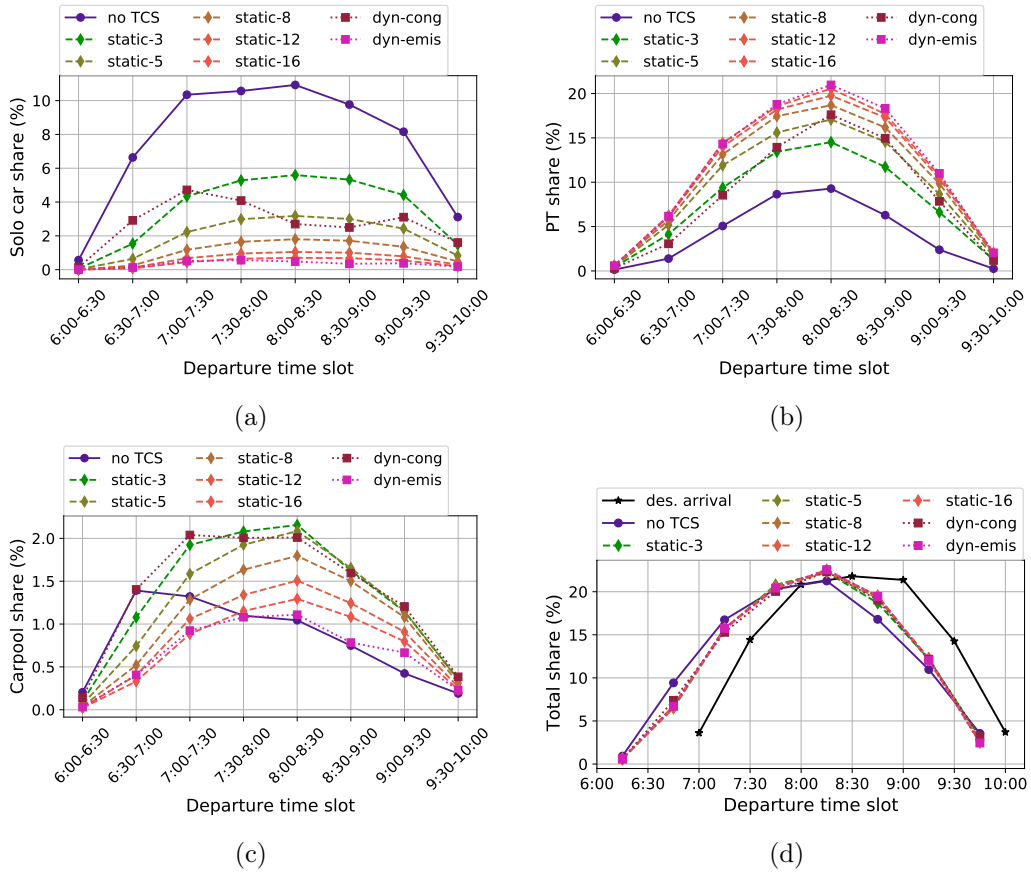

Figure 5.10: Evolution of the mode shares and the departure times for (a) solo car, (b) PT, (c) carpool, and (d) total shares.

decreases with dynamic charging during the peak demand, while it increases with static charging. This can be explained by two effects: it becomes expensive to take the car as the credit charge is high during the peak in the dynamic case. The credit charge is the same in the static case, but the travel demand is higher. The TCS 'cong' strongly reduces the car share for a limited time (8:00 to 9:00), while the TCS 'emis' creates a substantial reduction across the whole time frame to reach ambitious pollution targets. The PT share (Fig. 5.10(b)) increases with the charging profile as it requires no credits. The share of carpoolers is captured in Fig. 5.10(c). The carpooling mode is used more with TCS than without TCS. However, the carpooling share decreases with the charging profile when the credit charge is high, as a carpooler still needs to spend credits. When looking at the shares with respect to the charging slots for all modes in Fig. 5.10(d), the TCS seems to make travelers leave later. The traffic conditions are improved, the travel times decrease, and thus travelers start their trip later to arrive around their desired arrival time. There is, however, very little difference between the different TCS. The conclusion is that the TCS affects the mode choice more than the departure time distribution. This is partly due to the limitation of the maximum difference of one allocation κ between two consecutive charging periods. The gain of shifting one's departure time for a charging period with a lower credit charge does not exceed the early/late arrival penalty.

In Fig. 5.11, the traffic conditions with and without TCS are compared through the mean speeds. Without TCS, the mean speeds of PT and cars (represented in Fig. 5.11(a)) are similar during the peak demand. Although the equilibrium is not

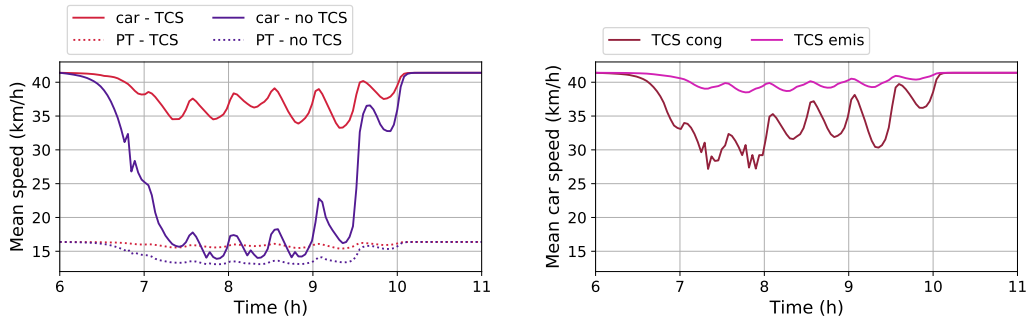

(a) (b)

Figure 5.11: Effect of the different dynamic TCS of the mean traffic speed: (a) mean car and PT speeds with dynamic TCS ('mid') and without TCS, and (b) mean car speed for the TCS 'cong' and 'emis'.

deterministic, the user costs are similar, as both modes are used. As expected, the TCS improves traffic conditions by reducing the number of circulating cars. The gain is considerable for cars, which circulate about 20 km/h faster during the peak period. The PT speed increases by about 4 km/h. The waves come from the discretization of the desired arrival times. This leads to several local demand peaks every half hour. Fig. 5.11(b) compares car speed for different objectives. When focusing on the total travel cost reduction, i.e., reducing the total travel cost, the TCS still allows mean speed reductions of more than 10 km/h. In particular, the credit charge is low before 8:00, and the demand is already high; thus, the mean car speed is lower than after 8:00. The TCS designed for emission reduction keeps the mean speed around 40 km/h. This is expected as the emissions decrease with the mean car speed for the range of urban speeds.

The change in departure time per trip length between equilibrium without TCS and with TCS is computed in Fig. 5.12. Most travelers depart later with the TCS,

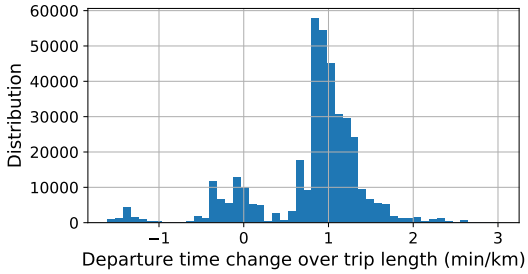

Figure 5.12: Variations in departure time normalized by the trip length. A positive value means the traveler starts their trip later with TCS (scenario 'mid') than without.

about one minute per kilometer after their departures without TCS. Their travel times are reduced thanks to the better traffic conditions; thus, they leave later to arrive around their desired arrival time at their destinations. Some travelers depart earlier because they switch to modes with longer travel times (carpooling and PT).

We look at the effect of TCS on the different travelers. As we consider heterogeneous travelers in terms of desired arrival times, OD pairs, and VoT, it is crucial to look at the equity of the TCS. By looking at the distributions of the gains provided by the TCS ('mid'), we can quantify the number of travelers who are better or worse

off with the policy proposed.

The gains are defined as the difference between travel costs (normalized or not by the VoT) with and without TCS. For a given set of traveler parameters (VoT, trip length, and desired arrival time), the TC gain Γ is the difference between the TC associated with the possible departure times and modes and weighted by the user distribution:

$$\Gamma = \frac{1}{d(c, i_l, i_{t_a})} \left(\sum_{i_{t_d}, m} f_{\text{no TCS}}(\omega) TC_{\text{no TCS}}(\omega) - f(\omega) TC(\omega) \right), \tag{5.27}$$

$$\omega = (c, i_l, i_{t_a}, i_{t_d}, m), \ \forall \ (c, i_l, i_{t_a}). \tag{5.28}$$

A positive gain is favorable for the traveler as it means its average TC decreases with the TCS. The distributions of the TC gains are shown in Fig. 5.13. Most travelers are

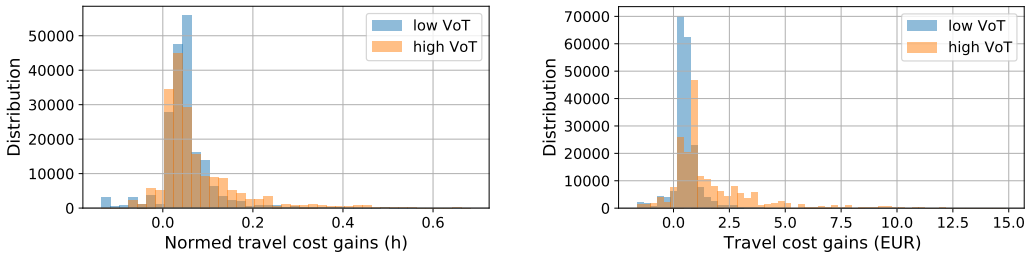

(a) (b)

Figure 5.13: Distribution of the travel cost gains: (a) normalized by the VoT and (b) absolute travel cost.

better off with the TCS in terms of normalized travel cost (by the VoT) and absolute travel costs. The majority see their TC equivalent decrease by 0 to 6 min (Fig. 5.13(a)) and 0 to 2 EUR (Fig. 5.13(b)). Wealthier travelers (higher VoT) are even better off since they will more readily buy credits to drive a car when the traffic conditions improve. The worst-off travelers lose the equivalent of several minutes with the TCS. Their TC increases by up to 1.6 EUR. The travelers who are better off decrease their TC by up to 14.7 EUR.

Let us have a look at the impact of the credit market. The trade gains from the market and the user cost gains (sum of travel cost and trade gains) are represented in Fig. 5.14. A positive trade gain means the traveler earns money by selling credits, while a negative gain means they spend money to buy credits. Fig. 5.14(a) gives an

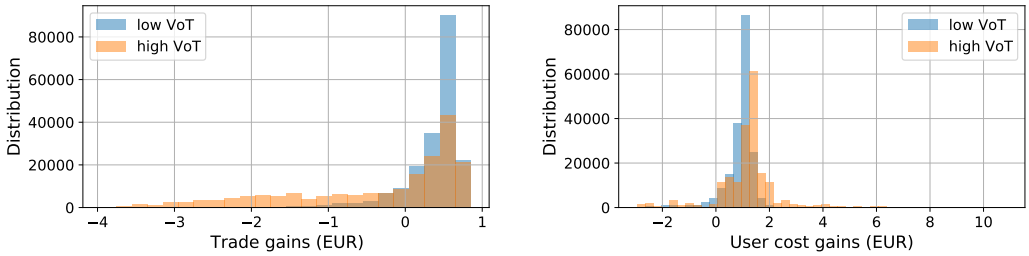

(a) (b)

Figure 5.14: Distribution of the benefits of the TCS: (a) trade gains (money earned or spent through the market) and (b) user cost gains.

overview of the market outcomes. Travelers with a high VoT tend to buy credits from travelers with a smaller VoT; thus, they earn less money through the market. A traveler can earn around 0.8 EUR by riding PT and spend around 5.4 EUR driving their car alone during the highest charging period. When weighting the trade gains by the user distribution, some travelers spend up to 4 EUR. In contrast, others earn up to 0.7 EUR, depending on their characteristics (VoT, trip length, and desired arrival time). The effect of TCS on the user cost (travel cost plus credit trade) is represented in Fig. 5.14(b). Most travelers are better off with the TCS, as they decrease their user costs by 0 to 2 EUR. About 6% of the travelers see their user costs increase with this TCS, meaning 94% benefit from the TCS. The worst off lose 2.9 EUR, while those better off earn up to 10.8 EUR. Note that those estimations do not account for the benefits linked to lower pollution levels, such as better air quality.

The TCS has different impacts on different travelers. We investigate the relationship between desired arrival times, the mode shift, i.e., the evolution of modal shares between before and after TCS (scenario 'mid'), and the user cost gains in Fig. 5.15. The mode shift (Fig. 5.15(a)) from car to PT is more pronounced for travelers want-

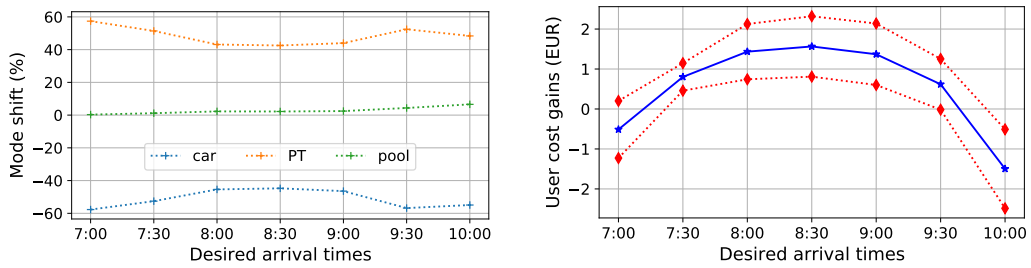

(a) (b)

Figure 5.15: (a) Mode shift and (b) user cost gains with respect to the desired arrival times. The blue line is the average, and the red lines are the average plus/minus the standard deviation.

ing to arrive outside the demand peak (before 7:30 or after 9:30), when up to 57% of the travelers leave their car to ride PT. Around 45% of the travelers with desired arrival times during the peak hour (between 8:00 and 9:00) switch from their cars to PT. This seems counterintuitive as the credit charge is higher during peak hours. The traffic conditions are bad during peak hours without TCS, and the car share is already lower than during peak hours. The user cost gain is positive for peak-hour users and negative for off-peak travelers (Fig. 5.15(b)). On-peak commuters benefit from better traffic conditions, which outweighs the burden of the TCS (mode shift or credit buy). On the contrary, the traffic conditions are already satisfying off-peak, and the slight improvement thanks to TCS does not outweigh additional TCS costs. We provide a similar analysis for the trip lengths in Fig. 5.16.

Travelers with short and long trips change modes differently with the TCS (Fig. 5.16(a)). For trips shorter than 6 km, the modal shift is almost exclusively from cars to PT, with 50% to 55% of the demand switching from cars to PT. On the contrary, for trips longer than 10 km, more travelers stick to solo car driving and prefer carpooling to PT. The mode share of solo car drivers decreases by only 32 to 33 points. The carpooling share increases by up to 39 points. Sharing a car ride is attractive for long trips. The extra costs (waiting time and credit charge) do not depend on the trip length. The user cost gains per distance (Fig. 5.16(b)) are, on average, positive for

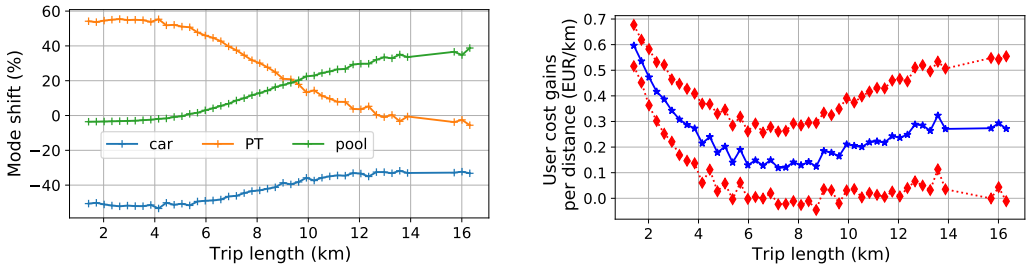

(a) (b)

Figure 5.16: (a) Mode shift and (b) user cost gains per distance with respect to trip lengths. The blue line is the average, and the red lines are the average plus/minus the standard deviation.

the range of trip lengths in this case study. Short trips tend to benefit more from the TCS, as those travelers tend to shift towards PT and earn money by selling credits.

5.4.3 Comparison with the trip-based MFD

We compute the trip-based MFD simulation for the reference test case without TCS and the intermediate 'mid' TCS to assess the discretization effects. The trip-based MFD, via its event-based resolution, provides the exact computation of the arrival times. It can be viewed as the plant model. It does not use any discretization. It is, however, significantly more time-consuming to compute the arrival times for a given assignment than the discretization of the bathtub. Typically, the computation time is longer by three orders of magnitude. The trip lengths are those from the continuous demand before the discretization. The departure times are smooth: the trip linked to a departure time index i_{t_d} in the bathtub corresponds to a departure time randomly drawn from the uniform distribution $[(i_{t_d} - 0.5)\Delta_t, (i_{t_d} + 0.5)\Delta_t]$. We only consider trips with a user distribution more than one traveler. Less than 2% of the travel demand is lost in the process. The mean car speeds are compared in Fig. 5.17. Some

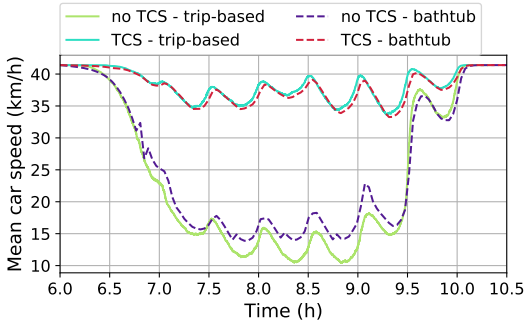

Figure 5.17: Comparison of the mean car speeds with and without TCS for the bathtub and trip-based MFD resolutions.

deviations, up to 4 km/h for car speed, can be observed in the no TCS case between the network speed in the MFD and the bathtub. Due to the affine transformation of Eq. (2.7), the PT speed error is below 0.5 km/h. The differences are barely noticeable with TCS. The generalized bathtub tends to underestimate the congestion.

To quantify the error made in congestion and pollution estimation with the bathtub, we compare the TCS and the carbon emissions both with and without TCS in Fig. 5.18. The errors stay below 3% for total travel cost (Fig. 5.18(a)) and 11% for

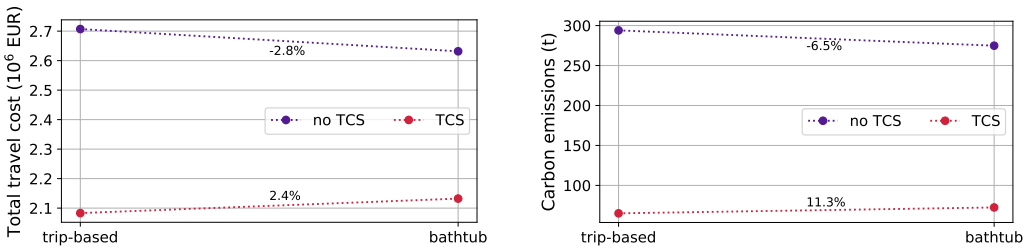

(a) (b)

Figure 5.18: Variations of the objectives measures between the bathtub and trip-based MFD: (a) total travel cost and (b) carbon emission.

carbon emissions (Fig. 5.18(b)). The numerical approximations of the multimodal generalized bathtub are below the differences between the scenarios with and without TCS. The numerical resolution of the bathtub still gives a reasonable quantification of the economic and environmental benefits of the TCS at a lower computational cost than the trip-based MFD. The trip-based approach thus validates the departure time and trip length discretization choices: the respective precisions of 145 s and 304 m.

5.5 Conclusions

We formulates a multimodal generalized bathtub to account for different types of vehicles and transportation modes. Each traveler's choices consist of mode and departure times. We add a TCS to foster mode shifts during the peak hour. PT users ride for free, solo car drivers pay the total charge, and carpoolers only half. We computed the SUE to account for the uncertainty of users' choices. A realistic scenario based on the morning commute in Lyon illustrated the methodology proposed.

The framework proposed makes it possible to compare the advantage of a dynamic TCS over a static one. The dynamic TCS accounts for the different demand levels depending on the time of day. It permits a better reduction of the total travel cost, i.e., the sum of all travelers' travel costs. The SUE is based on travel cost; thus, the shift of travelers' departure time is relatively limited. The biggest impact is the mode shift: PT and carpooling mode shares increase at the expense of the car share. We drew a Pareto front to present how TCS can lead to different total travel cost and carbon emission compromises. A TCS named 'cong' led to low total travel cost; another named 'emis' permitted significant carbon reduction, and 'mid' was a trade-off between both measures.

As TCS is a policy involving a marketplace and trading commodities (in this case credits), it raises the question of individual gains when people have different VoTs (different economic classes). The results showed no significant disadvantage for one category of VoT. With the 'mid' TCS, more than 94% of the population benefited from the TCS, as it reduced their user costs. However, it did not account for environmental aspects like air quality or noise. The numerical resolution of the multimodal generalized bathtub approximated the travel times. A comparison with the exact solution via trip-based MFD showed that the numerical error was below the order of benefits

of the TCS. Moreover, the methodology proposed was shown to efficiently assess and optimize the benefits of TCS. The framework used the advantages of macroscopic simulation to reduce the need for computation power and data collection.

Chapter 6

Rebalancing on-demand service operations with tradable credit scheme

The previous chapters take advantage of TCS to nudge travelers into more sustainable travel behaviors. This chapter proposes another approach based on TCS to improve the sustainability of the transportation network by regulating the transportation offer. The TCS is applied to ride-hailing drivers to mitigate the negative externalities of unregulated on-demand services and foster cooperation between ride-hailing and public transportation.

6.1 Motivation

Ride-Hailing (RH) companies like Uber, Didi, and Lyft introduced new options for mobility in many cities. Due to lesser regulations than traditional taxi companies, the fees are usually lower, and RH services have expanded significantly (OECD, 2018). However, these on-demand mobility services may negatively affect the transportation network. RH companies contributed to the congestion increase in San Francisco between 2010 and 2016, according to Erhardt et al., 2019. The study of Cats et al., 2022 concludes that RH companies mainly compete with Public Transportation (PT) alternatives, even if RH companies also provide trips not covered by the transit network.

RH services' objective is, as a private player, to increase their profits and thus dispatch their resources in high-demand areas which may already have good transit coverage. Those behaviors are usually not aligned with the collective optimum settings. We propose a TCS aimed at the RH drivers. Contrarily to traditional taxi license schemes, which regulate and redistribute the number of operating taxis in a given area in the long run, we envision a short-term and flexible framework. For now, TCS has only been proposed for demand management. Here, we want to extend the concept to the offer side. The goal is to encourage RH drivers to shift from the city center to the suburbs, where they can propose efficient first-/last-mile alternatives and complete the PT offers. The TCS restricts the number of RH vehicles driving in the city center and between the first rings. Thus, operating in the city center becomes less attractive due to the costs of acquiring the required credits. Travelers in the city center would find fewer RH drivers available to drive them and use PT to complete their trips. Increasing RH operations in the suburbs should foster cooperation between PT

and RH. Customers traveling from the suburbs to the center use RH services till the center and then ride PT.

For evaluating the TCS on RH services, the operation, and competition with other modes, it is essential to keep track of the transportation system dynamics, as congestion significantly impacts travel times and, thus, the service quality. We must also consider the service's full spatial extent and reproduce the vehicles' trajectories over the day. The trip-based MFD framework is an excellent candidate to simulate the RH trips under those conditions without the computational burden of detailed simulations. Several recent contributions regarding RH services are founded on the MFD concept. Nourinejad and Ramezani, 2020 study the equilibrium between RH offer, passenger demand, and service pricing. The model predictive controller represents the traffic dynamics with an MFD framework. Beojone and Geroliminis, 2021 nudge passengers to share their rides and park unmatched vehicles to reduce the impact of RH vehicles on congestion.

In this chapter, we implement a TCS to shift RH drivers from the city center to the suburbs. The trip-based MFD framework is used to track the position of the RH drivers and compute their trajectories: driving to pick up the passengers and then drop them at their destination. The RH drivers receive an initial credit allocation. Operating in different city regions requires credits. The credit charge is lower the further we are from the city center. The goal of the regulator is to promote the use of PT in the city center and a combination of RH and PT for trips between the center and the suburbs. In the following, we present the methodology in Sect. 6.2, i.e., how we represent the RH operations and travelers' trips with the MFD framework. The constraints of the TCS introduction are then developed in Sect. 6.3. The computation of the transportation network at equilibrium is described. A representation of the day-to-day dynamics is proposed to investigate the transitions between different TCS as the local authority adjusts the TCS from time to time. Sect. 6.4 develops a case study to illustrate the proposed TCS. The numerical results are then discussed in Sect. 6.5. Sect. 6.6 concludes this chapter. The main notations are summed up in D.1.

6.2 Methodology

The road network is divided into N_R different regions. Each region has a different travel demand distribution and PT coverage. The regions are indexed by increasing order from the center to the outskirts. We note $\mathcal{C}$ the set of travelers. Each traveler uses a travel mode $m \in \mathcal{M}$. The alternatives are RH service, riding the PT, or combining both. The transportation system is also populated with background traffic: regular users driving their own cars, influencing the congestion level and the network speed. We note $\mathcal{D}_0$ the set of potential drivers and $\mathcal{D} \subset \mathcal{D}_0$ the set of active RH drivers operating in the network. As we consider driver elasticity, some potential drivers may not operate because the earnings are too low. We assume each driver i has a reservation price P_i^{res}. When the average RH revenue exceeds the driver's reservation price, it will join the RH service. Otherwise, it leaves the service. The equilibrium is not straightforward: the more RH drivers, the more the total RH revenue is, but at the same time, the higher the denominator of the average revenue (the number of RH drivers) is.

The regulator aims to enforce a TCS to reduce competition between RH vehicles and the PT in the city districts where the transit offer is satisfying, usually the city

center and inside the first rings. Its strategy is to foster multimodal trips where RH drivers permit travelers from the outskirts to ride an RH vehicle to a transit hub at the border of the city center and then use the PT. Fig. 6.1 presents a schematic representation of the different travel alternatives for a traveler going from the suburbs (region 3) to the city center (region 1).

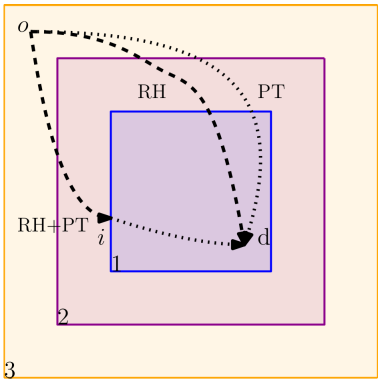

Figure 6.1: A trip between an origin o in region 3 and a destination d in region 1 has three alternatives: RH, PT, or RH till the border i and then PT.

We set a framework based on the trip-based MFD to study the effect of the TCS. It considers the congestion dynamics and the heterogeneity of the trips: each traveler has its own origin, destination, and departure time. Its trip length is retrieved from the actual multimodal network topology. We track the position of the RH vehicles. The drivers start at an initial position that corresponds to their homes. They move only to pick up or drive a customer to its destination. The rest of the time, they park on the street and wait to pick up another customer. Those idle drivers do not contribute to the congestion.

At their departure time t, the travelers request a trip through a Mobility-as-a-Service (MaaS) platform. The platform then chooses their travel alternatives (RH and/or PT) in order to minimize the sum of the travel costs. The user travel costs from origin o to destination d are defined by the travel times and the service prices:

$$C^t_{o,d,PT} = \alpha_j T_{PT,o,d} + f_{PT}; \tag{6.1}$$

$$C^t_{o,d,RH} = \alpha_j \left(L_{pu,o,d}/V_{r_o}(t) + \sum_{r=r_o}^{r_d} L^r_{o,d}/V_r(t) \right) + f_{RH} L_{o,d}; \tag{6.2}$$

$$\begin{aligned} C^t_{o,d,RH-PT} = \alpha_j & \left(L_{pu,o,i}/V_{r_o}(t) + \sum_{r=r_o}^{r_i} L^r_{o,i}/V_r(t) + T^*_{PT,i,d} \right) \\ & + f_{RH} L_{o,i} + f_{PT}; \end{aligned} \tag{6.3}$$

$$\begin{aligned} C^t_{o,d,PT-RH} = \alpha_j & \left(T^*_{PT,o,i} + L_{pu,i,d}/V_{r_i}(t) + \sum_{r=r_i}^{r_d} L^r_{i,d}/V_r(t) \right) \\ & + f_{RH} L_{i,d} + f_{PT}. \end{aligned} \tag{6.4}$$

α_j is the VoT of the traveler j. The PT travel cost consists of the travel time $T_{PT,o,d}$ plus the price of a unitary ticket f_{PT}. We assume the ticket price is independent of the trip. The RH travel cost consists of the pick-up time, the travel time, and the RH charge. The pick-up time is the pick-up distance $L_{pu,o,d}$ over the current average speed in the origin region $V_{r_o}(t)$. The estimated travel time is decomposed over the

different regions. In each region r, the travel time is the trip length in this region $L^r_{o,d}$ over the regional speed $V_r(t)$. The RH charge is the distance-based fee f_{RH} multiplied by the trip length. For the RH-PT alternative (RH then PT), the travel cost is the sum of the RH travel cost until the border i of the destination region and then the PT travel cost from this border to the destination. The same applies to PT-RH (PT then RH) in reverse: the traveler rides the PT and then takes an RH vehicle. We note $T^*_{PT,o,d}$ the PT travel time when combined with RH. It is usually smaller than $T_{PT,o,d}$ because the RH driver will pick up/drop the passenger close to the PT stop, reducing the access time.

Travelers starting at t from o to d send a request to the matching platform. The MaaS platform waits a few minutes to create a batch of departing travelers. It then assigns the travelers to a mode and an available RH driver. The assignment takes place to reduce the total travel cost of the current batch. The platform first removes the travelers for which the PT option is the cheapest alternative, even without accounting for the pick-up distance. Then if there are more travelers than drivers, the travelers with the highest pick-up distance are assigned to PT to ensure at least as many available RH drivers as travelers. These first steps reduce the size of the assignment problem. The assignment process correspond the following Integer Linear Problem (ILP):

$$\min \sum_{i,j,m \in \mathcal{D}\times\mathcal{C}\times\mathcal{M}} y^m_{i,j} C^m_{i,j} + \sum_{j\in\mathcal{C}} \left(1 - \sum_{i,m\in\mathcal{D}\times\mathcal{M}} y^m_{i,j}\right) C^{PT}_i \tag{6.5}$$

$$\sum_{j,m\in\mathcal{C}\times\mathcal{M}} y^m_{i,j} \leq 1, \forall i \in \mathcal{D} \tag{6.6}$$

$$\sum_{i,m\in\mathcal{D}\times\mathcal{M}} y^m_{i,j} \leq 1, \forall j \in \mathcal{C} \tag{6.7}$$

$$y^m_{i,j} = 0 \text{ if } lic_i > r^m_j, \forall i,j,m \in \mathcal{D}\times\mathcal{C}\times\mathcal{M} \tag{6.8}$$

m is the mode: RH or RH+PT (RH then PT or PT then RH); $C^m_{i,j}$ is the travel cost of j matched with i for mode m; C^{PT}_i the cost of the transit-only alternative; $y^m_{i,j} = 1$ if and only if the driver i is matched with passenger j for the alternative m (pure RH or combined trips), and zero otherwise. The first constraint Eq. (6.6) states that each driver is matched to at most one customer. The second Eq. (6.7) ensures each customer is matched to at most one driver. The third Eq. (6.8) ensures that the driver's license lic_i allows it to serve the trip. r^m_j is the required license to serve customer j following the alternative m.

6.3 Regulating fleet size in each region with TCS

The regulator introduces and enforces a TCS to regulate the RH operations in the city. Each active driver gets κ credits for free from the regulator per day. The drivers need to spend τ_r credits to acquire a license to operate (i.e., pick-up or drop-off passengers) in the regions with an index higher or equal to r for a day. Since the regions are defined for TCS purposes, we assume $\tau_r < \tau_{r-1},\ \forall r \in [1, N_R - 1]$. We let the option of operating in the region N_R free of credit charge, i.e., $\tau_{N_R} = 0$. Drivers can exchange their credits with a dedicated bank. It regulates the credit price p. The credit price evolves according to the offer and demand.

We note x_r the number of drivers with a license for region r, i.e., who can operate in regions $r' \geq r$. For an RH trip from an origin in region 3 to a destination in region 1, as in Fig. 6.1, the driver needs a license to operate in region 1 since it allows the driver to operate in regions 1, 2, and 3. However, for a combined trip (RH then PT) from 3 to 1, only a license for region 2 is needed as the last leg of the trip uses PT.

The framework distinguishes two timescales, as presented in Fig. 6.2. The drivers'

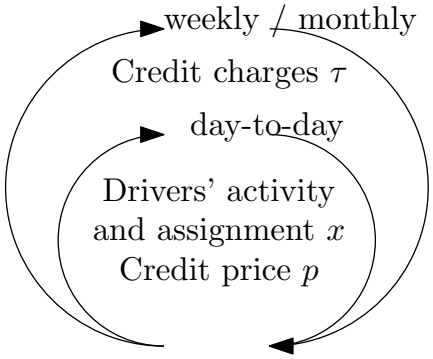

Figure 6.2: The two timescales of TCS: drivers' activity and assignment, and credit charge changes by the regulator.

activity and assignment, along with the credit price, are updated each day. The regulator adjusts the credit charge τ on a longer-term (weekly, monthly, or even yearly). In the following, we investigate two aspects. The first is the traffic state computation to estimate and predict the effect of TCS on the drivers' assignment and, thus, on the mode shares. The second is the evolution of the drivers' choice as a day-to-day process to represent the transition linked to the introduction of the TCS.

6.3.1 Calculating the equilibrium

We first focus on calculating the equilibrium. The drivers' assignment x, i.e., the choice of operating regions, balances two markets: the RH operation market, where travelers require RH services, and the credit market, where drivers buy and sell credits. Fig. 6.3 summarizes the different interactions. Travelers' mode choice impacts RH revenue for

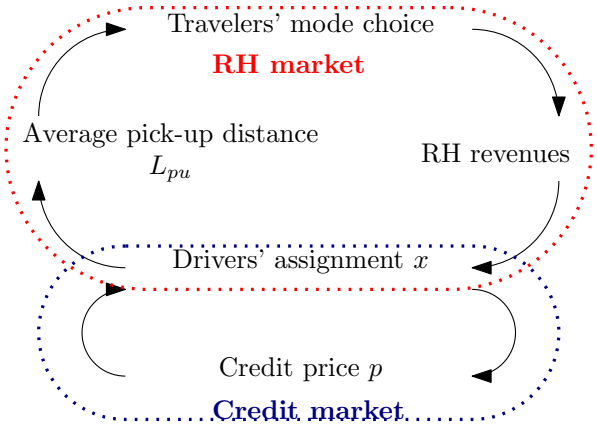

Figure 6.3: Inter-dependencies between drivers, travelers, and credit market.

drivers, which, with the credit price, will change drivers' assignments. The average

pick-up distance decreases as the number of drivers able to serve the trip increases. The pick-up distance affects the RH travel costs, thus modifying mode choices.

We jointly formulate the equilibrium of the number of active drivers, their assignment x, and credit price p. The RH revenue R_r is the volume of fees travelers pay for using RH (alone or combined with PT) for a trip requiring access to region r but not $r-1$.

The average RH gain G_r^{avg} for operating with license r is the sum of the average revenue for each region the license permit access to minus the price of the license:

$$G_r^{\text{avg}} = \sum_{r' \geq r} \frac{R_{r'}}{\sum_{r'' \leq r'} x_{r''}} - p\tau_r. \tag{6.9}$$

Note that we do not account for the value of the initial allocation as we only use the difference between average gains. We also define the average RH revenue for all regions combined R^{avg}:

$$R^{\text{avg}} = \frac{\sum_{r \in [1, N_R]} R_r}{|\mathcal{D}|}. \tag{6.10}$$

The equilibrium is reached when the chosen licenses correspond to the maximum gain value $G_{\max}^{\text{avg}} = \max_r(G_r^{\text{avg}})$ over the licenses. The equilibrium is formulated as

$$(G_{\max}^{\text{avg}} - G_r^{\text{avg}})x_r = 0, \ \forall r \in [1, N_R - 1]; \tag{6.11}$$

$$x_r \geq 0, \ \forall r \in [1, N_R]; \tag{6.12}$$

$$\sum_{r=1}^{N_R} x_r = |\mathcal{D}|; \tag{6.13}$$

$$P_i^{res} \leq R^{\text{avg}} \iff i \in \mathcal{D} \ \forall i \in \mathcal{D}_0; \tag{6.14}$$

$$\sum_{r=1}^{N_R} x_r(\tau_r - \kappa) \leq 0; \tag{6.15}$$

$$p \sum_{r=1}^{N_R} x_r(\tau_r - \kappa) = 0; \tag{6.16}$$

$$p \geq 0. \tag{6.17}$$

Eq. (6.11) means that any licenses chosen by at least one driver must yield the maximum gain. Eq. (6.12) states that the number of license holders is non-negative. Eq. (6.13) is the conservation of the number of drivers. Eq. (6.14) states that a driver is active if and only if its reservation price is below the average revenue. Eq. (6.15) is the credit cap (CC): the drivers cannot spend more credits than the distributed amount. Eq. (6.16) is the market clearing condition (MCC): all credits are used, or their price is zero. Eq. (6.17) means the credit price is non-negative. The last three constraints are specific to the TCS.

The equilibrium presented in Eq. (6.11-6.17) is theoretical and cannot be reached for most of the scenarios because the numbers of license holders are integer values. Furthermore, the computation of different parts of the equilibrium is implicit, such as the RH matching Eq. (6.5), or nonlinear, such as the average gains and revenues Eq. (6.9) and Eq. (6.10). For these reasons, we formulate a cost function corresponding to a state close to the equilibrium. This cost function is then minimized with heuristic methods.

We reformulate the equilibrium into the minimization of an objective function J. The first part J_1 means the average gains for which there are license holders are close to the maximum gain.

$$J_1 = \frac{1}{|\mathcal{D}_0|N_R} \sum_{r=1}^{N_R} (G_{\max}^{\text{avg}} - G_r^{\text{avg}}) x_r \tag{6.18}$$

The second part J_2 replaces constraint Eq. (6.14).

$$J_2 = \sum_{i \in \mathcal{D}_0} \delta(i, R^{\text{avg}}) \tag{6.19}$$

with $\delta(i, R^{\text{avg}})$ equals one when the driver i is active even though the average revenue is below its reservation price or when i is inactive, and the average revenue is higher than its reservation price, i.e.,

$$\delta(i, R^{\text{avg}}) = 1 \iff (i \in \mathcal{D} \wedge R^{\text{avg}} < P_i^{res}) \vee (i \notin \mathcal{D} \wedge R^{\text{avg}} > P_i^{res}) \,. \tag{6.20}$$

It is zero otherwise. The objective function is the sum of both costs.

$$J = J_1 + J_2 \tag{6.21}$$

Note that J is always non-negative.

We use the driver conservation Eq. (6.13) and the MCC Eq. (6.16) to reduce the size of the minimization problem. We assume the price is non-zero. Otherwise, the TCS is non-effective, and the state of the system is the same as without TCS, where all drivers can operate in all regions, i.e., $x_1 = |\mathcal{D}|$ and $x_r = 0$, $\forall r \in [2, N_R]$. Then the equality holds for the CC Eq. (6.15). We combine it with driver conservation to remove two variables. We choose to replace x_{N_R-1} and x_{N_R} with

$$\begin{aligned} x_{N_R-1} &= \frac{|\mathcal{D}|(\kappa - \tau_{N_R}) - \sum_{k=1}^{N_R-2}(\tau_k - \tau_{N_R})x_k}{\tau_{N_R-1} - \tau_{N_R}}; \\ x_{N_R} &= |\mathcal{D}| - \sum_{r=1}^{N_R-1} x_r. \end{aligned} \tag{6.22}$$

In total, the equilibrium computation consists in finding N_R variables: the credit price, the number of active drivers, and the assignment in the first $N_R - 2$ regions. The set of active drivers $\mathcal{D}$ is retrieved from the number of active drivers by selecting the ones with the lowest reservation prices.

6.3.2 Simulating the day-to-day markets evolution and the transition to equilibrium

To assess the equilibrium prediction quality, the convergence speed, and the smoothness of the transition, we represent the day-to-day transition between traffic states under different TCS constraints. The credit market size is tiny compared to the one presented in the previous chapters, as the number of commuters dwarfs the number of RH drivers. We thus assume the drivers do not trade directly with each other, as they may have trouble finding a seller or buyer and become frustrated. Instead, they exchange with a credit bank that buys and sells credits at a regulated price. However,

the credit cap might be violated in the transition between two TCS as every request to buy or sell credits at the regulated price is accepted. The price depends on the difference between the credit offer and demand as the bank aims to sell as many credits as it buys to reach a neutral budget. The different steps of the day-to-day process are presented in Fig. 6.4. Each day begins with an update of the TCS if the current TCS

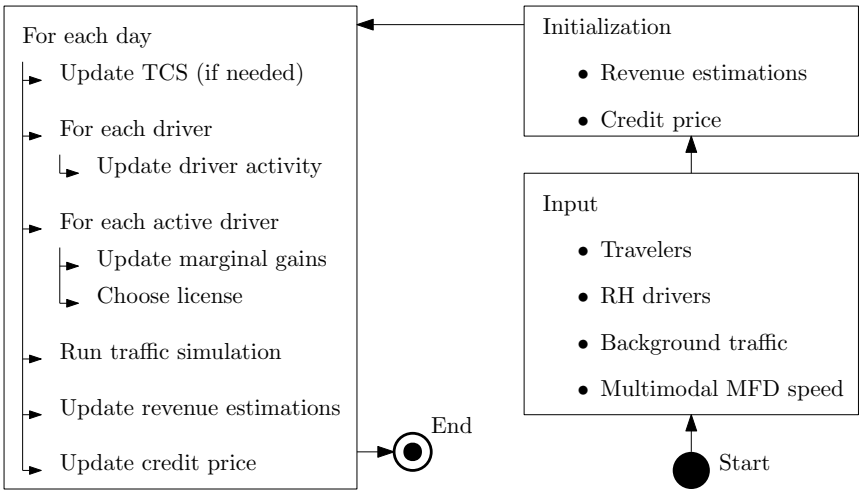

Figure 6.4: Simulation of the day-to-day RH operations.

differs from the previous day. Each driver chooses if it joins the RH service for the day or not. The active drivers then choose their licenses. The revenue estimations and the credit price are updated to provide a basis for the next day's decisions. Each step is detailed in the following paragraphs.

Update active car drivers

Every day, the number of active car drivers is updated using an estimation of the average RH revenue in the whole city (all regions combined) $\tilde{R}^{\text{avg}}$ based on past days' observations. The drivers decide if they want to join the RH service for the day. Note that the license choice occurs later. The RH drivers for whom the estimated RH revenue is higher than their reservation price will join the RH market and thus get their free allocation of credits. The other drivers do not take part in the RH services. They wait the next day to reevaluate the estimation of the RH revenue. Note that the credit price does not impact the average RH revenue because the credit consumption is balanced in the long term. Thus, the total money flow from the RH drivers to the regulator is null at equilibrium.

Car drivers choice of license

The active drivers then choose the license they will acquire with credits, buy the required credits or sell the extra ones. They consider the estimation of marginal gains for changing their license to a more expensive or cheaper one. We first define the marginal gain MG_r of adding access to region r for a driver who already can access the region $r+1$. The marginal gain is the average revenue of region r minus the price

of the additional credit charge:

$$\begin{aligned} MG_r &= \tilde{G}_r^{\text{avg}} - \tilde{G}_{r+1}^{\text{avg}} \\ &= \frac{\tilde{R}_r(day)}{\sum_{r' \leq r} x_r} - p(day)(\tau_r - \tau_{r+1}),\ \forall r \in [1, N_R - 1]. \end{aligned} \tag{6.23}$$

A positive marginal gain for region r means switching from license $r+1$ to r will increase the driver's profit. It means the additional revenue a driver can earn by operating in this additional is higher than the additional money needed to buy the required license. Conversely, negative marginal gain means accessing the new market is not worth the extra credit cost.

After each driver choice, the marginal gains MG_r are updated as the distribution of license holders x changes, and thus the denominator of the first term in Eq. (6.23) varies. For the case of a city split into $N_R = 3$ regions, the current RH driver chooses its next license following the diagram in Fig. 6.5. The license choice depends on

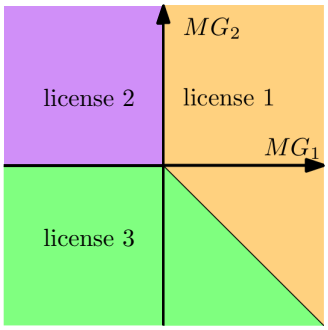

Figure 6.5: Driver assignment depending on the evaluation of the marginal gains.

the signs of MG_1, MG_2, and the sum $MG_1 + MG_2$. For example, MG_1 negative and MG_2 positive means a RH driver currently owning a license 3 has an interest in switching to license 2 (extra RH revenue higher than credit cost) but not to license 1 (extra credit cost higher than additional RH revenue).

Update revenue estimation

After the traffic simulation, the estimated RH revenue for each region $\tilde{R}_r$ is updated using the observed revenue for the current *day*:

$$\tilde{R}_r(day+1) = \tilde{R}_r(day) - \frac{1}{\sqrt{day - T_\tau}}(\tilde{R}_r(day) - R_r). \tag{6.24}$$

The update factor decays with time and is reset at each time T_τ the regulator modifies the credit charges. T_τ satisfies $T_\tau \leq day < T_{\tau+1}$, $T_{\tau+1}$ being the date of the next TCS change.

The estimated average revenue is also updated following the current day RH revenue:

$$\tilde{R}^{\text{avg}}(day+1) = \tilde{R}^{\text{avg}}(day) - \frac{1}{\sqrt{day - T_\tau}}\left(\tilde{R}^{\text{avg}}(day) - \frac{\sum_r R_r}{|\mathcal{D}|}\right). \tag{6.25}$$

Update credit price

The credit price is updated according to the credit consumption to reach a budget-neutral state.

$$p(day+1) = \max\left(0, p(day) + \frac{\Delta_p}{\sqrt{day - T_\tau + 1}} \sum_{i \in \mathcal{D}} (\tau_{lic_i} - \kappa)\right), \tag{6.26}$$

The factor associated with the credit balance also decays with the number of days since the last change of TCS, to smoothen the price and ensure convergence. The sensitivity of the price change to the credit balance Δ_p is set by the regulator. lic_i is the license chosen by the driver i.

6.4 Case study

We illustrate the proposed methodology with an example. The case study is designed to quantify the effect of different TCS on different stakeholders at different aggregated levels, such as mode shares, drivers' assignments, and total travel costs.

Transportation network

The fictive city is a square with a side length of 12 km. It is split into $N_R = 3$ regions, as presented in Fig. 6.1. The distance between two points is expressed with the Manhattan distance (the sum of the absolute difference between each coordinate), assuming the road network is a grid. PT mean speeds and access times depend on the departure and arrival regions, as presented in Table 6.1. Transit is faster and more frequent in the city center. The access times also account for the walking time from origin to station and from station to destination determined by the trip's highest region. The access time is divided by two for combined trips (RH and PT), as the RH vehicle picks up or leaves the passenger close to the transit station. The PT fare f_{PT}

Origin/Destination	1	2	3
1	7 (5)	6 (10)	6 (15)
2	6 (10)	6 (10)	5 (15)
3	6 (15)	5 (15)	5 (15)

Table 6.1: PT mean speeds (m/s) and headtimes (between brackets, min) for the different region OD pairs.

is set to 1 EUR per trip. The PT fare system is simplified as it does not depend on the distance traveled or the number of visited regions. It usually holds for small to medium cities but not for large metropolis. The city is represented as a unique MFD region for computing the trips. The following affine MFD speed function represents the congestion dynamics:

$$V(n) = V_{\max}\left(1 - \frac{n}{n_{\max}}\right). \tag{6.27}$$

The maximum speed $V_{\max}$ and the maximum accumulation $n_{\max}$ are set to 10 m/s and 5 000 vehicles, respectively.

Demand

We generate 1 000 travelers as individual travelers. Each agent has a VoT drawn from a uniform distribution between 20 and 100 EUR/h. Their departure times are drawn from a uniform distribution between 0 and 1 hour. The trips are generated by randomly picking up the origin and destination regions. The probability associated with each pair of regions is presented in Table 6.2. More trips depart or arrive in

Origin/Destination	1	2	3
1	5/34	4/34	4/34
2	4/34	4/34	3/34
3	4/34	3/34	3/34

Table 6.2: Demand distribution for the different region OD pairs.

regions close to the center. The origin and the destination are selected by randomly drawing a point for each region.

Background traffic is generated with 3 000 cars following the same distribution of trip lengths. The departure time distributions of the background traffic and MaaS customers are shown in Fig. 6.6.

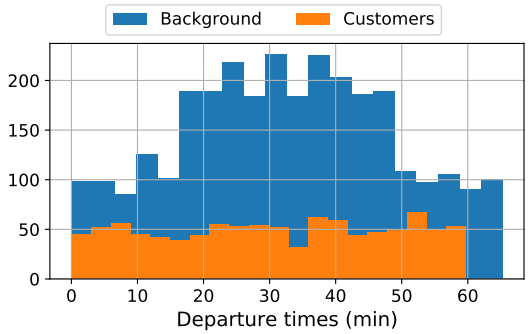

Figure 6.6: Departure time distribution of the background traffic and the MaaS customers.

These background vehicles only affect the traffic conditions, as those users do not change mode (thus do not request RH rides) and do not take part in the TCS. We simulate with only the background traffic first and add the car accumulation due to this background traffic when running the primary simulation with MaaS operations. We neglect the impact of RH drivers on the overall accumulation as their number is one order of magnitude below the number of background vehicles.

RH offer

We generated a pool of $|\mathcal{D}_0| = 150$ potential drivers, with reservation prices uniformly generated between 10 and 50 EUR. Note that the RH operations have a secondary impact on the traffic condition. The background traffic significantly affects the congestion level. We set the RH fee at 2 EUR/km. The matching period is 2 min. The RH requests are buffered during each matching period. Then a matching process assigns available RH drivers to the passengers. If a passenger is not matched, it will be sent to the next batch. After three failures, the passenger will ride PT.

TCS design

The regulator provides free $\kappa = 10$ credits to each *active* driver. It successively introduces TCS to restrict the access of regions 1 and 2. See Table 6.3. For the first

Day T_τ	Credit charge τ
10	[15, 10, 0]
50	[20, 10, 0]
90	[40, 20, 0]

Table 6.3: Credit charges and introduction day.

ten days, no TCS is applied, then a credit charge of [15,10,0], [20, 10, 0], and [40, 20, 0] are introduced every forty days. For example, a driver needs to spend 20 credits to operate in region 1 for a day between day 50 and day 89. It will require 40 credits afterward.

6.5 Numerical results

We first estimate the effect of TCS on the RH service at equilibrium. Thanks to the problem size reduction (6.22), there are only three unknowns: the number of active drivers $|\mathcal{D}|$, the number of license 1 holders x_1 and the credit price p. We use the tool *differential evolution* from the Python toolbox *SciPy* (Virtanen et al., 2020) to minimize the cost function J. The tool is based on genetic algorithm techniques, more precisely on the algorithm developed by Storn and Price, 1997. We only have to compute the number of active car drivers for the no TCS case. The cost function is J_2, i.e., only the error associated with active drivers.

We then look into the transition from the status quo to different TCS. The regulator gradually introduces the TCS for RH drivers in the following day-to-day scenario. The introduction of the TCS affects the average RH revenue and thus the number of active RH drivers, as seen in Fig. 6.7. As expected, the RH revenue (Fig. 6.7(a)) decreases with the TCS as the RH drivers are more constrained in the type of trip they can serve. When the TCS changes, the estimation of the average revenue undergoes some oscillations. The RH market needs some days to adapt to the new constraints the TCS sets. It converges after two to three days. As a consequence, the number of active RH drivers (Fig. 6.7(b)) decreases as the RH revenue does not exceed their reservation price anymore. The equilibrium computation reasonably estimates the number of RH drivers for the no TCS and the first two TCS with an error of less than 4%. The equilibrium computation overestimates the number of active drivers by 7% for the last TCS. We evaluate the value of the cost function with the average value over the last 10 days. The value is 24.9. It is far higher than the costs associated with the result of the equilibrium computation 0.2. The explanation is the equilibrium computation of minimizing J (difference with the maximum gain weighted by the number of license holders, Eq. (6.18)) is not equivalent to the day-to-day process, which involves assigning drivers to the most profitable licenses.

The cap of credits is not a hard constraint in the transient simulation as the bank can punctually sell more credits than the number it buys from RH drivers. The evolution of the credit balance (consumption minus allocation) and credit price is presented in Fig. 6.8. The credit balance and, consequently, the credit price are destabilized after each change of TCS, and it takes a few days to reach the new

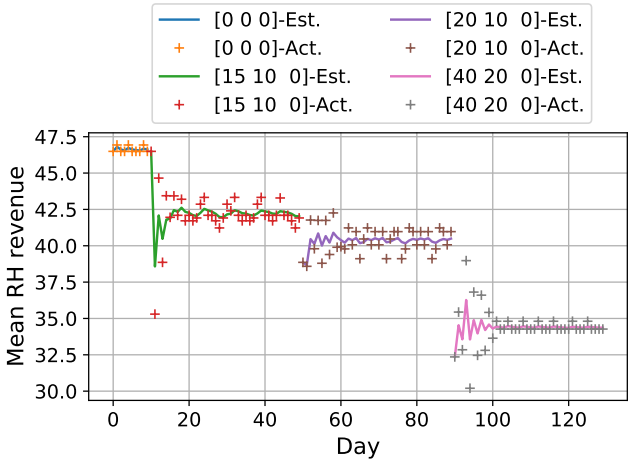

(a)

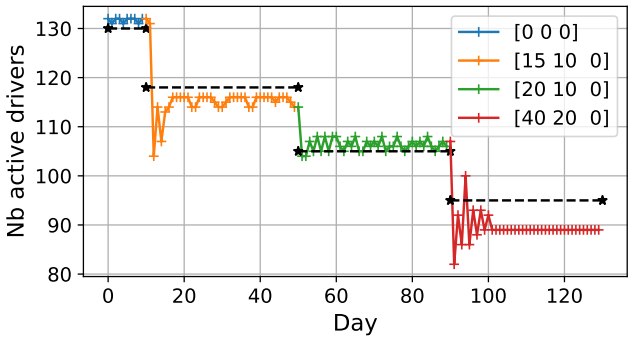

(b)

Figure 6.7: Evolution of (a) the average actual (Act.) RH revenue and its estimation (Est.) and (b) number of active RH drivers. The black dashed lines are the equilibrium values for the corresponding TCS computed with the heuristic method.

equilibrium with a balance of credit consumption. After introducing the first TCS, the overshoot represents about 100% of the equilibrium value. Based solely on the previous day's observation (no TCS), the RH drivers chose their assignment as per no TCS, resulting in a great credit imbalance and, thus, a proportional and strong price correction. The equilibrium computation (black dashed lines) gives a close estimate of the credit price, with an error of less than 7%. The credit price decreases as the TCS becomes more constraining. Note that, as the drivers require more credits to operate in the inner regions, the money required to operate in the city center usually increases even if the credit price decreases.

The evolution of the equivalent license prices, i.e., the out-of-pocket money spent or earned by buying or selling the required credits $(\tau_r - \kappa)p$, is presented in Fig. 6.9. The number of RH drivers buying the license for region 1 is also shown. The more constraining the TCS is, the more expensive the access to region 1 for RH drivers is. During the first two TCS, where $\tau_2 = \kappa$, the free allocation covers the need to access region 2. Its access is thus free. As no credits are required for region 3 ($\tau_0 = 0$), drivers only accessing region 3 earn money as they sell their credits. The equilibrium computation allows for a good prediction of the RH drivers' assignment. The error is at the maximum of 4%. The number of drivers operating in the city center decreases as the TCS becomes more constraining. Without TCS, 87% of the workforce operates

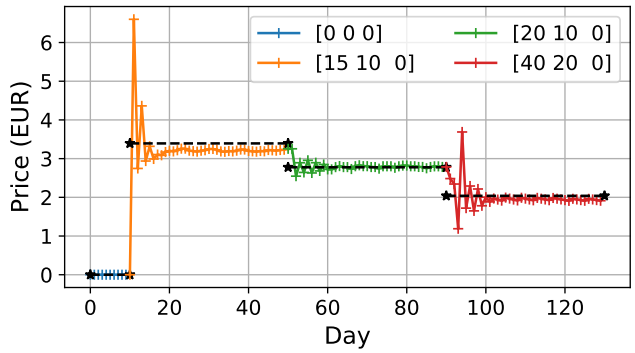

(a)

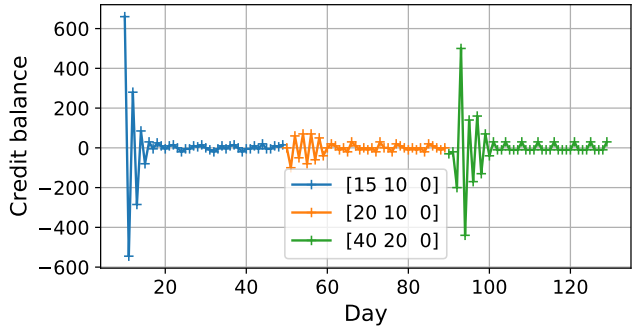

(b)

Figure 6.8: Evolution of (a) the credit price and (b) credit balance. The black dashed lines are the equilibrium values for the corresponding TCS.

in region 1 against 14% with the last TCS.

Fig. 6.10 shows the evolution of mode choice. The TCS decreases the number of active drivers and the number of drivers operating in the city center. Customers tend to shift to PT or combined trips (PT+RH) because they face higher RH travel costs, or RH drivers are unavailable. In absolute (Fig. 6.10(a)), the majority of the customers report on PT. However, the relative change (Fig. 6.10(b)) is higher for combined trips (PT+RH), with an increase of more than 2.5 for the last TCS.

Table 6.4 details the mode changes between the no TCS case and the last TCS ([40,20,0]) for each pair of regions of origin and destination. The TCS makes the shares of RH-only rides decrease for all trips, except for trips inside the outermost region 3, where RH share increases by 17 points. PT share increases, except for trips between 2 and 3 and inside 3, where it decreases by 8 to 19 points. The share of combined trips increases between regions 1 and 3 and 2 and 3. It reaches 0 for trips between 1 and 2. However, it was already small without TCS. The induced shortage of RH drivers allowed to operate in region 1 nudge travelers to use PT in the city center. Instead, the RH drivers are available in the periphery to drain passengers from the outside regions to PT stations at the center border and pick up passengers at those stations to drive them to their destination in the suburbs.

The transition of TCS leads to large overshoots for the credit price, number of active drivers, and driver assignment. We assume the regulator does not tolerate large oscillations, as the lack of smoothness renders the TCS unpopular with RH drivers and travelers having to change their travel habits drastically on consecutive days. We propose to use the knowledge of the credit price from the equilibrium computation

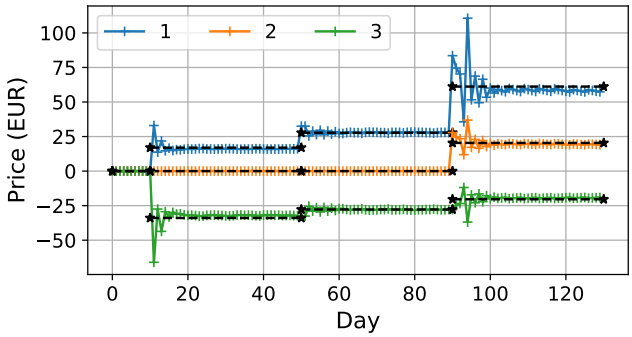

(a)

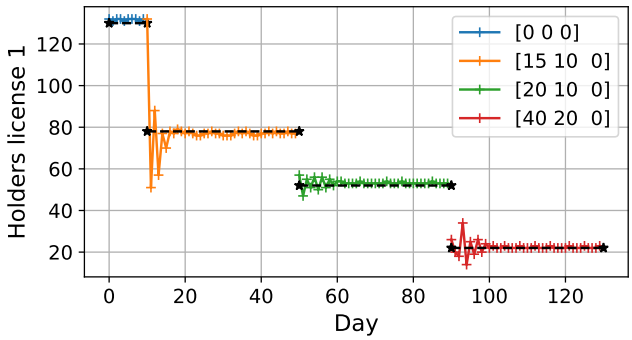

(b)

Figure 6.9: Evolution of (a) the equivalent license prices and (b) the number of RH drivers active in the city center. The black dashed lines are the equilibrium values for the corresponding TCS.

to provide a warm start: the credit price is set to the value from the equilibrium computation for the three days following the change of TCS. The evolution of the number of active drivers, credit price, and number of drivers operating in the city center is presented in Fig. 6.11. Thanks to the warm start from the equilibrium computation, the system avoids large overshoots when transitioning from one TCS to another. The communication of the equilibrium price value simultaneously with the introduction of the TCS allows the RH drivers to adapt to the new TCS faster. The equilibrium values are similar with and without warm starts. It is important for acceptability that the stakeholders can predict the effect of the TCS before its introduction. They can thus plan their response to the new TCS and not only react to the new schemes.

The global effect on the transportation system can be assessed by the total travel time and the total driven distance in Fig. 6.12. The first TCS leads to an increase of the travel time of 22%, travel cost of 20%, and a decrease of RH distance of 13%. The second TCS increases the travel time by 40%, travel cost by 35%, and decreases the RH distance by 21%. The third increases the travel time by 61%, the travel cost by 55%, and decreases the RH distance by 36%. To put the TCS into perspective, removing the RH service completely and having all travelers riding the PT increases the total travel time by 87% and the travel cost by 75%. The RH distance is zero. Total travel time (Fig. 6.12(a)) increases since some passengers using RH need to take PT with the introduction of the TCS. The effect of RH on traffic conditions is secondary to the background traffic. Thus, the decrease in RH activities does not significantly improve the driving conditions. The total travel cost (Fig. 6.12(b)) includes the travel times

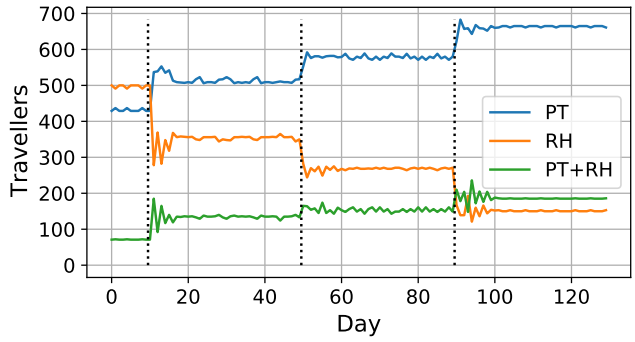

(a)

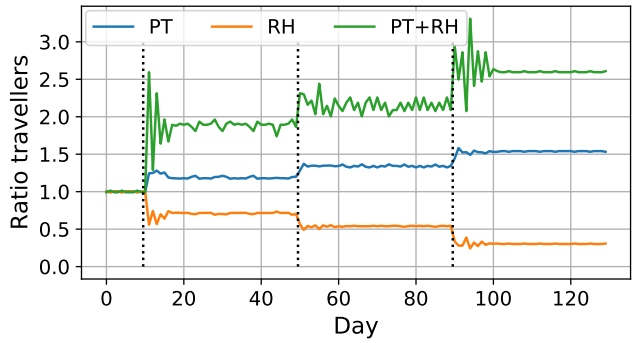

(b)

Figure 6.10: Mode choice evolution: (a) absolute and (b) relative. The reference is the no TCS case. The black vertical dotted lines mark the TCS changes.

weighted by the VoT and the fees paid for using RH and PT. The total driven distance (Fig. 6.12(c)) decreases since more commuters use PT only or in combination with RH. As a benchmark, the total travel time is represented when travelers can only ride transit.

The impacts of TCS on total travel time and driven distance are presented as a Pareto front in Fig 6.13 to highlight the compromises between the two objectives. The first seven days are removed to keep the states close to equilibrium. The total driven distance is a proxy for the negative externalities of RH. The TCS reduces the total driven distance and increases the total travel time. TCS is a tool to regulate RH continuously between the unregulated RH operations and the ban of RH services. It proposes different compromises regarding sustainability and minimum level of service for the regulator to match its objectives.

O/D	1			2			3		
	PT	RH	PT+RH	PT	RH	PT+RH	PT	RH	PT+RH
					no TCS				
1	48	52	-	43	54	3	33	51	16
2	42	38	16	45	55	-	39	55	6
3	47	41	12	41	53	6	48	52	-
					TCS [40,20,0]				
1	95	5	-	98	2	0	43	19	37
2	95	5	0	98	2	-	28	22	49
3	48	11	41	33	10	57	31	69	-

Table 6.4: Mode shares (%) without TCS and with the last TCS ([40,20,0]) for the different pairs of regions. Red means the mode share decreases with the TCS and blue means it increases.

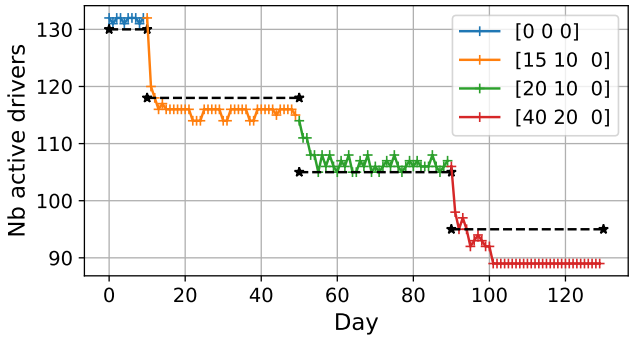

(a)

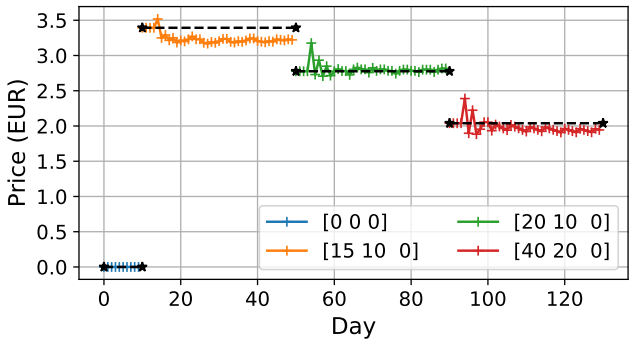

(b)

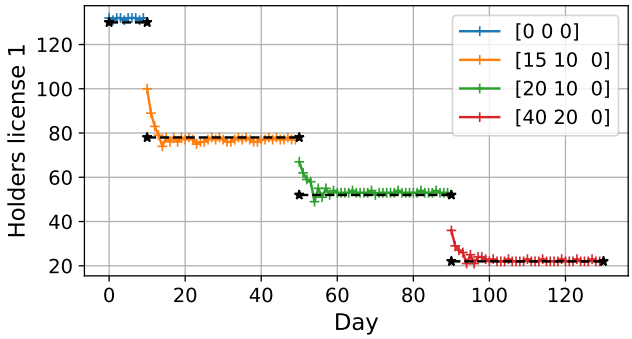

(c)

Figure 6.11: (a) Number of active drivers, (b) credit price, and (c) number of license 1 holders when providing a warm start for each TCS change.

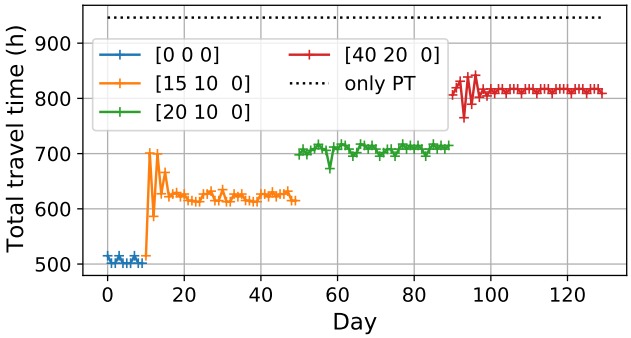

(a)

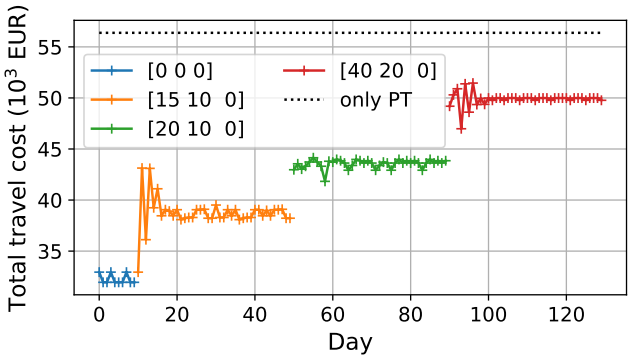

(b)

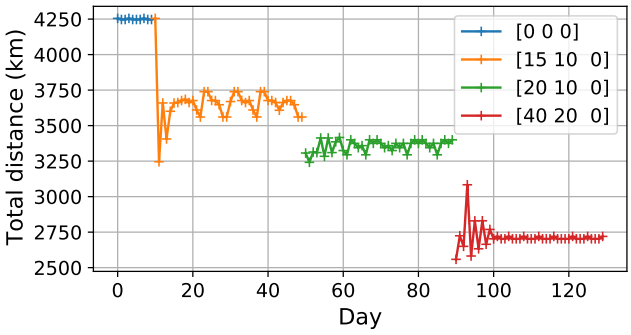

(c)

Figure 6.12: (a) Total travel time, (b) travel cost, and (c) driven distance (including pick-up distance). Without warm starts of the credit price.

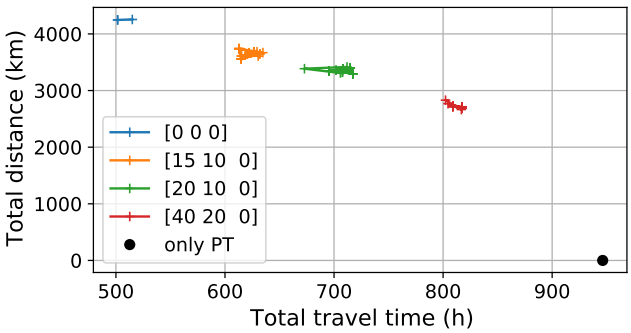

Figure 6.13: Total travel time and PT revenue.

6.6 Conclusions

In this chapter, we developed a policy based on TCS to regulate the RH services and foster a combination of RH and PT. The regulator provides a free allocation of credits to each active RH driver. Operating in different regions requires credits. The more central the region is, the more credits are needed, as the regulator wants RH drivers to operate in regions with low PT service levels. The novelty lies in regulating RH operations within a TCS framework. Indeed, TCS has been proposed in the literature (and in the previous chapters) to regulate the travel demand but not the transportation offer. We developed an MFD-based framework to compute the travel times and track the position of the RH drivers. Travelers are matched with Rh drivers or assigned to PT via a MaaS platform. We formulate the equilibrium under a TCS regarding the assignment of the drivers in the different regions, the offer elasticity, and the credit price. The equilibrium is computed with a heuristic method. The transition between the no TCS case and the TCS is represented by a day-to-day process where the credit price and driver choices (activity and operating regions) are updated daily depending on the credit balance and the RH revenues. A numerical case study illustrates the effect of the TCS. The TCS forces RH drivers to operate less in the city center and more in the suburbs. Consequently, travelers prefer riding PT or combining PT and RH to reach their destination. The total travel time increases, and the total traveled distance decreases. It offers a range of compromises for the regulator to protect the PT from the unfair RH competition instead of the binary choice of allowing/forbidding RH operations.

This study does not account for demand elasticity. Depending on the level of service of the proposed MaaS and the effect of the TCS on the operation of the RH drivers, some travelers may switch from private cars to PT+RH or, on the opposite, switch from RH to private cars. Future work should investigate TCS to reduce private car trips by replacing them with a combination of PT and RH and, in the long term, reduce car ownership.

Chapter 7

Conclusion

Different demand management policies have been proposed and applied to reduce traffic congestion in urban regions. TCS was proposed some decades ago. It is a cap and trade policy. Credits are issued to travelers, and each travel alternative requires a different amount of credits. The literature review in chapter 2 summarizes the past contributions related to TCS and similar policies. It helped us find research gaps in the literature and thus define research directions for this thesis. The main novelty in this thesis is the evaluation of TCS using the trip-based MFD to represent the congestion dynamics.

7.1 Contribution to the research questions

The following paragraphs detail how this thesis contributes to the research questions formulated in chapter 1.

Evaluation of TCS with a dynamic representation of the congestion

The chapter 3 answers the questions *How does the formulation change when introducing a dynamic representation of the network? How relevant is the introduction of trip heterogeneity and congestion dynamics for evaluating TCS?* The trip-based MFD is chosen to represent the congestion. It accounts for the congestion dynamics, trip length heterogeneity, and the effect of departure time distribution. A simulation framework for evaluating TCS with a trip-based MFD framework is formulated. The proposed TCS aims at nudging commuters from private cars to transit. The challenge lies in the implicit formulation of the trip-based MFD. The developed method finds the equilibrium by linearizing the problem formulation and solving a quadratic problem. The importance of the trip length and departure time distribution is assessed by modifying the trip length and departure time distribution. The results for Lyon show it significantly affects the TSC outcomes (e.g., travel choices and credit price). It thus highlights the limits of approaches based on the BPR function and Vickrey bottleneck.

Application to a realistic use case

Chapters 3, 4, and 5 answer the question *What impacts can we expect in the case of a real scenario?* Using a realistic network permits quantifying the gains brought by a TCS and provides an order of magnitude of the effects on the transportation network.

For example, chapter 3 concludes that a joint reduction of the total travel time by about 17% and carbon emissions by about 45% can be reached with TCS.

Comparison between TCS and other DMS

The chapter 4 compares different DMS to answer the questions: *What is the effect of being able to stock the credits earned one day to use on another day? What is the effect of trip-specific charges? How does TCS perform against other DMS?* To sum up, allowing for the credit to be stocked gives more flexibility to travelers and smoothens the credit price. Note that we assume travelers cannot sell credits they previously bought to prevent speculation. The TCS is better than LPR and TPS regarding compromises between total travel time, pollution, and flexibility. It is expected as TPS and LPR are less flexible. At equilibrium, the TCS, with the ability to stock credits, performs similarly to pricing. TCS has the additional advantages of being budget-neutral and allowing travelers not to spend out-of-pocket money by stocking credits. However, trying to account for the spatial difference regarding the PT alternative does not work well, as the day-specific need to use the car is more valuable for travelers.

The chapter 5 introduces time-dependent credit charge and thus answers the question *How is a time-dependent charging scheme better than a static one?*. A dynamic TCS permits to reach even better compromises between perceived travel costs and carbon emissions. The optimized time-dependent TCS permits to reduce the total travel cost by 20% compared to the no TCS scenario, whereas the static TCS reduces the total travel cost by 19%.

Effect on heterogeneous travelers

The chapter 5 includes different traveler profiles: VoT, desired arrival time, origin, and destination. The different VoT act as a proxy for different revenue levels. It thus partially answers the question *How does the TCS affect travelers with different revenue levels?*. Under the proposed TCS and case study, most of the users (94%) are better off with the TCS as their travel costs decrease. When looking closely at the VoT, the main trend is that high-VoT buy credits from low-VoT users. This result shows the developed framework can be used to assess the effect of TCS on heterogeneous users. As the trip-based MFD permits representing the travel demand as a set of agents, it leaves room for representing additional sources of heterogeneity, such as rationality or accessibility.

TCS for on-demand mobility services

The chapter 6 answers the questions *How could we use TCS to regulate transportation offers? What are the insights of using a TCS to regulate on-demand services?*. RH services are regulated through a TCS to nudge RH drivers to leave the city center for the suburbs, as competition with PT, where the PT coverage is excellent, is not wished for. The presented TCS promotes a combination of both offers for the RH service to complete the PT where the transit services are sparse.

7.2 Research perspectives

At the end of this thesis, we identified some research directions which would follow and extend the presented research.

The scope of the thesis is to provide a simulation framework to design, evaluate, compare, and optimize TCS. Travelers' decisions are approximated with logit-based models. The first research perspective is the run of pilot experiments to calibrate and validate the presented modeling frameworks and quantify the error resulting from the logit approximation of users' behavior. It would also provide insights regarding the acceptability of the TCS by the users.

The second direction is further investigating the relationship between the RH economy and the implementation of a TCS both for RH services as in chapter 6 and for commuters (chapters 3, 4, and 5). The TCS would nudge the commuters not to drive their personal cars and use the MaaS system (combination of PT and RH services) instead. It would also drive the RH service to operate in the suburbs to improve the MaaS level of service between the city center and the suburbs. The regulator can expect that a TCS improving and extending the MaaS coverage to the whole network will reduce car ownership.

The third direction concerns the application of TCS in an interurban context. The context differs from the one presented in this thesis as the network, and the demand have different patterns: the network is made of a few long links, and the number of different origins and destinations is low. The MFD framework is not suited anymore, as it was designed for urban networks. A pilot is underway with the *MedHighway* pilot in the EU project *DIT4TraM*. The pilot's objective is to use a TCS to regulate access to the portion of a Spanish Highway around the city of Girona to prevent the creation of congestion and react to temporary capacity drops.

Let us finish by formulating other challenges related to the practical application of the TCS. In this thesis, we suppose the TCS applies between the boundaries of the metropolis (the city and its close suburbs) and that every traveler or RH driver gets a portion of the free allocation. These hypotheses should be questioned to pave the way for realistic implementation. Is the city a good scale? Or is a regional or national level more adequate? Who should get free credits? People employed in the city? Inhabitants? Driving license holders?

Appendix A

Appendix Chapter 3

A.1 Notations

Parameters, variables, and other notations for Chapters 3 and 4 are respectively summed up in Tables A.1, A.2, and A.3.

Table A.1: Summary of parameters notations.

Notation	Meaning
α	VoT.
γ_i	Number of users in group i.
Γ	CO_2 weight for the credit charge optimization.
κ	Credit allocation.
κ^{TPS}	Macro permit allocation ratio.
κ_k^{TPS}	Allocation ratio of permit k.
τ	Macro credit charge.
τ_k	Credit charge k.
η	MCC weight for the QP.
η^{TPS}	MCC weight for the QP with TCS.
θ	Logit parameter.
c	Validity cycle length.
$C_{i,\text{PT}}$	Travel cost of group i by PT.
N	Number of groups.
N_K	Number of different charges (D or OD).
P_{carbon}	Carbon price.
r_i	Ratio of travellers in group i having access to a car.
$T_{i,\text{PT}}$	Travel time per PT of group i.
l_i	Trip length of group i.
t_i	Departure time of group i.
w_k	Quality of the PT alternative.

Table A.2: Summary of variables notations.

Notation	Meaning
$C_{i,\text{car}}$	Travel cost of group i by driving its car.
δ_v	Local slope of the gradient of the speed (taken as positive).
e, g	Event: either the entry or the exit of an group on the network.
$e_{i,e}$	Event when group i ends its trip.
$e_{i,s}$	Event when group i starts its trip.
E	Total network CO_2 emissions.
E_{dist}	CO_2 emission per distance.
$z(t)$	Distance traveled by the virtual traveler until time t.
i, j	Index of an group, which represents a group of travelers.
l_e	Distance traveled between the events e and $e+1$.
L_m	Mean traveled distance by car.
L_m^w	Mean traveled distance by car weighted by the absolute values of the gradient of the logit.
L_{tot}	Total traveled distance.
n	Accumulation at a given time.
$\bar{n}$	Typical accumulation.
N_c	Number of car users.
p_k	Price of toll k.
p^{TCS}	Credit price.
p_k^{TPS}	Price of permit. k
n	Accumulation at a given time.
t_e	Time at which the event e occurs.
T_e	Time between the events e and $e+1$.
T_i	Travel time per car of group i.
T_{dept}	Departure time window.
TT_{c}	Mean travel time per car.
TT_{c}^w	Mean travel time per car weighted by the absolute values of the gradient of the logit.
TT_{PT}^w	Mean travel time per PT weighted by the absolute values of the gradient of the logit.
TTT	Total travel time.
V	Mean speed in the network at a given time.
$\bar{V}$	Mean speed in the network over the whole simulation.
w_i	Absolute value of the gradient of the logit.
$\mathbf{x_d}$	Shares of groups taking the car on day d.
$\tilde{\mathbf{x}}$	Concatenation of modal shares for each day and credit price.
$\bar{\mathbf{x}}$	Concatenation of modal shares for each day and permits prices.
ψ	Modal decisions of the groups.
$\mathbf{\Psi}$	Concatenation of modal decisions for each day.

Table A.3: Other notations.

Notation	Meaning
$\cdot_0$	Reference value.
$\Delta\cdot$	Difference of the value of the variable compared to its reference.
$\nabla_\cdot\cdot$	Gradient.
$\nabla\cdot$	Gradient of the variable related to the modal shares.
$\tilde{\nabla}\cdot$	Gradient of the variable related to the modal shares and the credit price.

A.2 Numerical evaluation for the condition of uniqueness

We evaluate numerically the assumption Eq. (3.9) for the numerical use case in Sect. 3.5. 20 000 modal share vectors $\mathbf{x}$ are generated using a Latin Hypercube sampling. It represents about ten points per dimension. The Eq. (3.9) is computed for every pair of different points. The distribution of the dot product is represented in Fig. A.1. The assumption Eq. (3.9) seems to hold for our numerical example. The

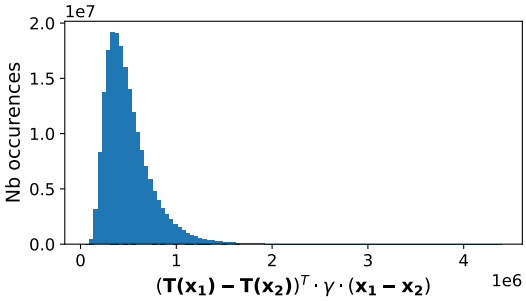

Figure A.1: Computation of the dot product of the car travel time differences and weighted modal share differences.

equilibrium might be unique.

A.3 Sensitivity of the PT travel times

To assess the effect of the PT level of service on the whole network, we change all the PT travel times by -20%, -10%, 10%, and 20%. A negative change means the transit alternative becomes faster, and thus the PT level of service is improved. We assess the effect on total travel time, carbon emissions, and toll equivalent $p^{\mathrm{TCS}}(\tau - \kappa)$ in Fig. A.2.

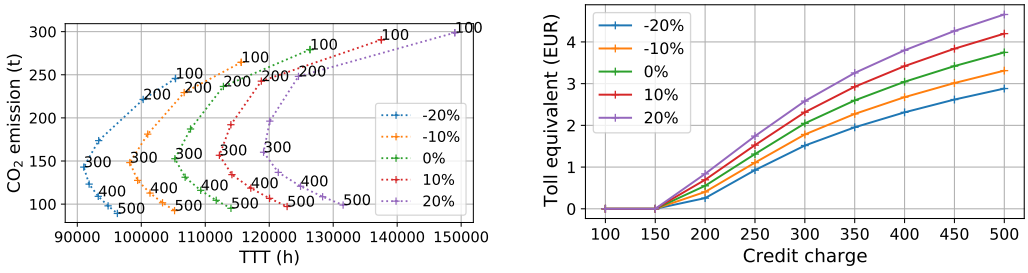

(a) (b)

Figure A.2: (a) Total travel time vs. carbon emissions and (b) toll equivalent for different variations of the PT travel times. The numbers in (a) are the credit charges.

The results are intuitive: with a reduction of the PT travel times, the total travel time decreases because (i) transit alternatives are faster and (ii) more travelers switch from car to PT because it is more competitive and there are fewer car drivers. Thus the traffic conditions are improved. A variation of the PT level of service of 20% leads to a total travel time variation of about 10%. The carbon emissions slightly decrease thanks to the better competitiveness of PT. The Pareto fronts are different, and we can quickly compute them thanks to our framework. The equivalent toll decreases

because the transit service is more attractive, and the advantage of driving a personal vehicle becomes less valuable. For a credit charge of 500 credits, the equivalent toll increases by about 1 EUR when the PT travel times increase by 20%, and it decreases by about the same when the PT travel times decrease by 20%.

A.4 Sensitivity of the threshold for the search space

To assess the sensitivity of the search for a modal equilibrium with regard to the maximum allowed variations ϵ_x and ϵ_p, different constant thresholds 0.01, 0.05, 0.1, 0.5, and 1 are compared to the inverse of the time step (Ref.) in Fig A.3 for no TCS, credit charge of 200, and 300 credits.

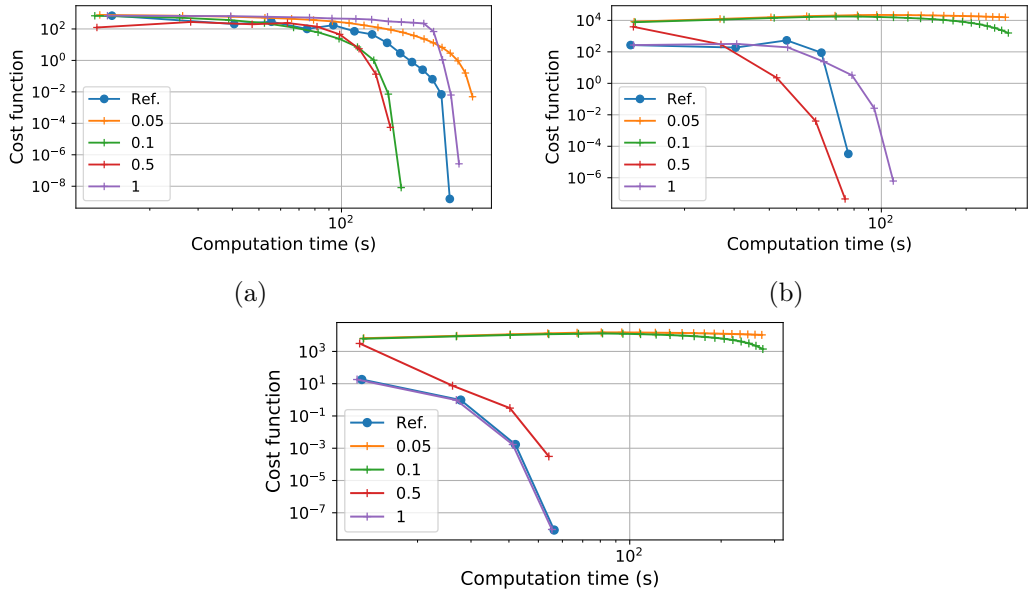

Figure A.3: Cost function values vs. computation time for different maximum allowed variations with (a) no TCS; (b) a credit charge of 200 credits; and (c) a credit charge of 300 credits.

Setting the allowed maximum variation too low makes the convergence more difficult. When convergence occurs, all the values lead to the same equilibrium. There is no best value for the maximum allowed variations in terms of computation time. The chosen approach with the inverse of the step size is a good compromise.

Appendix B

Appendix Chapter 4

B.1 Sensitivity of the PT penalty distribution

For actual implementation, the estimate of the distribution of the need to drive a car across the days is prone to uncertainty. To assess the robustness of the TCS, we perform a sensitivity study with regard to the distribution of the PT penalty over the days, we vary it by 20%. We present the penalty distributions, the car shares, equivalent toll prices, total travel times, satisfaction rates, carbon emissions, and social costs in Fig. B.1. At first, it is surprising that the mean car share without DMS

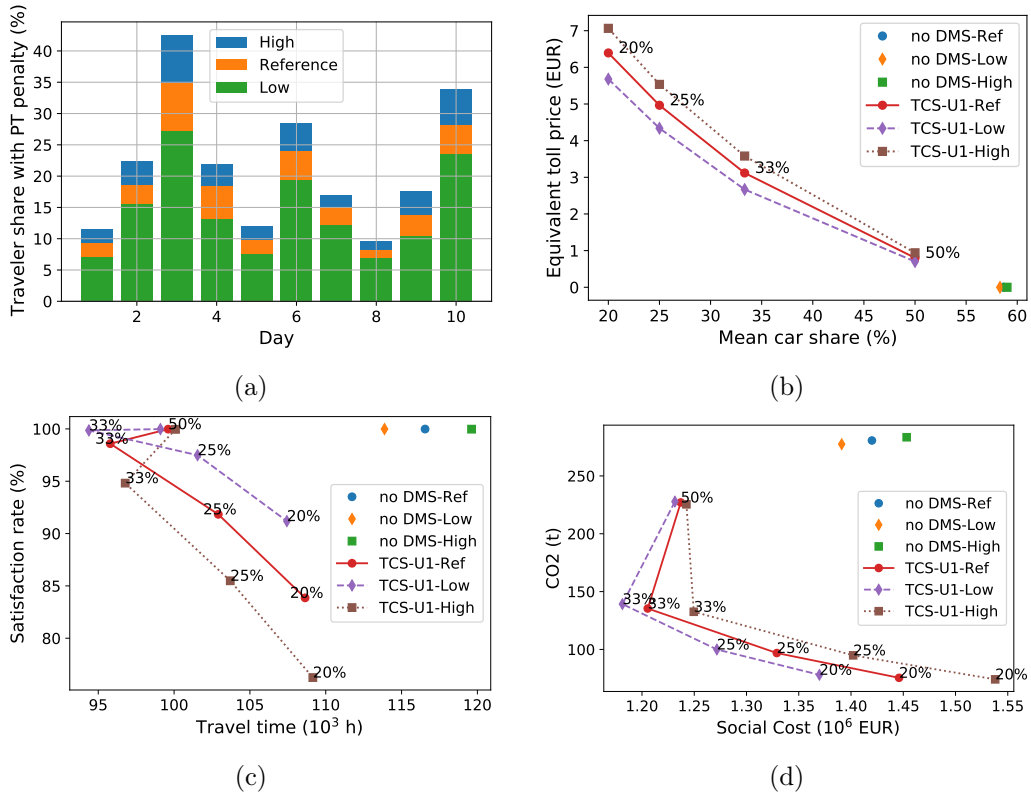

Figure B.1: TCS-U with different PT penalty distribution: (a) PT distribution; (b) toll equivalent vs. car share; (c) total travel time vs. satisfaction rate; and (d) social cost vs. carbon emissions.

does not change significantly and stays around 60%. The explanation is that travelers who need to drive their cars do so. In the case of a high car demand, the car traffic conditions worsen, and other travelers tend to prefer PT. The toll equivalent increases

as more travelers need to drive their cars. Indeed, the credit price increases as the credit demand increases. The satisfaction rate drops with an increasing number of travelers needing to take the car with TCS. For a credit ratio of 25%, the satisfaction rate loses 6 points between the reference and the high demand distribution. The total travel time increases for the no DMS scenario when the number of mandatory car users increases, whereas it stays similar to TCS. The credit cap permits to keep the car shares under control, regardless of the demand, at the expense of the satisfaction rate. As it becomes difficult to satisfy the demand, the cost of driving the car increases (because of the credit price). Some travelers would prefer to face the PT penalty rather than buy the necessary credits. The uniform TCS still reduces both carbon emissions and social costs. Still, the quality of the compromises decreases with a higher traveler share facing PT penalties as the penalty costs increase for a fixed carbon level. With TCS, the regulator needs to sacrifice the satisfaction rate to reach given pollution levels or total travel time.

Appendix C

Appendix Chapter 5

C.1 Notations

Parameters, variables, and other notations for Chapter 5 are summed up in Table C.1.

Table C.1: Summary of parameters and variables notations.

Notation	Meaning
Parameters	
Ω	Ensemble of travelers' characteristics and choices.
Ω_m^W	Subspace of Ω restricted to mode m and charging period W.
$\Omega_m^W\{l\}$	Ω_m^W further restricted to trips of length l.
$\mathcal{C}$	Ensemble of travelers classes (VoT).
c	Traveler's class.
α_c	VoT of class c.
$\tilde{\beta}_c$	Normalized marginal early cost of class c.
$\tilde{\gamma}_c$	Normalized marginal late cost of class c.
$\mathcal{L}$	Ensemble of trip lengths.
l	Trip length.
$\mathcal{M}$	Admissible modes.
$\mathcal{T}_a$	Ensemble of desired arrival times.
t_a	Desired arrival time.
$\mathcal{T}_d$	Admissible departure times.
$d(c, l, t_a)$	Travel demand distribution.
D	Total number of travelers.
χ_{opt}	Optimization parameter.
κ	Credit allocation.
$\tau(t_d, m)$	Credit charge for mode m starting at t_d.
T_{charges}	Duration of a charging period.
θ_c	Logit parameter of traveler class c.
ζ_m	Waiting time / penalty with mode m.
E^*_{CC}	Credit Cap error goal.
E^*_{MCC}	Market Clearing Condition error goal.
E^*_{SUE}	Stochastic User Equilibrium error goal.
Discret. param.	
Δ_l	Trip length resolution.
Δ_t	Departure time resolution.
Δ_{t_a}	Desired arrival time resolution.
i_l	Trip length index.
i_t	Simulation time index.

i_{t_d}	Departure time index.
i_{t_a}	Desired arrival time index.
$l_{\min}$	Minimum trip length.
$t_{a,\min}$	Minimum desired arrival time.
Variables	
ψ	Logit decision.
μ	Assignment update coefficient.
ω	Traveler's characteristics and choices.
$f(c, l, t_a, t_d, m)$	User distribution.
$F_m(x, t)$	Number of active trips with remaining distance longer than x at t.
$H_m(t)$	Accumulation at time t for mode m.
m	Mode index.
p	Credit price.
$\hat{t}_a$	Arrival time.
t_d	Departure time.
v_m	Instantaneous speed of mode m.
$z_m(t)$	Virtual traveler traveled distance at time t with mode m.
TT	Travel time.
TC	Travel cost.
UC	User cost.
r	Search index for SUE.
R	Normalized credit consumption excess.
E_{CC}	CC error.
E_{MCC}	MCC error.
E_{SUE}	SUE error.
$\mathcal{F}$	Travel characteristics to be updated.
$\bar{\mathcal{F}}$	Travel characteristics not to be updated.
W	Charging period index.
Obj_W	Objective function for charging period W.
ΔObj_W	Variation of the objective function for charging period W.
Γ	Travel cost gain.

C.2 Algorithm for credit charge optimization

`// Update the charging period with the largest absolute gradient.`
for Each time period W **do**
  Compute the gradient of objective function according to Eq. (5.26);
end
Select the charging period W^* with the highest absolute gradient $|Obj_{W^*}|$;
if $Obj_{W^*} < 0$ **then**
  $\tau(W^*) \leftarrow \tau(W^*) + \kappa$;
else
  $\tau(W^*) \leftarrow \max(\tau(W^*) - \kappa, \kappa)$;
end
`// Prevent large variations between two consecutive charging periods.`
for All previous charging periods $W < W^*$, in a decreasing order **do**
  if $\tau(W) < \tau(W+1) - \kappa$ **then**
    $\tau(W) \leftarrow \tau(W+1) - \kappa$;
  end
  if $\tau(W) > \tau(W+1) + \kappa$ **then**
    $\tau(W) \leftarrow \tau(W+1) + \kappa$;
  end
end
for All later charging periods $W > W^*$, in an increasing order **do**
  if $\tau(W) < \tau(W-1) - \kappa$ **then**
    $\tau(W) \leftarrow \tau(W-1) - \kappa$;
  end
  if $\tau(W) > \tau(W-1) + \kappa$ **then**
    $\tau(W) \leftarrow \tau(W-1) + \kappa$;
  end
end

Algorithm 2: Update of the credit charging profile.

C.3 Sensitivity of the carpooling penalty

Our case study is based on the assumption of a 10 min-penalty for carpoolers. This value is uncertain, and some additional traffic policies may decrease it, e.g., HOV lanes and carpooling parking places. We study the sensitivity of our case study with regard to the carpooling penalty. We compute the SUE for the intermediate TCS 'mid' with different values for the carpooling penalty ζ_{pool}: 5, 10 (reference case), and 15 min. The evolution of the carpooling shares is presented in Fig. C.1.

As expected, the carpool share increases as the penalty decreases. However, the difference between the 10 to 15 min penalty is small compared to the change between 5 and 10 min. We highlight the effects on other measures: modes shares, total travel cost, carbon emissions, and credit price.

The carpooling share decreases when the penalty increases, and both PT and car (solo) share increase. The effects on the system are not easy to predict: on one side, fewer carpoolers mean fewer cars, but on the other side, part of the former carpoolers may switch to solo car drivers. Compared to the reference case of a 10 min-penalty,

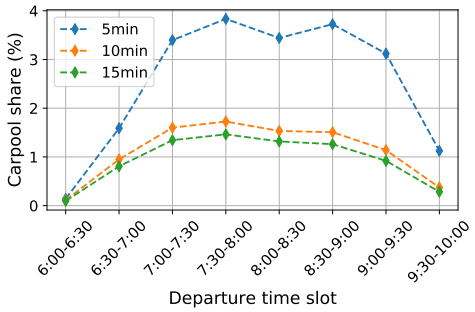

Figure C.1: Carpooling shares for the different carpooling penalties.

Table C.2: Sensitivity of the carpooling penalty.

Penalty (min)	5	10 (ref)	15
Car solo share (%)	5.4	11.2	11.9
PT share (%)	74.2	79.9	80.6
Carpool share (%)	20.4	8.9	7.5
Total travel cost change (%)	-2.8	-	+2.5
Carbon emissions change (%)	-4.3	-	+0.7
Price change (%)	+9.4	-	0

the total travel cost and the carbon emissions increase marginally with the penalty. The credit price decreases by about 10% with 5 min and stays the same between 10 and 15 min. In conclusion, the effect of the carpooling penalty stays marginal, as even a variation of ± 5 min (50%) leads to small changes (2.5% and less) in the leading indicators: total travel cost, carbon emissions, and credit price.

C.4 Total travel time and carbon emissions

The differences between no TCS, static, and dynamic TCS in terms of total travel time and carbon emissions are presented in Fig. C.2. Both static and dynamic ap-

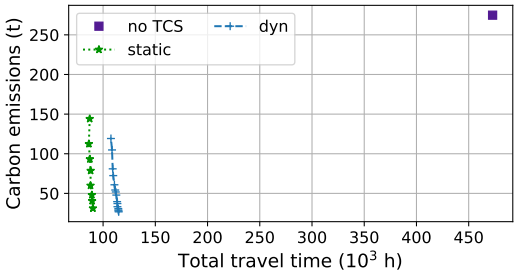

Figure C.2: Total travel time vs. carbon emissions for different static and dynamic TCS. The reference case (no TCS) is also presented.

proaches reduce total travel time and carbon emissions. Static TCS allows for better compromises between total travel time and carbon emissions than dynamic schemes. The reason is that the dynamic schemes are designed to minimize the total travel costs. This objective function considers early/late arrival costs and travel time. Furthermore, the travelers choose their departure time and travel mode based on their user costs: travel time plus early/late cost plus TCS-induced costs.

Appendix D

Appendix Chapter 6

D.1 Notations

Parameters, variables, and other notations for Chapter 6 are summed up in Table D.1.

Table D.1: Summary of parameters and variables notations.

Notation	Meaning
Parameters	
$\mathcal{C}$	Set of travellers.
$\mathcal{D}_0$	Set of potential RH drivers.
f_{PT}	Unitary PT fee.
f_{RH}	Distance-based RH fee.
$L_{o,d}$	Travel distance from o to d.
$L_{pu,o,d}$	Pick-up distance for a RH trip from o to d.
$\mathcal{M}$	Set of modes.
N_R	Number of regions.
P_i^{res}	Reservation price of driver i.
$T_{PT,o,d}$	PT travel time from o to d with transit.
$T^*_{PT,o,d}$	PT travel time from o to d with transit in connection with RH.
T_τ	Credit charge change date.
α_j	VoT of traveller j.
Δ_p	Price sensitivity to credit balance.
κ	Initial credit allocation.
τ_r	Number of credits for operating in region r.
Variables	
$C^t_{o,d,m}$	Travel cost from o to d at t with mode m.
$\mathcal{D}$	Set of active RH drivers.
lic_i	License of driver i.
G_r^{avg}	Average RH gain in region r.
J	Cost function.
MG_r	Marginal RH gain of region r.
p	Credit price.
R^{avg}	Average RH revenue.
R_r	RH revenue of region r.
$V(t)$	Mean car speed at t.
x_i	Number of license i holders.
$y^m_{i,j}$	Boolean for driver-traveller-mode matching.
Other	

$\tilde{\cdot}$	Day-to-day estimator of $\cdot$.

Bibliography

Akamatsu, T. (2007). *Tradable Network Permits: A New Scheme for the Most Efficient Use of Network Capacity*, Tohoku University.

Akamatsu, T., & Wada, K. (2017). Tradable network permits: A new scheme for the most efficient use of network capacity. *Transportation Research Part C: Emerging Technologies*, *79*, 178–195. https://doi.org/10.1016/j.trc.2017.03.009

Ameli, M. (2019). *Heuristic Methods for Calculating Dynamic Traffic Assignment* (Doctoral dissertation).

Ameli, M., Alisoltani, N., & Leclercq, L. (2021). Lyon Metropolis realistic trip data set including home to work trips with private vehicles during the morning peak. https://doi.org/10.25578/MLIDRM

Ameli, M., Faradonbeh, M. S. S., Lebacque, J.-P., Abouee-Mehrizi, H., & Leclercq, L. (2022). Departure Time Choice Models in Urban Transportation Systems Based on Mean Field Games. *Transportation Science*. https://doi.org/10.1287/TRSC.2022.1147

Ameli, M., Lebacque, J. P., & Leclercq, L. (2020). Cross-comparison of convergence algorithms to solve trip-based dynamic traffic assignment problems. *Computer-Aided Civil and Infrastructure Engineering*, *35*(3), 219–240. https://doi.org/10.1111/MICE.12524

Ameli, M., Lebacque, J. P., & Leclercq, L. (2021). Computational Methods for Calculating Multimodal Multiclass Traffic Network Equilibrium: Simulation Benchmark on a Large-Scale Test Case. *Journal of Advanced Transportation*, *2021*. https://doi.org/10.1155/2021/8815653

Andersen, M. S., Dahl, J., & Vandenberghe, L. (2021). CVXOPT: A Python package for convex optimization, version 1.2.6. https://cvxopt.org/

Arnott, R. (2013). A bathtub model of downtown traffic congestion. *Journal of Urban Economics*, *76*(1), 110–121. https://doi.org/10.1016/j.jue.2013.01.001

Arnott, R., de Palma, A., & Lindsey, R. (1990). Economics of a bottleneck. *Journal of Urban Economics*, *27*(1), 111–130. https://doi.org/10.1016/0094-1190(90)90028-L

Axhausen, K. W. (2016). *The Multi-Agent Transport Simulation MATSim*. Ubiquity Press. https://doi.org/10.5334/baw

Axhausen, K. W., Molloy, J., Tchervenkov, C., Becker, F., Hintermann, B., Schoeman, B., Götschi, T., Castro Fernández, A., & Tomic, U. (2021). *Empirical analysis of mobility behavior in the presence of Pigovian transport pricing* (tech. rep.). ETH Zürich. Bundesamt für Strassen (ASTRA) Eidgenössisches Departement für Umwelt Verkehr Energie und Kommunikation (UVEK). https://doi.org/10.3929/ETHZ-B-000500100

Aziz, H. M., Ukkusuri, S. V., & Romero, J. (2015). Understanding short-term travel behavior under personal mobility credit allowance scheme using experimental economics. *Transportation Research Part D: Transport and Environment*, *36*, 121–137. https://doi.org/10.1016/j.trd.2015.02.015

Balzer, L., Ameli, M., Leclercq, L., & Lebacque, J. P. (2023). Dynamic tradable credit scheme for multimodal urban networks. *Transportation Research Part C: Emerging Technologies*, *149*, 104061. https://doi.org/10.1016/J.TRC.2023.104061

Balzer, L., Ameli, M., Leclercq, L., & Lebacque, J.-P. (2022). Tradable Credit Scheme for Multimodal Urban Networks. *Symposium on Management of Future Motorway and Urban Traffic Systems (MFTS)*.

Balzer, L., Ameli, M., Leclercq, L., & Lebacque, J.-P. (2023). Modeling Tradable Credit Scheme for Multimodal Urban Networks with Departure Time: a Bathtub Approach. *Transportation Research Board Annual Meeting*.

Balzer, L., & Leclercq, L. (2022a). Mode share equilibrium with tradable credit scheme and license plate rationing. *Symposium of the European Association for Research in Transportation (hEART)*.

Balzer, L., & Leclercq, L. (2022b). Mode share equilibrium with tradable credit scheme over different time cycles. *Triennial Symposium on Transportation Analysis (TRISTAN)*.

Balzer, L., & Leclercq, L. (2022c). Tradable credit scheme: an alternative to license plate rationing and congestion pricing to foster modal shift. *Transportation Research Arena*.

Balzer, L., & Leclercq, L. (2022d). Trip-based MFD model with tradable credit scheme: investigating modal equilibrium. *Transportation Research Board Annual Meeting*.

Balzer, L., & Leclercq, L. (2022e). Mode shift with tradable credit scheme: a simulation study in Lyon. *Transportation Research Procedia*, *62*, 229–235. https://doi.org/10.1016/J.TRPRO.2022.02.029

Balzer, L., & Leclercq, L. (2022f). Modal equilibrium of a tradable credit scheme with a trip-based MFD and logit-based decision-making. *Transportation Research Part C: Emerging Technologies*, *139*, 103642. https://doi.org/10.1016/J.TRC.2022.103642

Balzer, L., & Leclercq, L. (2022g). Modal dynamic equilibrium under different demand management schemes. *Transportation*, 1–38. https://doi.org/10.1007/s11116-022-10338-0

Balzer, L., Provoost, J., Leclercq, L., & Cats, O. (2021). *Tradable mobility credits and permits: state of the art and concepts-Deliverable D4.1-Project DIT4TraM* (tech. rep.). https://dit4tram.eu/downloads/

Balzer, L., Provoost, J., Leclercq, L., & Cats, O. (2022). Tradable mobility credits and permits: state of the art and future research directions. *Transportation Research Arena*.

Bao, Y., Gao, Z., & Xu, M. (2016). Traffic Assignment Under Tradable Credit Scheme: An Investigation Considering Travelers' Framing and Labeling of Credits. *IEEE Intelligent Transportation Systems Magazine*, *8*(2), 74–89. https://doi.org/10.1109/MITS.2016.2533926

Bao, Y., Gao, Z., Xu, M., & Yang, H. (2014). Tradable credit scheme for mobility management considering travelers' loss aversion. *Transportation Research Part E: Logistics and Transportation Review*, *68*, 138–154. https://doi.org/10.1016/j.tre.2014.05.007

Bao, Y., Gao, Z., Yang, H., Xu, M., & Wang, G. (2017). Private financing and mobility management of road network with tradable credits. *Transportation Research Part A: Policy and Practice*, *97*, 158–176. https://doi.org/10.1016/j.tra.2017.01.013

Bao, Y., Verhoef, E. T., & Koster, P. (2019). Regulating dynamic congestion externalities with tradable credit schemes: Does a unique equilibrium exist? *Transportation Research Part B: Methodological*, *127*, 225–236. https://doi.org/10.1016/j.trb.2019.07.012

Bayer, P., & Aklin, M. (2020). The European Union Emissions Trading System reduced CO2 emissions despite low prices. *Proceedings of the National Academy of Sciences of the United States of America*, *117*(16), 8804. https://doi.org/10.1073/PNAS.1918128117

Beojone, C. V., & Geroliminis, N. (2021). On the inefficiency of ride-sourcing services towards urban congestion. *Transportation Research Part C: Emerging Technologies*, *124*, 102890. https://doi.org/10.1016/J.TRC.2020.102890

Bhatt, K., Higgins, T., & Berg, J. T. (2008). *Lessons Learned From International Experience in Congestion Pricing Final Report* (tech. rep.). K.T. Analytics, Inc.

Brands, D. K., Verhoef, E. T., Knockaert, J., & Koster, P. R. (2020). Tradable permits to manage urban mobility: Market design and experimental implementation. *Transportation Research Part A: Policy and Practice*, *137*, 34–46. https://doi.org/10.1016/j.tra.2020.04.008

Bureau of Public Roads. (1964). *Traffic Assignment Manual for Application with a Large, High Speed Computer*. (U.S. Government Printing Office, Ed.). https://books.google.fr/books?hl=en&lr=&id=CXMnAQAAMAAJ&oi=fnd&pg=PA1&ots=otJK0SVQVH&sig=wGd_OnmJmVwFW2tyNl5Va9ZVwCQ&redir_esc=y#v=snippet&q=figure&f=false

Cats, O., Kucharski, R., Danda, S. R., & Yap, M. (2022). Beyond the dichotomy: How ride-hailing competes with and complements public transport. *PLOS ONE*, *17*(1), e0262496. https://doi.org/10.1371/JOURNAL.PONE.0262496

Chen, Y.-J., Li, Z.-C., Lam, W. H. K., & Choi, K. (2016). Tradable location tax credit scheme for balancing traffic congestion and environmental externalities. *International Journal of Sustainable Transportation*, *10*(10), 917–934. https://doi.org/10.1080/15568318.2016.1187230

Chu, X. (1995). Endogenous Trip Scheduling: The Henderson Approach Reformulated and Compared with the Vickrey Approach. *Journal of Urban Economics*, *37*(3), 324–343. https://doi.org/10.1006/juec.1995.1017

Croci, E., & Douvan, A. R. (2016). *Urban Road Pricing: A Comparative Study on the Experiences of London, Stockholm and Milan*, IEFE - The Center for Research on Energy, Environmental Economics, and Policy at Bocconi University. www.iefe.unibocconi.it

Daganzo, C. F. (2007). Urban gridlock: Macroscopic modeling and mitigation approaches. *Transportation Research Part B: Methodological*, *41*(1), 49–62. https://doi.org/10.1016/j.trb.2006.03.001

Daganzo, C. F., & Sheffi, Y. (1977). On stochastic models of traffic assignement. *Transportation Science*, *11*(3), 253–274. https://doi.org/10.1287/trsc.11.3.253

Dakic, I., Yang, K., Menendez, M., & Chow, J. Y. (2021). On the design of an optimal flexible bus dispatching system with modular bus units: Using the three-dimensional macroscopic fundamental diagram. *Transportation Research Part B: Methodological*, *148*, 38–59. https://doi.org/10.1016/J.TRB.2021.04.005

de Kruijf, J., Ettema, D., Kamphuis, C. B., & Dijst, M. (2018). Evaluation of an incentive program to stimulate the shift from car commuting to e-cycling in the Netherlands. *Journal of Transport and Health*, *10*, 74–83. https://doi.org/10.1016/J.JTH.2018.06.003

de Palma, A., Proost, S., Seshadri, R., & Ben-Akiva, M. (2018). Congestion tolling - dollars versus tokens: A comparative analysis. *Transportation Research Part B: Methodological*, *108*, 261–280. https://doi.org/10.1016/j.trb.2017.12.005

Dogterom, N., Ettema, D., & Dijst, M. (2018). Behavioural effects of a tradable driving credit scheme: Results of an online stated adaptation experiment in the Netherlands. *Transportation Research Part A: Policy and Practice*, *107*, 52–64. https://doi.org/10.1016/j.tra.2017.11.004

Eliasson, J. (2014). *The Stockholm congestion charges: an overview*. www.cts.kth.se

Erhardt, G. D., Roy, S., Cooper, D., Sana, B., Chen, M., & Castiglione, J. (2019). Do transportation network companies decrease or increase congestion? *Science Advances*, *5*(5). https://doi.org/10.1126/SCIADV.AAU2670/SUPPL{_}FILE/AAU2670{_}SM.PDF

Ettema, D., Knockaert, J., & Verhoef, E. (2010). Using incentives as traffic management tool: Empirical results of the "peak avoidance" experiment. *Transportation Letters*, *2*(1), 39–51. https://doi.org/10.3328/TL.2010.02.01.39-51

Eurostat. (2017). Share of Member States in EU GDP - Products Eurostat News. https://ec.europa.eu/eurostat/web/products-eurostat-news/-/DDN-20170410-1

Fahrioglu, M., & Alvarado, F. L. (2000). Designing incentive compatible contracts for effective demand management. *IEEE Transactions on Power Systems*, *15*(4), 1255–1260. https://doi.org/10.1109/59.898098

Fosgerau, M., Hjorth, K., & Lyk-Jensen, S. V. (2007). *The Danish Value of Time Study* (tech. rep.). Danish Transport Research Institute. Lyngby.

Fosgerau, M., & Small, K. A. (2013). Hypercongestion in downtown metropolis. *Journal of Urban Economics*, *76*(1), 122–134. https://doi.org/10.1016/j.jue.2012.12.004

Gao, G., & Hu, J. (2015). Optimal tradable credits scheme and congestion pricing with the efficiency analysis to congestion. *Discrete Dynamics in Nature and Society*, *2015*. https://doi.org/10.1155/2015/801979

Gao, G., Liu, X. M., & Ren, C. X. (2019). An Average Cost Pricing Method on Electric Tradable Credits Scheme in Traffic Management. *IEEE Access*, *7*, 57276–57283. https://doi.org/10.1109/ACCESS.2019.2908184

Gao, G., Liu, X., Sun, H., Wu, J., Liu, H., Wang, W., Wang, Z., Wang, T., & Du, H. (2019). Marginal cost pricing analysis on tradable credits in traffic engineering. *Mathematical Problems in Engineering*, *2019*. https://doi.org/10.1155/2019/8461395

Gao, G., & Sun, H. (2014). Internalizing Congestion and Emissions Externality on Road Networks with Tradable Credits. *Procedia - Social and Behavioral Sciences*, *138*, 214–222. https://doi.org/10.1016/j.sbspro.2014.07.198

Gao, G., Sun, H., Wu, J., Liu, X., & Chen, W. (2018). Park-and-ride service design under a price-based tradable credits scheme in a linear monocentric city. *Transport Policy*, *68*, 1–12. https://doi.org/10.1016/j.tranpol.2018.04.001

Gao, G., Sun, H., Wu, J., & Zhao, H. (2016). Tradable credits scheme and transit investment optimization for a two-mode traffic network. *Journal of Advanced Transportation*, *50*(8), 1616–1629. https://doi.org/10.1002/atr.1418

Goddard, H. C. (1997). Using tradeable permits to achieve sustainability in the world's large cities. Policy design issues and efficiency conditions for controlling vehicle emissions, congestion and urban decentralization with an application to Mexico City. *Environmental and Resource Economics*, *10*(1), 63–99. https://doi.org/10.1023/A:1026444113237

Godfrey, J. W. (1969). The Mechanism of a Road Network. *Traffic Engineering and Control*, *11*(7), 323–327. https://trid.trb.org/view/117139

Gu, Z., Liu, Z., Cheng, Q., & Saberi, M. (2018). Congestion pricing practices and public acceptance: A review of evidence. *Case Studies on Transport Policy*, *6*(1), 94–101. https://doi.org/10.1016/j.cstp.2018.01.004

Guo, R. Y., Huang, H. J., & Yang, H. (2019). Tradable Credit Scheme for Control of Evolutionary Traffic Flows to System Optimum: Model and its Convergence. *Networks and Spatial Economics*, *19*(3), 833–868. https://doi.org/10.1007/s11067-018-9432-z

Han, F., & Cheng, L. (2016). The Role of Initial Credit Distribution Scheme in Managing Network Mobility and Maximizing Reserve Capacity: Considering Traveler's Cognitive Illusion. *Discrete Dynamics in Nature and Society*, *2016*. https://doi.org/10.1155/2016/7289621

Han, F., & Cheng, L. (2017). Stochastic user equilibrium model with a tradable credit scheme and application in maximizing network reserve capacity. *Engineering Optimization*, *49*(4), 549–564. https://doi.org/10.1080/0305215X.2016.1193357

He, F., Yin, Y., Shirmohammadi, N., & Nie, Y. (2013). Tradable credit schemes on networks with mixed equilibrium behaviors. *Transportation Research Part B: Methodological*, *57*, 47–65. https://doi.org/10.1016/j.trb.2013.08.016

HERE Developer. (2020). HERE API. https://developer.here.com/

Hu, X., Chiu, Y. C., & Zhu, L. (2015). Behavior Insights for an Incentive-Based Active Demand Management Platform. *International Journal of Transportation Science and Technology*, *4*(2), 119–133. https://doi.org/10.1260/2046-0430.4.2.119

Ingole, D., Mariotte, G., & Leclercq, L. (2020). Minimizing network-wide emissions by optimal routing through inner-city gating. *Transportation Research Part D: Transport and Environment*, *86*, 102411. https://doi.org/10.1016/j.trd.2020.102411

INSEE. (2021). Iris. https://www.insee.fr/en/metadonnees/definition/c1523

International Carbon Action Partnership. (2021). ICAP Allowance Price Explorer. https://icapcarbonaction.com/en/ets-prices

Jia, Z., Wang, D. Z., & Cai, X. (2016). Traffic managements for household travels in congested morning commute. *Transportation Research Part E: Logistics and Transportation Review*, *91*, 173–189. https://doi.org/10.1016/j.tre.2016.04.005

Jiang, N., Zhang, X., & Wang, H. (2017). Simultaneous optimization of road tolls and tradable credits in public-private mixed networks. *Promet - Traffic - Traffico*, *29*(6), 603–611. https://doi.org/10.7307/ptt.v29i6.2410

Jin, W.-L. (2020). Generalized bathtub model of network trip flows. *Transportation Research Part B*, *136*, 138–157. https://doi.org/https://doi.org/10.1016/j.trb.2020.04.002

Knockaert, J., Tsenga, Y. Y., Verhoef, E. T., & Rouwendal, J. (2012). The Spitsmijden experiment: A reward to battle congestion. *Transport Policy*, *24*, 260–272. https://doi.org/10.1016/J.TRANPOL.2012.07.007

Krabbenborg, L., Mouter, N., Molin, E., Annema, J. A., & van Wee, B. (2020). Exploring public perceptions of tradable credits for congestion management in urban areas. *Cities*, *107*. https://doi.org/10.1016/j.cities.2020.102877

Krabbenborg, L., van Langevelde-van Bergen, C., & Molin, E. (2021). Public support for tradable peak credit schemes. *Transportation Research Part A: Policy and Practice*, *145*, 243–259. https://doi.org/10.1016/j.tra.2021.01.014

Lamotte, R., & Geroliminis, N. (2018). The morning commute in urban areas with heterogeneous trip lengths. *Transportation Research Part B: Methodological*, *117*, 794–810. https://doi.org/10.1016/j.trb.2017.08.023

Lebacque, J.-P., Leclercq, L., & Ameli, M. (2022). Stochastic departure time user equilibrium with heterogeneous trip profile. *The 10th Symposium of the European Association for Research in Transportation.* https://hal.science/hal-03680843%20https://hal.science/hal-03680843/document

Leclercq, L., Sénécat, A., & Mariotte, G. (2017). Dynamic macroscopic simulation of on-street parking search: A trip-based approach. *Transportation Research Part B: Methodological*, *101*, 268–282. https://doi.org/10.1016/j.trb.2017.04.004

Lejri, D., Can, A., Schiper, N., & Leclercq, L. (2018). Accounting for traffic speed dynamics when calculating COPERT and PHEM pollutant emissions at the urban scale. *Transportation Research Part D: Transport and Environment*, *63*, 588–603. https://doi.org/10.1016/j.trd.2018.06.023

Lessan, J., Fu, L., & Bachmann, C. (2020). Towards user-centric, market-driven mobility management of road traffic using permit-based schemes. *Transportation Research Part E: Logistics and Transportation Review*, *141*. https://doi.org/10.1016/j.tre.2020.102023

Li, Q., & Gao, Z. (2014). Managing Rush Hour Congestion with Lane Reversal and Tradable Credits. *Mathematical Problems in Engineering*, *2014*. https://doi.org/10.1155/2014/132936

Lian, Z., Liu, X., & Fan, W. (2019). Does driving-day-based tradable credit scheme outperform license plate rationing? Examination considering transaction cost. *Journal of Modern Transportation*, *27*(3), 198–210. https://doi.org/10.1007/s40534-019-0189-y

Lindsey, R. C., Van den Berg, V. A., & Verhoef, E. T. (2012). Step tolling with bottleneck queuing congestion. *Journal of Urban Economics*, *72*(1), 46–59. https://doi.org/10.1016/j.jue.2012.02.001

Liu, R., Chen, S., Jiang, Y., Seshadri, R., Ben-Akiva, M., & Azevedo, C. L. (2022). Managing network congestion with a trip- and area-based tradable credit scheme. *Transportmetrica B: Transport Dynamics*, 1–29. https://doi.org/10.1080/21680566.2022.2083034

Liu, W., Yang, H., & Yin, Y. (2014). Expirable parking reservations for managing morning commute with parking space constraints. *Transportation Research Part C: Emerging Technologies*, *44*, 185–201. https://doi.org/10.1016/j.trc.2014.04.002

Liu, W., Yang, H., & Yin, Y. (2015). Efficiency of a highway use reservation system for morning commute. *Transportation Research Part C: Emerging Technologies*, *56*, 293–308. https://doi.org/10.1016/j.trc.2015.04.015

Loder, A., Ambühl, L., Menendez, M., & Axhausen, K. W. (2017). Empirics of multimodal traffic networks – Using the 3D macroscopic fundamental diagram. *Transportation Research Part C: Emerging Technologies*, *82*, 88–101. https://doi.org/10.1016/j.trc.2017.06.009

Loder, A., Bressan, L., Wierbos, M. J., Becker, H., Emmonds, A., Obee, M., Knoop, V. L., Menendez, M., & Axhausen, K. W. (2021). How Many Cars in the City Are Too Many? Towards Finding the Optimal Modal Split for a Multi-Modal Urban Road Network. *Frontiers in Future Transportation*, *0*, 5. https://doi.org/10.3389/FFUTR.2021.665006

Loder, A., Dakic, I., Bressan, L., Ambühl, L., Bliemer, M. C., Menendez, M., & Axhausen, K. W. (2019). Capturing network properties with a functional form for

the multi-modal macroscopic fundamental diagram. *Transportation Research Part B: Methodological*, *129*, 1–19. https://doi.org/10.1016/j.trb.2019.09.004

Mahmassani, H., Williams, J. C., & Herman, R. (1984). Investigation of Network-Level Traffic Flow Relationships: Some Simulation Results. *Transportation Research Record*, 121–130.

Mariotte, G. (2018). *Dynamic Modeling of Large-Scale Urban Transportation Systems* (Doctoral dissertation).

Mariotte, G., & Leclercq, L. (2019). Flow exchanges in multi-reservoir systems with spillbacks. *Transportation Research Part B: Methodological*, *122*, 327–349. https://doi.org/10.1016/j.trb.2019.02.014

Mariotte, G., Leclercq, L., Batista, S. F., Krug, J., & Paipuri, M. (2020). Calibration and validation of multi-reservoir MFD models: A case study in Lyon. *Transportation Research Part B: Methodological*, *136*, 62–86. https://doi.org/10.1016/j.trb.2020.03.006

Mariotte, G., Leclercq, L., & Laval, J. A. (2017). Macroscopic urban dynamics: Analytical and numerical comparisons of existing models. *Transportation Research Part B: Methodological*, *101*, 245–267. https://doi.org/10.1016/j.trb.2017.04.002

Miralinaghi, M., & Peeta, S. (2016). Multi-period equilibrium modeling planning framework for tradable credit schemes. *Transportation Research Part E: Logistics and Transportation Review*, *93*, 177–198. https://doi.org/10.1016/j.tre.2016.05.013

Miralinaghi, M., & Peeta, S. (2018). A Multi-Period Tradable Credit Scheme Incorporating Interest Rate and Traveler Value-of-Time Heterogeneity to Manage Traffic System Emissions. *Frontiers in Built Environment*, *4*, 33. https://doi.org/10.3389/fbuil.2018.00033

Miralinaghi, M., & Peeta, S. (2019). Promoting zero-emissions vehicles using robust multi-period tradable credit scheme. *Transportation Research Part D: Transport and Environment*, *75*, 265–285. https://doi.org/10.1016/j.trd.2019.08.012

Miralinaghi, M., & Peeta, S. (2020). Design of a Multiperiod Tradable Credit Scheme under Vehicular Emissions Caps and Traveler Heterogeneity in Future Credit Price Perception. *Journal of Infrastructure Systems*, *26*(3), 04020030. https://doi.org/10.1061/(asce)is.1943-555x.0000570

Miralinaghi, M., Peeta, S., He, X., & Ukkusuri, S. V. (2019). Managing morning commute congestion with a tradable credit scheme under commuter heterogeneity and market loss aversion behavior. *Transportmetrica B*, *7*(1), 1780–1808. https://doi.org/10.1080/21680566.2019.1698379

Nie, Y. (2012). Transaction costs and tradable mobility credits. *Transportation Research Part B: Methodological*, *46*(1), 189–203. https://doi.org/10.1016/j.trb.2011.10.002

Nie, Y. (2015). A New Tradable Credit Scheme for the Morning Commute Problem. *Networks and Spatial Economics*, *15*(3), 719–741. https://doi.org/10.1007/s11067-013-9192-8

Nie, Y. (2017a). Why is license plate rationing not a good transport policy? *Transportmetrica A: Transport Science*, *13*(1), 1–23. https://doi.org/10.1080/23249935.2016.1202354

Nie, Y. (2017b). On the potential remedies for license plate rationing. *Economics of Transportation*, *9*, 37–50. https://doi.org/10.1016/j.ecotra.2017.01.001

Nie, Y., & Yin, Y. (2013). Managing rush hour travel choices with tradable credit scheme. *Transportation Research Part B: Methodological*, *50*, 1–19. https://doi.org/10.1016/j.trb.2013.01.004

Nourinejad, M., & Ramezani, M. (2020). Ride-Sourcing modeling and pricing in non-equilibrium two-sided markets. *Transportation Research Part B: Methodological*, *132*, 340–357. https://doi.org/10.1016/J.TRB.2019.05.019

Ntziachristos, L., Gkatzoflias, D., Kouridis, C., & Samaras, Z. (2009). COPERT: A European road transport emission inventory model. *Environmental Science and Engineering (Subseries: Environmental Science)*, 491–504. https://doi.org/10.1007/978-3-540-88351-7{_}37

OECD. (2018). *Taxi, ride-sourcing and ride-sharing services - Background Note by the Secretariat* (tech. rep.). OECD. http://www.oecd.org/daf/competition/taxis-and-ride-sharing-services.htm

Paipuri, M., Barmpounakis, E., Geroliminis, N., & Leclercq, L. (2021). Empirical observations of multi-modal network-level models: Insights from the pNEUMA experiment. *Transportation Research Part C: Emerging Technologies*, *131*, 103300. https://doi.org/10.1016/J.TRC.2021.103300

Paipuri, M., & Leclercq, L. (2020). Bi-modal macroscopic traffic dynamics in a single region. *Transportation Research Part B: Methodological*, *133*, 257–290. https://doi.org/10.1016/j.trb.2020.01.007

Pigou, A. C. (1920). *The Economics of Welfare*. Palgrave Macmillan UK. https://www.palgrave.com/gp/book/9780230249318

Sakai, K., Kusakabe, T., & Asakura, Y. (2015). Analysis of tradable bottleneck permits scheme when marginal utility of toll cost changes among drivers. *Transportation Research Procedia*, *10*, 51–60. https://doi.org/10.1016/j.trpro.2015.09.055

Sakai, K., Liu, R., Kusakabe, T., & Asakura, Y. (2017). Pareto-improving social optimal pricing schemes based on bottleneck permits for managing congestion at a merging section. *International Journal of Sustainable Transportation*, *11*(10), 737–748. https://doi.org/10.1080/15568318.2017.1312646

Sbayti, H., Lu, C. C., & Mahmassani, H. S. (2007). Efficient Implementation of Method of Successive Averages in Simulation-Based Dynamic Traffic Assignment Models for Large-Scale Network Applications. *https://doi.org/10.3141/2029-03*, *2029*(2029), 22–30. https://doi.org/10.3141/2029-03

Schroten, A., van Essen, H., van Wijngaarden, L., Sutter, D., & Andrew, E. (2019). *Sustainable transport infrastructure charging and internalisation of transport externalities : executive summary.* (tech. rep.). European Commission. Brussels, Publications Office of the European Union. https://doi.org/10.2832/246834

Seilabi, S. E., Tabesh, M. T., Davatgari, A., Miralinaghi, M., & Labi, S. (2020). Promoting Autonomous Vehicles Using Travel Demand and Lane Management Strategies. *Frontiers in Built Environment*, *6*. https://doi.org/10.3389/fbuil.2020.560116

Sheffi, Y. (1985). *Urban Transportation Networks: Equilibrium Analysis With Mathematical Programming Methods*. Prentice-Hall.

Shirmohammadi, N., & Yin, Y. (2016). Tradable Credit Scheme to Control Bottleneck Queue Length. *Transportation Research Record: Journal of the Transportation Research Board*, *2561*(1), 53–63. https://doi.org/10.3141/2561-07

Shirmohammadi, N., Zangui, M., Yin, Y., & Nie, Y. (2013). Analysis and Design of Tradable Credit Schemes under Uncertainty. *Transportation Research Record: Journal of the Transportation Research Board*, *2333*(1), 27–36. https://doi.org/10.3141/2333-04

Simoni, M. D., Pel, A. J., Waraich, R. A., & Hoogendoorn, S. P. (2015). Marginal cost congestion pricing based on the network fundamental diagram. *Transportation*

Research Part C: Emerging Technologies, *56*, 221–238. https://doi.org/10.1016/j.trc.2015.03.034

Storn, R., & Price, K. (1997). Differential Evolution - A Simple and Efficient Heuristic for Global Optimization over Continuous Spaces. *Journal of Global Optimization*, *11*(4), 341–359. https://doi.org/10.1023/A:1008202821328/METRICS

Su, P., & Park, B. (2015). Auction-based highway reservation system an agent-based simulation study. *Transportation Research Part C: Emerging Technologies*, *60*, 211–226. https://doi.org/10.1016/j.trc.2015.07.018

Tian, L. J., Yang, H., & Huang, H. J. (2013). Tradable credit schemes for managing bottleneck congestion and modal split with heterogeneous users. *Transportation Research Part E: Logistics and Transportation Review*, *54*, 1–13. https://doi.org/10.1016/j.tre.2013.04.002

Tian, Y., & Chiu, Y. C. (2015). Day-to-Day Market Power and Efficiency in Tradable Mobility Credits. *International Journal of Transportation Science and Technology*, *4*(3), 209–227. https://doi.org/10.1260/2046-0430.4.3.209

Tian, Y., Chiu, Y. C., & Sun, J. (2019). Understanding behavioral effects of tradable mobility credit scheme: An experimental economics approach. *Transport Policy*, *81*, 1–11. https://doi.org/10.1016/j.tranpol.2019.05.019

Verhoef, E., Nijkamp, P., & Rietveld, P. (1997). Tradeable permits: their potential in the regulation of road transport externalities. *Environment and Planning B: Planning and Design*, *24*(4), 527–548. https://doi.org/10.1068/b240527

Vickrey, W. (2020). Congestion in midtown Manhattan in relation to marginal cost pricing. *Economics of Transportation*, *21*, 100152. https://doi.org/10.1016/j.ecotra.2019.100152

Vickrey, W. S. (1963). Pricing in Urban and Suburban Transport. *The American Economic Review*, *53*(2), 452–465. https://www.jstor.org/stable/1823886?seq=13#metadata_info_tab_contents

Vickrey, W. S. (1969). Congestion Theory and Transport Investment. *Source: The American Economic Review*, *59*(2), 251–260.

Virtanen, P., Gommers, R., Oliphant, T. E., Haberland, M., Reddy, T., Cournapeau, D., Burovski, E., Peterson, P., Weckesser, W., Bright, J., van der Walt, S. J., Brett, M., Wilson, J., Millman, K. J., Mayorov, N., Nelson, A. R., Jones, E., Kern, R., Larson, E., ... Vázquez-Baeza, Y. (2020). SciPy 1.0: fundamental algorithms for scientific computing in Python. *Nature Methods*, *17*(3), 261–272. https://doi.org/10.1038/S41592-019-0686-2

Wada, K., & Akamatsu, T. (2013). A hybrid implementation mechanism of tradable network permits system which obviates path enumeration: An auction mechanism with day-to-day capacity control. *Transportation Research Part E: Logistics and Transportation Review*, *60*, 94–112. https://doi.org/10.1016/j.tre.2013.05.008

Wang, G., Gao, Z., & Xu, M. (2019). Integrating link-based discrete credit charging scheme into discrete network design problem. *European Journal of Operational Research*, *272*(1), 176–187. https://doi.org/10.1016/j.ejor.2018.05.069

Wang, G., Gao, Z., Xu, M., & Sun, H. (2014a). Models and a relaxation algorithm for continuous network design problem with a tradable credit scheme and equity constraints. *Computers and Operations Research*, *41*(1), 252–261. https://doi.org/10.1016/j.cor.2012.11.010

Wang, G., Gao, Z., Xu, M., & Sun, H. (2014b). Joint link-based credit charging and road capacity improvement in continuous network design problem. *Transportation Research Part A: Policy and Practice*, *67*, 1–14. https://doi.org/10.1016/j.tra.2014.05.012

Wang, G., Li, Y., Xu, M., & Gao, Z. (2020). Operating a public–private mixed road network via determining tradable credits and road tolls: An equilibrium problem with equilibrium constraints approach. *International Journal of Sustainable Transportation*, *15*(2), 87–96. https://doi.org/10.1080/15568318.2019.1694110

Wang, G., Xu, M., Grant-Muller, S., & Gao, Z. (2020). Combination of tradable credit scheme and link capacity improvement to balance economic growth and environmental management in sustainable-oriented transport development: A bi-objective bi-level programming approach. *Transportation Research Part A: Policy and Practice*, *137*, 459–471. https://doi.org/10.1016/j.tra.2018.10.031

Wang, H., & Zhang, X. (2016). Joint implementation of tradable credit and road pricing in public-private partnership networks considering mixed equilibrium behaviors. *Transportation Research Part E: Logistics and Transportation Review*, *94*, 158–170. https://doi.org/10.1016/j.tre.2016.07.014

Wang, J. P., Liu, T. L., & Huang, H. J. (2018). Tradable OD-based travel permits for bi-modal traffic management with heterogeneous users. *Transportation Research Part E: Logistics and Transportation Review*, *118*, 589–605. https://doi.org/10.1016/j.tre.2018.08.015

Wang, P., Wada, K., Akamatsu, T., & Nagae, T. (2018). Trading mechanisms for bottleneck permits with multiple purchase opportunities. *Transportation Research Part C: Emerging Technologies*, *95*, 414–430. https://doi.org/10.1016/j.trc.2018.07.011

Wang, X., & Yang, H. (2012). Bisection-based trial-and-error implementation of marginal cost pricing and tradable credit scheme. *Transportation Research Part B: Methodological*, *46*(9), 1085–1096. https://doi.org/10.1016/j.trb.2012.04.002

Wang, X., Yang, H., Han, D., & Liu, W. (2014). Trial and error method for optimal tradable credit schemes: The network case. *Journal of Advanced Transportation*, *48*(6), 685–700. https://doi.org/10.1002/atr.1245

Wang, X., Yang, H., Zhu, D., & Li, C. (2012). Tradable travel credits for congestion management with heterogeneous users. *Transportation Research Part E: Logistics and Transportation Review*, *48*(2), 426–437. https://doi.org/10.1016/j.tre.2011.10.007

Wu, D., Yin, Y., Lawphongpanich, S., & Yang, H. (2012). Design of more equitable congestion pricing and tradable credit schemes for multimodal transportation networks. *Transportation Research Part B: Methodological*, *46*(9), 1273–1287. https://doi.org/10.1016/j.trb.2012.05.004

Wu, Z., Cai, X., Li, M., & Hu, L. (2020). Optimal mixed charging schemes for traffic congestion management with subsidy to new energy vehicle users. *International Transactions in Operational Research*, *00*, 1–18. https://doi.org/10.1111/itor.12869

Xiao, F., Long, J., Li, L., Kou, G., & Nie, Y. (2019). Promoting social equity with cyclic tradable credits. *Transportation Research Part B: Methodological*, *121*, 56–73. https://doi.org/10.1016/j.trb.2019.01.002

Xiao, F., Qian, Z., & Zhang, H. M. (2013). Managing bottleneck congestion with tradable credits. *Transportation Research Part B: Methodological*, *56*, 1–14. https://doi.org/10.1016/j.trb.2013.06.016

Xiao, L. L., Huang, H. J., & Liu, R. (2015). Tradable credit scheme for rush hour travel choice with heterogeneous commuters. *Advances in Mechanical Engineering*, *7*(10), 168781401561243. https://doi.org/10.1177/1687814015612430

Xiao, L. L., Liu, T. L., & Huang, H. J. (2016). On the morning commute problem with carpooling behavior under parking space constraint. *Transportation Research*

Part B: Methodological, *91*, 383–407. https://doi.org/10.1016/J.TRB.2016.05.014

Xiao, L. L., Liu, T. L., & Huang, H. J. (2021). Tradable permit schemes for managing morning commute with carpool under parking space constraint. *Transportation*, *48*, 1563–1586. https://doi.org/10.1007/s11116-019-09982-w

Xiao, L. L., Liu, T. L., Huang, H. J., & Liu, R. (2021). Temporal-spatial allocation of bottleneck capacity for managing morning commute with carpool. *Transportation Research Part B: Methodological*, *143*, 177–200. https://doi.org/10.1016/j.trb.2020.11.007

Xu, M., & Grant-Muller, S. (2016). Trip mode and travel pattern impacts of a Tradable Credits Scheme: A case study of Beijing. *Transport Policy*, *47*, 72–83. https://doi.org/10.1016/j.tranpol.2015.12.007

Yang, H., & Wang, X. (2011). Managing network mobility with tradable credits. *Transportation Research Part B: Methodological*, *45*(3), 580–594. https://doi.org/10.1016/j.trb.2010.10.002

Ye, H., & Yang, H. (2013). Continuous price and flow dynamics of tradable mobility credits. *Transportation Research Part B: Methodological*, *57*, 436–450. https://doi.org/10.1016/j.trb.2013.05.007

Yu, X., van den Berg, V. A., & Verhoef, E. T. (2019). Carpooling with heterogeneous users in the bottleneck model. *Transportation Research Part B: Methodological*, *127*, 178–200. https://doi.org/10.1016/j.trb.2019.07.003

Zang, G., Xu, M., & Gao, Z. (2018). High-occupancy vehicle lanes and tradable credits scheme for traffic congestion management a bilevel programming approach. *Promet - Traffic - Traffico*, *30*(1), 1–10. https://doi.org/10.7307/ptt.v30i1.2300

Zang, G., Xu, M., & Gao, Z. (2020). High-occupancy vehicle lane management with tradable credit scheme: An equilibrium analysis. *Transportation Research Part E: Logistics and Transportation Review*, *144*, 102120. https://doi.org/10.1016/j.tre.2020.102120

Zhang, F., Lu, J., & Hu, X. (2020). Traffic Equilibrium for Mixed Traffic Flows of Human-Driven Vehicles and Connected and Autonomous Vehicles in Transportation Networks under Tradable Credit Scheme. *Journal of Advanced Transportation*, *2020*. https://doi.org/10.1155/2020/8498561

Zhang, F., Lu, J., & Hu, X. (2021a). Tradable credit scheme design with transaction cost and equity constraint. *Transportation Research Part E: Logistics and Transportation Review*, *145*, 102133. https://doi.org/10.1016/j.tre.2020.102133

Zhang, F., Lu, J., & Hu, X. (2021b). Optimal Tradable Credit Scheme Design with Recommended Credit Price (C.-C. Lu, Ed.). *Journal of Advanced Transportation*, *2021*, 1–16. https://doi.org/10.1155/2021/6688803

Zhang, F., Lu, J., Hu, X., & Liu, T. (2021). Investigating the Impacts of Transaction Cost under a Tradable Credit Scheme with Heterogenous Users. *Mathematical Problems in Engineering*, *2021*. https://doi.org/10.1155/2021/6624300

Zhou, F., Wu, J., Xu, Y., & Yi, C. (2020). Optimization Scheme of Tradable Credits and Bus Departure Quantity for Travelers' Travel Mode Choice Guidance. *Journal of Advanced Transportation*, *2020*. https://doi.org/10.1155/2020/6665161

Zhu, C., Yue, J. S., Mandayam, C. V., Merugu, D., Abadi, H. K., & Prabhakar, B. (2015). Reducing Road Congestion Through Incentives: A Case Study. *Transportation Research Board 94th Annual Meeting*. https://www.microsoft.com/

en-us/research/publication/reducing-road-congestion-through-incentives-a-case-study/

Zhu, W., Ma, S., & Tian, J. (2017). Optimizing congestion and emissions via tradable credit charge and reward scheme without initial credit allocations. *Physica A: Statistical Mechanics and its Applications*, *465*, 438–448. https://doi.org/10.1016/j.physa.2016.08.045